Facile Synthesis of Durable and Bulk Superhydrophobic Materials

A thesis submitted by

Adil Majeed Rather

Roll No. 156122047

to

Indian Institute of Technology Guwahati

for

the award of the degree

of

Doctor of Philosophy

Department of Chemistry

Indian Institute of Technology Guwahati

Guwahati-781039, Assam

India

February-2019

Dedicated To My Grand Parents

INDIAN INSTITUTE OF TECHNOLOGY GUWAHATI
Department of Chemistry

STATEMENT

I hereby declare that the work incorporated in the thesis entitled **"Facile Synthesis of Durable and Bulk Superhydrophobic Materials"** is the result of investigations of research work carried out by me in the Department of Chemistry, under the supervision of Dr. Uttam Manna, Assistant Professor, Department of Chemistry, Indian Institute of Technology Guwahati, Assam, India.

Research material used in this thesis from any other source has been fully cited and acknowledged. This work is original and has not been submitted elsewhere for the award of any degree.

February, 2019

IIT Guwahati **Adil Majeed Rather**

INDIAN INSTITUTE OF TECHNOLOGY GUWAHATI
Department of Chemistry

CERTIFICATE

This is to certify that the work presented in this thesis entitled **"Facile Synthesis of Durable and Bulk Superhydrophobic Materials"** by **Adil Majeed Rather**, a Ph.D. student of Department of Chemistry, Indian Institute of Technology Guwahati, for the award of degree of Doctor of Philosophy has been carried out under my supervision and this work has not been submitted elsewhere for the award of any degree.

Dr. Uttam Manna
Thesis Supervisor
Department of Chemistry
Indian Institute of Technology Guwahati
Guwahati–781039
Assam, India.

February, 2019

Acknowledgements

First and foremost, I would like to express my earnest gratitude to my supervisor Dr. Uttam Manna for his expert supervision, encouragement, advice and prudent suggestions without which this work would not have been possible. I am fortunate enough to have worked under his guidance which has enlightened me about scientific research and life in general. I could not have imagined for a better mentor and advisor for my Ph.D. I am grateful to my doctoral committee members, Prof. Biplab Mondal (Chairman), Dr. Debapratim Das and Dr. Kalyan Raidongia for their ingenious advice, suggestions and critique which helped me in improving the thesis work. I am grateful to all the faculty members of Department of Chemistry, IIT Guwahati for their timely help and encouragement along with the non-teaching staff of the department for their technical support throughout my research work. I am also thankful to Central Instruments Facility (CIF), IIT Guwahati for the instrumental facilities. I thank Dr. Hemant Kumar Srivastava and Dr. Biman. B. Mondal for their assistance in collaborative work. I would like to acknowledge all my teachers at Aligarh Muslim University, Aligarh for their congeniality, excellent teaching, encouragement and treasurable advice which certainly had a great impact on me to further pursue my higher studies. I convey my special thanks to Ajaz Ahmad Dar, Akhter Hussain Malik, and Bilal Ahmad Mir, Tariq Ahmad Shah, Altaf Hussain Kawa, Basit Ahmad, Syed Abid, Khalid Ahmad, Sajad Ahmad for their continuous encouragement, invaluable advice and cherishable moments.

It has been a great learning experience while exploring science in the Bio-inspired Polymeric Material Lab of Dr. Uttam Manna at IIT Guwahati. I cherished every moment spent here with wonderful people around, who made it my second home. It was a pleasure to work with all of my labmates and I would like to express my deep sense of gratitude to all my dear labmates Dibyangana Parbat, Avijit Das, Kousik Maji, Nirban Jana, Arpita Shome, Supriya Das, Angana Borbara, Manideepa Dhar, Dr. Upama Baruah for providing a friendly environment in lab and making my days memorable. I am highly thankful to Arpita Shome for her unending and selfless support when it was utmost required. I would also like to thank Mrs. Tumpa Manna Janna and Irsia Manna for the happy memories that I will cherish lifelong. I am also thankful to various project students Prateeti Hazarika, Chetna Mohanty, Sulendar Mahanto, Arcot Yashwanth, Deepak Kumar Patel, Nasrin Benazir, who assisted me in carrying out various experiments during my research work.

Acknowledgements

I am highly thankful to the Almighty who bestowed me with friends like Arif Hassan Dar, Ryhan Abdullah Rather, Owais Mukhtar Wani, Liyakat Hussain Bhat without whom my life would have been incomplete. I would also like to express my deepest gratitude to my seniors, colleagues and juniors from AMU, Ajaz Ahmad Dar, Palashudin, Sameer Hussain, Wajid Ali, Akhtar Hussain, Shahnawaz Ahmad, Krapa Shankar, Ziaudin Ansari, Faheem Khan, Adil Afroz, Shaad Ansari, Kafeel Ahmad, Maimur Hussain, Akhtar Alam, Bilal Ahmad Mir, Tasleem Khan, Abshar Hassan, Munendra pal Singh, Nehal Zehra, Rabiul Islam, Suhaib Alam, Shavez Ahmad, Sagir Ali, Tipu Alam for giving me unforgettable experiences and cherishable moments. I would also like to acknowledge all the people I met in the hostel and various departments. I am also highly thankful to the staff members and administration at IITG who helped me and made my stay pleasant.

Finally, my PhD endeavor would have been incomplete without the boundless love, unending support, tolerance and prayers of my family. I would like to express my sincere gratitude to my family members who have given me lots of love, strength, support and prayers which helped me reach this stage. I am fortunate enough and blessed to have such caring and supportive parents Mr. Ab Majeed Rather and Mrs. Fahmeeda Begum, it is because of their prayers, sacrifice and struggle I am being able to live my dream to complete my higher education from a prestigious institute. I am grateful to my younger sister (Rahi Majeed) and brother (Shakir Majeed) for their eternal love, cooperation and emotional support which was immensely required to complete this work. Last but not the least, I would like to thank the Almighty Allah for his continuous blessings and for providing me an expert supervisor cum mentor, a loving and supportive family, and wonderful friends who have sincerely helped me to achieve my intellectual destiny.

Synopsis

In the past, lotus leaf-inspired extremely water repellent property that is widely recognized as superhydrophobicity, provided a facile basis for developing various functional materials. However, the synthesis of durable artificial superhydrophobic interfaces following a scalable and simple procedure is the major Achilles' heel at the helm of its practical use in severe and diverse scenarios. Here, a facile and rapid chemical reaction that is Michael addition reaction between acrylate and amine groups is strategically exploited in developing highly tolerant superhydrophobic materials for practically relevant applications. The content of this synopsis report entitled "**Facile Synthesis of Durable and Bulk Superhydrophobic Materials**" is presented in eight chapters. Chapter 1 accounts for a general overview on nature-inspired extremely water repellent interfaces, existing challenges associated with the fabrication of artificial superhydrophobic materials and the motivation for the thesis work. Chapter 2 illustrates the synthesis of amine reactive polymeric material through Michael addition reaction, where the salt assisted gelation of single polymer (i.e.; branched polyethylenimine (BPEI)) provided a durable and bulk superhydrophobic material that is capable of withstanding various kinds of physical (adhesive tape, sand drop, sand paper) and chemical (pH 1, pH 12, sea and river water) manipulations without compromising its anti-wetting property. Chapter 3 accounts the role of various alkali metal ions in the Michael addition reaction in controlling the rate of gelation and tailoring different hierarchical features in the polymeric material. Chapter 4 describes the experimental and computational study for examining the role of different alcoholic solvents in modulating the rate of gelation of polymer along with the change in various physical properties (shrinkage, stiffness, porosity). Chapter 5 illustrates the rapid gelation of BPEI polymer without using any reaction solvent and catalyst at ambient conditions. The inherently sticky material was successfully deposited on various substrates which displayed durable and bulk superhydrophobicity after post modification with octadecylamine. Chapter 6 describes the fabrication of highly stretchable and durable superhydrophobic membrane that can endure various physical (creasing, bending, twisting, 150% stretching) and chemical (pH 1, pH 12, river and sea water) manipulations without compromising the desired anti-wetting property. Furthermore, a process of gravity driven selective filtration of oil spills under various practically relevant challenging scenarios was

also illustrated. In Chapter 7, the fabrication of highly compressible, deformable and durable superhydrophobic material is described, where naturally abundant fibrous cotton was decorated with highly tolerant super-water repellent property for both absorption and filtration based separation of oil from oil/water mixtures with high separation efficiency and recyclability even under various practically relevant harsh chemical conditions. In Chapter 8, brief summary and possible future directions of the current work done in the thesis is proposed.

Chapter 1. Introduction

Naturally existing interfaces are designed with hierarchically featured special interfaces that are further optimized with appropriate chemistry as in the lotus leaf, butterfly wings, legs of water strider, mosquito eyes, gecko feet (Figure 1) etc. which display extreme water repellency, with advancing water contact angle above 150° and roll off angle below 10°.

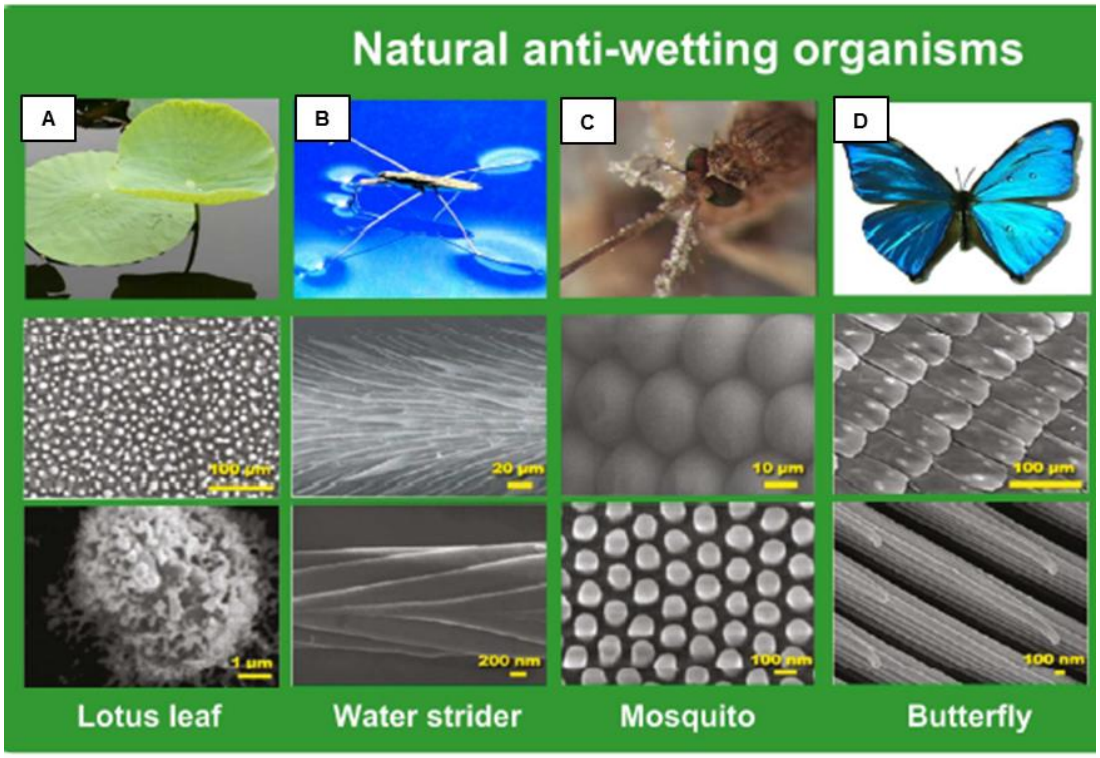

Figure 1. (A-D) Digital images and microscopic images of various natural superhydrophobic interfaces including Lotus leaves (A), Water strider legs (B), Mosquito's compound eyes (C), Butterfly wings (D) respectively. All species exhibit hierarchical structures with appropriate chemical functionality. Reprinted with permission from (*J. Am. Chem. Soc*. **2016**, *138*, 1727−1748), Copyright 2016, American Chemical Society.

Such interfaces are formally defined as nonadhesive superhydrophobic interfaces. Detailed investigation of topography and chemical composition of these naturally existing interfaces demonstrated that the co-existence of hierarchical structures and essential low surface energy coating are the pre-requisites for adopting superhydrophobicity. Since then, various top-down and bottom-up methods have been introduced in the literature to fabricate artificial superhydrophobic interfaces. Such interfaces are potent for various practically relevant applications including self-cleaning, drag reduction, anti-corrosion, anti-icing, anti-fogging, oil/water separation etc. However, the stability and longevity of these artificially synthesized superhydrophobic interfaces remains a challenge, since many of these early synthesized interfaces compromise their embedded extreme water repellency on exposure to even a gentle finger or tissue paper wipe, as the loosely physically deposited low surface energy coating on the hierarchically featured interface is easily eroded. Over the last decade, post repairable and self-healing materials were introduced to combat these poor durability issues, where the compromised anti-wetting property due to various severe abrasive physical/chemical exposures, can be either repaired or self-healed after application of suitable post treatments on the damaged interfaces, but the utility of such approaches are limited to certain healing/repairing cycles. Recently, bulk superhydrophobicity has been introduced in the literature, where the developed material has the extreme water repellent property three dimensionally including the top interface and the interior of the material. Such synthesized materials are inherently capable of sustaining various practically relevant severe physical and chemical challenges without the aid of any external intervention. The examples for designing materials having appropriate and three dimensional co-existence of essential chemistry and hierarchical features that conferred bulk superhydrophobicity, are limited in the literature. Furthermore, the reported bulk superhydrophobic materials are fabricated either following complicated and multiple synthetic procedures or the chemicals involved are too expensive to be executed for practical applications. Here, in this thesis work, various bulk and durable superhydrophobic materials are developed by adopting a facile and rapid Michael addition reaction at ambient conditions and some of these synthesized durable superhydrophobic materials were further exploited for eco-friendly remediation of oil spills from aqueous phase under practically relevant challenging scenarios.

Chapter 2. Synthesis of 'Amine' Reactive Polymeric Material

In this chapter, a porous polymeric material with essential topography and surface chemistry has been developed through 1, 4-conjugate addition reaction between amine and acrylate groups of branched polyethylenimine (BPEI) and dipentaerythritol pentaacrylate (5-Acl) respectively (Figure 2A). The reaction mixture of BPEI/5-Acl in ethanol solvent formed the polymeric gel via formation of chemically reactive nanocomplex intermediate (Figure 2B). Fourier-transform infrared (FTIR) spectroscopy confirmed the existence of characteristic peaks at 1410 cm^{-1} and 1739 cm^{-1} (black spectrum; untreated polymeric gel) for the C−H bond for the β carbon of the vinyl group and ester carbonyl stretching respectively, indicating the presence of residual acrylate groups in the synthesized material. Furthermore, the intensity of peak at 1410 cm^{-1} significantly depleted after post chemical modification (red spectrum; after decylamine treatment) of the polymeric material with amine containing small molecules, validating that the residual acrylate groups remained chemically reactive to primary amine groups (Figure 2C). During the course of reaction, the transparent reaction mixture of BPEI and 5-Acl appeared as a turbid solution (Figure 2D) due to the formation of polymeric nanocomplexes in the reaction mixture, and further random aggregation of these nanocomplexes presumably led to the formation of semi-solid polymeric material. After solvent evaporation, this aerogel provided a porous polymeric material with significant amount of shrinkage, however, the integrity and shape of the material remained intact. On addition of a tiny amount (200-600 µg/mL) of NaCl in the reaction mixture, the rate of gelation was significantly accelerated and the shrinkage reduced drastically after solvent evaporation. The synthesized material displayed superhydrophobicity with advancing contact angle 159º (Figures 2I-J), after post covalent modification with decylamine. Moreover, the synthesized material was embedded with bulk superhydrophobicity (Figures 2L-M) as it displayed extreme water repellency when arbitrarily sliced into multiple pieces. Further, this polymeric material was exposed to various other physical (sand paper, adhesive tape, sand drop, scratch) and chemical (pH 1, pH 12, river and sea water) insults, however, the embedded superhydrophobicity remained intact. The synthesized material can be molded into desired complex and arbitrary shapes that remains unaffected even after shrinkage of the material (Figure 2P). This unaffected integrity and shape after solvent evaporation is likely due to the presence of covalent crosslinking (Michael addition reaction between amine and acrylate) in the material. This current approach provides an easy way

to optimize water wettability from hydrophilic to adhesive (rose petal) and nonadhesive (lotus leaf) superhydrophobic through appropriate post chemical modification of the residual acrylate groups in the polymeric material with amine containing small molecules. The superhydrophobic material displayed self-cleaning property wherein the deposited dust on the extreme water repellant interface was removed on exposure to water (Figures 2Q, R) and the self-cleaning performance remained unaffected even after incurring physical damages to the superhydrophobic material. In the recent past, 3D superhydrophobic materials have emerged as a potential approach for developing a long-term and sustainable

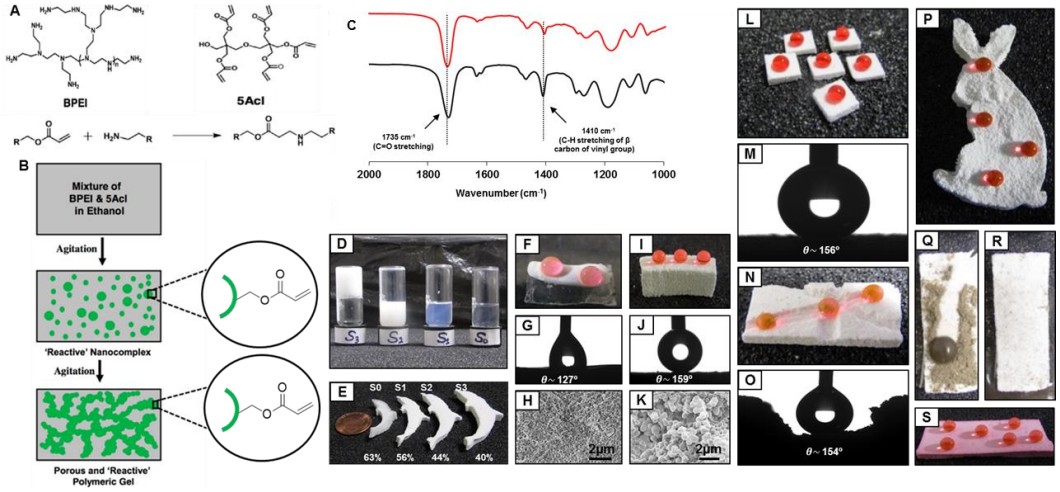

Figure 2. (A) Chemical structures of BPEI and 5-Acl and the 1, 4-conjugate addition reaction between primary amine and acrylate groups. B) Transformation of BPEI/5-Acl mixture to amine reactive polymeric gel via formation of "reactive" nanocomplex intermediate. C) FTIR spectra of polymer gel before (black) and after (red) post chemical modification with decylamine molecules. The spectra was normalized with respect to carbonyl streching (1735 cm^{-1}). D) Gelation of BPEI/5-Acl mixture in presence of various concentrations of NaCl including S0 (without any salt) S1 (200 µg/mL NaCl), S2 (400 µg/mL NaCl), S3 (600 µg/mL NaCl). E) Digital image displaying the shrinkage of polymeric material doped with various concentrations of NaCl. F-K) Digital images (F, I), water contact angle images (G, J) and FESEM images (H, K) of the synthesized material that is prepared in absence (F, G, H) and in presence of salt (600 µg/mL NaCl) (I, J, K) respectively. L-O) Digital images and contact angles image of beaded water droplet on the material (post modified with decylamine) after slicing it in different pieces (L-M) and after random and deep scratches (N-O). P) Digital image of beaded water droplet of polymeric material (post modified with decylamine) with rabbit shape. Q-R) Self-cleaning behavior of synthesized superhydrophobic interface. S) Digital image of beaded water droplet on synthesized material (post modified with decylamine) after loading with rhodamine-6G (a hydrophilic dye molecule).

small-molecules release system. This synthesized porous polymeric material can also be used for developing such slow and sustained drug delivery system, where the hydrophilic small molecules (model drug molecules) can be successfully post loaded within the porous material without compromising the anti-wetting property (Figure 2S). These unique features and the scalability of the current synthetic approach, can substantially extend the potential utility of the biomimicked wettability for various practical applications.

Chapter 3. Alkali Metal Salts in Controlled Tailoring of Topography in Superhydrophobic Material

In the previous chapter, the mixture of BPEI/5-Acl in ethanol rapidly transformed into a polymeric gel in the presence of alkali metal salt (NaCl) displaying bulk and robust superhydrophobicity. In this chapter, the impact of other alkali metal salts was examined in details in the gelation of polymeric material. The growth of the nanocomplexes in the BPEI/5-Acl mixture varied in the presence of different alkali metal salts and eventually the rate of gel formation was observed to be different (Figure 3A). Interestingly, the topography of the materials prepared in the presence of different alkali metal salts was significantly changed (Figures 3B, C). All the alkali metal salt assisted synthesized materials that have different hierarchical topography are loaded with chemically reactive residual acrylate groups, and thus, providing a facile basis for tailoring the essential chemical functionality. The polymeric materials with different hierarchical topography displayed nonadhesive superhydrophobicity after post-treatment with decylamine. This simple study independently revalidated that the superhydrophobic interfaces are not very sensitive towards the specific arrangements of hierarchical features. Next, the polymeric material that is with appropriate hierarchical topography was post functionalized with different amine containing small molecules such as decylamine, octylamine and hexylamine, and the water wettability was examined. The polymeric material (10 mM LiCl) having the same topography, but on post treatment with different chemical functionalities displayed different wettabilities (Figures 3D-F). For example, the decylamine treated material appeared highly shiny under water, and displays nonadhesive superhydrophobicity due to the presence of a large amount of metastable trapped air, whereas the same interface when treated with octylamine was found to be less shiny and adhesive superhydrophobic as shown in Figure 3G-J. Further, no shiny interface was noted for the same hierarchically

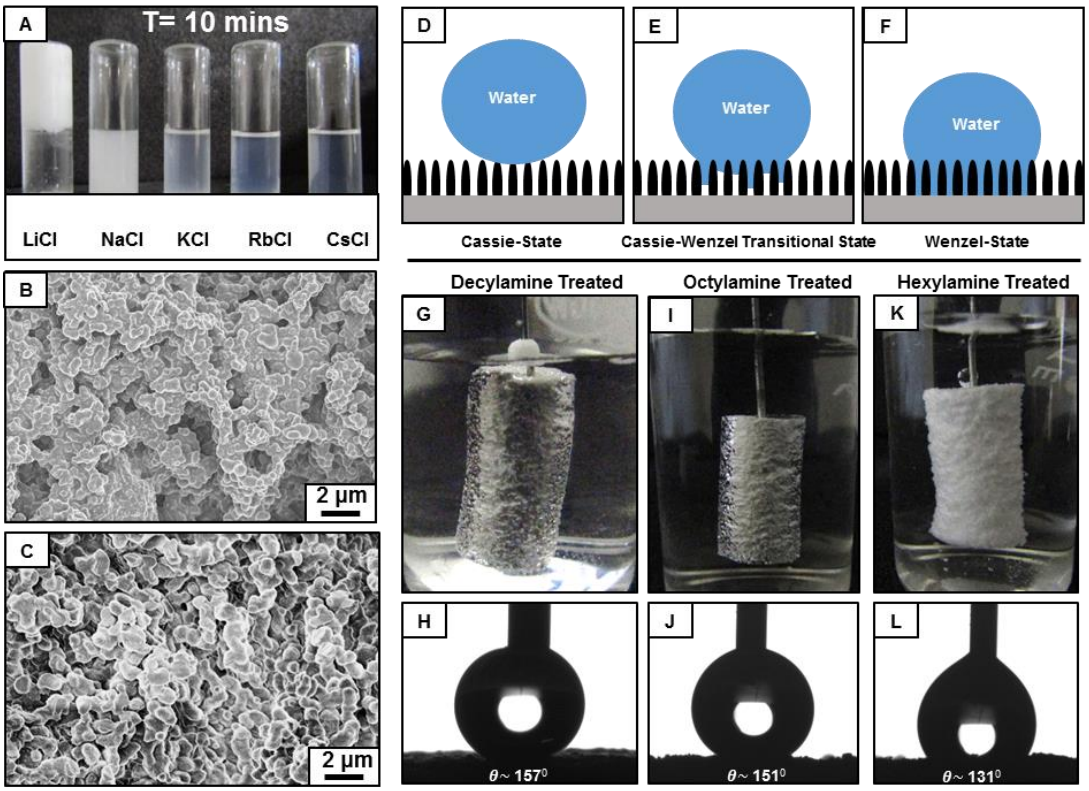

Figure 3. (A) Digital image accounting the visual change in the reaction solution of BPEI/5-Acl mixtures that are prepared individually in presence of various alkali metal salts including LiCl, NaCl, KCl, RbCl and CsCl respectively over 10 mins. B-C) FESEM images of polymeric material that are prepared in presence of LiCl (B) and CsCl (C). D-F) Schematic illustration of the heterogeneous (Cassie state (D) and Cassie–Wenzel transition state (E) and homogeneous (Wenzel state) (F) wetting. G-L) Digital images and contact angle of the material having the same hierarchical topography but with different post chemical modifications with decylamine (G-H), octylamine (I-J) and hexylamine (K-L). The polymeric interfaces with decylamine and octylamine modifications appeared shiny due to the presence of meta-stable trap air, and no trap air was noticed in hexylamine treated material.

featured interfaces treated with hexylamine as it displayed homogeneous water wettability as shown in Figures 3K-L. Thus, the current investigation clearly suggested that the biomimicked interfaces are more sensitive to the chemistry, in comparison to the hierarchical topography as a small variation in the hydrocarbon tail length can have a dramatic impact on water wettability. The hierarchical topography is essential, but it does not demand any specific arrangement of micro/nano domains paving its way for several fundamental and applied studies including tissue engineering, catalysis etc. Moreover, the synthesized material was explored in remediation of oil spills from aqueous phase. The

material successfully and selectively absorbed oil, but the collection of absorbed oil by squeezing the material is not possible as the material breaks in pieces.

Chapter 4. Solvent-Controlled Michael Addition Reaction for Modulating Multiple Physical Properties in Polymeric Material

In the previous chapters, a bulk superhydrophobic material was developed following salt assisted gelation approach which was found to be highly brittle in nature. In this chapter, a more flexible and tolerant superhydrophobic material was synthesized in the absence of any external additives. The alteration of reaction solvents with higher analogues of methanol allowed to tailor various associated physical properties in the synthesized material. In the previous chapters, it was noticed that BPEI and 5-Acl molecules mutually reacted in ethanol at ambient condition through 1, 4-conjugate reaction and the reaction mixture converted into polymeric gel after 210 mins. Here in this chapter, the BPEI and 5-Acl were separately mixed (in appropriate proportion) in various alcoholic solvents starting from methanol to pentanol. The reaction mixture of BPEI/5-Acl in pentanol rapidly transformed into an opaque gel material within 15 mins (Figure 4A), whereas, the same reaction mixture of BPEI/5-Acl in butanol appeared as a milky suspension due to the formation of nanocomplexes (NC) as confirmed by the DLS study (Figure 4B). The growth of NC was delayed on decreasing the hydrocarbon chain length of the respective alcoholic solvents in the reaction mixture. To understand the phenomenon of rapid gelation of BPEI/5-Acl mixture in pentanol compared to methanol solvent, a preliminary computational study was performed. The intermolecular bond distance r (O⋯H) and r (C⋯N) for the transition state in various alcoholic solvents was calculated, and concluded that the intermolecular bond distance steadily decreased with increase in the hydrocarbon chain length in alcoholic solvents. A shorter distance is likely to facilitate the reaction and the probable reason for rapid gelation in pentanol and the slowest gelation in methanol. Furthermore, the topography of the synthesized material prepared in various alcoholic solvents was characterized by FESEM study where significant change in morphology was observed. The material prepared in pentanol solvent consists of dominant micro-domains and the population of these granular domains decreased with the decrease in the alkyl chain length of alcoholic solvent and it was observed that the granular domains were absent in the material prepared in ethanol (Figures 4D-E). The alteration in the alcoholic solvent also

had a significant impact on the shrinkage of polymeric material after solvent evaporation.

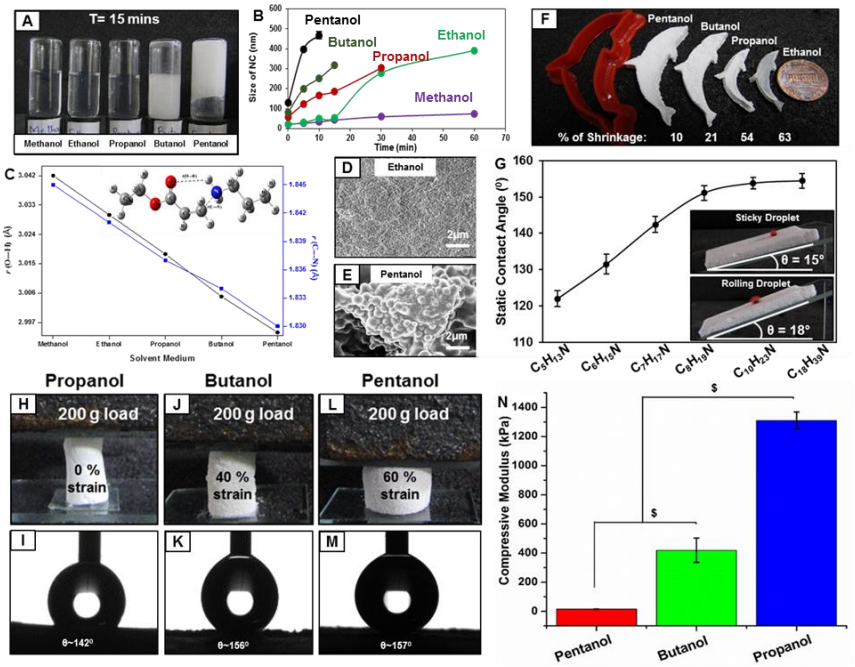

Figure 4. (A) Digital image of BPEI/5-Acl mixture in methanol, ethanol, propanol, butanol and pentanol solvent after 15 mins. B) DLS study on the mixture of 5-Acl/BPEI in pentanol, butanol, propanol, ethanol and methanol illustrating the gradual progression in growth of the nano-complex in different alcoholic solvents. C) Intermolecular bond distance r (O---H, black line) and r (C---N, blue line) in the transition state of the reaction between primary amine and acrylate group in different solvent mediums calculated at B3LYP/6-311++G(2d,2p) level of theory. D-E) FESEM images of materials that are prepared separately in ethanol (D) and pentanol (E). F) Digital image provides the qualitative estimation of shrinkage of polymeric material prepared in pentanol, butanol, propanol, ethanol solvents after the removal of the respective solvents. Dolphin-shaped dough cutter (red) was used as a template for incurring the dolphin shape to each polymeric gel. G) The plot accounts the static contact angles of water droplet on the polymeric gel material (that is prepared in pentanol solvent) after the post modification with pentylamine, hexylamine, heptylamine, octylamine, decylamine and octadecylamine, respectively. Digital images (inset) show the behavior of water droplet (red color aids visual inspection) on octylamine post-modified material, which was tilted with angles of 15° (top) and 18° (bottom), the water droplet completely rolled off at 18° angle, while the same water droplet was adhered on inclining the interfaces at 15°. H-M) Digital images (H, J, L) and contact angle images (I, K, M) of polymeric material depicting the percentage of compressive strain and anti-wetting property after the application of 200 g load on the materials that were prepared in propanol (H-I), butanol (J, K), and pentanol (L, M) respectively. N) The plot accounting the compressive modulus of the materials that are prepared in pentanol, butanol and propanol.

The polymeric material in pentanol showed 10% shrinkage compared to ethanol (63%) (Figure 4F). The presence of residual acrylate groups (as confirmed with FTIR analysis) in the polymeric material synthesized in pentanol allowed to tailor the water wettabilities from hydrophilic to superhydrophobic (adhesive and nonadhesive). The adhesive superhydrophobicity (after post modification with octylamine) was extended for the demonstration of no-loss transfer of tiny water droplets by controlling the tilting angle of the interface (Figure 4G). In addition to that, the deformation behavior of the polymeric materials, which were prepared in various alcoholic solvents, was examined under a constant load of 200 g (Figures 4H, J, L). The materials that were synthesized in butanol and pentanol were subjected to 40% and 60% compressive strain, whereas the material prepared in propanol and ethanol media were significantly less deformable. Thus, the hardness and softness of the polymeric material can be also tailored depending on the selection of appropriate alcoholic solvent. Moreover, the materials prepared in butanol and pentanol after post modification with ODA displayed superhydrophobicity whereas ethanol and propanol developed materials only showed hydrophobicity due to the lack of appropriate combination of hierarchical topography in the materials. Hence, this simple and environment-friendly approach could be useful in developing various functional materials for several relevant and prospective applications. This superhydrophobic material was further extended for absorption based separation of oil spills and the absorbed oil was collected by squeezing the polymeric material.

Chapter 5. Rapid and Solvent-free Synthesis of bulk Superhydrophobic Coating

Here, in this chapter, rapid and facile synthesis of chemically reactive and hierarchically featured polymeric coating was demonstrated without using any reaction solvent and external additives. The molar ratio of BPEI (the mole amount is calculated with respect to the repeating unit) and 5-Acl was varied from 1:3 to 1:5 for optimizing (a) essential topography and (b) the appropriate chemistry that conferred biomimicked superhydrophobicity was optimized by post covalent functionalization. The colorless liquid mixture of BPEI and 5-Acl was mixed rapidly to form an opaque gel within 30 s as shown in Figure 5B. The synthesized polymeric gel (molar ratio of BPEI/5-Acl 1:5) was observed to be inherently sticky and hydrophilic but after treatment with octadecylamine (ODA) molecule, extremely water repellent property was observed with water contact angle above

150º (Figures 5D-E). Moreover, the polymeric gel was arbitrarily sliced into two parts to expose the interior of the material and it was observed that the interior was also superhydrophobic with WCA above 150° (Figure 5G). The microscopic morphology of the polymeric gel was examined with FESEM study, where both the top interface and bulk of the material was noticed to have random porous structures (Figure 5F). This simple approach provided a facile basis for coating various hydrophilic substrates including wood, paper, card board, plastic etc. to confer the extreme water repellency with high contact angles (above 150°) and low contact angle hysteresis (below 10°) as shown in Figures 5H-Q. The integrity as well as the anti-wetting property of the polymeric coating on various

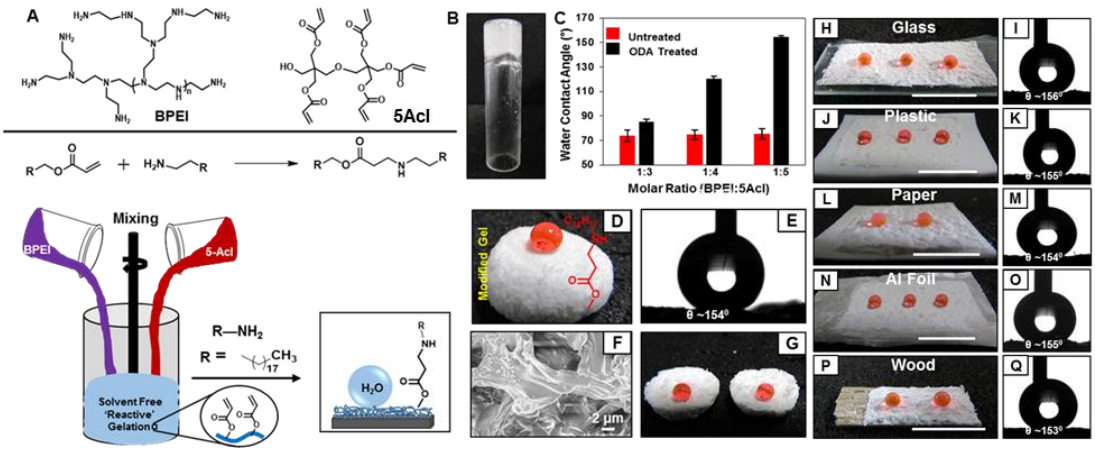

Figure 5. (A) Schematic illustrating the spontaneous and rapid synthesis of chemically 'reactive' polymeric gel on continuous mixing of polymer (BPEI) and small molecule (5-Acl) without using any external reaction solvent and catalyst, and the material displays superhydrophobicity after appropriate post chemical modification. B) Digital image showing the mixture of liquid reactants (BPEI and 5-Acl) after gelation. C) The plot accounting the change in contact angle of the chemically 'reactive' polymeric gels that are prepared by mixing BPEI and 5-Acl with different molar ratio, before (red) and after (black) post treatment with ODA molecules. D-E) Digital image and water contact angle image of the 'reactive' polymeric gel (that is synthesized by mixing BPEI and 5-Acl with 1:5 molar ratio) after post modification with ODA. F) FESEM image of solvent-free polymeric gel prepared by mixing of BPEI and 5-Acl with 1:5 molar ratio. G) Digital image showing the beaded water droplets after slicing the polymeric material in two pieces. H-Q) Digital images and contact angle images of beaded water droplet on reactive polymeric material coated substrates after post modification with ODA molecules, where coated glass (H-I), plastic (J-K), paper (L-M), aluminum foil (N-O) and wood (P-Q) display robust superhydrophobicity.

substrates remained intact under various physical (sand drop, adhesive tape, UV radiations) and chemical (pH 1, 12, sea and river water) insults. This approach can be further exploited for developing functional biointerfaces and chemically patterned interfaces. This approach can be further exploited for developing functional biointerfaces and chemically patterned interfaces. Thus the current approach provided substrate independent bulk superhydrophobic coating–following a facile deposition process.

Chapter 6: Synthesis of Stretchable Superhydrophobic Interfaces

Recently, stretchable superhydrophobic materials have emerged as a prospective avenue for developing ultra-flexible electronics, flexible microfluidics, gas sensors, functional textiles, wearable devices etc. However, the synthesis of highly stretchable superhydrophobic interfaces that is tolerant towards various abrasive exposures is highly challenging. In the previous chapters (2–4), the reaction mixture of BPEI and 5-Acl transformed into a polymeric gel via formation of turbid solution of polymeric nanocomplex in ethanol. Here, in this chapter, fibrous, stretchable and hydrophilic polyurethane (PU) membrane (Figures 6A, B) was selected as the substrate. The PU substrate was first functionalized with BPEI polymer, prior to transfer into the reaction solution of growing nanocomplexes in ethanol. The polymeric nanocomplex coated fibrous PU matrix was post modified with octadecylamine (ODA) after which it displayed nonadhesive superhydrophobic property with advancing contact angle of 157º and contact angle hysteresis 4º respectively (Figures 6C, D). The topography of the PU fibers was examined with FESEM imaging, where smooth and featureless native PU fibers were found to be uniformly coated with random granular domains due to successful immobilization of growing nanocomplexes from BPEI/5-Acl mixture in ethanol as shown in Figures 6E-F. To examine the durability, the synthesized material was exposed to various physical (bending, creasing, twisting, rubbing, sand paper, sand drop, adhesive tape, UV radiations) and chemical (pH 1, pH 12, river and sea water) manipulations and was observed that it could withstand such challenging and complex scenarios (Figures 6G-J, N) with advancing contact angle above 150º and contact angle hysteresis below 10º. Next, the substrate was exposed to 150% tensile strain for 1000 times and a stream of water readily bounced back after 150% streching from the interface and the anti-wetting property remained intact with advancing water contact angle above 150º and contact angle hysteresis below 10º during

the entire process (Figures 6K-M). The stretchable membrane was further explored for gravity-driven and energy efficient oil/water separation. For the proof of concept, an oil/water separation prototype was built in the lab using a centrifuge tube and the stretchable membrane was wrapped on the opening of the tube, and a hole was made at the other end of the tube for pouring the oil/water mixture and collecting the separated aqueous

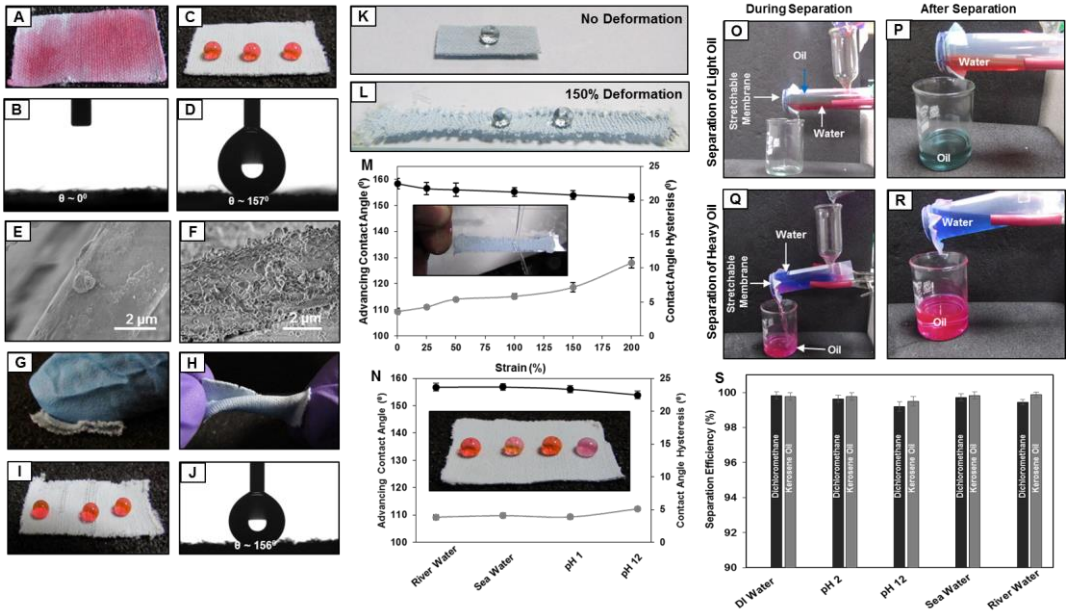

Figure 6. (A-F) Digital images (A, C), water contact angle images (B, D) and FESEM images (E, F) of uncoated (A, B, E) and nano-complex coated (C, D, F) polyurethane (PU) based fibrous substrate (post functionalized with ODA molecule). G, H) Digital images of superhyrophobic PU substrate that is manually creasing (G) and twisting (H). I-J) Digital image (I) and water contact angle image (J) of the beaded water droplets on superhydrophobic PU fabric after adhesive tape peeling test. K-L) Digital images of beaded water droplet on the superhydrophobic fibrous PU substrate before (K) and after physical deformation (L) with 150% strain. M) The plot accounting the advancing contact angle (black) and contact angle hysteresis (grey) of water droplet on the superhydrophobic PU substrate that was gradually deformed with 200% strain and digital image (inset) depicting the bouncing of a jet of water on deformed (with 150% strain) superhydrophobic substrate. N) The plot showing the advancing contact angle (black) and contact angle hysteresis (grey) of acidic (pH 1), alkaline (pH 12), sea, and river water droplet on the superhydrophobic PU fabric. O-R) Digital images illustrating the separation of both lighter (kerosene) and heavier oils (dichloromethane) from corresponding oil/water mixtures using lab-made prototype. S) Plot accounted the oil collection efficiency for both the heavier and lighter oils from corresponding mixture of oil and complex aqueous (extremes of pH, sea water, river water) phases.

phase from the prototype. The oil/water separation was demonstrated with kerosene oil (model light oil) and dichloromethane (DCM, model heavy oil). The mixture of respective oil/water mixtures were poured into the prototype, the oil phase was selectively and readily passed through the stretchable superhydrophobic fibrous substrate (Figures 6O-R), and finally collected in a separate beaker with separation efficiency of 99.7%. Furthermore, these oils (kerosene and DCM) can also be separated from complex and harsh environments, where DI water is replaced with extremes of acidic and basic water, sea and river water.

Chapter 7: Compressible, Deformable and Durable Superhydrophobic Material for Absorption and Filtration Based Oil/Water Separation

In the previous chapter, a stretchable superhydrophobic material was demonstrated for gravity-driven selective filtration of oil spills from the aqueous phase. Water pollution due to oil-contamination from petro-chemical industrial discharge, accidental oil spillages during oil production and transportation has severe impact on the marine ecosystem. Generally, separate fabrication processes and geometrically different substrates are used for selective absorption-based and filtration-based oil/water separations. Hence, the development of a single superhydrophobic material through a simple and scalable fabrication process, which would be capable of both filtration-based and absorption-based oil/water separation, is essential for comprehensive and environmental friendly oil/water separation in practically relevant circumstances. In this current chapter, a naturally abundant and inherently hydrophilic fibrous cotton was selected as a substrate (Figures 7A, B). This fibrous cotton was first functionalized with BPEI polymer and subsequently coated with amine reactive nanocomplexes (NC) followed by post-chemical modification with octadecylamine (ODA) molecules through 1, 4-conjugate addition reaction. The material displayed extreme water repellency with advancing contact angles of 161° as shown in Figures 7C, D. Furthermore, FESEM images confirmed the uniform coating of nanocomplexes on the fibrous substrate where the smooth and featureless fibrous cotton fibers are coated with random granular domains (Figures 7E, F), providing the essential topography to confer the extreme water repellency. The physical integrity and the anti-wetting property of the material remained intact after 1) performing physical deformations

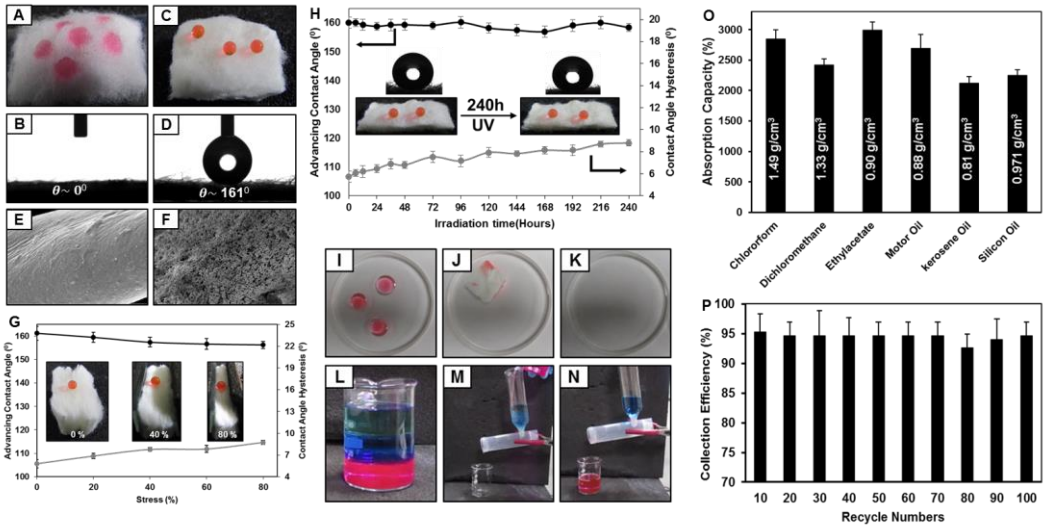

Figure 7. (A-F) Digital images (A, C) water contact angle images (B, D) and FESEM images (E, F) of uncoated (A, B, E) and nano-complex coated (C, D, F) cotton (post functionalized with ODA molecule). G) Plot showing the advancing contact angle (black) and contact angle hysteresis (grey) of beaded water droplets on SHC that were manually deformed to different extents, starting from 0% to 80% compressive strains. The inset digital images represent the beading of water droplets before (left image) and after deforming the material with 40% (middle image) and 80% (right image) compressive strains. H) Plot displaying the change in advancing contact angle (black) and contact angle hysteresis (grey) of beaded water droplets on SHC after irradiating the material under UV light, the inset is the contact angle images of beaded water droplets on SHC before and after exposure to UV radiation for 10 days. I-K) Digital images demonstrating the collection of multiple (three) droplets of vegetable oil from the air/water interface using SHC. L-N) Digital images illustrating the separation of a complex oil/water mixture that consists of three phases, light oil (kerosene), heavy oil (DCM, red color) and water (blue color), through gravity-driven filtration using SHC. O) Plot illustrating the capacity of SHC for absorbing various oils irrespective of chemical compositions, densities and viscosities of the oils. P) Plot showing the ability of SHC for repetitive use in gravity-driven filtration of an oil/water mixture for 100 times.

i.e. bending, twisting, creasing, compressing with 80% strain (Figure 7G), 2) prolonged exposure to UV radiation (Figure 7H). Due to the existence of inherent high porosity and durable anti-wetting property, the superhydrophobic cotton (SHC) was explored for oil/water separations of lighter and heavier fraction of oils through absorption and filtration based methods. The SHC floats on the air/water interface due to its inherent light weight and the presence of extreme water repellent property provided a facile basis for the complete removal of floating multiple oil droplets from the oil/water interface, as depicted

in Figures 7I-K. The absorption capacity of the synthesized SHC was calculated to be well above 2000 wt% irrespective of the density and viscosity of the oils (Figure 7O). Furthermore, gravity-driven selective filtration of oils from a complex oil/water mixture, where the aqueous phase was sandwiched between heavy (DCM) and light (kerosene) oils was also carried out. Both the heavy and light oils were actively filtered and collected in a separate container while as aqueous phase remained on the top of the SHC as noted in Figures 7L-N. The material was repetitively used for oil/water separation for 100 times with high separation efficiency. This material has potential for both (a) preventing oil contamination by adopting an active-filtration process and (b) cleaning up accidental oil-spills from vast and open water resources (seas, rivers, lakes etc.) through the selective absorption of oil from oil/water mixture.

Chapter 8. Conclusion and Future Directions

In conclusion, a facile chemical strategy was adopted to develop functional polymeric monoliths and coatings through strategic use of Michael addition reaction between amine and acrylate functionalities. The impact of salt in the reaction mixture was studied in details. The reaction solvent has a significant impact on tailoring various physical properties in the polymeric material. Moreover, some important fundamental aspects of superhydrophobicity was explained with the synthesized materials. The detailed understanding of Michael addition reaction between BPEI and 5-Acl molecules provided a facile basis to develop various superhydrophobic materials, which were explored for the demonstration of self-cleaning of deposited dust, no-loss transfer of liquid droplets and remediation of oil spills under various challenging settings. Some of the synthesized materials are highly capable of sustaining large (upto 150%) tensile deformation for multiple times (1000 times), without compromising the embedded antifouling property. Moreover, such interfaces are extremely tolerant towards exposures to various severe physical and chemical challenges. These initial findings are very encouraging and likely to pave the way for various other practically relevant applications including design of chemically patterned interfaces for biomedical applications and water harvesting etc. Stretchable superhydrophobicity is likely to provide a suitable avenue for developing smart and wearable electronic devices. Further, the bulk superhydrophobicity allowing post loading of external hydrophilic small molecules without compromising embedded extreme

water wettability. This principle provided facile basis for developing sustained and prolonged drug delivery systems. Thus, this current approach of developing bulk and durable superhydrophobicity has immense scope for developing different functional materials for practically relevant applications in the recent future.

Table of Contents

Chapter 1: Introduction

1.1. Biomimicry: Smart Inventions Inspired from Nature

Nature remains an open source of inspiration for various important and relevant scientific and technological developments in the past. For hundreds of years, people have observed and inspired by the variety of natural species. For instance, the discovery of aeroplane was inspired through observation of birds flying in air, in fact the word aeroplane is derived from the Latin word '*avis*' means bird. Leonardo da Vinci was one of the pioneer in the use of biomimicry of birds for developing revolutionary designs, in the hope of enabling human flight. Although he was not successful, but his ideas lived on and became source of inspiration for the Wright Brothers. They finally succeed in creating and flying the first airplane in 1903.[1] The origin of 'Velcro' is another fascinating discovery by George de Mestral[2], a Swiss mechanical engineer who observed many small burrs attached themselves to the hair of his dog's legs on walking through the forest. Another great invention was the 'bullet train' inspired from the bill of kingfisher bird. After several failed attempts, the designers observed that the kingfisher bird dives into water with minimal splashing compared to other similar sized birds. The inventors concluded that the structural design of the kingfisher's bill reduces air friction enabling the bird to dive into the water, thus, carving the proposition that led to the invention of bullet train.[3] Whale fish inspired the better design of ocean turbine blades, a 'Biologist' Frank-Fish after looking at the picture of a humpback whale and noted the pointy bumps along its fins and he discovered that these bumps called 'tubercles' are the natures secret design to allow the whale fish of big size to take tight turns and capture the prey with outstanding ability. This energy efficient nature-inspired design proved useful in developing turbines, compressor, pumps, fans etc.[4]

It is astounding that nature has answers to all the challenging and complex problems perturbing the mankind and therefore, the concept of 'bio-mimicking' was introduced. The mimicking of natural materials to prepare their exact replica due to their unique properties has become one of the potent research topics in the academia as well as in industries. In that context, the extremely liquid (oil/water) repellent interfaces that are observed on lotus-leaf and fish scale, emerged recently as an important avenue for designing various functional materials for wide range of applications. We will discuss on this in more details in the following section.

1.2. Liquid Wettability on Solid Surface

Wetting of a solid surface by liquids is an important phenomenon appeared to be of potential interests for various fundamental studies and practical applications.[5,6] When a liquid droplet is dispensed on a solid surface, the adhesive forces (force between unlike molecules) between the liquid and the solid surface causes the liquid droplet to spread over the surface and the cohesive forces (force between like molecules) causes the liquid droplet to ball up and lessen the contact with the solid surface.[7] The wetting of a solid surface by liquid is quantified by measuring the contact angle, which can be defined as the tangent angle of the liquid/vapor interface at the three phase boundary as shown in Figure 1.1A. Further, the dynamic contact angles—that are advancing (θ_{Adv}) and receding (θ_{Rec}) contact angles (Figure 1.1B, C) are important for characterizing the extreme liquid repellency.[8] In general, for highly liquid repellent interfaces, advancing contact angle is measured for a growing droplet on the interface (Figure 1.1B), while the receding contact angle is measured during the process of withdrawing of beaded liquid droplet from the solid interface (Figure 1.1C). The difference between advancing and receding contact angle is known as contact angle hysteresis (θ_{Hys}), which is equivalent to the roll off angle of beaded liquid on tilted interface.[9] On the basis of contact angle of aqueous phase, the solid surfaces can be classified as hydrophilic, hydrophobic and superhydrophobic.[10] The solid interface

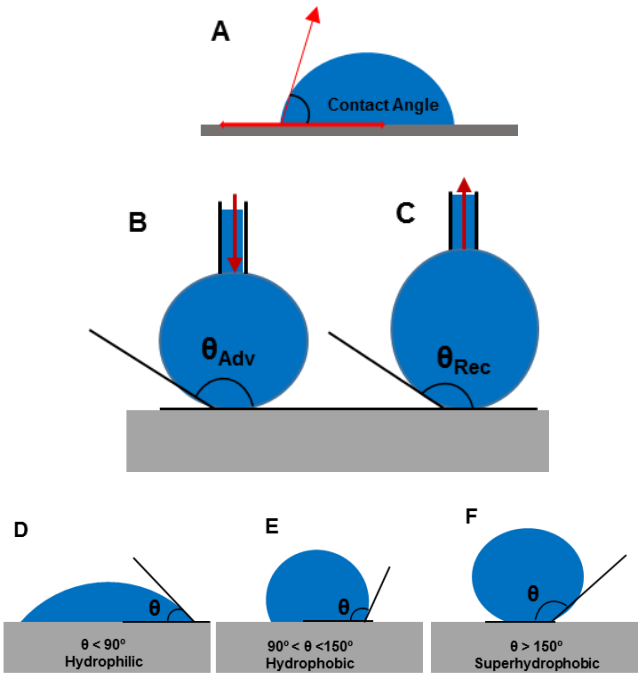

Figure 1.1. (A) The contact angle θ is defined as the angle between the droplet, and the substrate at the three phase contact point. B-C) The advancing contact angle (B) and receding contact angle (C). D-F) Surfaces in contact with water display a contact angle of less than 90° are hydrophilic (D), surfaces with contact angles of more than 90° are hydrophobic (E) and surfaces with contact angle of more than 150° are superhydrophobic (F).

having water contact angle (θ) lesser than 90º is recognized as hydrophilic and the aqueous phase readily spreads over the large area on such solid interface (Figure 1.1D), whereas the water contact angle (θ) greater than 90º signifies that the interface is hydrophobic, and the solid surface starts repelling the beaded water droplet (Figure 1.1E). The extremely water repelling property known as superhydrophobicity is formally defined as the interface having water contact angle above 150º,[11] where the water droplet beaded on the solid interface with minimum physical contact as shown in Figure 1.1F. The nonadhesive superhydrophobic interfaces are with advancing water contact angle above 150° and contact angle hysteresis below 10º. Over the time, different wetting models have been proposed to understand this liquid wettability in more details.

1.2.1. Various Wetting Models

1.2.1.1. Young Model

The concept of wettability traces its history around two hundred years ago beginning with the introduction of Young's equation in 1805.[12] When a liquid droplet is dispensed on a solid smooth surface, the adhesive force overpowers the cohesive force which leads to droplet spreading over the surface until all the acting interfacial tensions are balanced. This phenomenon was first observed by a British physicist—Thomas young, and he proposed an equation which is known as Young's equation to measure the contact angle on a solid smooth surface, where all the interfacial forces that are acting on the beaded liquid is balanced and the equation is proposed;

$$\cos\theta_Y = \frac{\gamma_{SV} - \gamma_{SL}}{\gamma_{LV}} \quad \text{…….……..} (1)$$

Where γ_{SV}, γ_{SL}, γ_{LV} are the interfacial tensions of solid-vapor, solid-liquid and liquid-vapor interfaces respectively and θ_Y refers to Young's contact angle.

The molecules at the surface are at a different environment compared to the bulk. Energy is required to bring a molecule from the bulk to the surface, known as 'interfacial energy'. When the interfacial energy of solid-vapour interface (γ_{sv}) is higher than that of solid-liquid interface ($\gamma_{SV} > \gamma_{SL}$), then the right side of young's equation is positive and contact angle will be in between 0º to 90º. The theoretical calculations of water contact angle following

Young's equation resembles well with the experimental results for featureless and smooth solid surfaces.

1.2.1.2. Wenzel Model

The Young model fails to explain the water contact angle of beaded droplet on a rough solid surface. In 1936, the Wenzel Model[13] was proposed, where the Young's contact angle equation was modified by associating the roughness factor (r) as shown in equation 2.

$$\cos \theta_W = r \cos \theta_Y \quad \text{.................................} \quad (2)$$

Where θ_w is the contact angle of liquid on the rough surface (Wenzel contact angle), θ_Y is the contact angle of liquid on the smooth surface (Young's contact angle), 'r' is the roughness factor which is defined as the ratio of actual surface area to the projected surface area. Wenzel equation implies that a hydrophilic surface will become more hydrophilic and hydrophobic surface will become more hydrophobic due to the incorporation of roughness factor. The schematic representation of the model is shown in Figure 1.2B. However, this homogenous wetting model on the rough interface is unable to explain the superhydrophobicity.

1.2.1.3. Cassie-Baxter Model

Both the Young's and Wenzel's wetting models are derived assuming a homogenous wetting surface by the liquids. Later, Cassie and Baxter introduced a fundamentally different concept of liquid wettability on solid interfaces,[14] where liquid droplet beaded on the solid interfaces with discontinuous contact—due to the entrapment of third external

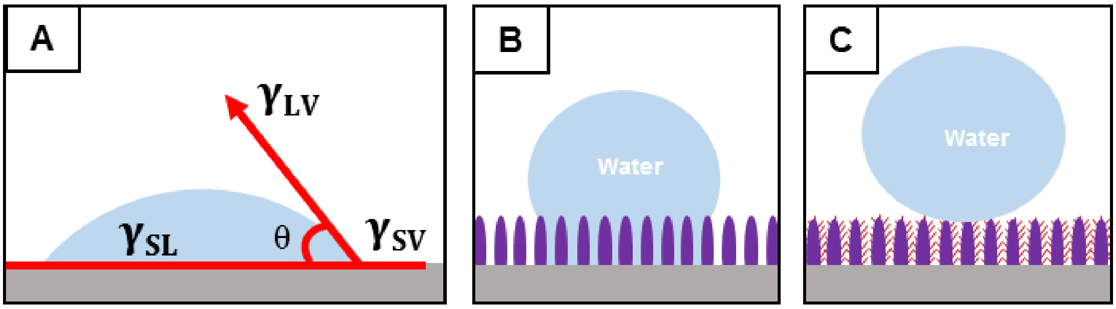

Figure 1.2. Schematic representation of a water droplet on a smooth surface (A), following the Young's equation, and on a rough surface (B), following the Wenzel equation and the Cassie–Baxter state (C).

phase in the asperities of rough solid surface. In case of lotus-leaf mimicked superhydrophobicity, the third external phase is meta-stable trapped air that leads to a discontinuous contact between beaded water and the lotus leaf as shown in Figure 1.2C.

The apparent contact angle of this vapor/liquid/solid interface is the contribution from different phases:

$$\cos\theta_{CB} = f_1 \cos\theta_1 + f_2 \cos\theta_2 \ldots\ldots\ldots\ldots\ldots\ldots\ldots\ldots\ldots\ldots (3)$$

Where f_1 and f_2 are the geometrical fractional areas of solid/liquid and liquid/air interface (where $f_1 + f_2 = 1$), θ_1 and θ_2 are the contact angles of beaded liquid on solid surface and in air respectively. The suspended contact angle of water in air is 180°, then the modified Cassie- Baxter equation can be written as:

$$\cos\theta_{CB} = f_1 \cos\theta_1 + (1-f_1) \cos 180^o \ldots\ldots\ldots\ldots\ldots\ldots\ldots\ldots (4)$$

$$\cos\theta_{CB} = f_1 \cos\theta_1 + f_1 - 1 \ldots\ldots\ldots\ldots\ldots\ldots\ldots\ldots\ldots (5)$$

$$\cos\theta_{CB} = f_1 (\cos\theta_1 + 1) - 1 \ldots\ldots\ldots\ldots\ldots\ldots\ldots\ldots\ldots (6)$$

The parameters f_1 ranges from 0 to 1, when $f_1 = 0$, the liquid droplet doesn't wet the surface and when $f_1 = 1$, the surface is completely wetted by the liquid with contact angle 0º. In the Cassie-Baxter state, entrapped third external phase, reduces the contact between the liquid and solid surface, and eventually allows the droplet to roll off easily from the slightly tilted solid interface.

1.3. Naturally Existing Superhydrophobic Interfaces

From plant leaves to insect legs nature presents numerous examples of anti-wetting surfaces.[15–17] However, lotus leaf (*Nelumbo Nucifera*) is an archetype of all and is considered as a sign of purity in Asian culture due to its inherent self-cleaning nature. In 1997, two German Botanists, Neinhuis and Barthlott[18] unprecedentedly revealed the reason behind the self-cleaning property of lotus leaf. Scanning electron microscope (SEM) images of the louts leaf confirmed that the surface contains randomly distributed papillae (bumps; 5–10 μm) which are further decorated with hairy nanostructures (diameter of 100–200 nm) on top (Figure 1.3A). The hierarchical structures that are coated with an epicuticular wax film of the lotus leaf display superhydrophobicity with water contact angle of ~160º and roll off angle below ~5º.[19,20] The aqueous/air interface of the rolling water droplet is capable of collecting the deposited dust and dirt particles, and eventually the lotus leaf is self-cleaned. Furthermore, some insects and birds are also possessed with such extreme water repellency. For example, water striders have non-wetting legs that allows them to walk on water (Figure 1.3B).[17] SEM imaging of the water strider's legs reveals the

existence of the micro-scale setae which contains nanoscale grooves at the surface. The presence of these hierarchical structures that are decorated with hydrophobic wax renders the superhydrophobicity and allowed to freely walk on aqueous phase. Additionally, feathers of many birds are superhydrophobic, and this extreme water repellency help in keeping the feathers dry even after prolonged exposure to aqueous phase.[21]

Nature also provides examples of anisotropic super-water-wettability. For example, water droplets easily roll along the direction parallel to rice leaf edges but not in the perpendicular direction.[22] This property is attributed to the anisotropic arrangement of microstructures on

Figure 1.3. (A) Lotus leaves demonstrate low adhesion, superhydrophobic, and self-cleaning properties, due to randomly distributed micro-papillae covered by branch-like nanostructures. B) Water strider legs have robust superhydrophobicity attributed to the directional arrangements of needle like micro-setae with helical nano-grooves. C) Mosquito's compound eyes have superhydrophobic function due to micro-ommatidia covered by nano-nipples. D) Butterfly wings exhibit directional adhesion and superhydrophobicity due to the multiscale structures. E) A gecko's feet present highly adhesive superhydrophobic functions due to the aligned microsetae splitting into hundreds of nanospatulae. Reprinted with permission from (*J. Am. Chem. Soc.* **2016**, *138*, 1727−1748), Copyright 2016, American Chemical Society.

the leaves. The distribution of the papillae follows a quasi-one-dimensional order parallel to the leaf edge rather than a uniform arrangement like lotus leaf. As a consequence, the beaded water droplets roll along a specific direction on such interface. Similar to rice leaves, butterfly wings (Figure 1.3D) also exhibit anisotropic rolling of beaded water

droplet,[23] the water droplets on butterfly wings easily rolls away along the radial outward (RO) direction, but their movement was strongly inhibited in the opposite direction. SEM analysis of the wings shows periodic hierarchical scales along the RO direction. Each scale is composed of well-oriented nanostripes, which are stacked stepwise by tilted periodic lamellae along the RO direction. Interestingly, the nanoscale tips on the top of stripes tilted slightly upward, allow the water droplets to roll along them but pinning the droplets when rolling against the tips. In addition to these examples of low-adhesion superhydrophobic surfaces, some organisms also display highly adhesive superhydrophobicity such as gecko feet (Figure 1.3E).[24–26] The surface of gecko feet consists of well-aligned microhairs called setae (approximately 5 μm in diameter and 110 μm in length), which are decorated with hundreds of smaller nanoscale ends called spatulae. Liu *et al.*[24] reported that the adhesive force between the gecko feet and the water droplet is in the range of 10−60 μN, depending on conformational changes in the surface setae proteins upon exposure to water. These natural examples continues to inspire researchers to develop artificial interfaces that are rationally decorated with adhesive and nonadhesive superhydrophobicity for wide range of prospective and practically relevant applications.

1.4. Essential Criteria to Develop Artificial Superhydrophobic Interfaces

In 1997, Barthlott *et al.*[18] postulated that the microstructures of lotus leaf are the key reasons for its superhydrophobic property. However, microstructure based artificial superhydrophobic materials were noticed to be mostly adhesive in nature. Later, in 2002 Jiang *et al.*[22] designed a smart interface for examining the role of both micro/nano features in the hierarchical interface that displayed nonadhesive superhydrophobicity. The hierarchically featured interface became highly adhesive to the beaded water droplet, after destroying the nano structures selectively. This study unambiguously confirmed that the existence of the appropriate combination of micro and nanoscale two-tier structures are essential for developing lotus leaf mimicked nonadhesive artificial superhydrophobicity. Further, Koch *et al.*[20] revalidated this fundamental study with an independent design, where the hierarchical structures were developed—directly from lotus leaf by adopting fast and precise molding process and natural lotus wax was deposited by thermal evaporation to create the waxy nanostructures. The authors also demonstrated the behaviour of water droplet on artificial interface that were exclusively decorated with either the nano or micro

features. However, only the hierarchically featured (micro/nano) surfaces displayed the anti-wetting property similar to lotus leaf. Therefore, these fundamental studies concluded that the two essential criteria required to develop the artificial superhydrophobic surfaces are the presence of 1) dual (micro/nano) scale of roughness and 2) essential low surface energy coating on top of the hierarchical features.[27]

1.5. Approaches to Develop Artificial Superhydrophobic Interfaces

In general, fabrication of hierarchical structures on arbitrary substrates (mostly hydrophilic), followed by its essential chemical modification with low surface energy materials or developing hierarchical features out of inherently hydrophobic substrate are primary principles for synthesizing artificial superhydrophobic interfaces. Over the last two decades, various top-down and bottom-up approaches were adopted for fabricating artificial superhydrophobic interfaces. Most of the reported designs are associated with multistep procedures, challenging reaction conditions, expensive reagents and sophisticated equipments.

1.5.1. Top Down Approaches

Top-down approach sometimes known as step-wise design is the breaking down of a system into its sub-systems in a reverse engineering fashion. Top-down approach is a general term in microelectronics referring to the fabrication of materials and devices by carving, molding or machining bulk materials with tools and lasers.[28] Some of the top down approaches that are adopted for developing superhydrophobic interfaces are briefly discussed in the following section.

1.5.1.1. Lithography

The term lithography, is blend of two Greek words—Litho (means stone) and graphy (means writing), generally refers to the process of writing on hard surfaces like stones and metals.[29] Initially, a process of printing using a nonpolar ink on a hydrophilic master plate was considered as lithography.[30,31] Nevertheless, such general principle was extended later in developing organized topography in micro/nano scales.[32–36] In the early progress on the artificial superhydrophobic interfaces, the lithographic methods that provide a good control over surface structuring and pattering were widely used for preparing extreme water repellent interface. Rough surfaces patterned with various shapes (e.g.; circular, square, star etc.) of pillars, with different dimensions has been developed by adopting various

lithographic techniques.[37–40] In 1994, a seminal report by Kawai Nagata utilized photolithography to develop micro-patterned interfaces for examining the water wettability, the water wettability was gradually increased with enhancing the aspect ratio (formally defined as length ratio between the bottom space and pattern height).[41] Later, McCarthy *et al.*[42] have extended this photolithography process for developing a series of silicon surfaces possessed with posts of different sizes, shapes, and separations (Figure 1.4) and have studied the water wettability on such strategically patterned interfaces. The water contact angles were noticed to be independent of the post height from 20 to 140 μm, and

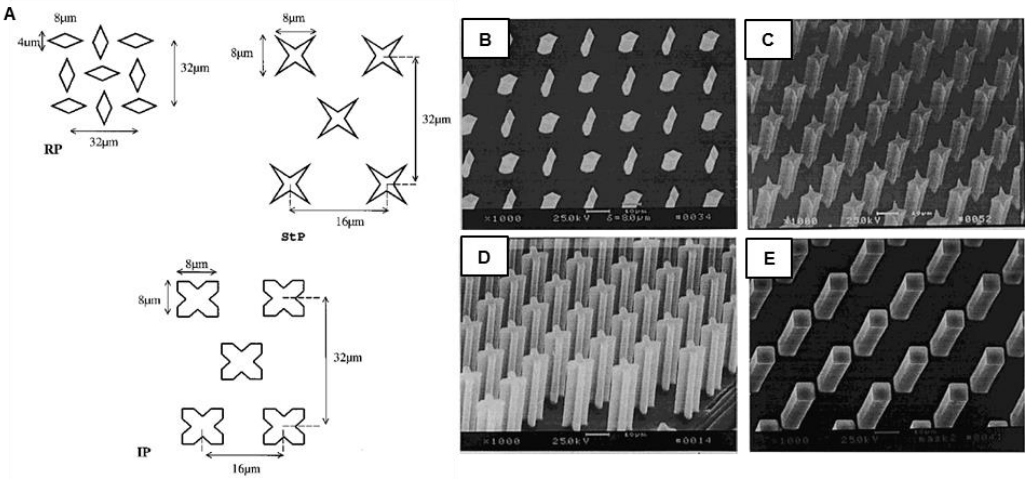

Figure 1.4. (A) Two dimensional representation of surfaces containing different geometry posts; RP (rhombus), StP (four armed star shaped posts), IP (Indented square posts). B-E) SEM images of different surfaces including RP (D), StP (C), IP (D) and hexagonally arrayed square posts (E) respectively. Reprinted with permission from (*Langmuir*, **2000**, *16*, 7777–7782), Copyright 2000, American Chemical Society.

the maximum length scale of roughness that conferred the superhydrophobicity was measured to be ~32 μm for the interface having square shaped posts (Figure 1.4E). Later, other research groups exploited this lithography technique for re-examining the impact of rationally organized topography on the water wettability,[43] and the controlled change in topography provided a basis for tailoring water wettability.[40]

1.5.1.2. Plasma Etching

Plasma etching is a dry etch technique in which reactive atoms or ions (oxygen, chlorine, fluorine) are generated in a gas discharge reaction.[44] Reactive ion etching makes use of the fact that ions are accelerated in the boundary layer between plasma and substrate with high

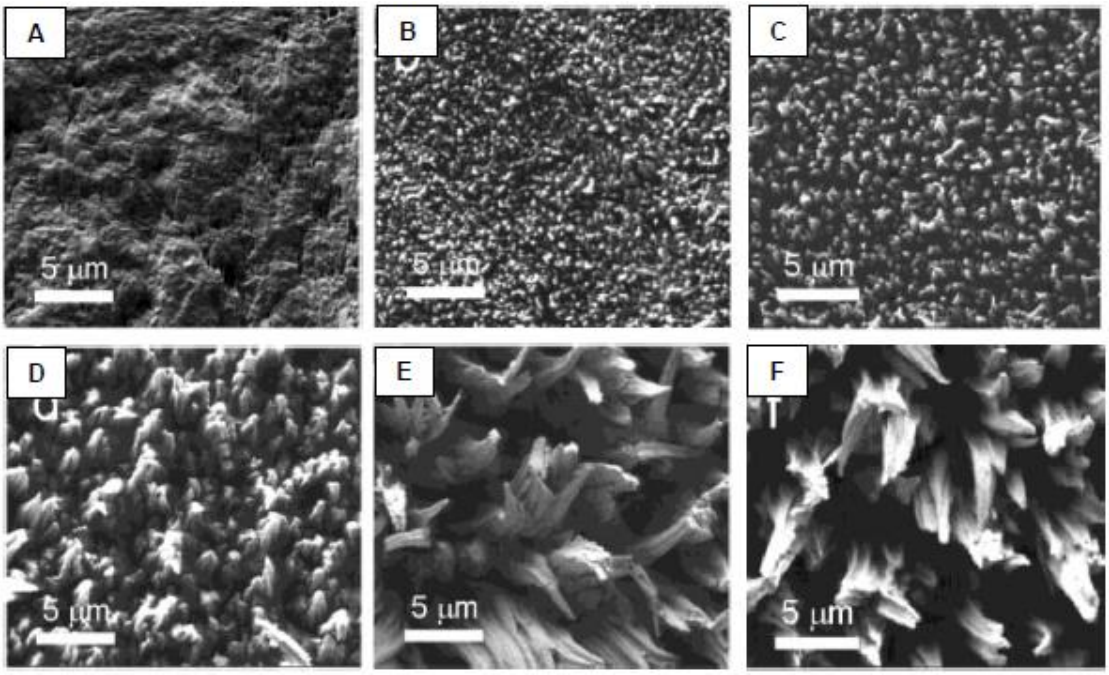

Figure 1.5. (A-F) SEM images of PTFE foils untreated A), treated with oxygen plasma for 60 secs (B), 120 secs, (C), 5 mins (D), 10 mins (E), and ammonia for 1 min (F). Reprinted with permission from (*J. Am. Chem. Soc.* **2003**, *125*, 3896−3900), Copyright 2003, American Chemical Society.

directivity and thus this process is able to create deep grooves with steep walls.[45] Plasma treatment of solid surface can cause a considerable change in the surface topography because of anisotropic etching of the top surface of the selected substrates.[46] Several reports have been published on the increase in wettability of Poly(tetrafluoroethylene) (PTFE) substrate on exposure to radio frequency (RF) oxygen plasma.[47−51] Minko *et al.*[49] have strategically exploited both oxygen and ammonia plasma treatment for developing hierarchical topography with two-level surface features on PTFE substrate as shown in Figures 1.5. The surface roughness was gradually increased with extending the duration of plasma etching, and eventually allowed to optimize the extreme water repellency. The oxygen plasma etched PTFE surface provided an appropriate surface topography for exhibiting water contact angle of 160º. Later, O_2 plasma etching of PTFE substrate was performed with different applied DC bias voltage and water wettability was examined. The high-power plasma treatment provided superhydrophobicity, whereas the low-power plasma treated PTFE interface failed to display extreme water repellency.[50]

Moreover, this plasma etching approach was extended to modify other polymeric substrates for adopting superhydrophobicity.[51] Both the poly(methyl methacrylate) (PMMA) and poly(ether ether ketone) (PEEK) substrates were exposed to O_2 plasma etching prior to depositing fluorocarbon (i.e.; C_4F_8). The physically deposited fluorocarbon provided essential low surface energy, where, the water droplet beaded with advancing contact angle above 150º and the contact angle hysteresis was noted below 5º. However, such interfaces are susceptible to compromise superhydrophobicity under severe physical challenges (i.e.; scratching, creasing etc.).

1.5.1.3. Templation

In nature, superhydrophobic property exists on various surfaces. Hence, approach for replicating the naturally existing surface is direct and facile method for synthesizing artificial superhydrophobic interface. The hierarchical topography of the lotus-leaf inspired surface is adopted by using this naturally existing featured interface as the template to mimic its embedded water wettability on poly(dimethylsiloxane) (PDMS, soft material) substrate.[52] During the replication of water wettability from lotus-leaf, the templation approach was associated with fabrication of negative template, and this negative template

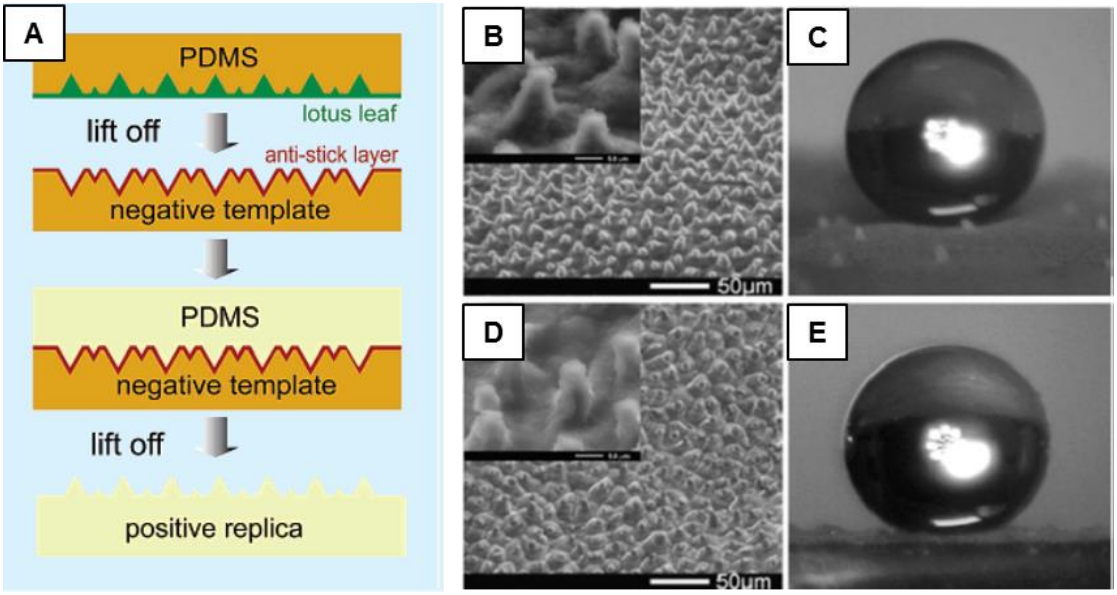

Figure 1.6. (A) Schematic illustration of the lotus leaf replication process and fabrication of superhydrophobic surface from the replica. B-E) SEM images and water contact angle images of lotus leaf (B, C) and the superhydrophobic PDMS (D, E) developed by templation of lotus leaf. Reprinted with permission from (*Langmuir*, **2005**, *21*, 8978−8981*)*, Copyright 2005, American Chemical Society.

allowed to replicate the topography and water wettability similar to the lotus leaf as shown in Figure 1.6B-E. Primarily, the casting of PDMS mold directly on the fresh lotus leaf, provided a negative template. A mono layer of trimethylchlorosiloxane (TCMS) was deposited on the negative replica to obtain a non-sticky interface on the top and thereafter, a second layer of PDMS was casted to obtain the positive replica of these features. In this way, the hierarchical surface topography of lotus leaf was directly transferred to the PDMS surface, and the electron microscopic images of both positive replica and the lotus leaf revealed the existence of the same surface morphology decorated with small papillate hills as shown in Figure 1.6B, D. As expected, the positive replica exhibited the similar anti-wetting property as that of lotus leaf (Figure 1.6C, E). Furthermore, the artificial superhydrophobicity was developed using a synthetic template, where anodic aluminium oxide (AAO) surface was used as a template.[53] The array of platinum nanofibers were developed by electrodeposition of platinum into the pores of AAO template followed by removal of template in the alkaline medium as shown in Figure 1.7. The synthesized platinum nanowires with "hills-and-valleys" topography exhibited superhydrophobicity after post modification with fluoroalkylsilane. The thin layer of low surface energy coating on the top of hierarchically featured interfaces is likely to compromise on exposure to practically relevant abrasive challenges.

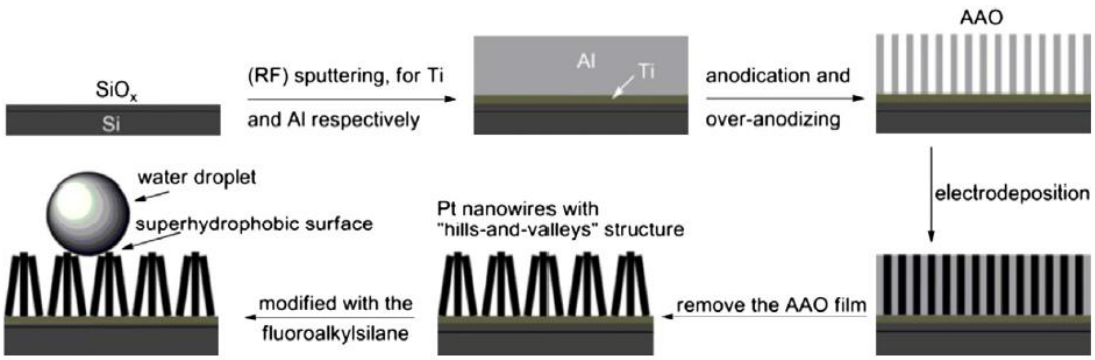

Figure 1.7. Schematic representation for preparing "hills-and-valley" structure made of Pt nanofiber. Such interfaces provided superhydrophobic after essential modification with fluoroalkylsilane. Reprinted with permission from (*Nanotechnology* **2008**, *19*, 55707−55711*)*, Copyright 2008, American Institute of Physics.

1.5.2. Bottom Up Approaches

The bottom-up approaches inherently allows to decorate large and complex substrates with appropriate hierarchical topography and essential chemical functionality, which confer the extreme water repellency. In the bottom-up approaches, small building blocks (nano/micro) colloidal particles, polymers, polyelectrolytes etc.) and chemical components are strategically integrated for developing rough interfaces that consisted of dual (nano/micro) scale features. Commonly used bottom-up approaches are briefly accounted with few examples in the following section;

1.5.2.1. Sol-gel Method

In sol-gel process, a precursor is converted into a glassy material via a series of hydrolysis and polycondensation reactions.[54] A large amount of solvent is associated in the network formation process and eventually the reaction solution is transformed to a gel material.[55] The sol can be applied either directly or combined with fillers such as micro and nanoparticles. The surface roughness can be controlled by varying the components in the reaction mixture. Various sol-gel methods have been used to develop superhydrophobic surfaces on various substrates including textiles and wood.[56–60] In earlier demonstrations, orthosilicates were mostly used for preparing silica sol based superhydrophobic coatings.[61]

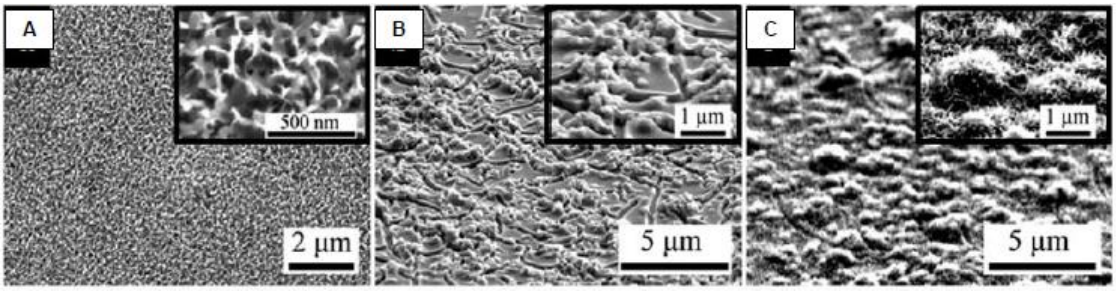

Figure 1.8. (A-C) SEM images of alumina gel films. A) Undoped film after immersion in boiling water. B-C) alumina nanoparticles doped films before (B) after immersion in boiling water (C). Reprinted with permission from (*Chem. Commun*. **2012**, *48*, 6824−6826*)*, Copyright 2012, The Royal Society.

In 2005, Shang *et al.*[59] have prepared an optically transparent superhydrophobic coatings by adopting sol-gel process. The appropriate hierarchical features were tailored through controlled regulation of hydrolysis and condensation reactions of various silica precursors. The selected substrates were decorated with such featured topography by dipping the substrates into the silica sols, and the post modification of the deposited coating with

tridecafluoro-1, 1, 2, 2-tetrahydrooctyldimethylchlorosilane (TFCS) provided extreme water repellency. The water droplet beaded on such coated interfaces with advancing water contact angle of 165º, and an optical transparency of above 90% was achieved for such superhydrophobic coating. Further, nonadhesive artificial superhydrophobicity was achieved using an alumina sol, where aluminum tri-sec-butoxide was used as a precursor for preparing the appropriate gel network.[60] The sol was doped with alumina nanoparticles (80 nm) for optimizing appropriate dual degree of roughness, the aggregation of nanoparticles provided micro-scale features. Further, a nanoscale roughness was achieved by immersing this interface in boiling water for 5 mins as shown in Figure 1.8C. The resultant surface presented a flower-like structure with nano-scale (20 to 50 nm) features, likely due to reaction between gel and boiling water. Finally, a self-assembly of fluoroalkyl phosphonic acid provided essential low surface energy on top of this hierarchical interface for obtaining the nonadhesive artificial superhydrophobicity.

1.5.2.2. Layer by Layer Deposition (LBL)

Layer-by-Layer (LBL) deposition process was first adopted in developing multilayers of colloidal particles,[62] and then this facile approach was extended for preparing multilayers of polyelectrolytes.[63–65] In this coating process, two oppositely charged polyelectrolytes are alternately deposited on selected substrates by taking advantage of the electrostatic

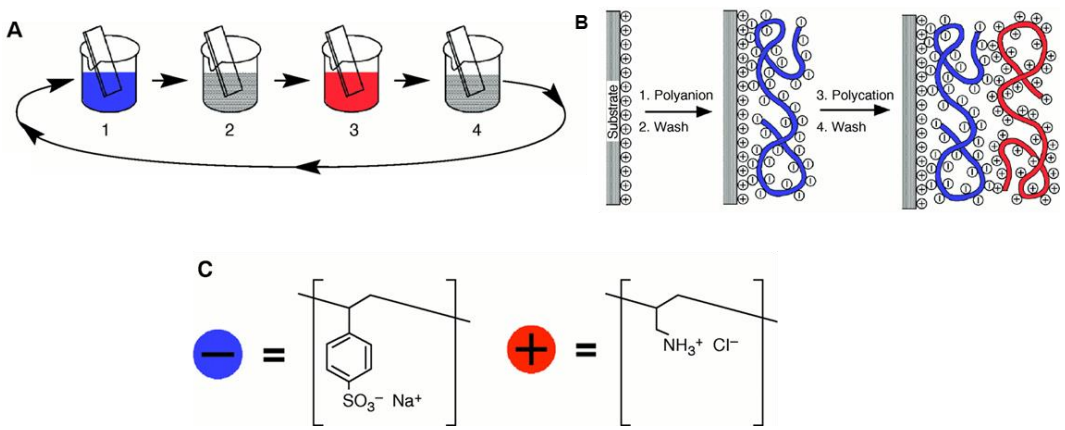

Figure 1.9. (A) Schematic of film deposition process. Step 1 and 3 represents the deposition of polyanion and polycation, step 2 and 4 are washing steps. B) Schematic representation of first two adsorption steps. C) Chemical structure of two polyions. Reprinted with permission from (*Science* **1997**, *277*, 1232−1237*)*, Copyright 1997, American Association for the Advancement of Science.

interactions (Figure 1.9).[65] Loosely bound or excess polyelectrolytes were removed by rinsing the multilayers at regular intervals during the LbL deposition process. In addition to electrostatic interaction, hydrogen bonding and covalent bondings are also strategically exploited in developing different functional polymeric multilayers. The LbL deposition approach was further extended in fabrication of multilayers of different nanomaterials (i.e., clay, graphene, nanotube etc.).[66−72] This coating approach provided facile basis for controlling thickness and topography on various substrates, irrespective of the dimensions and geometry of selected substrates.[73,74] Zhai *et al.*[75] have introduced multilayers of polyallylamine hydrochloride (PAH) and polyacrylic acid (PAA) for preparing artificial superhydrophobic coating, where the multilayers of polymer provided honeycomb like structures on strategic acidic treatment as shown in Figure 1.10B. These featured multilayers were further decorated with silica nano particles for adopting essential hierarchical topography. Next, the semi fluorinated silane molecules were deposited on this

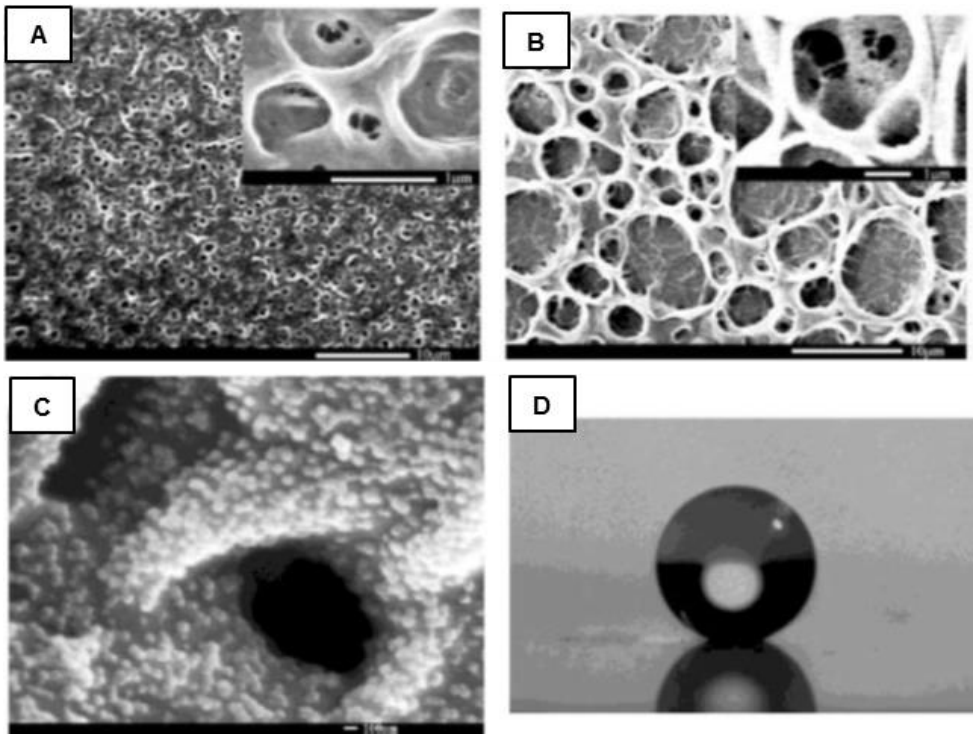

Figure 1.10. (A-C) SEM images of $(PAH/PAA)_{100}$ films after single acid (A) and combined acid (B) treatments and after deposition of silica nanoparticles (C). D) Beaded water droplet on the multilayer film after post chemical modification (D). Reprinted with permission from (*Nano Lett.* **2004**, *4*, 1349−1353), Copyright 2004, American Chemical Society.

hierarchically featured multilayers for achieving the artificial superhydrophobicity as shown in Figure 1.10D. Later, various other nanomaterials[76] were associated through layer-by-layer deposition process for successfully developing the artificial superhydrophobicity. Even though, this simple synthetic approach is efficient in tailoring morphology and allowed to coat various types of substrates, but this deposition approach is associated with laborious multi step process and mostly chemically weak interactions and bondings are associated for synthesis of superhydrophobic interfaces.

1.5.2.3. Chemical Vapour Deposition (CVD)

Chemical and physical vapour depositions (CVD, PVD) are other types of chemical deposition techniques in which gaseous reactants can be deposited onto a substrate to form

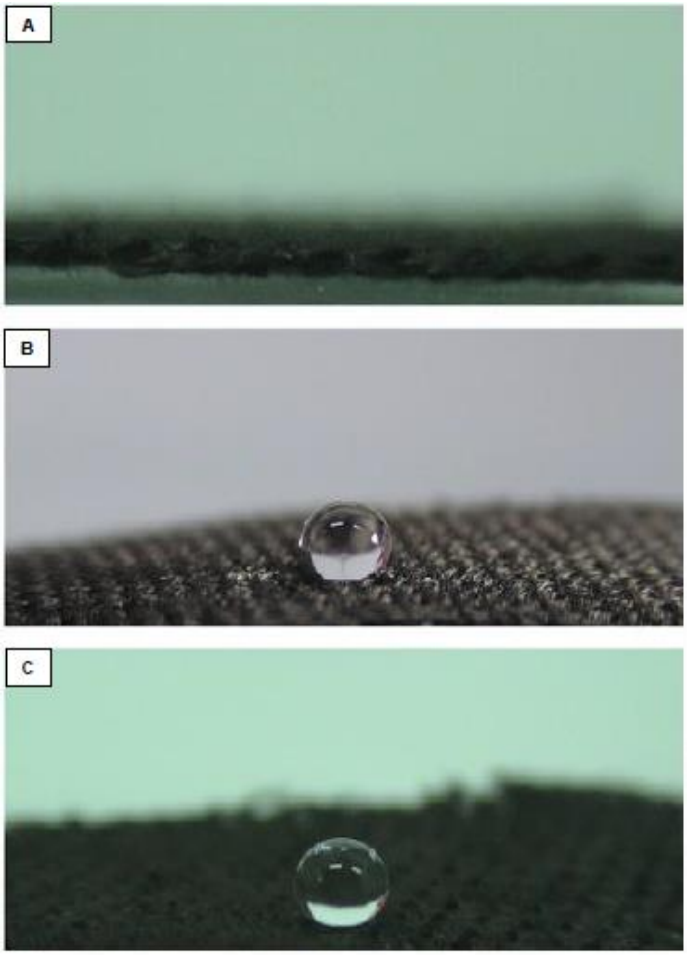

Figure 1.11. (A-C) Digital images of carbon fabric developed through chemical vapor deposition. Untreated cotton fabric (A), fluorinated carbon fabric (B), fluorinated carbon fabric with dual scale of roughness (C). Reprinted with permission from (*Carbon* **2008**, *46*, 1218−1224), Copyright 2008, Elsevier.

a non-volatile solid layer with desired topography by appropriate selection of precursors. Vapour deposition approach is often preferred for optimizing essential low surface energy on the hierarchical featured interfaces for adopting superhydrophobicity.[77–80] As for example, Hseish *et al.*[81] introduced a catalytic chemical vapour deposition (CCVD) for decorating carbon fibers with carbon nano tubes (CNTs) and subsequent post-fluorination of the hierarchically featured interface resulted in superhydrophobic coating on the selected substrate as is shown in Figure 1.11C. Such approach was further extended for developing thin superhydrophobic coatings on various other objects.[82–83]

1.5.2.4. Electrospinning

Electrospinning is recently emerging as one of the leading method for fabricating continuous polymeric fibers with various diameters—starting from few nanometers to tens

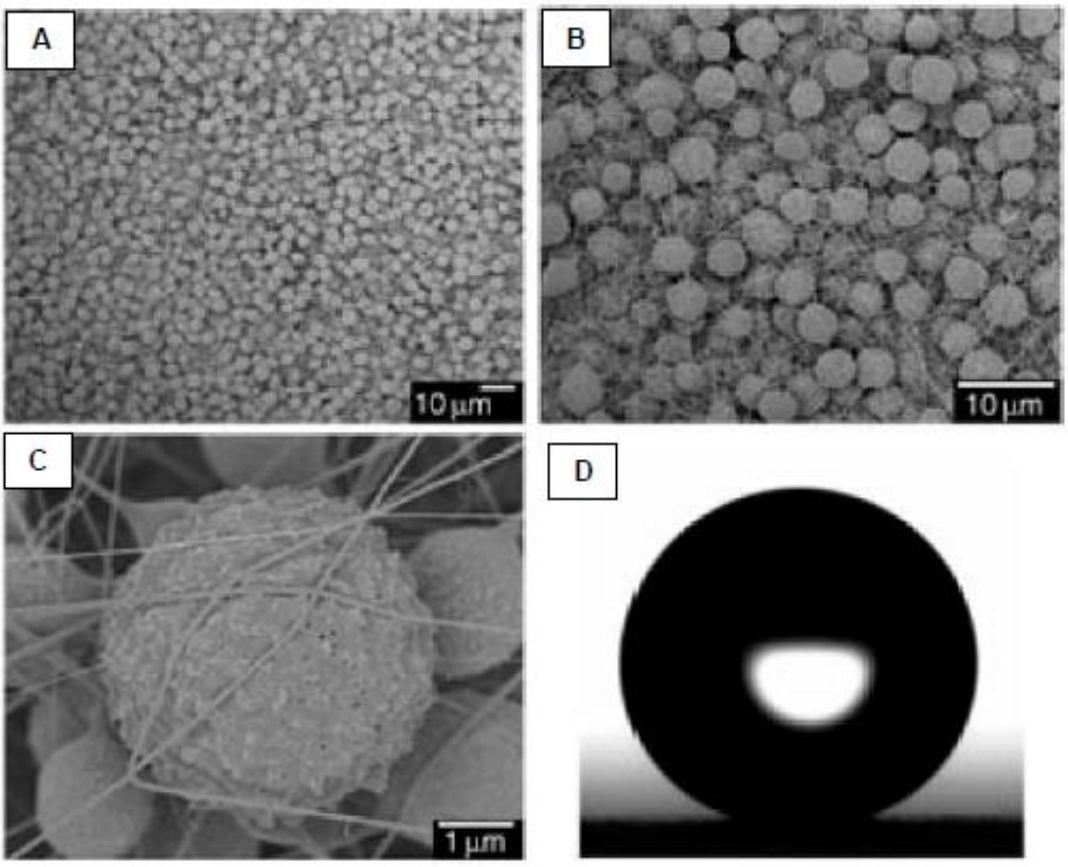

Figure 1.12. (A-C) SEM images of porous microsphere/nanofiber composite film (PMNCF) of polystyrene in different magnifications; D) Contact angle image of beaded water droplet on PMNCF. Reprinted with permission from (*Angew. Chem. Int. Ed.* **2004**, *43*, 4338–4341*)*, Copyright 2004, Wiley-VCH.

of micrometers, and such approach is further extended for tailoring hierarchical topography for adopting superhydrophobicity. In a seminal report, Jiang *et al.*[84] exploited electro hydrodynamic method for synthesizing porous microsphere/nanofiber composite film (PMNCF) from solution of polystyrene (PS, 7 wt %) in Dimethylformamide. The fabricated polystyrene fibers consisting of porous microspheres and nanofibers exhibiting excellent anti-wetting property as shown in Figure 1.12D. Later, this inherently simple approach was extended by various research groups for developing artificial superhydrophobic interfaces using various other polymers.[85–87]

1.6. Applications of Superhydrophobicity

According to the recent statistics of ISI web of Science,[88] the research publications in the field of superhydrophobicity has tremendously increased from hundreds to thousands per annum over the last decade (Figure 1.13A). This significant increase in the research is due to their ample number of practically relevant and potential applications for the real world scenario (Figure 1.13B). Some of the important applications are discussed in the following section.

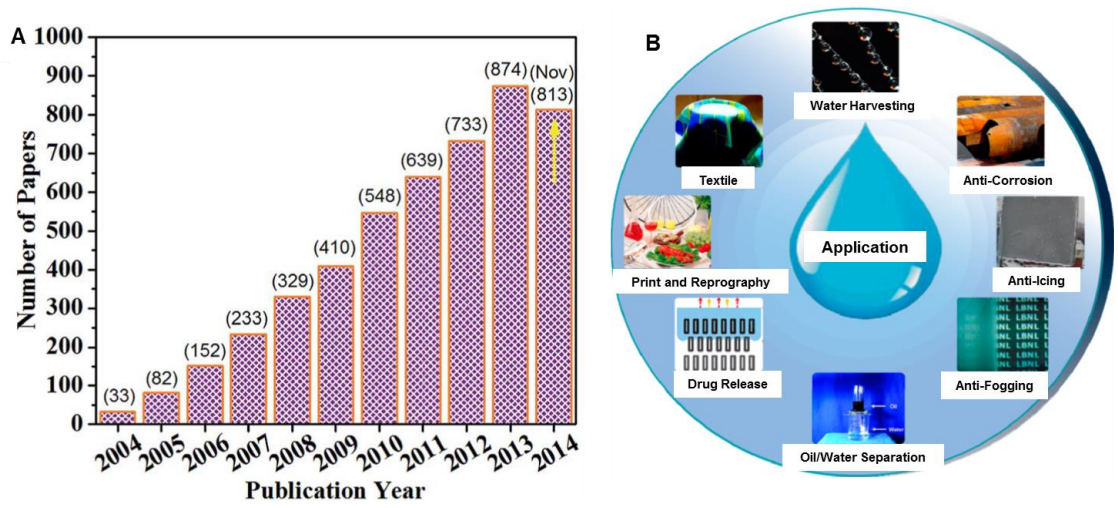

Figure 1.13. (A) Plot displaying the number of papers published on superhydrophobic surfaces (Source: ISI Web of Science). B) Schematic illustration of the representative applications of superhydrophobic surfaces. Reprinted with permission from (*J. Mater. Chem. A* 2015, *3*, 3224–3251*)*, Copyright 2015, The Royal Society (A). Reprinted with permission from (*Chem. Rev.* **2015**, *115*, 8230−8293*)*, Copyright 2015, American Chemical Society (B).

Inspired from the self-cleaning phenomenon of lotus leaf, plenty of research has been devoted in fabricating self-cleaning materials.[89–92] For instance, Wang *et al.*[89] reported a transparent and abrasion resistant superhydrophobic coating with self-cleaning ability in air and under oil. Further, this extreme water repellency property was extended for developing corrosion resistant coating on metals and metal alloys for addressing the massive economic loss due to the corrosion related challenges. As for example, Jiang *et al.*[94] decorated the Mg alloy with durable superhydrophobicity for the successful demonstration of promising anticorrosion performance. Later, many other research groups have extended this approach for addressing the corrosion related challenges.[95–101] The ice accumulation on solid surfaces is a well-known phenomenon that causes grave damages at the outdoor settings. For instance, the accumulation of ice on aircraft limits the wind flow upto 50% leading to flight accidents and an ice accumulation on electric transmission lines threatening the safe operation of electric railways and networks.[102,103] Moreover, ice formation on the roads can disrupt traffic and bring inconvenience in daily life. Numerous methods have been developed to prevent ice formation such as an outer insulating layer for high cold highways.[104–106] Recent demonstrations in the literature revealed that the superhydrophobic interfaces can effectively prevent the ice formation. The presence of entrapped air layer in the superhydrophobic surfaces could provide the thermal insulation and hence, delays the freezing process on superhydrophobic surfaces.[107–109] Water pollution causes due to frequent oil spill accidents and continuous discharge of oil contaminated wastewater from oil-refinery plants imposed severe worldwide challenges.[110–114] For instance, the oil spill accident that occurred in the Gulf of Mexico in 2010 is considered as the largest oil spill accident in the history of petroleum industry and caused severe damage to the marine eco-system. Hence, the oil/water separation is an important emerging subject of interest in both academic and industrial research. Conventional measures, including chemical dispersants, in situ burning, skimming etc[115,116] for removal of oil spills are either associated with secondary pollutions or involved with highly energy consuming process. Therefore, the development of eco-friendly and energy efficient approach for separating the oil/water mixture is highly essential in the current context. The lotus-leaf inspired superhydrophobic interfaces are inherently superoleophilic, and allowed to spread oil and oily liquids instantly and selectively. In 2004, Feng *et al.*[118]

unprecedentedly exploited this principle in gravity driven selective filtration of oil from oil/water mixture. A stainless steel mesh was first decorated with lotus leaf-inspired superhydrophobicity (Figure 1.14A-F). The water droplet beaded on the superhydrophobic mesh with contact angle of 156.2º, while oil passed immediately through the membrane as shown in Figure 1.14E, F. This principle was successfully used for gravity driven filtration based separation of oil/oily contaminates from oil/water mixture. Later, this

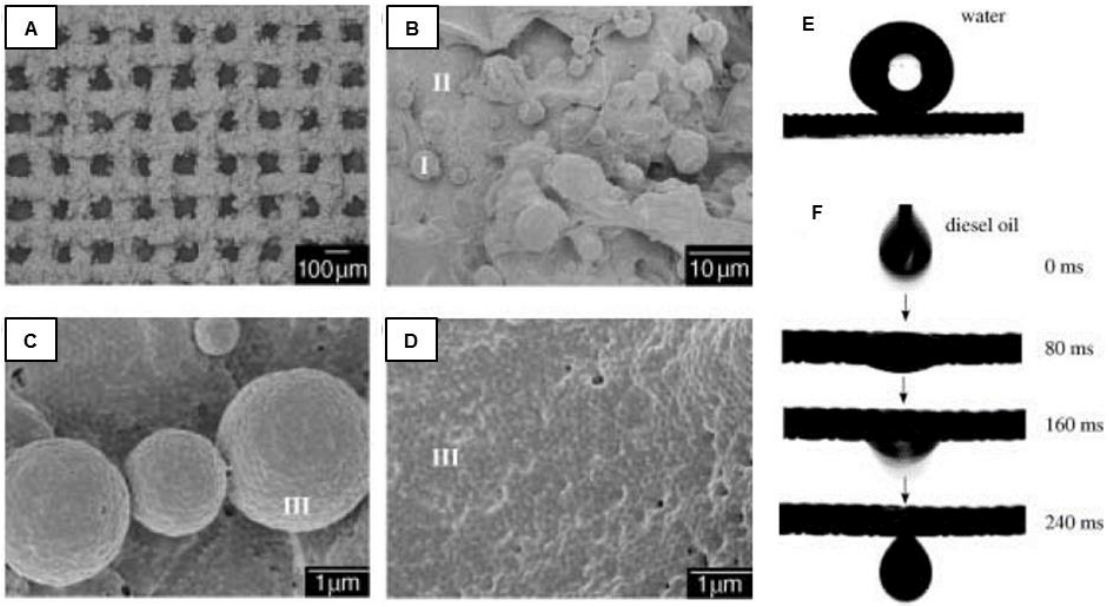

Figure 1.14. (A-D) SEM images of coated mesh with lower (A, B) and higher (C, D) magnifications. E-F) shape of water (E) and oil (F) droplet on the superhydrophobic mesh. Reprinted with permission from (*Angew. Chem. Int. Ed.* **2004**, *43*, 2012 –2014*)*, Copyright 2004, Wiley-VCH.

superhydrophobicity was extended for selective absorption based oil/water separation, where porous superhydrophobic materials were used to collect the oil spills, selectively, from aqueous phase.[119–120] However, the demonstration of oil/water separation in the practically relevant severe settings is rare in the literature, likely due to poor durability of the artificial superhydrophobicity under challenging scenarios.

Further, the meta-stable trapped air in the extremely water repellent interfaces provides facile basis for long-term release of small bioactive molecules.[121–123] Even, such superhydrophobic interfaces are strategically exploited in developing anti-bioadhesion interfaces.[124–126] Furthermore, the patterned superhydrophobic interfaces were exploited in

various bioengineering applications, water harvesting and synthesis of open microfluidic devices[127–129] etc.

1.7. Approaches for Synthesizing Durable Superhydrophobicity

Superhydrophobic surfaces have received enormous attention from the last couple of decades due to their string of applications including self-cleaning, drag reduction, anti-corrosion, anti-icing, anti-fogging, oil/water separation[130–134] etc. However, the poor durability of many of these artificially synthesized superhydrophobic interfaces is emerged as a major challenge for their practical applications at the outdoor settings, as the slight perturbation in the chemistry or topography is believed to causes severe or permanent damage to the synthesized extreme water repellent property.[135,136] Most of the superhydrophobic materials developed through top down and bottom up approaches are associated with weak or delicate chemistries, including functionalization with various analogues of silane,[137–139] metal thiol bonds,[140,141] metal ion interaction[142,143] etc., for optimization of low surface energy on the top of hierarchical features. The metal-thiol

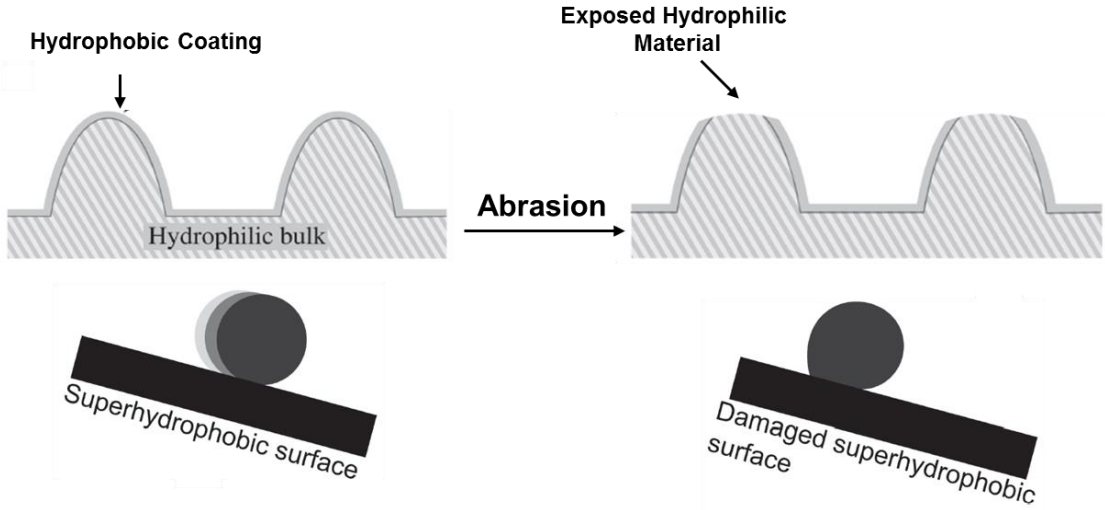

Figure 1.15. Schematic representation displaying the coating on a roughness pattern may get easily worn off, and hydrophilic bulk material will be exposed as a result. Reprinted with permission from (*Adv. Mater.* **2011**, *23*, 673–678*)*, Copyright 2011, Wiley-VCH.

bonds and metal-ion interactions are generally susceptible to damage under harsh chemical conditions (extremes of pH, river and sea water) and silane bonding is known to labile under prolonged UV exposure.[144] Moreover, the optimized low surface energy nano-scale

coating on the top of hierarchical features are physically removed away during exposures to severe physical abrasion processes and the underneath hydrophilic bulk is exposed and eventually the embedded superhydrophobicity is compromised as shown in Figure 1.15. In some cases, the appropriate hierarchical features made of brittle metal oxides are likely to get damaged under applied pressure or scratching process and thus, the use of such prospective interfaces are limited for practical applications. In nature, superhydrophobic surfaces such as lotus leaf maintain their anti-wettability by regenerating the epiticular wax layer after it is damaged, but it is difficult for artificially fabricated surfaces to follow the nature's way when the property is damaged. Nevertheless, over the time, various strategies were adopted for synthesizing highly durable superhydrophobic materials, some of those important approaches are briefly accounted in the following sections;

1.7.1. Post Repairable Approach

Synthetic interfaces having roughness at two length scales and low surface energy thin coating on top, ensure a stable Cassie state. However, physical/chemical abrasions are likely to damage both the essential low surface energy coating and appropriate hierarchical features that confer superhydrophobicity. In post repairable approach, the hierarchical structures and essential low surface energy coatings are regenerated on the damaged areas and hence, superhydrophobicity is restored.[145,146] For example, Zhu *et al.*[145] developed the mechanically durable and easily repairable superhydrophobic surface, where polymer/metal composite was prepared with hot (180°C) pressing (4 MPa) approach, and then Ag deposition provided appropriate hierarchical topography and surface fluorination was adopted to optimize the essential low surface energy in the synthesized material. The composite surface displays mechanical durability and rough surface textures after abrasion test. After a long abrasion time, the surface became smooth with decreased concentration of fluorine and thus, superhydrophobicity was lost. However, after repeating the Ag deposition and surface fluorination process, the material regained its superhydrophobicity with advancing contact angle of 163º as is shown in Figure 1.16C. Meanwhile, Zhu *et al.*[146] also fabricated the regenerable superhydrophobic coating by spraying the metal alkylcarboxylate dispersion. The dispersion is prepared by the reaction of metal salt and alkylcarboxyl acid in ethanol solution. The superhydrophobic performance can be easily repaired by spraying the dispersion when the features and essential chemistry are damaged.

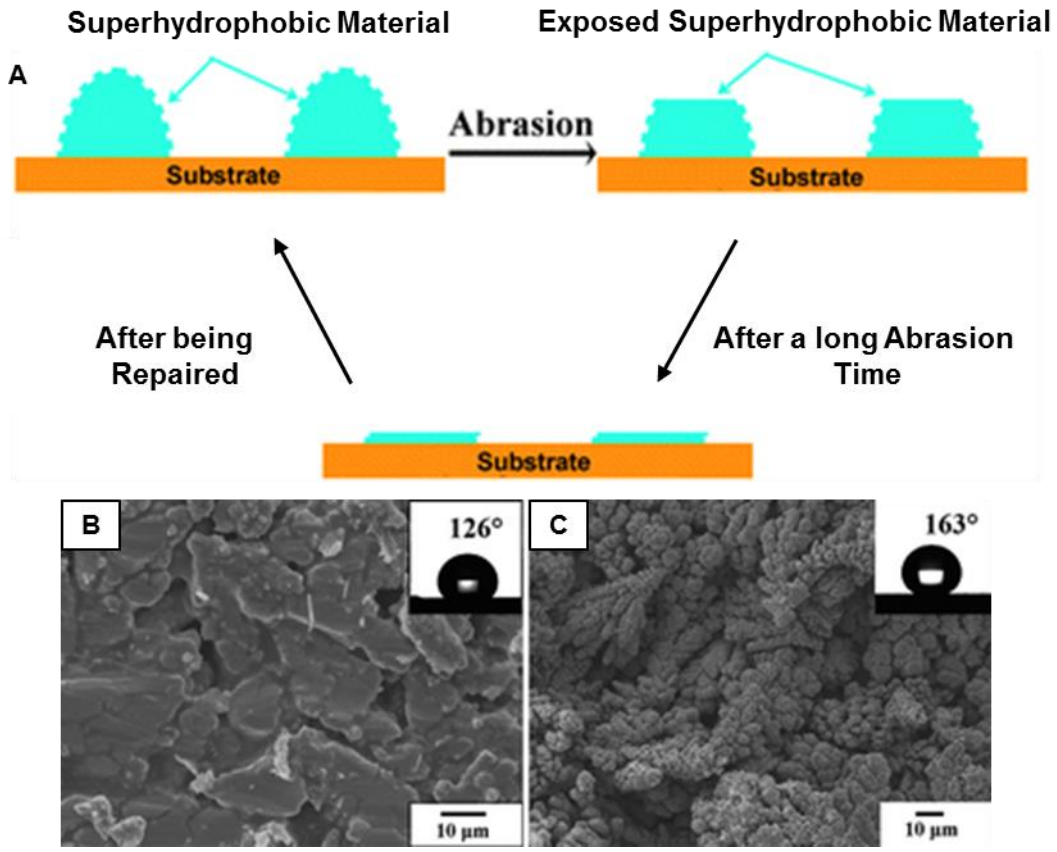

Figure 1.16. (A) Schematic illustration of regeneration of superhydrophobicity after abrasion of topography and chemical functionality. B-C) FESEM images of composite after long abrasion (B) and after repairing the damage (C). Reprinted with permission from (*J. Mater. Chem.* **2011**, *21*, 15793–15797), Copyright 2011, The Royal Society.

However, in general, the post repairable approach is less realistic for practical applications, as the regeneration of damaged features and chemistry would be difficult on site having in diverse and severe practical settings.

1.7.2. Self-healing Approach

Naturally existing superhydrophobicity that is present in plant leaves and insect wings sustain various damages and their water repelling property remained unperturbed due to continuous and natural healing tendency of the damaged topography and chemistry. Inspired from this fact, different designs were introduced for developing self-healing artificial superhydrophobicity. For instance, Li *et al.*[147] developed a superhydrophobic surface with a self-healing ability, where polymeric multilayers was constructed by adopting the electrostatic LbL deposition of a complex of poly(allylamine hydrochloride)

(PAH) and sulfonated poly(ether ether ketone) (SPEEK) and polyacrylic acid (PAA). This sequential deposition cycle was repeated for more than 60 times to obtain hierarchically featured and porous polymeric multilayers $(PAH\text{-}SPEEK/PAA)_{60.5}$. The coating was rendered superhydrophobic after the chemical vapour deposition (CVD) of 1H, 1H, 2H, 2H-perfluorooctyltriethoxysilane (POTS) at 120ºC for 3 hours. The deposition of POTS was strategically kept in excess in this porous polymeric multilayers for achieving the self-healing of extreme water repellency in the chemically damaged interface. To demonstrate the self-healing ability, the superhydrophobic interface was exposed to oxygen (O_2) plasma for decomposing the low-surface-energy POTS layer, and eventually the multilayers became hydrophilic. However, this same interface restored the superhydrophobicity after keeping this damaged multilayers in humid condition, where the humidity triggered migration of preserved healing agent—fluoroalkylsilane from bulk of the coating to the

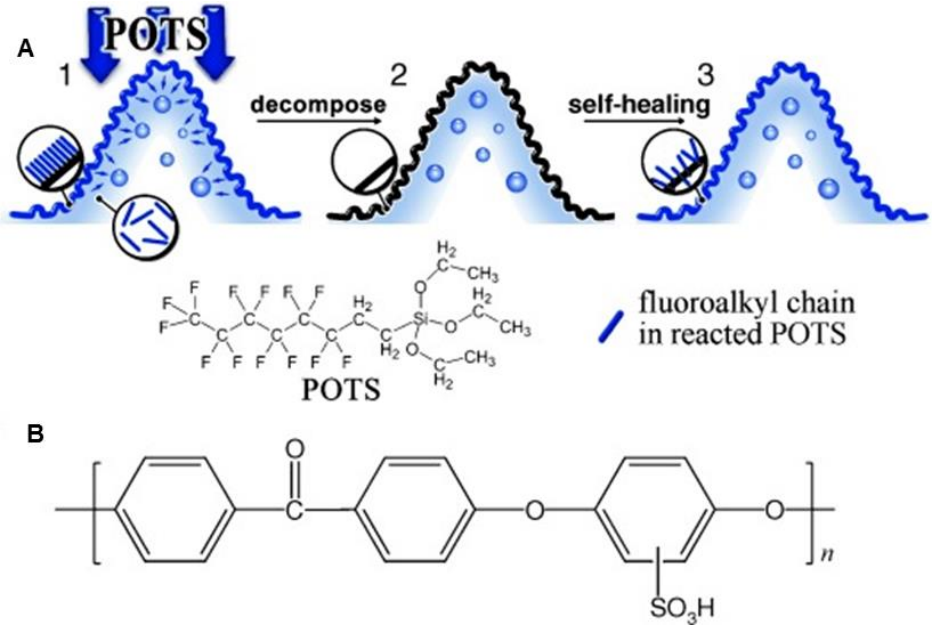

Figure 1.17. (A) The schematic illustrating the working principle of self-healing of artificial superhydrophobicity, where 1) a porous polymer multilayers coating with micro and nanoscaled hierarchical structures can preserve an excess of healing agent fluoroalkylsilane (POTS) in the bulk of the coating; 2) the top fluoroalkylsilane layer is decomposed under oxygen plasma treatment and the coating loses its superhydrophobicity; 3) the preserved healing agents migrated to the damaged interface under humid environment and heal the superhydrophobicity. B) Chemical structure of sulfonated poly-(ether ether ketone) (SPEEK), one of the key component in the design of self-healing superhydrophobic interface. Reprinted with permission from (*Angew. Chem. Int. Ed*. **2010**, *49*, 6129–6133*)*, Copyright 2010, Wiley-VCH.

damaged interface was reoptimized the essential low surface energy as shown in Figure 1.17. This damage/healing cycle was successfully conducted for 6 times.

Furthermore, various other reports of self-healing[148–150] were introduced recently, where the damaged water wettability can be healed with the aid of humidity, acidic water and elevated temperature. However, limited healing cycles due to gradual loss of preserved low surface energy molecules, difficulties in the maintenance of appropriate stimuli and the stability of physically deposited healing agents on top of the interface are likely to impose a serious durability concern for practical utility of the synthesized superhydrophobic material under severe settings.

1.7.3. Bulk Superhydrophobicity

In addition to the above mentioned approaches, recently a new approach has been developed known as bulk superhydrophobicity, where the anti-wetting property is not limited to the surface of the material but is present three dimensionally (*i.e.* both surface and bulk). Thus, the anti-wetting property remains intact even after physical removal of the top interface of the material. The concept of bulk superhydrophobic surfaces is a simple approach for encountering the existing challenges related to the durability of artificial superhydrophobicity. Fundamentally, bulk superhydrophobic approach is different from the conventional thin and 'surface-only' superhydrophobicity, the bulk

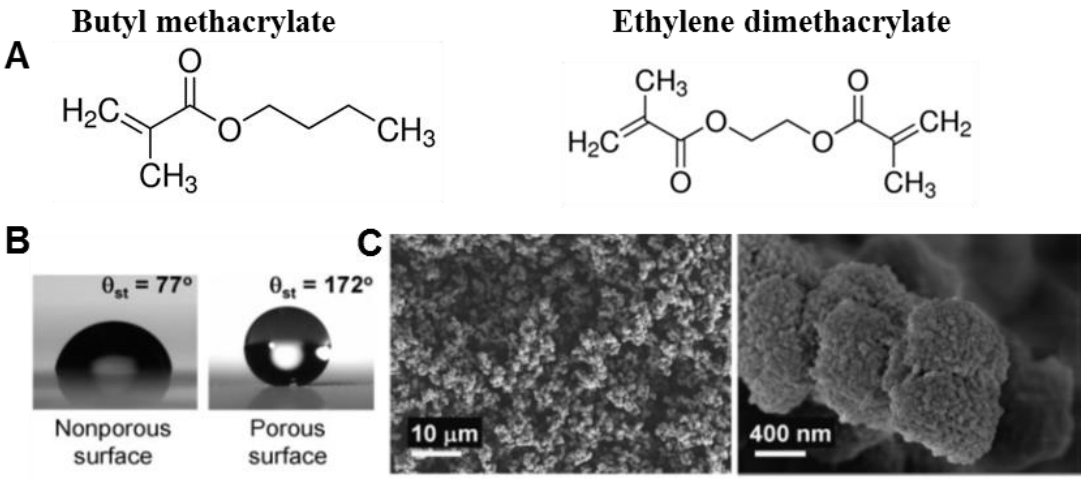

Figure 1.18 (A) Chemical structure of butyl methacrylate and ethylene dimethacrylate. B) Beaded water droplet on smooth and porous polymer layers. C) FESEM images of porous polymeric material prepared by copolymerization of butyl methacrylate and ethylene dimethacrylate. Reprinted with permission from (*Adv. Funct. Mater.* **2009**, *19*, 1993–1998*)*, Copyright 2009, Wiley-VCH.

superhydrophobicity demands appropriate optimization of hierarchical topography and essential low surface energy—three dimensionally, including the top surface and the interiors, which is highly challenging to achieve. The evolution of promising bulk superhydrophobic property has progressed recently with limited examples. For instance, Levkin *et al.*[151] developed a bulk superhydrophobic coating by copolymerization of two monomers followed by phase separation. The copolymerization of butyl methacrylate and ethylene dimethacrylate in the solvent mixture of cyclohexanol and 1-decanol, provided highly porous polymeric material that displayed superhydrophobicity with θ_{adv} and θ_{rec} of 174.8º and 171.8º respectively as is shown in Figure 1.18. For examining the existence of bulk superhydrophobicity, the top surface of the material was physically abraded—following standard adhesive tape peeling test, where the newly exposed interior of the porous polymeric material continued to display superhydrophobicity, thus affirming the existence of bulk superhydrophobicity. Later, Vollmer *et al.*[152] introduced an optically transparent and bulk superomniphobicity (repel both oil and water simultaneously in air), where the candle soot was used as a porous template for achieving three dimensional hierarchical topography. A coating of silica shell was deposited on the candle soot using catalysed chemical vapour deposition of tetraethoxysilane. Later, the silica coated soot was calcinated at 600ºC for two hours, and subsequently, semifluorinated silane was deposited by adopting CVD process for developing optically transparent superhydrophobicity and superoleophobicity. The interior of the synthesized coating is also capable of displaying extreme water repellency. Next, covalent LbL and electrospinning deposition approaches were adopted for developing bulk superhydrophobicity.[121–123] However, in general most of these existing approaches are either associated with tedious/complex fabrication process or associated with expensive chemicals that have adverse effect on health and environment.[153] Therefore, this area of research requires further development for synthesizing such inherently durable materials that survives under various severe settings,[122] following facile and scalable chemical approach. In that context, Michael addition reaction between acrylate and amine groups at ambient conditions recently provided simple basis to develop various functional materials. Some of the strategic uses of this chemical approach is accounted in the following section.

1.8. Michael Addition Reaction in Synthesis of Various Functional Materials

The Michael addition reaction named after 'Arthur Michael' also known as conjugate addition reaction is a facile chemical reaction between nucleophiles and an activated olefins in which nucleophile adds across a carbon-carbon multiple bond.[154] More specifically Michael addition reaction is a conjugate 1, 4-addition reaction in which nucleophile attacks

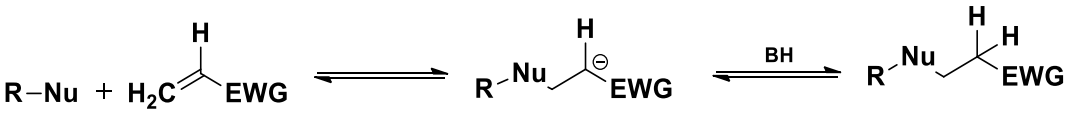

Figure 1.19. Schematic representation of Michael addition reaction

on β-carbon of α, β unsaturated carbonyl group resulting in a negatively charged enolate ion and subsequently forms the product by de-protonating the catalyst (Figure 1.19). Though, Michael addition reaction is generally considered the addition of enolate nucleophiles to activated olefins, a wide range of other functional moieties possesses sufficient nucleophilicity to act as Michael donors.[155] Reactions involving non-enolate nucleophiles such as amines, thiols and phosphines also typically take part in Michael addition reactions. This facile approach to generate C-C, C-N, C-O, C-S etc. is being used for the synthesis of small organic molecules for over hundreds of years.[156–159] Depending on the selection of reactants, Michael addition reactions is further categorized into oxa-Michael reactions,[160] aza-Michael reactions,[161] thiol-Michael reactions[162] all of which have been exploited over the years in organic synthesis and material science. Here, the strategic uses of 1, 4-conjugate addition reaction between amine and acrylate groups instead of oxa-Michael reactions,[160] aza-Michael reactions,[161] thiol-Michael reactions in developing various functional materials are briefly discussed;

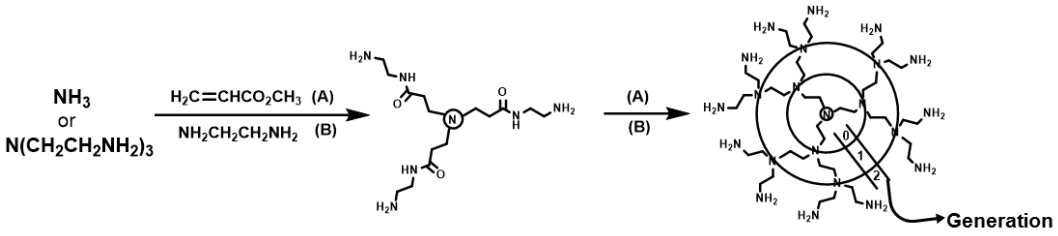

Figure 1.20. Synthesis of PAMAM dendrimer through alternate Michael addition reaction and Amidation.

Dendrimers are branched macromolecules, typically symmetric around the core and adopts a spherical three dimensional morphology. Michael addition reaction between amine and

acrylate groups are successfully exploited for synthesising dendrimers at mild reaction conditions. Tomalia *et al.*[163] shows the dendrimeric synthesis of poly (amido amine) (PAMAM) through the alternating Michael addition reaction of methyl acrylate with primary amines as shown in Figure 1.20. The PAMAM dendrimers are known as effective gene transfection agents due to the presence of large number of terminal amine groups for

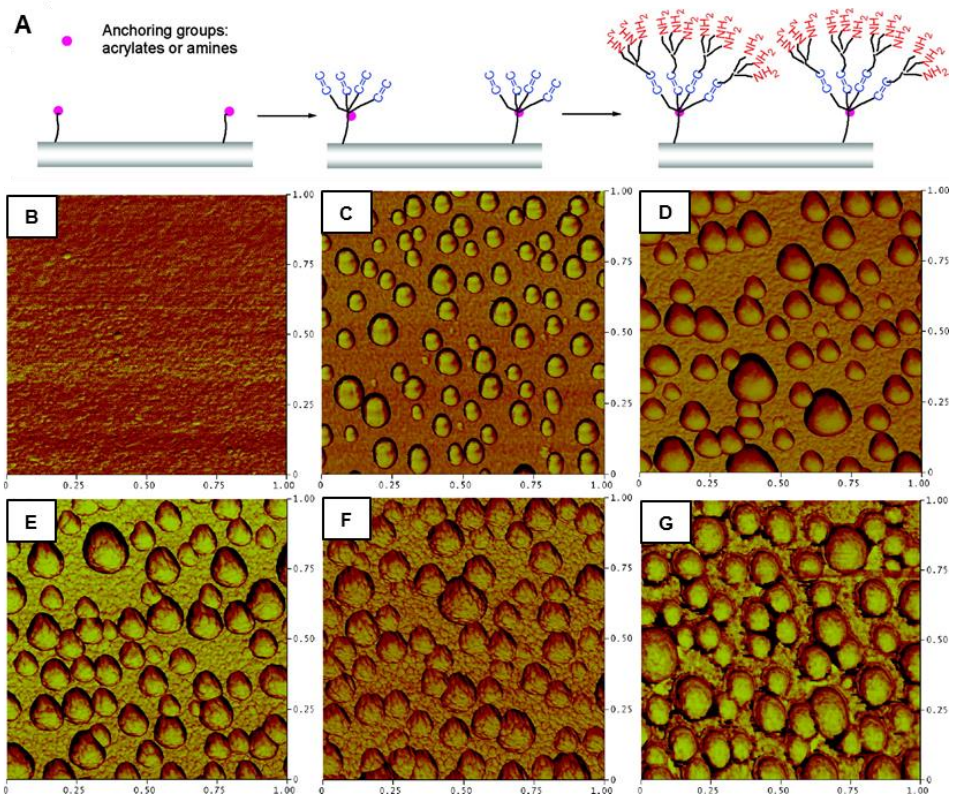

Figure 1.21. (A) Schematic illustration of hyperbranched polyester amine. B-G) AFM images of SU-8 surface at different surface functionalization stages including bare SU-8 surface (B), nano-cranberries (C), nano-strawberries (E), nano-raspberries (F), nano-pineapples (G) respectively on SU-8 surface. (Scale bar-1µm×1µm). Reprinted with permission from (*Chem. Mater.* **2009**, *21*, 476−483*)*, Copyright 2009, American Chemical Society.

complexation with negatively charged DNA phosphate backbone.[164] Further, such facile chemical approach was successfully extended for developing bio-conjugates, hydrogel and amplification of functional groups etc, for various relevant applications.[165−174]

In the recent past, Michael addition reaction was explored by Ford *et al.*[175] for developing polymeric coatings with various nano-structures, where branched poly (ethyleneimine) (BPEI) and small molecules (having multiple acrylate functionalities) were consecutively

deposited by adopting covalent LbL coating process as shown in Figure 1.21A-G. Later, Lynn *et al.*[176] extended this covalent LbL deposition of BPEI and dipentaerythritol penta-acrylate for 80 cycles to achieve thick (750 nm) and porous 'chemically reactive' polymeric multilayers. The developed multilayers consisted of residual acrylate functionalities that allowed to post-modify the porous multilayers with amine containing small molecules. After decylamine treatment, the multilayer coating became highly hydrophobic with contact angle of 138º as shown in Figure 1.22G. There are further possibilities for synthesizing durable superhydrophobic material through appropriate use of this 1, 4-conjugate addition reaction. In this thesis work, I have unprecedently extended this chemical approach in synthesizing durable superhydrophobic interfaces—following simple synthetic procedures.

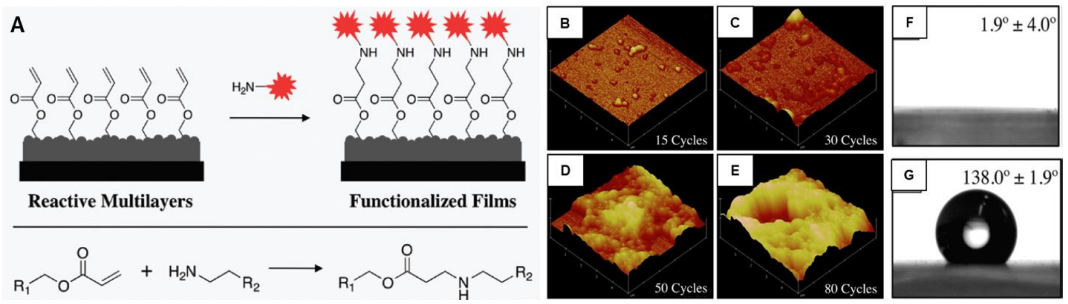

Figure 1.22. (A) Schematic illustration of reactive multilayer and its post functionalization with amine containing small molecules. B-E) AFM images of PEI/5-Ac films fabricated on silicon substrate after 15 (B), 30 (C), 50 (D) and 80 (E) dipping cycles. F-G) Contact angle images of beaded water droplet on film after 80 dipping cycles (after post modification with glucamine (F) and decylamine (G) respectively. Reprinted with permission from (*Biomacromolecules* **2012**, *13*, 1523−1532*)*, Copyright 2012, American Chemical Society.

1.9. Objectives and Motivation

Conventional thin superhydrophobic interface that is achieved through optimization of essential chemistry on top of the hierarchical featured interfaces—associating delicate chemistry is less appropriate for sustaining various severe challenges at practical settings. In the recent past, few approaches including mechanically durable, post repairable, self-healing etc., provided more durable artificial superhydrophobicity. However, in that context, bulk superhydrophobic materials that displays super-water-wettability both on the top interface as well as in the interiors, are most promising for applications under various severe settings. The bulk superhydrophobic materials are inherently loaded with more metastable trapped air, in comparison to the conventional superhydrophobic thin interface. Moreover, the rate of infiltration of water in the bulk superhydrophobic material is very sluggish as confirmed by X-ray computed tomography study.[177] Additionally, bulk superhydrophobicity is inherently capable of withstanding range of physical/chemical challenges without compromising the embedded superhydrophobicity, even after physical erosion of top of the synthesized material.[150–152] However, most of the reported bulk superhydrophobic materials are associated with complex synthetic procedures, expensive starting materials and sophisticated instrumental set-ups.[150,152] In the past, layer by layer deposition[150] and electrospinning technique[121] was explored for the fabrication of bulk superhydrophobic interfaces. For instance, Lynn *et al*[150] developed a bulk superhydrophobic coating through layer by layer deposition of PVDMA and PEI, which involves subsequent dipping in respective polymeric solutions for 600 times and attained only 80µm thick film after 100 bilayers of deposition. Hence, this approach is very laborious and time consuming. Next, the electrospinning technique, which is dependent on various variables including applied voltage, solution flow rate, polymer concentration, solution viscosity, nature of solvent, solution conductivity is applied to achieve the desired nanofiber morphology. So, the development of bulk superhydrophobic materials using a facile and scalable synthetic approach is essential and would be useful in addressing various practically relevant challenges. Furthermore, the synthesis of stretchable and compressible superhydrophobic interfaces that withstands various abrasive challenges are extremely rare in the literature,[178–180] however, such materials would be highly relevant for various fundamental and applied contexts.

To address these above mentioned challenges, my research was mostly focused towards developing highly durable superhydrophobic materials by adopting a facile and scalable synthetic approach. In my approach, I have exploited 1, 4-conjugate addition reaction between amine and acrylate functionalities at ambient conditions for developing robust superhydrophobicity. The work reported here was motivated from the previously reported functional polymeric coatings that were developed through strategic use of the 1, 4-conjugate addition reactions.[175,176] Amplification of desired functional groups and optimization of topography is successfully achieved following LbL deposition process, where polyamines (polyethylenimine branched, PEI) consecutively reacted with small molecule having multiple acrylate moieties (dipentaerythrotritol penta-acrylate, 5-Ac) through 1, 4-conjugate addition reaction between amine and acrylate functionality.[175,176] The gradual stepwise growth of multilayers allowed to control different shapes of nanostructures in the polymeric coating.[175] The polymeric multilayers were possessed with residual acrylate groups that provided facile basis to tailor the chemistry of synthesized material through strategic selection of primary amine containing small molecules.[176] After decylamine treatment, the polymeric multilayers was found to be highly hydrophobic with water contact angle of 138º. Based on these prevailing reports, I assumed that these reactive nanostructures that were developed directly on the solid interface following sequential deposition process, can be further extended to prepare dispersion of chemically reactive nanocomplex in organic solvent and the strategic associations of this nanomaterial is likely to provide various functional materials. Thus, grounded on these hypothesis, I extended the above mentioned systems rationally to obtain a chemically reactive nanocomplex and porous polymeric material. In the current thesis work, this simple chemical approach further addressed various prospective applications of bulk superhydrophobic interfaces including energy efficient oil/water separation, self-cleaning of deposited dust, no loss transfer of tiny water droplets etc.

References

(1) Wilbur and Orville Wright *U.S. Patent 821*, **1906,** 393-395.

(2) Mestral, G. D. *U. S. Patent 2, 717*, **1955**, 437–439.

(3) Verbrugge, K. *Harvard Review*, **2011**, 16–19.

(4) Fish, F. E.; Weber, P.W.; Murray, M. M.; Howle. L. E. *Integrative and Comparative Biology* **2011**, *51*, 203–213.

(5) Coninck, J. D.; Ruijter, M. J. de.; Voue, M. *Curr. Opin. Colloid Interface Sci.* **2001**, *6*, 49–53.

(6) Onda, T.; Shibuichi, S.; Satoh, N.; Tsujii, K. *Langmuir* **1996**, *12*, 2125–2127.

(7) Adamson, A. W.; Gast, A. P. *John Wiley and Sons: New York*, **1997**, 371–372.

(8) Zhang, X.; Shi, F.; Niu, J.; Jiang, Y.; Wang, Z. *J. Mater. Chem.* **2008**, *18*, 621–633.

(9) Eral, H.B.; 't Mannetje, D. J. C. M.; Oh, J. M. *Colloid Polym Sci*. **2013**, *291*, 247–260.

(10) Douglas J. C. G.; N. C. de, Souza.; Silva. J. R. *Measurement* **2013,** *46*, 3623–3627.

(11) Latthe, S. S.; Terashima, C.; Nakata, K.; Fujishima. A. *Molecules* **2014**, *19*, 4256–4283.

(12) Young, T. *Phil. Trans. R. Soc. Lond.* **1805,** *95*, 65–87.

(13) Wenzel, R. N. *Ind. Eng. Chem.* **1936**, *28*, 988–994.

(14) Cassie A. B. D.; Baxter, S. *Trans. Faraday Soc.* **1944**, *40*, 546–551.

(15) Liu, K.; Yaob, X.; Jiang. L. *Chem. Soc. Rev*. **2010**, *39*, 3240–3255.

(16) Gao, X. F.; Yan, X.; Yao, X.; Xu, L.; Zhang, K.; Zhang, J. H.; Yang, B.; Jiang, L. *Adv Mater*. **2007**, *19*, 2213–2217.

(17) Gao, X.; Jiang, L. *Nature* **2004**, *432*, 36–36.

(18) Barthlott, W.; Neinhuis, C. *Planta* **1997**, *202*, 1–8.

(19) Nishimura, R.; Hyodo, K.; Sawaguchi, H.; Yamamoto, Y.; Nonomura, Y.; Mayama, H.; Yokojima, S.; Nakamura, S.; Uchida, K. *J. Am. Chem. Soc.* **2016**, *138*, 10299−10303.

(20) Koch, K.; Bhushan, B.; Jung Y. C.; Barthlott W. *Soft Matter* **2009**, *5*, 1386–1393.

(21) Bin, S.; Ye, T.; Lei, J. *J. Am. Chem. Soc*. **2016**, *138*, 1727–1748.

(22) Feng, L.; Li, S. H.; Li, Y. S.; Li, H. J.; Zhang, L. J.; Zhai, J.; Song, Y. L.; Liu, B. Q.; Jiang, L.; Zhu, D. B. *Adv. Mater*. **2002**, *14*, 1857−1860.

(23) Zheng, Y. M.; Gao, X. F.; Jiang, L. *Soft Matter* **2007**, *3*, 178−182.

(24) Liu, K. S.; Du, J. X.; Wu, J. T.; Jiang, L. *Nanoscale* **2012**, *4*, 768−772.

(25) Autumn, K.; Sitti, M.; Liang, Y. C. A.; Peattie, A. M.; Hansen, W. R.; Sponberg, S.; Kenny, T. W.; Fearing, R.; Israelachvili, J. N.; Full, R. J. Proc. *Natl. Acad. Sci.* **2002**, *99*, 12252−12256.

(26) Autumn, K.; Liang, Y. A.; Hsieh, S. T.; Zesch, W.; Chan, W. P.; Kenny, T. W.; Fearing, R.; Full, R. J. *Nature* **2000**, *405*, 681−685.

(27) Manna, U.; Carter, M. C. D.; Lynn, D. M. *Adv.Mater.* **2013**, *25*, 3085–3089.

(28) Azo Nano. Lithography, Photolithography, Electron Beam Lithography and X-Ray Lithography – *Nano Fabrication Techniques* **2004**, 1−3.

(29) Brooks, W.; Vincent F. *Cambridge University Press* **1911**, *16*, 785–789.

(30) Hartsuch, P. *Lithographic Technical Foundation: New York* **1961**, 198–203.

(31) Peter, W. *The Technique of Lithography. London: B.T. Batsford* **1964**, 49–53.

(32) Chou, S. Y.; Krauss, P. R.; Zhang, W.; Guo, L. G.; Zhuang, L. *Vac. J. Sci. Technol. B* **1997,** *15*, 2897–2904.

(33) Herbertson, D. L.; Evans, C.R.; Shirtcliffe, N. J.; McHale, G.; Newton, M. I. *Sens. Actuators, A* **2006**, *130*, 189–193.

(34) Callies, M.; Chen, Y.; Marty, F.; Pepin, A.; Quere, D. *Microelectron Eng*. **2005**, *78*, 100–105.

(35) Martines, E.; Seunarine, K.; Morgan, H.; Gadegaard, N.; Wilkinson, C. D. W.; Riehle, M. O. *Nano Lett*. **2005**, *5*, 2097–2103.

(36) Fresnais, J.; Benyahia, L.; Poncin-Epaillard, F. *Surf. Interface Anal*. **2006**, *38*, 144–149.

(37) Chou, S.Y.; Keimel, C.; Gu, J. *Nature* **2002**, *417*, 835–837.

(38) Zhu, L.; Feng, Y.; Ye, X.; Zhou, Z. *Sens. Actuators, A* **2006**, *130*, 595–600.

(39) Furstner, R.; Barthlott, C.; Neinhuis, C.; Walzel, P. *Langmuir* **2005**, *21*, 956–961.

(40) Pozzato, A.; Zilio, S. D.; Fois, G.; Vendramin, D.; Mistura, G.; Belotti, M.; Chen, Y.; Natali, M. *Microelectron. Eng*. **2006,** *83*, 884–888.

(41) Kawai, A.; Nagata, H. *Jpn. J. Appl. Phys.* **1994**, *33*, 1283–1285.

(42) Oner, D. and T. J. McCarthy, *Langmuir* **2000**, *16*, 7777–7782.

(43) Zhu, L.; Feng, Y. Y.; Ye, X. Y.; Zhou, Z. Y. *Sens. Actuators, A* **2006**, *130*, 595–600.

(44) Coburn, J. W.; Winters, H. F. *J. Vac. Sci. Technol.* **1979**, *16*, 391–403.

(45) Cardinaud, C.; Peignon, M.-C.; Tessier. P.-Y. *Appl Surface Sci*. **2000** *164*, 72–83.

(46) Celia, E.; Givenchy, E.T. de.; Amigoni, S.; Guittard, F. *Soft Matter* **2011**, *7*, 10057–10062.

(47) Lee, E. J.; Jung, C.H.; Hwang, I. T.; Choi, J. H.; Cho, S. O.; Nho, Y. C. *ACS Appl. Mater. Interfaces* **2011**, *3*, 2988–2993.

(48) Vandencasteele, N.; Nisol, B.; Viville P.; Lazzaroni, R.; Castner D. G.; Reniers, F. *Plasma Process. Polym.* **2008**, *5*, 661–671.

(49) Minko, S.; Muller, M.; Motornov, M.; Nitschke, M.; Grundke, K.; Stamm, M. *J. Am. Chem. Soc.* **2003**, *125*, 3896–3900.

(50) Vandencasteele, N.; Merche, D.; Reniers, F. *Surf. Interface Anal*. **2006**, *38*, 526–530.

(51) Tsougeni, K.; Vourdas, N.; Tserepi, A.; Gogolides, E. *Langmuir* **2009**, 25, 11748–11759.

(52) Sun, M. H.; Luo, C. X.; Xu, L. P.; Ji, H.; Qi, O. Y.; Yu, D. P.; Chen, Y. *Langmuir* **2005**, *21*, 8978–8981.

(53) Qu, M.; Zhao, G.; Wang, Q.; Cao, X.; Zhang, J. *Nanotechnology* **2008**, *19*, 055707–055711.

(54) Shang, H.M.; Wang, Y.; Limmer, S. J.; Chou, T.P.; Takahashi, K.; Cao, G. Z. *Thin Solid Films 472*, **2005**, 37–43.

(55) Sia, Y.; Guo, Z. *Nanoscale* **2015**, *7*, 5922–5946.

(56) Tadanaga, K.; Morinaga, J.; Matsuda, A.; Minami, T. *Chem. Mater*. 2000, *12*, 590–592.

(57) Manca, M.; Cannavale, A.; Marco, L. D.; Arico, S.A.; Cingolani, R.; Gigli, G. *Langmuir* **2009**, *25*, 6357–6362.

(58) Xu, Q.F.; Wang, J. N.; Sanderson, K. D. *ACS Nano* **2010**, *4*, 2201–2209.

(59) Shang, H.M. Wang, Y.; Limmer, S. J.; Chou, T. P.; Takahashi, K.; Cao, G. Z. *Thin Solid Films*, **2005**, *472*, 37–43.

(60) Ma, W.; Wu, H.; Higaki, Y.; Otsuka, H.; Takahara, A. *Chem. Commun*. **2012**, *48*, 6824–6826.

(61) Brinker, C.J.; Keefer, K.D.; Schaefer, D.W.; Ashley, C. S. *J. Non-Crystalline Solids* **1982**, *48*, 47–64.

(62) Iler, R. *J. Colloid Interface Sci.* **1966**, *21*, 569−594.

(63) Decher, G.; Hong, J. Berich. B. *Gesell.* **1991**, *95*, 1430−1434.

(64) Decher, G.; Hong, J. D. *Makromol. Chem. Macromol. Symp.* **1991**, *46*, 321–327.

(65) Decher, G. *Science* **1997**, *277*, 1232−1237.

(66) Lee, S. W.; Kim, B. S.; Chen, S.; Horn, Y. S.; Hammond. P. T. *J. Am. Chem. Soc*. **2009**, *131*, 671–679.

(67) Zhang, Y.; Arugula, M. A.; Williams, S. T.; Minteer, S. D.; Simonian. A. L. *Journal of Electrochemical Society* **2016,** *163*, 449–454.

(68) Kong, B. S.; Geng. J.; Jung. H. T. *Chem. Commun*. **2009**, 2174–2176.

(69) Kulkarni, D. D.; Choi, I.; Singamaneni, S. S.; Tsukruk, V. V. *ACS Nano* **2010**, *4*, 4667−4676.

(70) Hu, M.; Mi. B. *Journal of Membrane Science* **2014,** *469*, 80–87.

(71) Ahn, E.; Lee,T.; Gu ,M.; Park, S v.; Min, H.; Kim, B S. *Chem. Mater.* **2017**, *29*, 69−79.

(72) Zhuk, A.; Mirza, R.; Sukhishvili, S. *Acs Nano* **2011**, *5***,** 8790–8799.

(73) Lee, H.; Lee, Y.; Statz, A. R.; Rho, J.; Park, T. G.; Messersmith, P. B. *Adv Mater.* **2008**, *20*, 1619–1623.

(74) Tang, Z.; Wang,Y.; Podsiadlo, P.; Kotov, N. A. *Adv. Mater*. **2006**, *18*, 3203–3224.

(75) Zhai, L.; Cebeci, F. C.; Cohen, R. E.; Rubner, M. F. *Nano Lett*. **2004**, *4*, 1349–1353.

(76) Han, J. T.; Zheng, Y.; Cho, J. H.; Xu, X.; Cho, K. *J. Phys. Chem. B* **2005**, *109*, 20773–20778.

(77) Zhang, L.; Sun, J. *Macromolecules* **2010**, *43*, 2413–2420.

(78) Hozumi, A.; Cheng, D.F.; Yagihashi, M. *J. Colloid Interface Sci.* **2011**, *353*, 582–587.

(79) Liu, X.; Dai, B.; Zhou, L.; Sun, J. *J. Mater. Chem*. **2009**, *19*, 497–504.

(80) Yao, L.; Zheng, M.; He, S.; Ma, L.; Li, M.; Shen, W. *Appl. Surf. Sci*. **2011**, *257*, 2955–2959.

(81) Hsieh, C. T.; Chen, W. Y.; Wu, F. L. *Carbon* **2008**, *46*, 1218–1224.

(82) Zimmermann, J.; Reifler, F. A.; Fortunato, G.; Gerhardt, L. C.; Seeger. S. *Advanced Functional Mat.* **2008**, *18*, 3662−3669.

(83) Sun, M.; Luo, C.; Xu, L.; Ji, H.; Ouyang, Q.; Yu, D.; Chen. Y. *Langmuir* **2005**, *21*, 8978–8981.

(84) Jiang, L.; Zhao, Y.; Zhai, J. *Angew. Chem. Int. Ed*. **2004**, *43*, 4338–4341.

(85) Liu, Z. J.; Wang, H. Y.; Wang, E. Q.; Zhang, X. G.; Yuan, R. X.; Zhu, Y. J. *Polymer* **2016**, *82*, 105–113.

(86) Park, S. H.; Lee, S. M.; Lim, H. S.; Han, J. T.; Lee, D. R.; Shin, H. S.; Jeong, Y.; Kim, J.; Cho, J. H. *ACS Appl. Mater. Interfaces* **2010**, *3*, 658–662.

(87) Zhan, N.; Li, Y.; Zhang, C.; Song, Y.; Wang, H.; Sun, L.; Yang, Q.; Hong, X. *Journal of Colloid and Interface Science* **2010,** *345*, 491–495.

(88) Nagappan, S.; Ha, C.S. *J. Mater. Chem. A* **2015**, *3*, 3224–3251.

(89) Wang, P.; Chen, M.; Han,H.; Fan, X.; Liua, Q.; Wang, J. *J. Mater. Chem. A* **2013**, *4*, 7869–7874.

(90) Zhiqing, Y.; Hong, C.; Jide, Z.; Dejian, Z.; Yuejun, L.; Xiaoyuan, Z.; Song, L.; Pu, S.; Jianxin, T.; Xin, C. *Sci. Technol. Adv. Mater.* **2008,** *9*, 045007–045012.

(91) Nakajima, A.; Hashimoto K.; Watanabe T. *Langmuir* **2000**, *16*, 7044-7047.

(92) Lu, Y.; Sathasivam, S.; Song, J.; Crick, C. R.; Carmalt, C. J.; Parkin, I. P. *Science* **2015**, *6*, 1132–1135.

(93) Latthe, S. S.; Sudhagar, P.; Devadoss, A.; Kumar, A. M.; Liu, S. H.; Terashima, C. ; Nakata, K.; Fujishima, A. *J. Mater. Chem. A* **2015**, *3*, 14263–14271.

(94) Liu, K. S.; Zhang, M. L.; Zhai, J.; Wang, J.; Jiang, L. *Appl. Phys. Lett*. **2008**, *92*, 183103−183106.

(95) Xu, W.; Song, J.; Sun, J.; Lu, Y.; Yu, Z. *ACS Appl. Mater. Interfaces* **2011**, *3*, 4404−4414.

(96) Ishizaki, T.; Saito, N. *Langmuir* **2010**, *26*, 9749−9755.

(97) Liu, Q.; Chen, D.; Kang, Z. *ACS Appl. Mater. Interfaces* **2015**, *7*, 1859–1867.

(98) Guo, Z. G.; Liu, W. M.; Su, B. L. *Appl. Phys. Lett.* **2008**, *92*, 063104–063106.

(99) Huang, Z. B.; Zhu, Y.; Zhang, J. H.; Yin, G. F. *J. Phys. Chem. C* **2007**, *111*, 6821–6825.

(100) Liu, H. Q.; Szunerits, S.; Xu, W. G.; Boukherroub. R. *ACS Appl. Mater. Interfaces* **2009**, *1*, 1150–1153.

(101) Zhang, F.; Zhao, L.; Chen, H.; Xu, S.; Evans, D. G.; Duan, X. *Angew. Chem. Int. Ed.* **2008**, *47*, 2466–2469.

(102) Broeren, A. P.; Lee, S.; Clark, C. *J. Aircr.* **2016**, *53*, 451–462.

(103) Lv, J. Y.; Song, Y. L.; Jiang, L.; Wang, J. J. *ACS Nano* **2014**, *8*, 3152–3169.

(104) Kim, A.; Lee, C.; Kim, H.; Kim, J. *ACS Appl. Mater. Interfaces* **2015**, *7*, 7206–7213.

(105) Boreyko, J. B.; Collier, C. P. *ACS Nano* **2013**, *7*, 1618–1627.

(106) Miljkovic, N.; Preston, D. J.; Enright, R.; Wang, E. N. *ACS Nano* **2013,** *7*, 11043–11054.

(107) Cao, L.; Jones, A. K.; Sikka, V. K.; Wu, J.; Gao, D. *Langmuir* **2009**, *25*, 12444–12448.

(108) Lo, C. W.; Sahoo, V.; Chang, M. *ACS Nano* **2017,** *11*, 2665–2674.

(109) Kim, A.; Lee, C.; Kim, H.; Kim, J. *ACS Appl. Mater. Interfaces* **2015,** *7*, 7206–7213.

(110) Lei, W.; Portehault, D.; Liu, D.; Qin, S.; Chen, Y. *Nat. Commun.* **2013**, *4*, 1777–1783.

(111) Yuan, J.; Liu, X.; Akbulut, O.; Hu, J.; Suib, S. L.; Kong, J.; Stellacci, F. *Nat. Nanotechnol.* **2008**, *3*, 332–336.

(112) Lahann, J. *Nat. Nanotechnol.* **2008**, *3*, 320–321.

(113) Joye, S. B. *Science* **2015**, *349*, 592–593.

(114) Schrope, M. *Nature* **2011**, *472*, 152–154.

(115) Kleindienst, S.; Paul, J. H.; Joye, S. B. *Nat. Rev. Micro*. **2015**, *13*, 388–396.

(116) Rasmussen, J. F.; Wegeberg, S.; Gustavson, K. *Water Air Soil Pollut*. **2015**, *226*, 329–340.

(117) Feng, L.; Zhang, Z. Y.; Mai, Z. H.; Ma, Y. M.; Liu, B. Q.; Jiang, L.; Zhu, D. B. *Angew. Chem. Int. Ed.* **2004**, *43*, 2012–2014.

(118) Li, B.; Li, L.; Wu, L.; Zhang, J.; Wang, A. *Chem- Plus Chem*. **2014**, *79*, 850–856.

(119) Gui, X.; Wei, J.; Wang, K.; Cao, A.; Zhu, H.; Jia, Y.; Shu, Q.; Wu, D. *Adv. Mater.* **2010**, *22*, 617–621.

(120) Ruan, C.; Ai, K.; Li, X.; Lu, L. *Angew. Chem. Int. Ed.* **2014**, *53*, 5556–5560.

(121) Yohe, S. T.; Colson, Y. L.; Grinstaff, M. W. *J. Am. Chem. Soc*. **2012**, *134*, 2016−2019.

(122) Manna, U.; Kratochvil, M. J.; Lynn, D. M. *Adv. Mater*. **2013**, *25*, 6405–6409.

(123) Wolinsky, J. B.; Yohe, S. T.; Colson, Y. L.; Grinstaff, M. W. *Biomacromolecules* **2012**, *13*, 406−411.

(124) Fan, H. L.; Chen, P. P.; Qi, R. M.; Zhai, J.; Wang, J. X.; Chen, L.; Chen, L.; Sun, Q. M.; Song, Y. L.; Han, D.; Jiang, L. *Small* **2009**, *5*, 2144–2148.

(125) Sun, T. L.; Tan, H.; Han, D.; Fu, Q.; Jiang, L. *Small* **2005**, *1*, 959–963.

(126) Cho, E. C.; Jian, C. W. C.; Chen, H. C.; Chuang, K. S.; Zheng, J. H.; Hsiao, Y. S.; Lee, K. C.; Huang, J. H. *Chem. Eng. J.* **2017**, *314*, 347–357.

(127) Zahner, D.; Abagat, J.; Svec, F.; Fréchet, J. M. J.; Levkin, P. A. *Adv. Mater*. **2011**, *23*, 3030–3034.

(128) Seo, J.; Lee, S.; Lee, J.; Lee, T. *ACS Appl. Mater. Interfaces* **2011**, *3*, 4722−4729.

(129) Zhai, L.; Berg, M.C.; Cü, F.; Cebeci; Kim,Y.; Milwid, J.M.; Rubner, M. F.; Cohen, R. E. *Nano Lett.* **2006**, *6*, 1213–1217.

(130) Wang, Y.; Xue, J.; Wang, Q.; Chen, Q.; Ding, J. *ACS Appl. Mater. Interfaces* **2013**, *5*, 3370–3381.

(131) Wang, P.; Chen, M. J.; Han, H. L.; Fan, X. L.; Liu, Q.; Wang, J. F. *J. Mater. Chem. A* **2013,** *4*, 7869–7874.

(132) Wang, S. T.; Feng, L.; Jiang, L. *Adv. Mater.* **2006**, *18*, 767−770.

(133) Cebeci, F. C.; Wu, Z. Z.; Zhai, L.; Cohen, R. E.; Rubner, M. F. *Langmuir* **2006**, *22*, 2856–2862.

(134) Feng, L.; Zhang. Z.; Mai. Z.; Ma, Y.; Liu, B.; Jiang, L.; Zhu, D. *Angew. Chem. Int. Ed.* **2004**, *43*, 2012–2014.

(135) Verho, T.; Bower, C.; Andrew, P.; Franssila, S.; Ikkala, O.; Ras, R. H. A. *Adv. Mater*. **2011**, *23*, 673–678.

(136) Li, X. M.; Reinhoudt, D.; Grego-Calama, M. *Chem. Soc. Rev.* **2007**, *36*, 1350–1368.

(137) Crick, C. R.; Gibbons, J. A.; Parkin, I. P. *J. Mater. Chem. A* **2013**, *1*, 5943–5948.

(138) Zhou, X. Y.; Zhang, Z. Z.; Xu, X. H.; Guo, F.; Zhu, X. T.; Men, X. H.; Ge, B. *ACS Appl. Mater. Interfaces* **2013**, *5*, 7208–7214.

(139) Wang, Z.; Wang, Y.; Liu, G. *Angew. Chem., Int. Ed*. **2016**, *55*, 1291–1294.

(140) Wang, B.; Guo, Z. G. *Chem. Commun*. **2013**, *49*, 9416–9418.

(141) Osicka, J.; Il˘cikov´, M.; Popelka, A.; Filip, J.; Bertok, T.; Tkac, J.; Kasak, P. *Langmuir* **2016**, *32*, 5491–5499.

(142) Han, Z.; Li, B.; Mu, Z.; Niu, S.; Zhang, J.; Ren, L. *Small* **2017**, *13*, 1701121–1701131.

(143) Zhou, C.; Chen, Z.; Yang, H.; Hou, K.; Zeng, X.; Zheng, Y.; Cheng, J. *ACS Appl. Mater. Interfaces* **2017**, *9*, 9184–9194.

(144) Kwak, G.; Lee, M.; Yong, K. *Langmuir* **2010**, *26*, 9964–9967.

(145) Zhu, X. T.; Zhang, Z. Z.; Men, X. H.; Yang, J.; Wang, K.; Xu, X. H.; Zhou, X. Y.; Xue, Q. J. *J. Mater. Chem.* **2011**, *21*, 15793–15797.

(146). Yang, J.; Zhang, Z. Z.; Men, X. H.; Xu, X. H.; Zhu, X. T. *Colloids Surf. A* **2010**, *367*, 60−64.

(147) Li, Y.; Li, L.; Sun, J. *Angew. Chem. Int. Ed.* **2010**, *49*, 6129–6133.

(148) Wang, H. X.; Xue, Y. H.; Ding, J.; Feng, L. F.; Wang, X. G.; Lin, T. *Angew. Chem., Int. Ed.* **2011**, *50*, 11433−11436.

(149) Wang, X. L.; Liu, X. J.; Zhou, F.; Liu, W. M. *Chem. Commun*. **2011**, *47*, 2324−2326.

(150) Manna, U.; Lynn, D. M. *Adv. Mater.* **2013**, *25*, 5104−5108.

(151) Levkin, P. A.; Svec, F.; Frechet, J. M. *J. Adv. Funct. Mater.* **2009**, *19*, 1993–1998.

(152) Deng, X.; Mammen, L.; Butt, H. J.; Vollmer. D. *Science* **2012,** *335*, 67–69.

(153) Hu, X. C.; Andrews, D. Q.; Lindstrom, A. B.; Bruton, T. A.; Schaider, L. A.; Grandjean, P.; Lohmann, R.; Carignan, C. C.; Blum, A.; Balan, S. A.; Higgins, C. P.; Sunderland, E. M. *Environ. Sci. Technol. Lett.* **2016**, *3*, 344–350.

(154) Little, R. D.; Masjedizadeh, M. R.; Wallquist, O.; McLoughlin, J. I. *Org. React*. **1995**. *47*, 315–352.

(155) Mather, B.D.; Viswanathan, K.; Miller, K. M.; Long T. E. *Prog. Polym. Sci.* **2006**, *31*, 487–531.

(156) Michael, A. *Am. Chem. J.* **1887**, *9*, 115−117.

(157) Nising, C. F.; Brase, S. *Chem. Soc. Rev*. **2008**, *37*, 1218−1228.

(158) Vicario, J. L.; Badia, D.; Carrillo, L. *Synthesis* **2007**, *14*, 2065−2092.

(159) Sundararajan, G.; Prabagaran, N. *Org. Lett.* **2001**, *3*, 389−392.

(160) Enders, D.; Haertwig, A.; Raabe, G.; Runsink, J. *Angew. Chem., Int. Ed. Engl.* **1996**, *35*, 2388−2390.

(161) Sani, M.; Bruche, L.; Chiva, G.; Fustero, S.; Piera, J.; Volonterio, A.; Zanda, M. *Angew. Chem. Int. Ed.* **2003**, *42*, 2060−2063.

(162) Yadav, J. S.; Reddy, B. V. S.; Baishya, G. *J. Org. Chem*. **2003,** *68*, 7098−7100.

(163) Tomalia, D. A.; Baker, H.; Dewald, J.; Hall, M.; Kallos, G.; Martin, S.; Roeck, J.; Ryder, J.; Smith, P. *Polymer Journal* **1985**, *17*, 117–132.

(164) Bielinska, A.; Kukowska-Latallo, J. F.; Johnson, J.; Tomalia, D. A.; Baker, J. R. *Res* **1996**, *24*, 2176–2182.

(165) Roy, R.; Laferriere, C. A. *J. Chem. Soc. Chem. Commun.* **1990**, *23*, 1709–1711.

(166) Harris, J.M.; Kozlowski, A. *US Patent:* **2003**, *6*, 664, 331–332.

(167) Elbert, D.L.; Hubbell, J.A. *Biomacromolecules* **2001**, *2*, 430–441.

(168) Goodson, R.J.; Katre, N.V. *Biotechnology* **1990**, *8*, 343–346.

(169) Vernon, B.; Tirelli, N.; Bachi, T.; Haldimann, D.; Hubbell, J. *J. Biomed Mater Res* **2003**, *64*, 447–456.

(170) Rizzi, S. C.; Hubbell, J. A. *Biomacromolecules* **2005**, *6*, 1226–1238.

(171) Tsubokawa, N.; Takayama, T. *React Funct Polym.* **2000**, *43*, 341–350.

(172) Weatherspoon, M. R.; Dickerson, M. B.; Wang, G.; Cai, Y.; Shian, S.; Jones, S. C.; Marder, S. R.; Sandhage, K. H. *Angew. Chem. Int. Ed.* **2007**, *46*, 5724−5727.

(173) Wang, G. J.; Fang, Y. N.; Kim, P.; Hayek, A.; Weatherspoon, M. R.; Perry, J. W.; Sandhage, K. H.; Marder, S. R.; Jones, S. C. *Adv. Funct. Mater.* **2009**, *19*, 2768−2776.

(174) Lynn, D. M.; Langer, R. *J. Am. Chem. Soc*. **2000**, *122*, 10761−10768.

(175) Ford, J.; Marder, S. R.; Yang, S. *Chem. Mater*. **2009**, *21*, 476−483.

(176) Bechler, S. L.; Lynn, D. M. *Biomacromolecules* **2012**, *13*, 1523−1532.

(177) Yohe, S. T.; Freedman, J. D.; Falde, E. J.; Colson, Y. L.; Grinstaff, M. W. *Adv. Funct. Mater*. **2013**, *23*, 3628–3637.

(178) Wang, Y.; Shi, Y.; Pan, L.; Yang, M.; Peng, L.; Zong, S.; Shi, Y.; Yu, G. *Nano Lett.* **2014**, *14*, 4803–4809.

(179) Cho, S. J.; Nam, H.; Ryu, H.; Lim, G. *Adv. Funct. Mater.* **2013**, *23*, 5577–5584.

(180) Lee, W. K.; Jung, W. B.; Sidney, R.; Nagel, T.; Odom, W. *Nano Lett.* **2016**, *16*, 3774–3779.

Chapter 2: Synthesis of 'Amine' Reactive Polymeric Material*

A chemically "reactive" polymeric gel material is developed by adopting the robust and facile 1, 4-conjugate addition reaction between acrylate and primary amine groups for synthesizing chemically cross-linked and bulk (including interior and surface) superhydrophobic material. A mixture of dipentaerythritol penta-acrylate (5-Acl) and branched poly (ethylenimine) (BPEI) can rapidly form a self-standing and shapeable gel network. On removal of solvent molecules, the synthesized gel network provided a highly porous and chemically reactive polymeric material. The residual acrylate groups provided a facile basis for modifying the chemistry and eventually allowed to tailor the liquid water wettability on the synthesized material. This approach provided a facile and rapid process for fabricating a bulk superhydrophobic material of arbitrary shapes and sizes. The anti-wetting property of the material remained intact even after incurring various standard physical and chemical insults. This synthetic strategy could be useful to develop multifunctional materials for various applications including self-cleaning of deposited dust, loading of hydrophilic small molecules etc.

* Rather. A. M.; U. Manna. *Chem. Mater*. **2016**, *28*, 8689−8699.

Chapter 2

2.1. Introduction

Bio-inspired superhydrophobic materials[1,2] (having advancing contact angle $\theta_{adv} > 150°$ and contact angle hysteresis $\theta_{hys} < 10°$), which are extremely liquid water repelling, provide a general platform to design materials for widespread applications including self-cleaning, oil/water separation, water harvesting, guided water and gas bubble transfer, drug release, protein crystallization, etc.[1–9] Detailed investigation on natural superhydrophobic surfaces (e.g., lotus leaf) revealed that these surfaces are composed of hierarchical micro/nano features coated with a low surface energy coating.[1] Since then, several top-down and bottom-up synthetic approaches have been developed to attain two essential criteria's: (1) a hierarchical topography, generally using hydrophilic elements, and (2) a thin layer of low surface energy coatings on top, achieved mostly by chemical vapor deposition of fluorinated inert molecules.[10,11] This general procedure has been widely adopted to develop superhydrophobic materials, and some of them have been used for demonstrations of various prospective applications. However, the use of such materials is restricted in practical scenarios where such artificial superhydrophobic interfaces are likely to subject at different physical (scratching, creasing, bending etc.) and chemical (extremes of pH, sea and river water) insults. These severe physical/chemical exposures are likely to remove the essential low surface energy coatings and the resulted exposure of interior of the coating expected to compromise the anti-wetting property of the superhydrophobic materials.[12–14] Thus, the development of chemically and physically durable superhydrophobic materials remains an important challenge in both fundamental and applied contexts.[15–24]

In the recent past, only a few approaches have been introduced i.e. (a) post-repairable [25–27] and (b) self-healing[28–32] approaches where the compromised anti-wettability can be either repaired or self-healed after application of appropriate post treatments to the damaged materials; however, the sustainability of these approaches is limited to a finite number of healing/repairing cycles and also requires external stimuli which may associate severe inconvenience at diverse practical scenarios. In addition to these approaches, a new class of superhydrophobic materials (known as "bulk superhydrophobic") have recently been introduced by few research groups.[17,33–38] In these materials, the anti-wetting property is not limited to the surface, but exhibit three-dimensional (3D) anti-wetting property including the surface and the bulk of the material. Thus, the anti-wetting property remained

intact even after abrasion of the top surface of the material during severe physical insults (scratching, creasing, etc.).[17,33–38] The evolution of "bulk" superhydrophobicity has progressed recently with limited examples; however, further development and progress in this research area would be of potential interest for various fundamental and applied contexts.

In this chapter, a chemically reactive and porous polymeric material is introduced using a salt assisted gelation approach of branched polymer for fabricating a chemically and physically durable superhydrophobic material. This approach is inherently facile and provides the following major advantages: (i) residual chemical reactivity of the polymeric gel can be used in tuning the desired liquid wettability (e.g., adhesive and nonadhesive superhydrophobicity, superhydrophilicity, etc.); (ii) facile chemical post functionalization of the porous polymeric material provided a bulk superhydrophobic material that is covalently crossed-linked through 1, 4-conjugate addition reaction;[39–43] (iii) as a consequence, the material is embedded with chemically and physically durable superhydrophobicity. Moreover, the synthesis of bulk superhydrophobic material following this salt-assisted rapid polymeric gelation approach provides a platform to develop three-dimensionally free-standing superhydrophobic materials of complex shape and size, which is unprecedented in the literature. The current work is inspired by the past studies which introduced different approaches to develop various functional materials using the robust and facile Michael addition reaction between primary amines and acrylates. The 1, 4-conjugate addition reaction has been strategically exploited for synthesizing different functional materials,[39–43] i.e. (a) dendritic amplification of desired functional groups,[42] (b) selective and 3D functionalization of polymer microstructures[39] and (c) synthesis of polymer coatings with complex nanostructures,[41, 43] providing a simple basis to design materials with both desired chemical functionalities and surface topography.[39–43]

2.2. Materials and Methods

2.2.1. Materials

Branched poly (ethylenimine) (BPEI, $M_W \approx 25,000$ Da), dipentaerythritol penta-acrylate (5-Acl, $M_W \approx 524.51$ g/mol), nile red dye, propylamine, butylamine, pentylamine, hexylamine, heptylamine, octylamine, decylamine, octadecylamine, methylene blue were purchased from Sigma-Aldrich (Bangalore, India). Reagent-grade THF and NaCl were

purchased from RANKEM (Maharashtra, India), and absolute ethyl alcohol (CAS Registry No. 64-17-5, Lot 1005150) was purchased from TEDIA Company (United States of America). HCl was obtained from Fischer Scientific (Mumbai India). Microscopic glass slides were procured from JSGW (Jain Scientific Glass Works) India. Play-dough cutters in the shapes of dolphin, elephant, and rabbit were purchased from Fabric Castell (India). NaOH was obtained from Emparta (Merck Specialties Private Limited). Rhodamine-6G was purchased from Labo Chemie (Laboratory Reagents and Fine Chemicals Mumbai India). Sandpaper was procured from a local shop in Guwahati City (Assam, India). UV cabinet used for continuous exposure of UV radiations was purchased from Relitech (Bengaluru India). Adhesive tape was obtained from Jonson Tapes (India). Sand was collected from a construction site at IIT-Guwahati and was rinsed thoroughly prior to use. All materials and chemicals were used as obtained without further purification.

2.2.2. General Considerations

Contact angle measurements were performed using a KRUSS Drop Shape Analyzer-DSA25 instrument with an automatic liquid dispenser at ambient temperature. Advancing and receding contact angles were measured with deionized water droplets at four different locations on each sample. Field Emission Scanning Electron Microscope (FESEM) images were obtained using a Carl Zeiss field emission scanning electron microscope, and a thin layer of gold was coated (using a sputterer) on each sample prior to imaging. Atomic force microscope (AFM) images were acquired using an Agilent model 5500 series microscope. Dynamic light scattering (DLS) study was performed using a Zetasizer Nano ZS90 instrument (model no. ZEN3690). Surface area and pore size analyzer (Quantachrome Autosorb-IQ MP) was used for estimation of pore volume and surface area. Fourier Transform Infrared (FTIR) spectra were recorded using a Perkin-Elmer instrument at normal temperature, and the sample was grinded with KBr prior to analysis. Digital pictures were captured using a Canon Power Shot SX420 IS digital camera. Milli-Q grade water was used for all experiments.

2.3. Methods

2.3.1. Preparation of ‘Amine Reactive’ Polymeric Gel

First, BPEI and 5-Acl solutions were prepared by dissolving 0.5 g of BPEI and 1.325 g of 5-Acl in 10 mL of ethanol solvent discretely. These two reactant solutions BPEI and 5-Acl

were mixed in various compositions [each composition is designated with a certain abbreviation related to its polymeric composition (PC) consists of 5-Acl and BPEI with different volumes: PC-1 (1 mL 5-Acl+0.10 mL BPEI), PC-2 (1 mL 5-Acl+0.25 mL BPEI), PC-3 (1 mL 5-Acl+0.30 mL BPEI), PC-4 (1 mL 5-Acl+0.40 mL BPEI), PC-5 (1 mL 5-Acl+0.50 mL BPEI), and PC-6 (0.5 mL 5-Acl+0.50 mL BPEI) see results and discussion section for more details]. After mixing some of the polymeric compositions were transformed from colorless mixtures to opaque white gels (PC-3, PC-4, and PC-5), and one of them transformed to a translucent gel (PC-6), while other compositions appeared as a turbid milky liquid (PC-1) or white precipitate (PC-2). All the synthesized gels (PC-3, PC-4, PC- 5 and PC-6) were rinsed with THF for 1 h prior to treatment with decylamine (DA) solution (0.5 mL of DA in 10 mL of THF). Then these gel materials were further rinsed with THF for 1 hour to remove unreacted decylamine molecules and allowed to dry at ambient conditions. The water wettability was further examined by dispensing a water droplet on the surface of the synthesized material, and it was found that only one composition, i.e., PC-3, showed hydrophobicity, while all the other compositions displayed an insignificant influence of decylamine treatment.

2.3.2. Effect of NaCl on Water Wettability of Polymeric Material

It was observed that the PC-3 sample shows hydrophobicity with contact angle 127° after decylamine treatment; however, the water contact angle (WCA) was far away from superhydrophobicity. To further improve the water wettability, I first aimed to tailor the morphology of the material, and during the course of the study, it was observed that the same composition [PC-3, which we renamed as S0 (without salt)] displayed the improved hydrophobicity after decylamine treatment when the polymeric gel was prepared in the presence of a small amount [concentrations of 200 μg/mL (polymeric gel denoted as S1) and 400 μg/mL (polymeric gel denoted as S2)] of NaCl salt. On further increasing the salt doping amount, (600 μg/mL NaCl salt) the polymeric gel (S3) exhibited artificial superhydrophobicity after post chemical modification of the material with decylamine. The solvent was doped with salt as follows: first the desired concentration of salt (S1, S2, and S3) was optimized by dissolving the required amount of salt in ethanol, and then solutions of BPEI and 5-Acl were separately prepared using the salt-doped ethanol. Next, the salt added 1 mL of 5-Acl and 0.3 mL of BPEI (as followed for PC-3) were mixed and kept on

shaking until they formed a gel and thereafter, gel was taken out, washed with THF and finally immersed in decylamine solution for overnight. To remove the traces of the salt from the material, it was further washed with deionized water several times under magnetic stirring and dried in air. Water wetting behavior was examined with digital images and contact angle measurements.

2.3.3. Tailoring of Water Wettability

The synthesized chemically reactive material (S3) was washed with THF for 1h and was subsequently transferred to solutions of different alkyl chain amines including propylamine (30 mg/mL), butylamine (30 mg/mL), pentylamine (30 mg/mL), hexylamine (30 mg/mL), octylamine (30 mg/mL), decylamine (30 mg/mL) and octadecylamine (5 mg/mL) individually and were kept for overnight. Afterwards, the materials were rinsed with THF to remove the unreacted small molecules and dried at ambient conditions. The water wettability of the materials were inspected with digital images and contact angle measurements.

2.3.4. Physical and Chemical Durability of the Superhydrophobic Material

Various types of physical and chemical insults were performed on the synthesized superhydrophobic material to examine the durability of the embedded anti-wetting property. The detailed procedures of all physical and chemical abrasion tests are discussed in the following section.

2.3.4.1. Sandpaper Abrasion Test

Sandpaper was first immobilized on a glass slide using adhesive tape, the superhydrophobic polymer sample was placed on it, and a weight of 100 g was placed on top of the material with the help of microscopic glass slide. The polymeric material was rubbed manually across a 5 cm distance back and forth for multiple (six) times. After this abrasion procedure, the anti-wetting property was examined with digital images and contact angle measurements.

2.3.4.2. Adhesive Tape Test

The double-sided adhesive tape was used for the experiment, where one surface of adhesive tape was placed on a glass slide and the other surface was exposed to the material with 500 g applied load for pressing the sample uniformly onto the adhesive surface to ensure improved contact with the adhesive surface. The material was manually peeled from the

adhesive tape surface and both the abraded surface and the peeled portion that is attached to adhesive surface were inspected through digital images and contact angel measurement.

2.3.4.3. Sand Drop Test

In this test, the superhydrophobic material was fixed on a microscopic glass slide using adhesive tape. Then, 150 g of sand grains were dropped from the height of 20 cm with continuous flow on the material inclined at 45° angle. Afterwards, the anti-wetting property of the material was observed by visual inspection and contact angle measurement.

2.3.4.4. Scratch Test

The synthesized superhydrophobic material was manually scratched with a sharp pointed needle of depth around 1 mm all over the surface of the materials. Subsequently, the anti-wetting property was examined on the scratched as well on the non-scratched interfaces by visual inspection and contact angle measurement.

2.3.4.5. Chemical Durability

Chemical durability of the superhydrophobicity was examined on exposing the synthesized materials to various harsh aqueous chemical conditions including highly alkaline solution (0.01 M NaOH; pH 12), acidic solution (0.01 M HCl; pH 1), artificial seawater and river (Brahmaputra, Assam, India) water for prolonged duration. Afterwards, the superhydrophobic property was investigated through digital images and contact angle measurements. Artificial seawater was prepared by mixing $MgCl_2$ (0.226 g), $MgSO_4$ (0.325 g), NaCl (2.673 g), and $CaCl_2$ (0.112 g) in 100 mL of deionized water.

2.3.4.6. Self-cleaning Property

The self-cleaning property of the synthesized superhydrophobic surface was examined by placing the dust particles on the surface of the material and subsequently exposed to a stream of liquid water resulting in the accumulation of dust particles on the air/water interface. This water droplet with accumulated dust particles instantly rolled off on the tilted interface and leave behind a dust-free, cleaned and dry interface.

2.4. Results and Discussion

2.4.1. Fabrication and Characterization of Polymeric Gel

Here, I adopt Michael addition reaction to fabricate a bulk superhydrophobic material through covalent gelation of single polymer. Studies from the recent past, have shown that dipentaerythritol penta-acrylate (5-Acl) and similar molecules can readily react with

branched poly (ethylenimine) (BPEI) through 1, 4-conjugate addition process during the fabrication of multilayer construction,[41, 43] and provided interfaces with different nano-complex features. Moreover, porous multilayers with residual acrylate chemical functionalities was successfully exploited for post modification with various amine containing small molecules for obtaining different interesting properties. Based on these previous studies, I hypothesized that the mixture of BPEI and 5-Acl in ethanol might provide a chemically reactive nanocomplexes decorated with residual acrylate functional

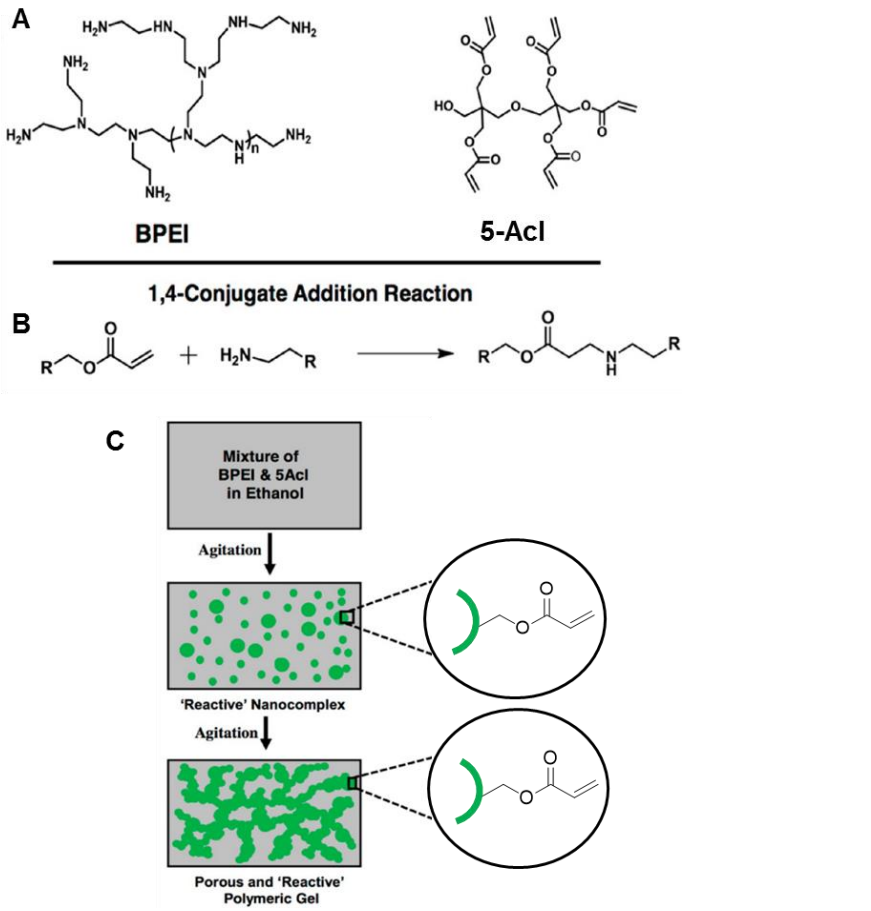

Figure 2.1. (A) Chemical structures of branched poly (ethylenimine) (BPEI) and dipentaerythritol penta-acrylate (5-Acl). B) 1, 4-conjugate addition reaction between primary amine and acrylate groups. C) Transformation of BPEI/5-Acl mixture to reactive polymeric gel via "Reactive" Nanocomplex intermediate.

groups and over the time, these nanocomplexes would further covalently aggregated to form a porous polymeric gel network, as depicted in Figure 2.1. Hence, a series of studies were performed with various polymeric compositions (PCs) of 5-Acl and BPEI in ethanol

solvent at ambient conditions, as listed in Table 1, to develop an appropriately porous and "reactive" polymeric material which can be transformed into a bulk superhydrophobic material upon essential post chemical modification. On mixing of BPEI and 5-Acl solutions in ethanol, the physical appearance of the mixture was noted to be turbid solution (PC-1), white precipitate (PC-2), etc., as listed in Table 2.1. At one particular composition (PC-3), colorless BPEI/5-Acl mixture transformed into a faint turbid solution and over the time, an intensely milky turbid solution was observed. After 3.5 h, a polymeric gel was recovered

Composition	5-Acl (mL)	BPEI (mL)	Physical State of the Composition	Contact Angle (º)	
				Before Treatment	After Treatment
PC-1	1.00	0.10	Turbid Liquid	N/A	N/A
PC-2	1.00	0.25	White precipitate	N/A	N/A
PC-3 (S0)	1.00	0.30	White Gel	0	127.3
PC-4	1.00	0.40	White Gel	0	68.2
PC-5	1.00	0.50	White Gel	0	85.8
PC-6	0.50	0.50	Translucent Gel	0	84.2

Table 2.1. Displays the mixture of 5-Acl/BPEI with various compositions and their water wettability after decylamine treatment.

from the glass vial, as shown in Figure 2.2A. The other compositions (PC-4, PC-5, and PC-6) similarly transformed to gel materials, as noted in Table 2.1. On complete evaporation of solvent (ethanol) molecules from each of the gel materials, a dried white polymeric solid material was obtained and found to be hydrophilic with water contact angle (WCA) of 0°. However, after post chemical modification with decylamine molecules (hydrophobic molecule), the WCA increased to ~127°, ~68°, ~85°, and ~84° for PC-3, PC- 4, PC-5, and PC-6, respectively. Thus, the polymeric gel that was prepared using PC-3 (which is further renamed as S0) was found to be most hydrophobic compared to the other gel materials (PC-4, PC-5, and PC-6) after same post chemical treatment—that is modification with DA. I selected this particular composition (S0) for optimizing the desired bulk superhydrophobic property. The gelation of polymer proceeded through formation of polymeric nanocomplex as characterized with AFM imaging. AFM image in Figure 2.2B

provides information about the morphology of the nano-complex, where each of these nanocomplexes have nearly spherical shape with some random roughness as is depicted in line profile diagram. The gelation of polymeric material after mixing of BPEI/5-Acl is very

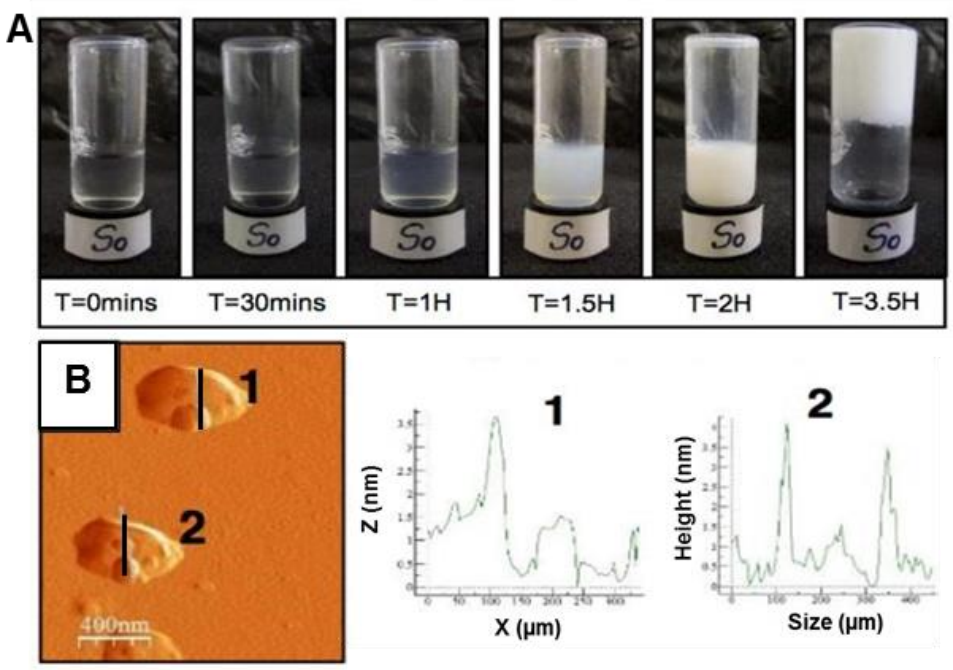

Figure 2.2. (A) Digital images from left to right panel illustrating the polymeric gel formation process with time on mixing of BPEI and 5-Acl in ethanol (S0). B) AFM image of nano-complexes (formed on mixing of BPEI and 5-Acl) reveals the shape of the nano-complex and line profiles (1 and 2) on nanocomplexes further indicates the existence of nano-topography on the surface of each nanocomplex.

slow and completes in 210 mins as is shown in Figure 2.2A. During the course of this study, we noticed that the rate of gelation can be enhanced by addition of a tiny amount (on the order of µg/mL concentration) of salt (NaCl) in the reaction mixture, as shown in Figure 2.3A, B [salt-doped samples are indicated as S1 (200 µg/ mL), S2 (400 µg/mL), and S3 (600 µg/mL), with increasing order of added NaCl]. The mixture of 5-Acl and BPEI that was doped with 600 µg/mL NaCl rapidly (within 20 mins) transformed to a polymeric gel material. Dynamic light scattering (DLS) study also revealed the formation of nanocomplexes during this polymeric gel synthesis process and the size of these nanocomplexes increased with enhancing the concentration of salt as shown in the reaction mixture of BPEI/5-Acl Figure 2.3C. The synthesized polymeric material can be molded into different and complex shapes with strategic use of appropriate template as shown in

Figure 2.3D. However, significant shrinking of these polymeric gels was noticed during the air drying process on removal of solvent molecules (ethanol), but the shape remained intact. This unaffected integrity and intact shape of the material, even after removal of solvent molecules, is mainly because of the covalent cross-linked (through 1, 4-conjugate addition

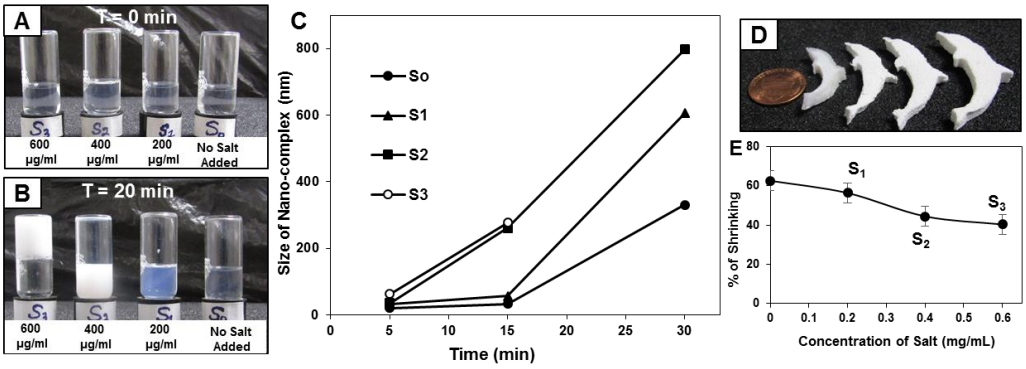

Figure 2.3. (A, B) Gelation process of colorless mixtures (A) of BPEI and 5-Acl in ethanol both in the absence (S0) and in the presence of salt (NaCl: S1, 200 µg/mL; S2, 400 µg/mL; and S3, 600 µg/mL). After 20 min (B), S3 formed a gel (which sticks to the bottom of the inverted vial), while S2 and S1 formed more (S2) and less (S1) turbid solutions, and the turbidity was even less for S0. C) DLS study of S0, S1, S2, and S3 samples, showing that the progression in growth of the nanocomplex is faster for higher salt-doped mixtures of BPEI and 5-Acl. D) Digital image of gel materials in the shape of dolphins that were prepared using a play-dough shape-cutter, the size of each dolphin was same before drying. After drying, the dolphins were found to shrink to different sizes, based on the amount of salt added in the mixture. E) Graph accounting for the effect of salt doping on shrinkage of material upon air drying.

reaction between amine and acrylate) nature of the material. The synthesized materials with the shape of a dolphin were noticed to shrink less with increasing concentration of the added salt in the reaction mixture as shown in Figure 2.3D. The change in percentage of shrinking of these materials with added salt is detailed in Figure 2.3E, the polymeric gel that is prepared without added salt (S0) was shrinked to 60 ± 2%, and this shrinking could be restricted to 40 ± 1% on increasing the salt doping concentration up to 600 µg/mL (S3). To understand this behavior, a detailed FESEM study was performed. A significant change in morphology of the polymeric material is noticed, depending on the concentration of added NaCl in the reaction mixture. The globular features appeared to be larger in size for salt-doped materials as compared to the salt free and the arrangement of these globular domains

in the covalently cross-linked polymeric network is found to be more irregular on increasing salt doping (Figure 2.4). These morphological changes contribute to the enhanced porosity in the polymeric materials, as confirmed by BET pore volume analysis for S0 (no salt added) and S3 (600 μg/mL doping of NaCl) are estimated to be 0.023 and 0.031 cm^3/g respectively. From these results, it was hypothesized that the enhanced porosity, because of the irregular arrangements of granular domains (smaller/bigger) in the polymeric material on increasing the concentration of added salt, controls the rate of shrinkage of the synthesized material during air drying process. However, the exact role of the added salt in evolving the essential random porous structure is not thoroughly understood, the added salt might screen the potential charge of each nanocomplex, and thus it might accelerate the random aggregation of nanocomplex, eventually helping in forming a highly porous and reactive polymeric network. FTIR spectroscopy was further performed to understand the availability of functional groups in the chemical structures of BPEI/5-Acl polymeric gels. The characteristic peak at 1410 cm^{-1} and 1739 cm^{-1} in the IR spectrum (black) of the polymeric gel without salt, as shown in Figure 2.5A are the characteristic peaks of symmetric deformation of the C−H bond for the β carbon of the vinyl group and carbonyl stretching.[41, 43] Thus, these IR signatures unambiguously suggested the presence of residual acrylate groups that could be further used for post chemical modification of the entire polymeric gel. The characteristic peak for residual acrylate groups at 1410 cm^{-1} (red spectrum in Figure 2.5A) depleted compared to the untreated counterpart (black spectrum) significantly after treating the polymeric gel with decylamine molecules and the IR spectra was normalized with respect to the signature at 1739 cm^{-1}. This suggests successful post chemical modification of the synthesized material with amine containing small molecules. Moreover, no visible change in the appearance of the polymeric gel was noticed after post chemical functionalization with decylamine molecules in THF. However, a remarkable change in the water wettability was noticed on post chemical modification of the polymeric matrix with DA molecule. The water droplet was brought in contact with the air dried material and the aqueous phase was readily soaked on the chemically reactive polymer gel with 0º contact angle while the water droplets beaded with a contact angle of 127º on the same polymeric matrix after decylamine functionalization (Figure 2.5B, C). Further, a significant improvement in hydrophobicity (S1, ~146º; S2, ~150º) was observed for

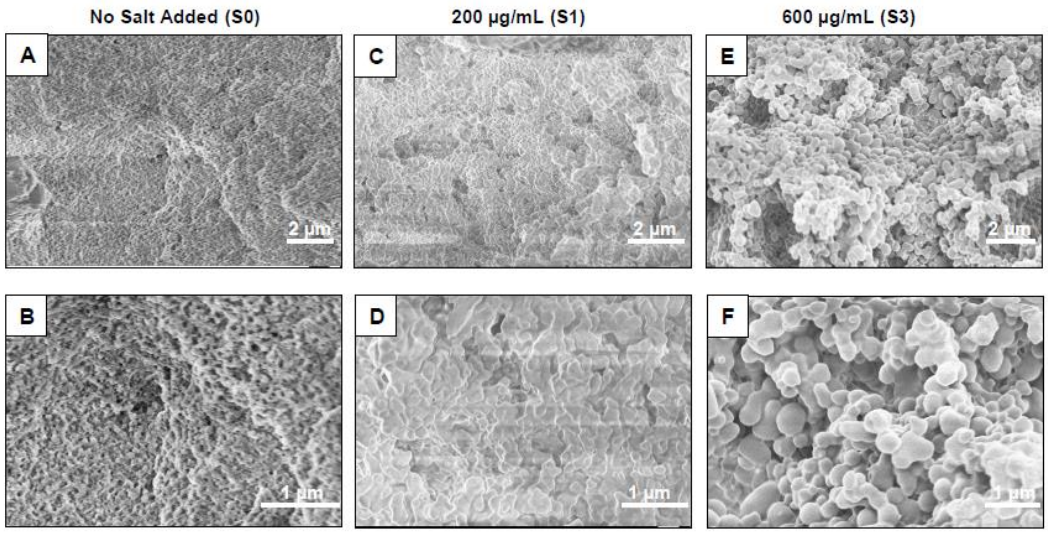

Figure 2.4. (A-F) FESEM images of polymeric gel without any salt (A, B), with 200 µg/mL (C, D) and with 600 µg/mL of NaCl (E, F) with lower (A, C, E) and higher (B, D, F) magnifications respectively.

decylamine treated polymeric materials that were synthesized in the presence of NaCl salt (Figure 2.5E-I). On further increasing the salt doping level (600 µg/mL), the polymeric gel (S3) transformed from superhydrophilic (with contact angle 0°, Figure 2.5K) to nonadhesive superhydrophobic (θ_{adv} ≈ 159° and with roll-off angle of 3°, Figure 2.5L) after post chemical treatment with decylamine molecules. The post chemical modification of the polymeric materials (that is synthesized in presence of salt) with decylamine molecule were analyzed with FTIR spectra as shown in Figure 2.5 D, G, J. Moreover, a significant decrement in surface energy was noted in the synthesized material (S3) after decylamine treatment (24.14 mN/m) in comparison to that of the untreated sample (72.71 mN/m), which further reveals that the post chemical functionalization of the "reactive" polymeric material with decylamine molecules provided the essential low surface energy to display the superhydrophobic property.

An aqueous droplet (5 µL) dispensed from 7 mm height made an impact on the horizontal superhydrophobic surface and rebounded three times (Figure 2.6A-E) before it settled on the polymeric interface. A stream of liquid water that was sprayed on a tilted (~45°) superhydrophobic material for 30 min bounced away from the surface continuously after hitting the material (inset of Figure 2.7A left side). The superhydrophobic property remained intact even after around 1000 droplets (~5 µL each) were imparted on the same

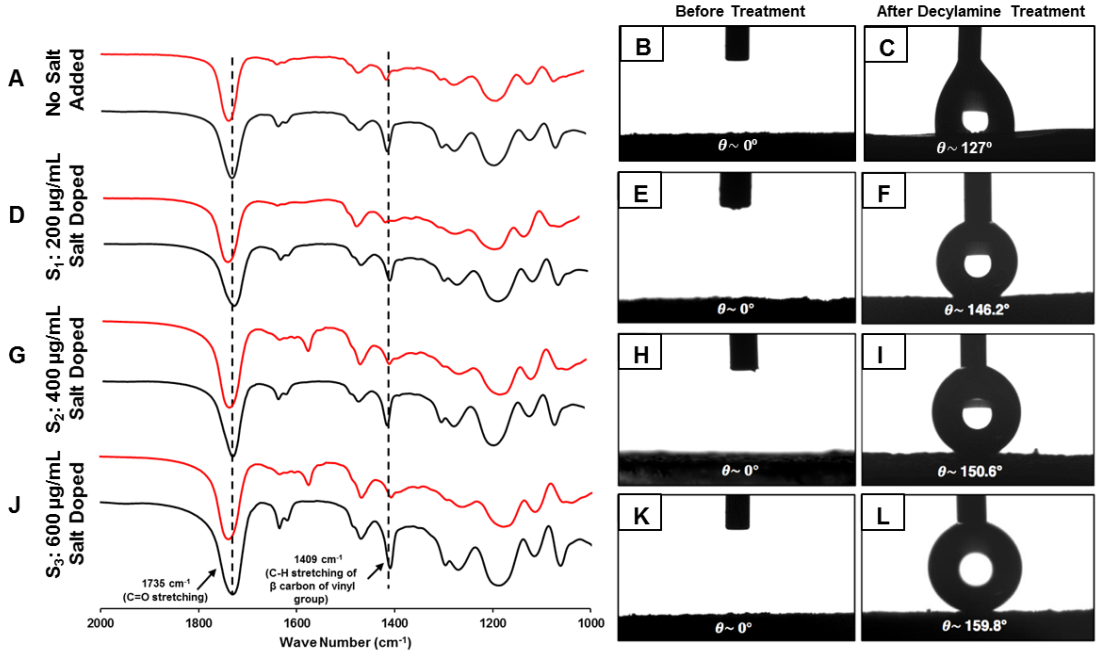

Figure 2.5 (A, D, G, J) FTIR spectra reveals the post chemical modification. The residual acrylate peak at 1410 cm^{-1} (black spectrum) intensity was significantly depleted after post chemical modification (red spectrum) with decylamine molecules B-L) water contact angle images reveals the effect of post chemical functionalization (with decylamine molecule) on the liquid water wettability. Polymeric gels without any salt (B-C) (S1:200 µg/mL; S2:400 µg/mL; S3:600 µg/mL) that are doped with salts (NaCl), changed from hydrophilic (0˚; B, E, H, K) polymeric gels to highly hydrophobic (C, θ_{adv}~127º), (F, θ_{adv}~146º), adhesive superhydrophobic (I, θ_{adv}~150º, θ_{hys}~11º) and nonadhesive superhydrophobic (L, θ_{adv}~159º, θ_{hys}~4º) materials on post chemical treatment with decylamine molecules.

area of the superhydrophobic material. Moreover, the material appeared shiny and reflective when it was submerged in water, because of the presence of trapped air (can be

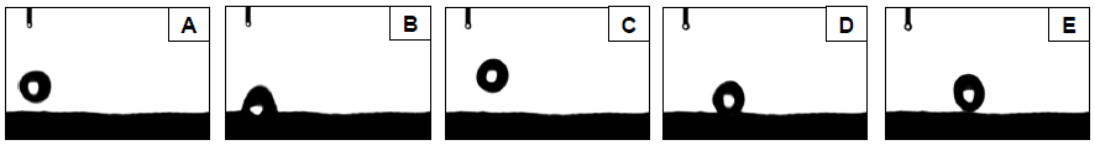

Figure 2.6. (A-E) Images of a bouncing water droplet on the horizontal superhydrophobic material.

explained based on Cassie−Baxter model) within the material, (inset Figure 2.7A right side), and superhydrophobicity remained unaltered even after continuous submersion in water for more than 50 days as is evident in Figure 2.7A.

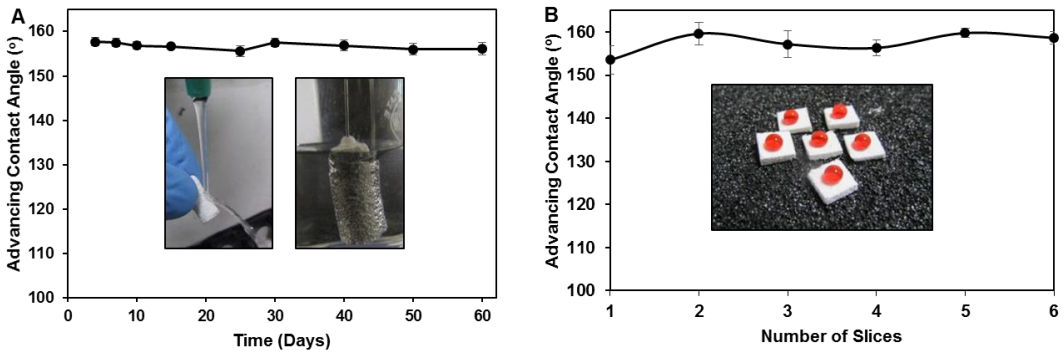

Figure 2.7. (A) Plot accounts the anti-wettability of the decylamine treated material that was submerged in water for 60 days and the superhydrophobicity of the material remained intact. Inset is the digital images showing the stream of water is readily bounced away after hitting the superhydrophobic surface (left) and shiny liquid water-polymeric material interface (right), which reveals the presence of metastable trapped air. B) Accounts the anti-wetting property of the aqueous droplet on arbitrarily sliced interior of the polymeric bulk (inset) super hydrophobic material.

2.4.2. Physical and Chemical Durability of Bulk Superhydrophobic Material

Additional experiments were performed to examine the durability of the embedded superhydrophobicity in the material The superhydrophobic material was arbitrarily sliced to expose the interior of the polymeric material (Figure 2.7B) and interestingly, the water droplets beaded on the freshly exposed interface (solid/air) with advancing contact angle above 155° (Figure 2.7B). Thus, this study suggests that both the interior and the top surface of the material are capable of displaying superhydrophobicity. Various other severe physical abrasions that are well known to disrupt the anti-wetting property of conventional superhydrophobic materials were performed on the synthesized material to examine its overall durability. For instance, in sand drop test, 150 g of sand grains was poured onto the material from a height of 20 cm (Figure 2.8A). No apparent physical change or damage was noticed after this treatment; moreover, the superhydrophobicity remained intact as confirmed with contact angle measurements (Figure 2.8B, C). In sand paper abrasion test, the surface of the superhydrophobic material was rubbed with abrasive sand paper (Figure 2.8D) multiple times resulting in significant loss of material in the form of white powder (found on the surface of the sandpaper), however, both this sacrificed white powder and the exposed underlying surfaces displayed strong repellency to liquid water with advancing contact angle above 155° as shown in Figure 2.8E-F. In scratch test, the material was deeply

scratched manually (Figure 2.8G), but the anti-wetting property remained unperturbed on the scratched region of the material as is shown in Figure 2.8G, H. In adhesive tape test, the exterior of the material was manually brought in contact with adhesive tape with applied load of 500 g and then the tape was peeled off. This process led to random cleaving and transfer of some material to the adhesive tape surface (Figure 2.8I); however, the exposed surface still displayed anti-wetting property (Figure 2.8J, K). These results further supports the existence of "internal" superhydrophobicity within the material. The current studies confirm that the anti-wetting property of the material can withstand a wide range of physical

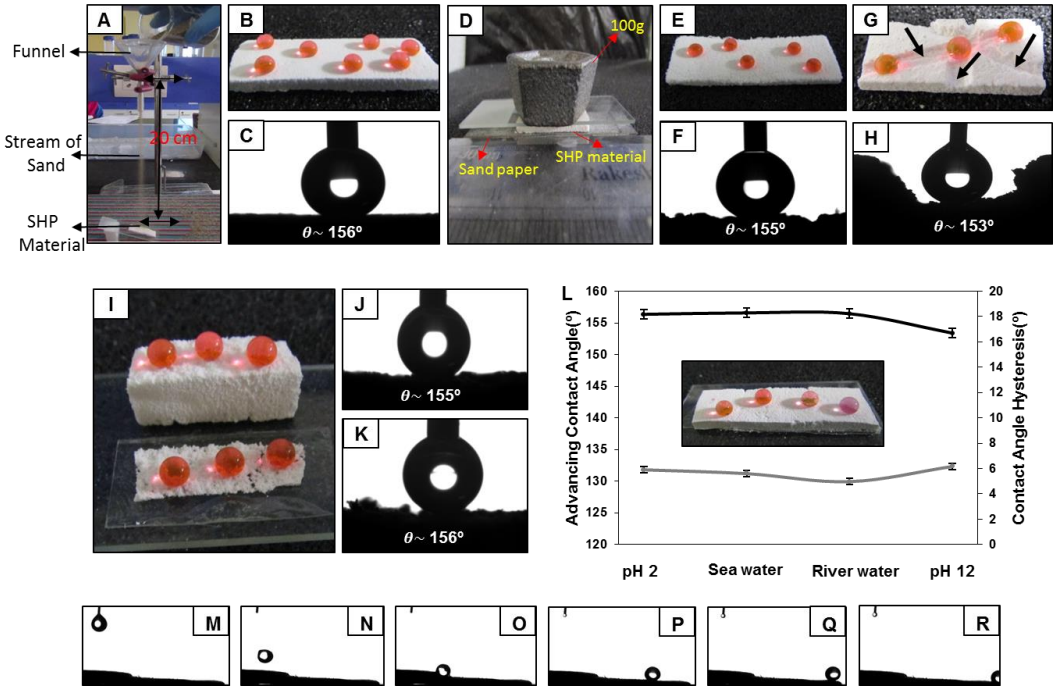

Figure 2.8. (A) Schematic depiction of experimental setups is used for sand drop. B-C) Digital image (B) and contact angle image (C) of beaded water droplets on the superhydrophobic material after sand drop test. D) Schematic depiction of experimental setup used for sand paper abrasion. E-F) Digital image (E) and contact angle image (F) of beaded water droplets on the superhydrophobic material after sand paper abrasion test. G-H) Digital image (G) and contact angle image (H) of beaded water droplets on the superhydrophobic material after scratch test. I-K) Digital image (I) and contact angle images (J, K) of beaded water droplet on the exposed interior of the material after adhesive tape peeling test. L) Plot showing the advancing contact angle (black) and contact angle hysteresis (grey) of acidic solution (pH 1), alkaline solution (pH 12), artificial seawater and river (Brahmaputra, Assam, India) water on the superhydrophobic surface. M-R) Images showing the rolling of water droplet on the scratched (top) and sand paper abrasion (bottom) superhydrophobic surface at tilt angle of 5°.

insults, including various physical damages to the material. The chemical durability of the superhydrophobic material was further explored in which the superhydrophobic surface was exposed to various harsh chemical environments, including extremes of pH (2 and 12), artificial seawater and river (Brahmaputra, Assam, India) water. The anti-wetting property of the material remained intact even after exposure to such harsh chemical environments (Figure 2.8L) for 1 h. Moreover, the rolling of beaded water droplet from the tilted (5º) superhydrophobic material even after incurring scratches and sand paper abrasions on the surface of the superhydrophobic material is shown in Figure 2.8M-R. These results implies that the as synthesized material can withstand various physical and chemical insults without compromising its nonadhesive anti-wetting property.

2.4.3. Tailoring the Shape and Water Wettability of the Polymeric Material

The existence of residual acrylate groups in the covalently cross-linked and porous polymeric gel (salt-doped, S3) network provides a means for tailoring the water wettability in the material by facile post chemical functionalization with appropriate amine-containing small molecules as shown in Figure 2.9A, from propylamine (C3) to decylamine (C10). The post chemical modification was characterized with FTIR spectral analysis, where the characteristic signature for residual acrylate groups at 1410 cm^{-1} (which appears because of the symmetric deformation of the C−H bond for the β carbon of the vinyl group) was noticed to be reduced significantly upon treatment of the polymeric material with strategically (propylamine, short hydrocarbon tail, to decylamine, long hydrocarbon tail) selected primary amine containing small molecules, as shown in Figure 2.9B. The significant change in wetting behavior (θ_{adv} = 143°) compared to that of untreated material (0°) is first observed upon post chemical functionalization with pentylamine (C5) molecules (Figure 2.10E, F) and hydrophobicity further improved on modification with more hydrophobic small molecules (C6, θ_{adv} = 145°; C7, θ_{adv} = 149°). Adhesive (with θ_{Hys} ≈ 14°) superhydrophobicity (θ_{adv} = 152°, Figure 2.10K, L) was observed on covalent immobilization of octylamine (C8), while nonadhesive (with roll off angle 3°) superhydrophobicity (θ_{adv} = 159°, Figure 2.10M, N) was noticed after treatment with decylamine molecules. Thus, the result here provides facile basis for systematic tailoring of liquid water wettability of material in air from hydrophilic to adhesive and nonadhesive superhydrophobic. Moreover, various rigid substrates (Zn metal, glass) can be further

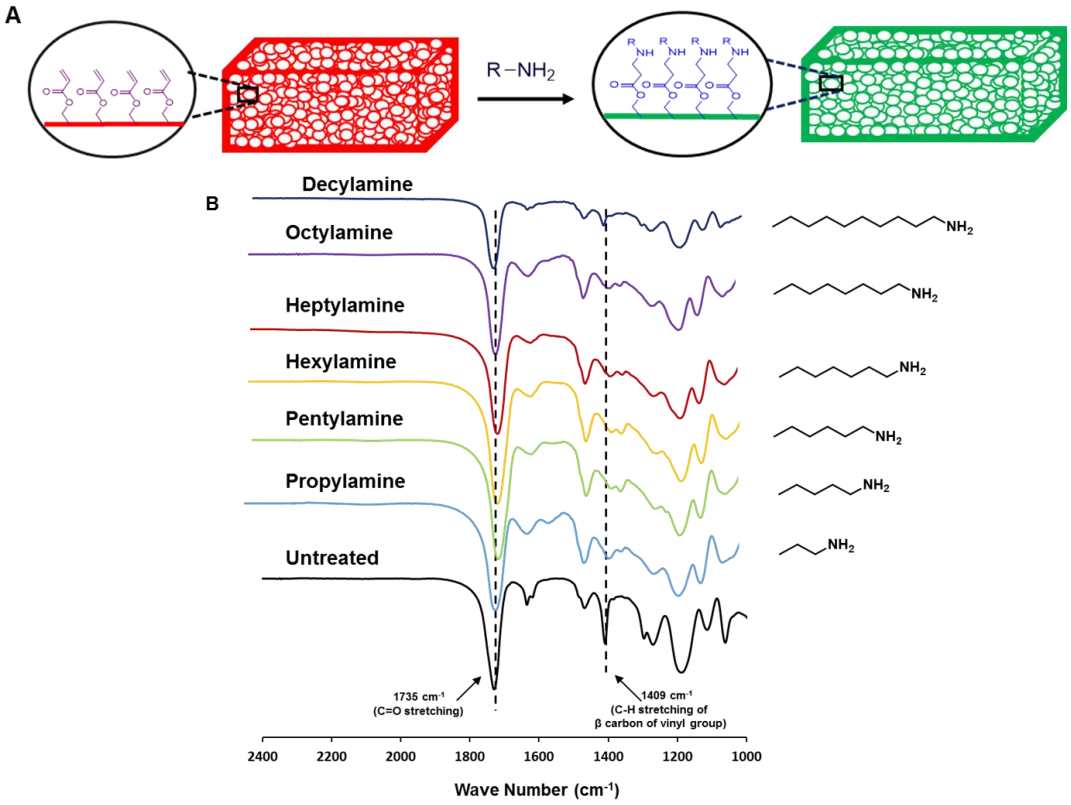

Figure 2.9. (A) Schematic illustration of porous and "reactive" polymeric material with random granular structures and residual acrylate groups that can be used in post modification of the material with amine-containing small molecules via 1, 4-conjugate addition reaction. B) FTIR spectra of salt doped polymeric material (S3) before (black) and after post chemical modification (propylamine; blue, pentylamine; green, hexylamine; yellow, heptylamine; red, octylamine; violet and decylamine; dark blue) with primary amine containing small molecules (propylamine, butylamine, pentylamine, hexylamine, heptylamine, octylamine and decylamine). The peaks at 1736 cm^{-1} and 1410 cm^{-1} denoted the carbonyl stretching and symmetric deformation of the C−H bond for the β carbon of the vinyl group respectively. Peaks at 1410 cm^{-1} are significantly reduced in the polymeric material (S3) after post chemical modification with primary amine containing small molecules in comparison to untreated.

coated with this superhydrophobic material (Figure 2.11A-D). In the recent past, 3D superhydrophobic materials have emerged as a potential approach for developing a long-term and sustained small molecules release systems.[36,44–46] The as synthesized materials can be further loaded with small hydrophilic molecules (e.g., rhodamine-6G) without compromising the anti-wetting property (Figure 2.11G, H) and such loaded molecules are distributed uniformly, including the surface and interior of the material. This might

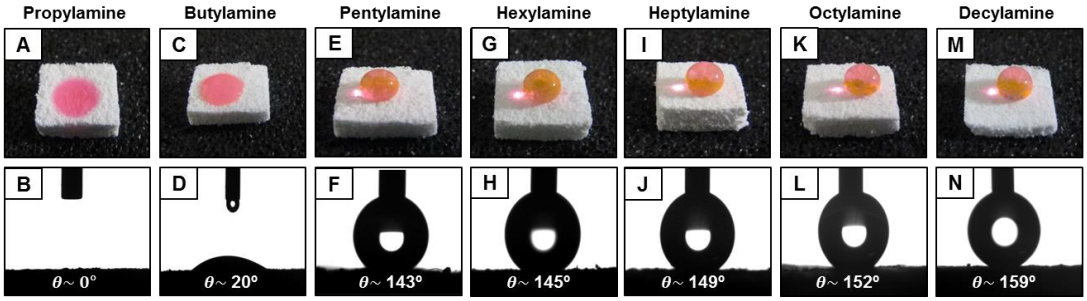

Figure 2.10. (A-N) Digital images (A, C, E, G, I, K, M) and contact angle images (B, D, F, H, J, L, N) of beaded water droplets on propylamine (A, B), butylamine (C, D), pentylamine (E, F), hexylamine (G, H), heptylamine (I, J), octylamine (K, L) and decylamine (M, N) treated polymeric materials.

certainly be of use in developing sustained drug delivery vehicles. Furthermore, the self-cleaning property was also demonstrated where the deposited dust is removed on exposing the superhydrophobic surface to liquid water as shown in Figure 2.12A-D, and the self-cleaning performance was compared with the bare glass where the deposited dust turned muddy on exposing to liquid water (Figure 2.12E-H). These unique properties, along with the ability to coat several substrates and the scalability of the material with arbitrary shapes

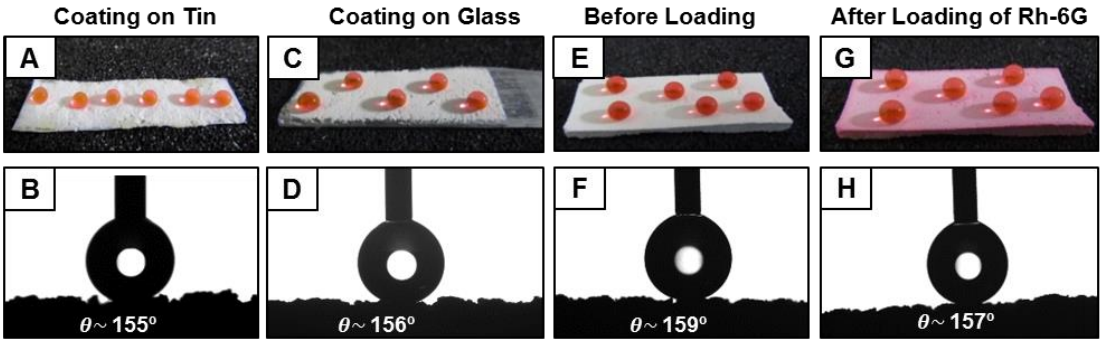

Figure 2.11. (A-D) Digital images (A, C) and contact angle images (B, D) of beaded water droplet on bulk superhydrophobic material coating on a tin metal plate (A, B) and glass (C, D). E-H) Digital images (E, G) and contact angle images (F, H) of beaded water droplet on superhydrophobic material before (E, F) and after (G, H) loading of Rhodamine-6G.

and sizes, can substantially extend the potential utility of this system in different practical settings compared to conventional thin 'surface only' chemically and physically less durable synthetic water repellant surfaces. However, some important applications of our

material are restricted in comparison to other materials[47] due to its lack of transparency to visible light.

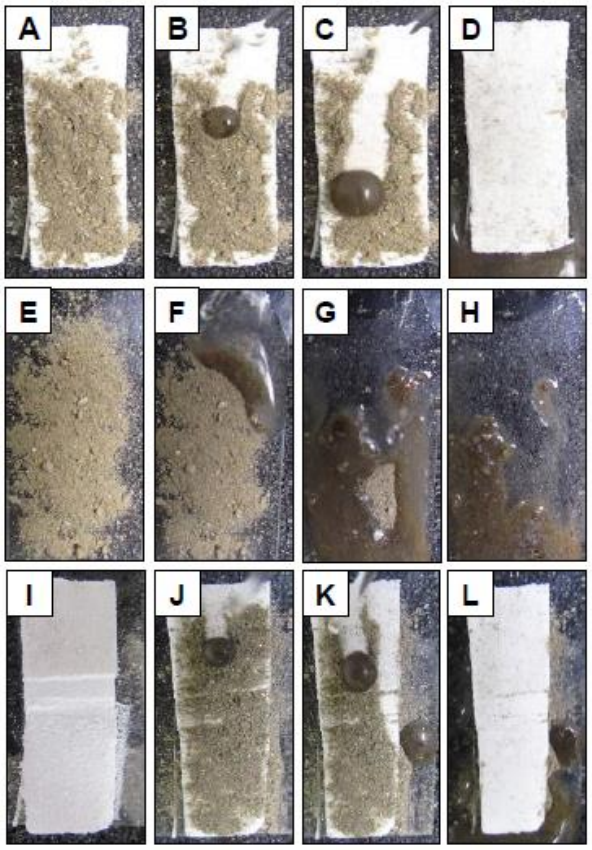

Figure 2.12. (A-D, I-L) Digital images illustrating the self-cleaning process on superhydrophobic surface before (A-D) and after (I-L) abrasion (scratched (middle) and sand paper abrasion (bottom) processes. Polymeric surfaces were first made dirty with dust grains (A, J) prior to drop (B-C, J-K) water droplets on the non-abraded (A) and abraded (J) superhydrophobic materials.

2.5. Conclusion

In this chapter, a scalable, robust and bulk superhydrophobic material using a salt-doped "reactive" polymeric gelation approach is presented. During the fabrication process, the semi-solid polymeric gel material provides an opportunity to manipulate the shape and size of the material. The anti-wetting property of the material is highly durable, even at harsh chemical and physical settings. The liquid water wettability of the polymeric material can be tailored either by changing the salt doping level (manipulating the topography of material) in polymeric gel synthesis process or by selection of appropriate post chemical

modification of the chemically reactive polymeric material with different functional small molecules. We anticipate that this synthetic strategy will be useful in developing advanced and multifunctional materials for further extending the application of this anti-wetting property in practical scenarios.

References

(1) Liu, Y. L.; B. Q.; Jiang, L.; Zhu, D. B. *Adv. Mater*. **2002**, *14*, 1857−1860.

(2) Li, X. M.; Reinhoudt, D.; Crego-Calama, M. *Chem. Soc. Rev*. **2007**, *36*, 1350−1368.

(3) Zhang, X.; Shi, F.; Niu, J.; Jiang, Y. G.; Wang, Z. Q. *J. Mater. Chem*. **2008**, *18*, 621−633.

(4) Yao, X.; Song, Y.; Jiang, L. *Adv. Mater*. **2011**, *23*, 719−734.

(5) Ueda, E.; Levkin, P. A. *Adv. Mater*. **2013**, *25*, 1234−1247.

(6) Wen, L.; Tian, Y.; Jiang, L. *Angew. Chem. Int. Ed*. **2015**, *54*, 3387−3399.

(7) Gao, A.; Wu, Q.; Wang, D.; Ha, Y.; Chen, Z.; Yang, P. *Adv. Mater*. **2016**, *28*, 579−587.

(8) Li, C.; Boban, M.; Snyder, S. A.; Kobaku, S. P. R.; Kwon, G.; Mehta, G.; Tuteja, A. *Adv. Funct. Mater*. **2016**, *26*, 6121−6131.

(9) Yu, C.; Cao, M.; Dong, Z.; Wang, J.; Li, K.; Jiang, L. *Adv. Funct. Mater*. **2016**, *26*, 3236−3243.

(10) Yan, Y. Y.; Gao, N.; Barthlott, W. *Adv. Colloid Interface Sci.* **2011**, *169*, 80−105.

(11) Feng, X.; Jiang, L. *Adv. Mater*. **2006**, *18*, 3063−3078.

(12) Artus, G. R. J.; Jung, S.; Zimmermann, J.; Gautschi, H. P.; Marquardt, K.; Seeger, S. *Adv. Mater*. **2006**, *18*, 2758−2762.

(13) Verho, T.; Bower, C.; Andrew, P.; Franssila, S.; Ikkala, O.; Ras, R. H. A. *Adv. Mater*. **2011**, *23*, 673−678.

(14) Ionov, L.; Synytska, A. *Phys. Chem. Chem. Phys*. **2012**, *14*, 10497−10502.

(15) Zimmermann, J.; Reifler, F. A.; Fortunato, G.; Gerhardt, L. C.; Seeger, S. *Adv. Funct. Mater*. **2008**, *18*, 3662−3669.

(16) Deng, X.; Mammen, L.; Zhao, Y.; Lellig, P.; Mullen, K.; Li, C.; Butt, H. J.; Vollmer, D. *Adv. Mater*. **2011**, *23*, 2962−2965.

(17) Deng, X.; Mammen, L.; Butt, H. J.; Vollmer, D. *Science* **2012**, *335*, 67−70.

(18) Xue, C. H.; Ma, J.-Z. *J. Mater. Chem. A* **2013**, *1*, 4146−4161.

(19) Yao, X.; Xu, L.; Jiang, L. *Adv. Funct. Mater*. **2010**, *20*, 3343−3349.

(20) Jung, Y. C.; Bhushan, B. *ACS Nano* **2009**, *3*, 4155−4163.

(21) Deng, X.; Mammen, L.; Zhao, Y.; Lellig, P.; Mullen, K.; Li, C.; Butt, H.-J.; Vollmer, D. *Adv. Mater*. **2011**, *23*, 2962−2965.

(22) Zimmermann, J.; Reifler, F. A.; Fortunato, G.; Gerhardt, L.−C.; Seeger, S. *Adv. Funct. Mater*. **2008**, *18*, 3662−3669.

(23) Mates, J. E.; Bayer, I. S.; Palumbo, J. M.; Carroll, P. J.; Megaridis, C. M. *Nat. Commun*. **2015**, *6*, 8874−8881.

(24) Paven, M.; Fuchs, R.; Yakabe, T.; Vollmer, D.; Kappl, M.; Itakura, A. N.; Butt, H. − J. *Adv. Funct. Mater.* **2016**, *26*, 4914−4922.

(25) Yang, J.; Zhang, Z. Z.; Men, X. H.; Xu, X. H.; Zhu, X. T. *Colloids Surf. A* **2010**, *367*, 60−64.

(26) Zhu, X. T.; Zhang, Z. Z.; Men, X. H.; Yang, J.; Wang, K.; Xu, X. H.; Zhou, X. Y.; Xue, Q. J. *J. Mater. Chem*. **2011**, *21*, 15793−15797.

(27) Wu, M.; Li, Y.; An, N.; Sun, J. *Adv. Funct. Mater*. **2016**, *26*, 6777−6784.

(28) Li, Y.; Li, L.; Sun, J. Q. *Angew. Chem. Int. Ed*. **2010**, *49*, 6129-6133.

(29) Wang, H. X.; Xue, Y. H.; Ding, J.; Feng, L. F.; Wang, X. G.; Lin, T. *Angew. Chem. Int. Ed.* **2011**, *50*, 11433−11436.

(30) Wang, X. L.; Liu, X. J.; Zhou, F.; Liu, W. M. *Chem. Commun*. **2011, 4***7*, 2324−2326.

(31) Manna, U.; Lynn, D. M. *Adv. Mater*. **2013**, *25*, 5104−5108.

(32) Manna, U.; Carter, M. C. D.; Lynn, D. M. *Adv. Mater*. **2013**, *25*, 3085−3089.

(33) Levkin, P. A.; Svec, F.; Frechet, J. M. *Adv. Funct. Mater*. **2009**, *19*, 1993−1998.

(34) Manna, U.; Broderick, A. H.; Lynn, D. M. *Adv. Mater*. **2012**, *24*, 4291−4295.

(35) Zhu, X. T.; Zhang, Z. Z.; Ren, G. N.; Yang, J.; Wang, K.; Xu, X. H.; Men, X. H.; Zhou, X. Y. *J. Mater. Chem*. **2012**, *22*, 20146−20148.

(36) Yohe, S. T.; Colson, Y. L.; Grinstaff, M. W. *J. Am. Chem. Soc*. **2012**, *134*, 2016−2019.

(37) Ramakrishna, S.; Kumar, K. S. S.; Mathew, D.; Nair, C. P. R. *Sci. Rep*. **2015**, *5*, 18510−18521.

(38) Yohe, S. T.; Freedman, J. D.; Falde, E. J.; Colson, Y. L.; Grinstaff, M. W. *Adv. Funct. Mater*. **2013**, *23*, 3628−3637.

(39) Farrer, R. A.; LaFratta, C. N.; Li, L.; Praino, J.; Naughton, M. J.; Saleh, B. E. A.; Teich, M. C.; Fourkas, J. T. *J. Am. Chem. Soc*. **2006**, *128*, 1796−1797.

(40) Weatherspoon, M. R.; Dickerson, M. B.; Wang, G.; Cai, Y.; Shian, S.; Jones, S. C.; Marder, S. R.; Sandhage, K. H. *Angew. Chem. Int. Ed*. **2007**, *46*, 5724−5727.

(41) Ford, J.; Marder, S. R.; Yang, S. Shu Yang. *Chem. Mater*. **2009**, *21*, 476−483.

(42) Wang, G.; Fang, Y.; Kim, P.; Hayek, A.; Weatherspoon, M. R.; Perry, J. W.; Sandhage, K. H.; Marder, S. R.; Jones, S. C. *Adv. Funct. Mater*. **2009**, *19*, 2768−2776.

(43) Bechler, S. L.; Lynn, D. M. *Biomacromolecules* **2012**, *13*, 1523−1532.

(44) Manna, U.; Kratochvil, M. J.; Lynn, D. M. *Adv. Mater*. **2013**, *25*, 6405−6409.

(45) Wang, J.; Kaplan, J. A.; Colson, Y. L.; Grinstaff, M. W. *Angew. Chem. Int. Ed.* **2016**, *55*, 2796−2800.

(46) Kratochvil, M. J.; Welsh, M. A.; Manna, U.; Ortiz, B. J.; Blackwell, H. E.; Lynn, D. M. *ACS Infect. Dis*. **2016**, *2*, 509−517.

(47) Aslanidou, D.; Karapanagiotis, I.; Panayiotou, C. *Mater. Des.* **2016**, *108*, 736−744.

Chapter 3: Role of Alkali Metal Salts in Synthesis of Michael Addition Mediated Superhydrophobicity*

In general, lotus leaf and rose petal-inspired wettabilities are artificially developed through the integration of hierarchical topography and essential chemical functionality. However, a fundamental and important aspect of this nature-inspired wettability has not yet been addressed i.e. amongst hierarchical topography and essential chemical functionality, which is the more sensitive parameter for these nature-inspired special wettability? The design of a common approach for tailoring both the hierarchical topography and chemical functionality is highly essential for investigating such a relevant fundamental aspect, however, the synthesis of such material is extremely difficult in reality. In this chapter, Michael addition reaction mediated gelation of BPEI/5-Acl mixture was found to be facilitated in the presence of alkali metal salts. Interestingly, the mixture of BPEI and 5-Acl in ethanol transformed into a chemically reactive polymeric gel with tailored hierarchical features depending on the selection of appropriate alkali metal salts in the reaction mixture. This chapter investigates the impact of change in hierarchical topography on the nature-inspired super-wettability while the chemical functionality remains intact. On the other side, the residual chemical reactivity of the hierarchical interfaces allowed us to examine the change in the chemical functionalities independently and precisely. The post-covalent modification with longer and shorter hydrocarbon tails has a significant impact in controlling the metastable trapped air in the artificially biomimicked interfaces, and eventually controls the Wenzel, Cassie–Wenzel and Cassie–Baxter transition states. This current approach also allows us to modulate other relevant physical properties in the material including the shrinkage and compressive modulus of the material after removal of the reaction solvent. The materials with durable physical properties were successfully exploited for the separation and collection of different forms of oil spills through both selective absorption and gravity-driven filtration process, even under practically relevant severe settings.

*****Rather, A. M.; Shome, A.; Kumar, S.; Bhunia, B. K.; Mandal, B. B.; Srivastava, H. K.; Manna. U. *J. Mater. Chem. A* **2018**, *6*, 17019–17031.

Chapter 3

3.1. Introduction

In general, chemistry and topography are instrumental in the synthesis of various smart and functional materials. In this context, polymeric materials with hierarchical topography (refers to the co-existence of micro/nano scale features) are widely recognized for their prospective applications in gas storage, separation, bioengineering, support for catalysts, drug delivery, sensing and removal of pollutants, etc.[1–5] Furthermore, the strategic integration of appropriate hierarchical topography with essential chemistry is the general basis for developing materials with nature-inspired wettability.[6,7] As mentioned in chapter 1, several top down and bottom up approaches were introduced to synthesize hierarchical topography on selected substrates in the last few decades.[8–10] The appropriate optimization of chemistry on these hierarchically featured interfaces provided thin and conventional coatings that displayed lotus leaf-inspired wettability.[11–18] Few fundamental studies were carried out to examine the role of this hierarchical topography in nature-inspired wettability, where interfaces with (1) micro-features, (2) nano-features and (3) hierarchical (combination of micro/nano) features were separately synthesized maintaining the same chemistry.[19,20] Nonadhesive superhydrophobicity was only observed for interfaces having lotus leaf mimicked hierarchical features.[19,20] Furthermore, the bouncing of water droplets on various natural (i.e., wings of Morpho butterfly, lotus leaf and nasturtium leaf) and biomimetic artificial interfaces having different hierarchical topography (that are prepared following different synthesis procedures) was also examined.[21] The arrangement and dimensions of the nano/micro features in natural hierarchical interfaces followed a specific pattern;[21–23] however, several lotus leaf-inspired artificial hierarchical interfaces have random hierarchy as reported in the literature.[8–10] Nevertheless, the impact of this change in artificial hierarchy in the synthesized material on the biomimicked wettability is not examined in detail. A design where hierarchical topography and chemical functionality can be tailored appropriately is imperative for investigating the nature of dependency of the biomimetic wettability on physical and chemical parameters. Appropriate chemistry and hierarchical topography are primary requirements for synthesizing artificial superhydrophobic materials,[8–10,19,20] but which (hierarchical topography or chemistry) is the more sensitive parameter for lotus-leaf inspired wettability is yet to be addressed in the literature. In this chapter, an alkali metal salt assisted Michael addition reaction is exploited

to design a material to examine the impact of change on (a) the topography and (b) chemical optimization on the bio-inspired wettability. Here, in this current approach, a branched polymer is directly and covalently converted into a polymeric material with (i) readily amine reactive tailored hierarchical topography and (ii) tunable relevant physical properties (e.g., elasticity, shrinkage, porosity, etc.). In the chapter 2, I, have discussed that a mixture of branched polyethylenimine (BPEI) and dipentaerythritol pentaacrylate (5-Acl) in ethanol was transformed into a polymeric gel, and in the presence of NaCl salt, this sol-gel transformation was rapid and the polymeric gel was capable of displaying three dimensional and robust superhydrophobicity.[24] Here in this chapter a detailed study of various alkali metal salts on the gelation of polymeric material was performed. This current chemical approach provided a facile basis for tailoring hierarchical topography and other relevant physical properties in the polymeric material. Furthermore, the synthesized material with tailored topography is observed to be chemically reactive with primary amine groups due to the presence of residual acrylate groups. Thus, this current chemical approach provided (i) chemically reactive and (ii) tailored hierarchical topography which is strategically exploited in examining the fundamental and important aspects of this lotus leaf-inspired wettability. The nature-inspired interfaces are found to be more sensitive to chemical functionality, rather than the change in hierarchical topography in the super-water repellent interfaces. Interestingly, this current facile chemical approach also allowed us to modulate the mechanical properties of the synthesized polymeric material without using any external nanomaterials (e.g., graphene, carbon nanotubes, clay, etc.) which are commonly used in tailoring the mechanical properties of polymer based soft materials. Furthermore, this biomimicked polymeric material is exploited in demonstration of selective absorption and filtration based oil/water separation from respective oil/water mixtures. Such functional polymeric materials with tailored hierarchical topography and mechanical properties are of potential interest in various other applications including tissue engineering, catalysis, etc.

3.2. Materials and Methods

3.2.1. Materials

Hexane and ethyl acetate and various alkali metal salts including LiCl, KCl, RbCl and CsCl were purchased from RANKEM (Maharashtra, India). Motor oil was purchased from

Castrol India Limited. Dichloromethane (DCM), chloroform were obtained from Merck Life Science Pvt Ltd (Bangalore, India). Methylene blue was purchased from Sigma-Aldrich (Bangalore, India). The details of all other materials and chemicals used in this work were discussed previously in material section of chapter 2.

3.2.2. Preparation of Polymeric Materials with Tailored Topography

The polymeric materials were synthesized following the same procedure as mentioned in the chapter 2. Before preparation of solution of respective reactants (BPEI, 5-Acl), various alkali metal salts including LiCl, NaCl, KCl, RbCl and CsCl were separately dissolved in ethanol maintaining the desired molar concentrations. Then the branched poly(ethyleneimine) (BPEI) and dipentaerythritol penta/hexaacrylate (5-Acl) solutions were prepared separately by dissolving 1.325 g of 5-Acl and 0.5 g of BPEI in 10 mL of ethanol that is doped with different alkali metal salts. Next, the 5-Acl and BPEI were mixed in definite proportions (1 mL of 5-Acl and 0.3 mL of BPEI) and was kept for continuous agitation to form the polymeric gel. The material that was prepared in presence of various alkali metal salt required different time for transforming into gel. The topography of the material was also changed based on the selection of the alkali metal ions in the reaction mixture. The topography of the polymeric gel materials were characterized with FESEM.

3.2.3. General Considerations

The instruments used in this section for characterization of synthesized materials were same as discussed previously in chapter 2.

3.2.4. Tailoring of Water Wettability on Polymeric Material

The water wettability of the synthesized polymeric materials prepared in presence of various alkali metal salts with different amine containing small molecules was carried out using the previously established procedure mentioned in chapter 2.

3.2.5. Physical and Chemical Abrasions

Various physical and chemical abrasions performed in this section were already discussed in chapter 2.

3.2.5.1. UV Exposure

In this test, the synthesized polymeric materials were exposed to UV radiations at short (264nm) and long (385nm) wavelengths with continuous exposure for 30 days and the anti-

wetting property was examined at regular intervals following the water contact angle measurements.

3.2.6. Oil/Water Separation

The oils of density lighter (motor oil, silicon oil, vegetable oil) as well as heavier (chloroform) than water were separated using the synthesized superhydrophobic material following both selective absorption and filtration processes. For the demonstration of floating oil collection, light oil phase was placed on the air/water interface and then the polymeric material was exposed to the floating oil phase and the floating oil phase was selectively absorbed by the polymeric material. To separate the heavier sediment oil under water, chloroform was used as a model oil in which 5 mL of chloroform was placed under a 20 mL of aqueous phase. Then, the polymeric material was exposed to oil/water mixture and the sediment oil phase under water was selectively absorbed by the material. The same material was also used in gravity driven filtration of both heavy and light oils from respective oil/water mixtures, where a prototype was developed using centrifuge tube and wide opening of the tube was closed with the superhydrophobic monolith and a surface hole was made for pouring the respective oil/water mixtures. The polymeric monolith allowed selective filtration of respective oil phase.

3.3. Results and Discussion

3.3.1. Impact of Alkali Metal Salts on the Controlled Gelation of BPEI Polymer

The 1, 4-conjugate addition of carbon/heteroatoms of nucleophiles to conjugated electrophiles is widely recognized for the synthesis of various important organic molecules. In the past, transition-metals, including zinc, copper, cobalt, rhodium, nickel and palladium, have been strategically and effectively used in performing the desired organic synthesis under mild conditions.[25–32] Recently, Michael addition reaction between unsaturated esters and primary amines under mild conditions was exploited for developing functional polymeric materials.[33–36] Furthermore, the same reaction solution of BPEI/5-Acl rapidly transformed into a polymeric gel in the presence of NaCl[24] as discussed in previous chapter. In this chapter, a detailed study was performed to assess the gelation of polymeric material in presence of different alkali metal salts, where the rate of gelation (that primarily occurred through the Michael addition reaction), hierarchical topography and compressive modulus in the synthesized polymeric materials are tailored in a single step through appropriate

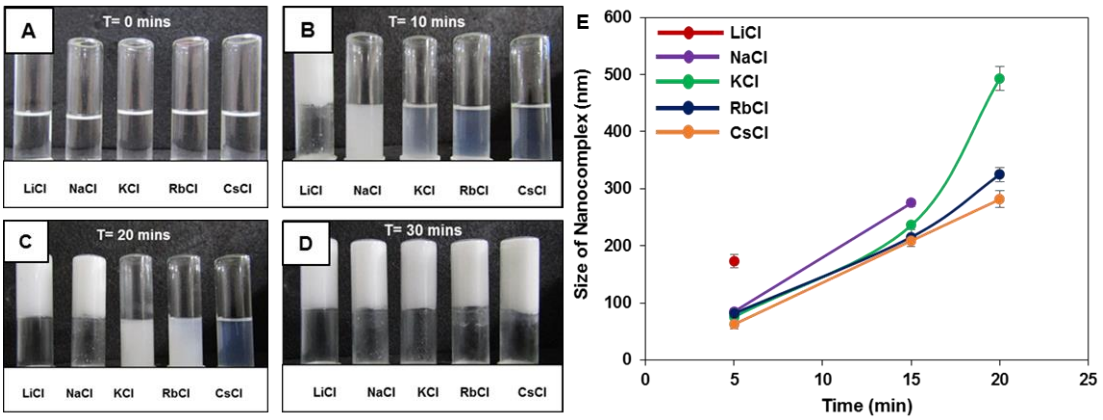

Figure 3.1. (A-D) Digital images showing the visual change in the reaction solution of BPEI/5Acl mixtures that are prepared individually in the presence of various alkali metal salts including LiCl, NaCl, KCl, RbCl and CsCl respectively after 0 mins (A), 10 mins (B), 20 mins (C), 30 mins (D). E) DLS study on the growth of the polymeric nanocomplex forms in the reaction (BPEI/5-Acl) mixtures that are prepared in the presence of various alkali metal salts.

selection of alkali metal salts in the reaction mixture of BPEI/5-Acl in ethanol. BPEI readily reacts with 5-Acl through the Michael addition reaction and yields a milky white solution, which eventually transforms into a gel material after 210 mins. The reaction mixture is transformed into a polymeric gel material through the formation of a reactive nanocomplex as shown in Figure 3.1A-D. Here, different alkali metal salts (e.g., LiCl, NaCl, KCl, RbCl and CsCl) are strategically and independently added to the reaction mixture of BPEI/5-Acl in ethanol. The appearance of milky turbidity in the reaction of BPEI/5-Acl was observed to be faster on decreasing the size of alkali metal ions from CsCl to LiCl, likely due to the faster growth of the nanocomplexes in the reaction mixture as characterized with dynamic light scattering (DLS) (Figure 3.1E). After 5 mins, the size of the nanocomplex in the reaction mixture of BPEI/5-Acl was estimated to be 19 nm in the absence of any alkali metal salt; however, in the presence of alkali metal salts, a sharp increase in the size of the nanocomplex was noted. The size of the nanocomplex was measured to be in the range of 60 to 80 nm in the reaction mixture of BPEI/5-Acl in the presence of metal salt from CsCl to NaCl, and the same reaction mixture was found to have a much bigger nanocomplex (having a mean size of 172 nm) in the presence of LiCl. Eventually, this highly turbid reaction mixture of BPEI/5-Acl (Figure 3.1A, left most glass vial) that was prepared in the presence of LiCl (concentration of 10 mM) in ethanol transformed into a polymeric gel

within 10 mins, and the reaction mixtures (BPEI/5-Acl) that are prepared in the presence of other alkali metal salts remained in the solution state with less or more turbidity depending on the selection of appropriate alkali metal salts as shown in Figure 3.1B. The nanocomplexes that are formed in the reaction mixtures further aggregated through the 1, 4-conjugate addition reaction and eventually transformed into a polymeric gel. The conversion of the reaction mixture into a gel material was found to be slower on increasing the size of alkali metal of the salt as shown in Figure 3.1C, D. Thus, this simple covalent gelation between the branched polymer and 5-Acl molecule in the presence/absence of alkali metal ions have the dramatic impact on the 1, 4-conjugate addition reaction mediated gelation process.

3.3.2. Tailoring of Hierarchical Topography and Other Relevant Physical Properties

The growth of the nanocomplexes that were appeared in the reaction mixture of BPEI/5-Acl was noted to vary in the presence of different alkali metal salts. These differently growing nanocomplexes covalently cross-linked over the time and eventually transformed into a polymeric gel. The topography of the polymeric gels that are prepared in the presence of different alkali metal ions is also noticed to be significantly different as shown in Figure 3.2A-F. In the presence of LiCl, the reaction mixture of BPEI/5-Acl rapidly transformed into a polymeric gel. Even though, at the given time frame, the growth of the nanocomplex

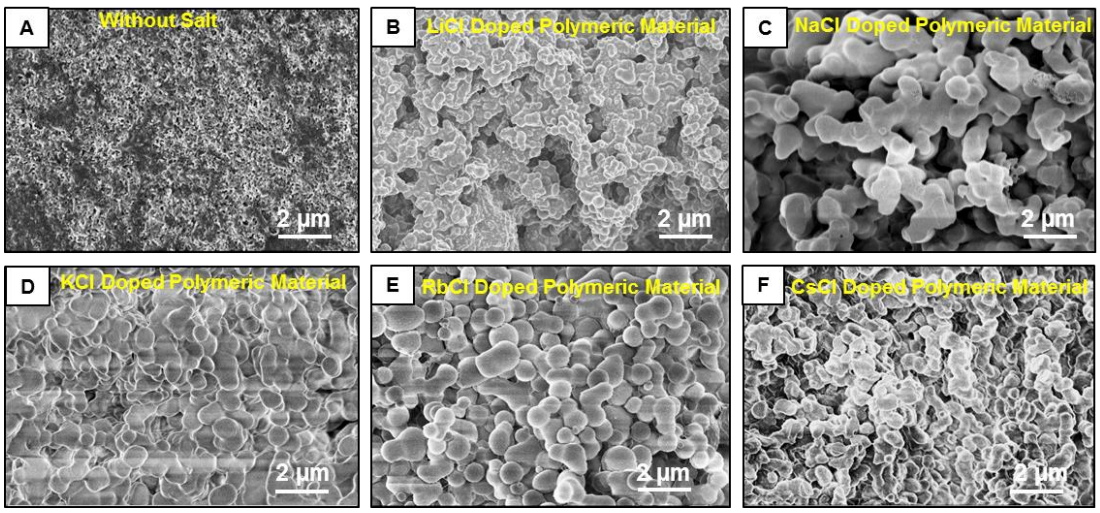

Figure 3.2. (A-F) FESEM images of polymeric materials that are prepared in absence of salt (A) and in presence of various alkali meta salts including LiCl (B), NaCl (C), KCl (D), RbCl (E) and CsCl (F) respectively. (Scale bar: 2 µm).

was estimated to be maximum in comparison to other reaction mixtures that are prepared in the presence of other alkali metal ions, but the rapid conversion of this reaction solution into the polymeric gel led to the formation of covalently cross-linked hierarchical topography that consisted of randomly aggregated smaller granular domains in comparison to other alkali metal assisted gel materials as shown in Figure 3.2B. The size of these granular domains was estimated to be in the range of 200–300 nm. However, the same reaction mixture that is prepared in the presence of CsCl was found to have completely different topography as shown in Figure 3.2F. The reaction mixture of BPEI/5-Acl in the presence of CsCl was converted into a polymeric gel after 30 mins and this gelation rate was three times slower in comparison to the gelation of the same reaction mixture that was prepared in the presence of LiCl and during this time, the polymeric nanocomplexes grew bigger in size and the random association of these bigger nanocomplexes in the polymeric gel provided a completely different topography to the synthesized material (Figure 3.2F). The size of the granular domains was observed to be bigger (in the range of 600 to 700 nm). Thus, the synthesized materials that are prepared from the same composition of BPEI and 5-Acl but in the presence of different alkali metal salts provided different hierarchical topography as shown in Figure 3.2B-F. In addition to change in topography, few other relevant and important properties in the synthesized material were also observed. The shrinkage of the polymeric gel after the evaporation of the volatile reaction solvent (i.e., ethanol) led to reduction in the effective volume of the synthesized material. The polymeric gel that was prepared in the absence of any alkali metal salt shrunk to ~ 60%; however, in the presence of alkali metal salts, the shrinkage of the material after air drying was suppressed as shown in Figure 3.3A. The smaller alkali metal ion salts are more effective in preventing shrinkage of the material; the polymeric gel that is prepared in the presence of LiCl salt shrunk less (25%) compared to that of cesium chloride salt doped polymeric gel (54%) after air drying as shown in Figure 3.3A. The shrinkage of the polymeric material is further reduced by increasing the concentration of alkali metal salt from 10 mM to 30 mM in the reaction mixture of BPEI/5-Acl in ethanol. The percentage of shrinkage of the synthesized polymeric gel during air drying was reduced further from 25% to 15% with the change in the concentration (from 10 mM to 30 mM) of added LiCl in the reaction mixture of BPEI/ 5-Acl as is noted in Figure 3.3A. A very similar trend was noticed for other alkali

metal salts that were present in the reaction mixture during the synthesis of polymeric materials and the shrinkage of the synthesized materials gradually decreased with an increase in the concentration of the respective alkali metal salt in the reaction solution (Figure 3.3A). The polymeric material that was prepared in the presence of LiCl (concentration of 30 mM) was observed to have the least shrinkage (15%) after evaporation of solvent (i.e., ethanol). Furthermore, the topography of the polymeric monoliths that were

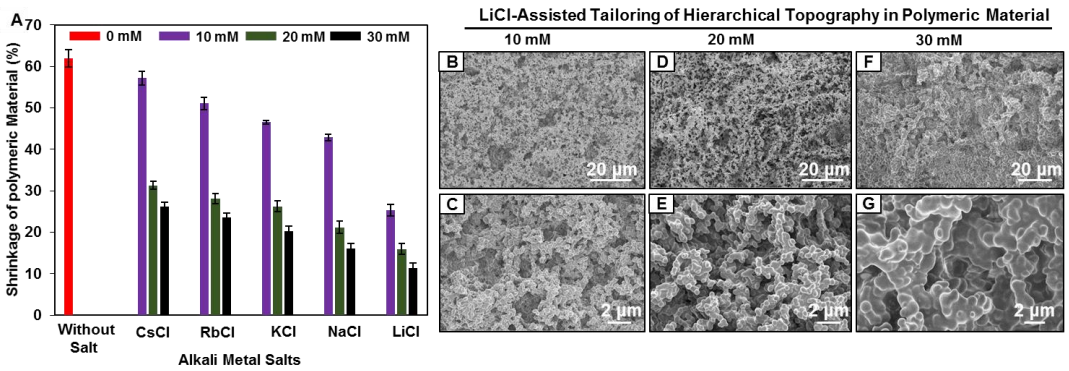

Figure 3.3. (A) Plot illustrating the shrinkage of polymeric materials that are synthesized in the absence (red) and presence (purple, green, and black) of various alkali metal salts including CsCl, RbCl, KCl, NaCl and LiCl after the evaporation of volatile reaction solvent (i.e., ethanol). The impact of change in concentrations (10 mM (purple), 20 mM (green) and 30 mM (black)) of the added alkali metal salts on the shrinkage of the polymeric material is also shown in the graph. B-G) FESEM images of polymeric materials that are prepared in presence of LiCl with different concentrations including 10 mM (B, C), 20 mM (D, E) and 30 mM (F, G) at lower magnifications (B. D, F; scale bar: 20 µm) and higher magnifications (C, E, G; scale bar: 2 µm).

prepared in the presence of different concentrations of LiCl was examined with FESEM study as shown in Figure 3.3B-G. On increasing the concentration of LiCl in the reaction mixture, the hierarchical topography of the polymeric materials was noticed to be different (Figure 3.3B, D, F) and the granular domains were found to be more diffused (Figure 3.3C, E, G). These changes in the topography is likely to help in preventing the shrinkage of the synthesized materials.

Interestingly, another physical property that is the mechanical property of the synthesized polymeric material can be altered depending on the selection of appropriate alkali metal salts in the same reaction mixture of BPEI/5-Acl. The polymeric material that was prepared in the presence of LiCl was most compressible and the material could be compressed to

40% compressive strain after the application of a 200 g load. However, the materials that were prepared in the presence of other alkali metal salts were found to be less compressible under the same applied load (200 g) as shown in Figure 3.4A, C, E, G, I. The compressed materials are fully capable of restoring their initial shape once the applied load was released as shown in Figure 3.4B, D, F, H, J. Furthermore, the compressive modulus was estimated for each of the materials prepared in the presence of various alkali metal salts (Figure 3.4K).

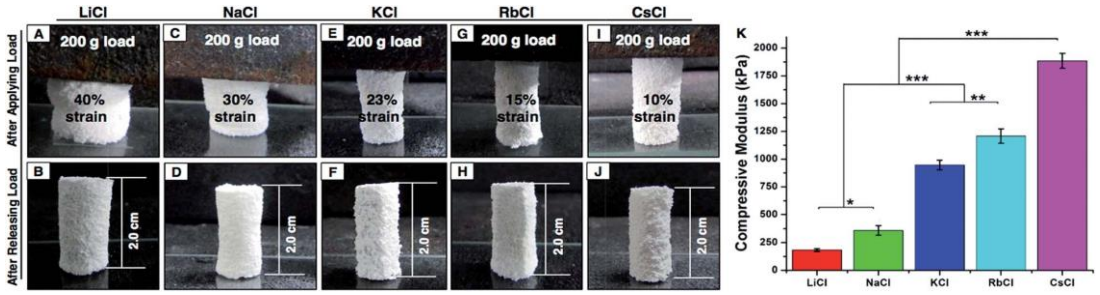

Figure 3.4. (A-J) Digital images depicting the impact of an external applied load (200 g) on the polymeric materials that are synthesized in the presence of LiCl (A, B), NaCl (C, D), KCl (E, F), RbCl (G, H) and CsCl (I, J). Once the load is released, all polymeric materials recovered back to their original shapes and sizes (B, D, F, H, J). K) Plot showing the compressive modulus of polymeric materials that are prepared individually in the presence of various alkali metal salts including LiCl (red), NaCl (green), KCl (blue), RbCl (aqua) and CsCl (magenta), respectively. (K) Data represent mean SD (n = 3), where *p # 0.05, **p # 0.01 and ***p # 0.001.

The polymeric materials that are prepared in the presence of CsCl have the highest compressive modulus of 1884.05±67.09 kPa, whereas the polymeric material prepared in the presence of LiCl displayed the lowest (182.19±12.62 kPa) compressive modulus as shown in Figure 3.4K. Thus, the polymeric materials were more elastic when smaller alkali metal ion salts are added in the reaction mixtures. The variation in the random distribution of the micro/nano features in the presence of different alkali metal salts likely contribute in controlling the compressive modulus of the synthesized material, however, the exact role of alkali metal ion on controlling the mechanical property of the material is not clear yet.

3.3.3. Lotus-Leaf/Rose Petal Inspired Superhydrophobicity

The alkali metal salt assisted synthesized materials with tailored mechanical properties and diverse hierarchical features would be useful for the synthesis of various smart materials. In this context, the hierarchical topography is instrumental for the synthesis of various

nature-inspired interfaces. In this chapter, synthesized materials with different hierarchical topographies were strategically explored for the preparation of durable superhydrophobic

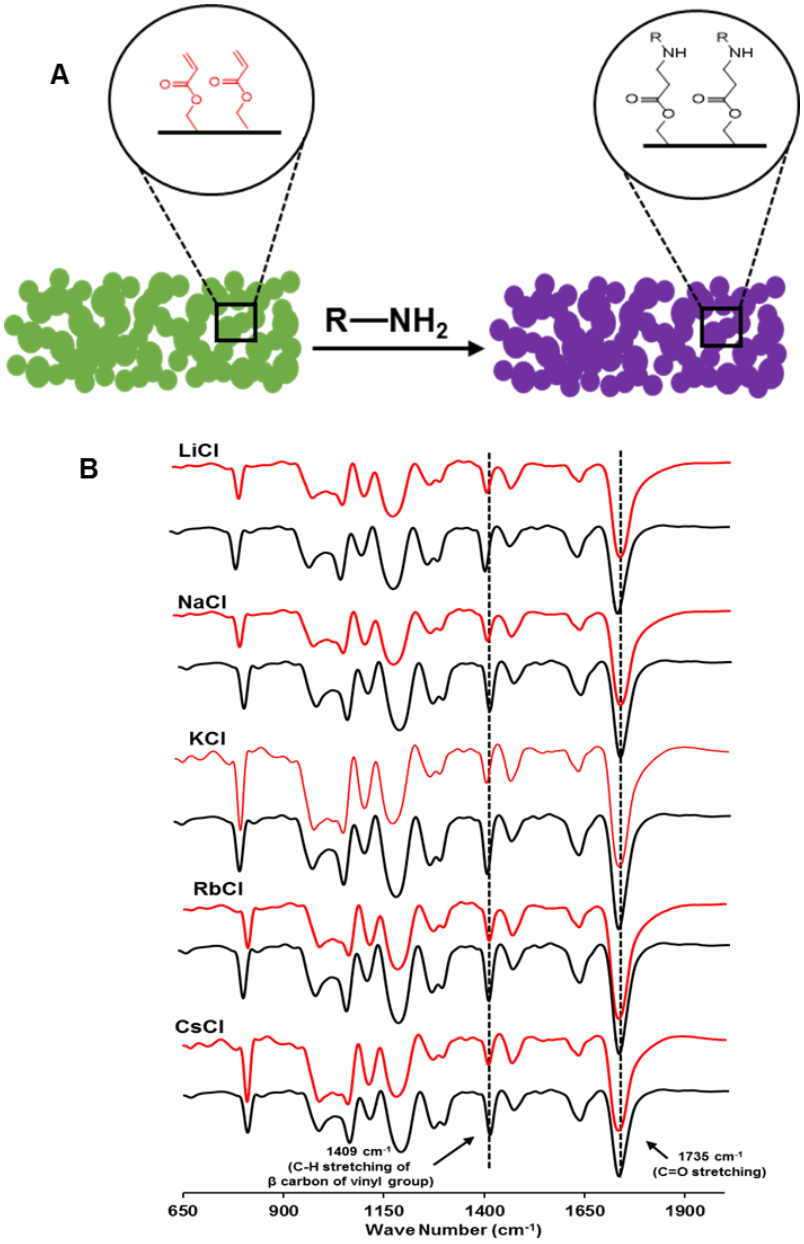

Figure 3.5. (A) Schematic illustration of porous polymeric materials with random granular structures having residual acrylate moieties that can be further post modified with amine containing small molecules via the 1, 4-conjugate addition reaction. B) FTIR spectra of polymeric materials that are synthesized in the presence of various alkali metal salts including LiCl, NaCl, KCl, RbCl and CsCl before (red) and after post chemical modification with decylamine (black). The peak at 1735 cm^{-1} and 1409 cm^{-1} corresponds to carbonyl stretching and symmetric deformation of C–H stretching of β carbon of the vinyl group.

materials. The available reactive chemical functionality (Figure 3.5A) in the synthesized polymeric materials prepared in the presence of different alkali metal salts was examined with FTIR spectral analysis as shown in Figure 3.5B. All the alkali metal salt synthesized materials consist of residual acrylate groups (all red spectra in Figure 3.5B) as confirmed by the presence of characteristic IR peaks at 1409 cm^{-1} and 1735 cm^{-1} that correspond to symmetric deformation of the C–H bond for β carbon of the vinyl group and carbonyl stretching of the ester groups. These residual acrylate functional groups in the synthesized materials provided a facile access for post-covalent modification with primary amines containing small molecules through the 1, 4-conjugate addition reaction. In general, the lotus leaf-inspired special interfaces are developed through appropriate chemical functionalization on top of the essential hierarchical topography mainly following vapor deposition of fluorinated small molecules.[8–10] In the past, mostly silane-based chemistry was associated for the covalent modulation of essential low surface energy coatings[8–20,48] but such chemistry is susceptible under prolonged exposure to UV radiations.[49] In this current work, the essential low surface energy is provided through a robust 1, 4-conjugate addition reaction. The amine reactive polymeric materials were strategically made to react with decylamine molecules (DA) for the covalent optimization of the required low surface energy environment and the successful chemical modification through the 1, 4-conjugate addition reaction was confirmed by FTIR analysis. The IR peaks (black spectra in Figure 3.5B) at 1409 cm^{-1} (characteristic of the symmetric deformation of the C–H bond for β carbon of vinyl groups) depleted significantly with respect to the normalized IR peak at 1735 cm^{-1} (for carbonyl stretching). The carbonyl groups remain preserved during the 1, 4-conjugate addition reaction. Thus, the depletion of the IR peak at 1409 cm^{-1} in the polymeric material after treatment with DA molecules revealed the successful covalent modification with desired chemical functionality as shown in Figure 3.5B. After post modification, the water wettability in air was examined by contact angle measurements. The polymeric materials that are prepared in the presence of different alkali metal salts (with 10 mM concentrations; black bars in Figure 3.6A, B) are capable of displaying lotus leaf-inspired non-adhesive superhydrophobicity with an advancing contact angle above 150º and contact angle hysteresis less than 5º (Figure 3.6A, B). The polymeric materials that are prepared in the presence of higher concentrations (20 mM and 30 mM) of alkali

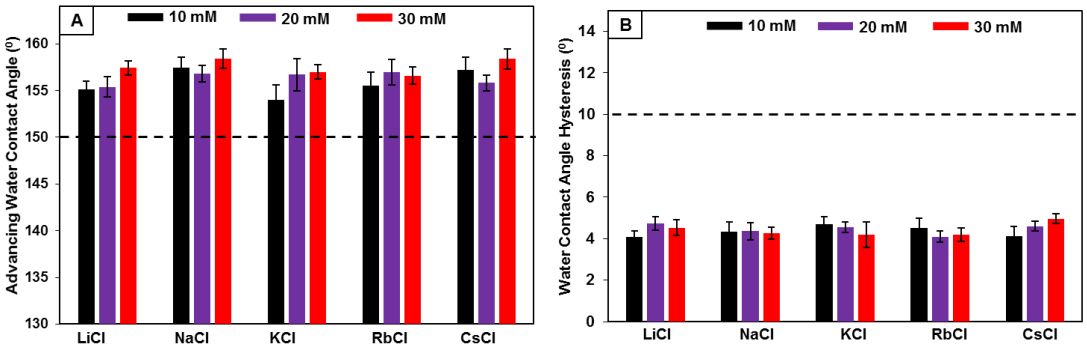

Figure 3.6. (A-B) Plots illustrating the advancing contact angle (A) and contact angle hysteresis (B) of beaded water droplet on polymeric materials that are developed by changing the concentrations (10 mM (black), 20 mM (violet) and 30 mM (red)) of various alkali metal salts, including LiCl, NaCl, KCl, RbCl and CsCl, after post-modifications with decylamine molecules through the 1, 4-conjugate addition reaction.

metal salts also have the appropriate hierarchical topography for displaying non-adhesive superhydrophobicity after post-covalent modifications with DA molecules as shown in Figure 3.6A, B. Thus, all the as synthesized polymeric materials with different hierarchical topography are highly effective in the synthesis of non-adhesive superhydrophobic materials. Next, such hierarchically featured materials are post modified with other amine containing small molecules having shorter hydrocarbon tails including hexylamine and octylamine molecules. The same hierarchical topography (that is prepared in the presence of 10 mM alkali metal salts in the reaction mixture) modified with octylamine molecules provided rose petal inspired adhesive-superhydrophobicity (formally defined as an interface that repels beaded water droplets with an advancing water contact angle above 150º and contact angle hysteresis above 10º) with an advancing contact angle above 150º and contact angle hysteresis around 13º, while the post chemical modification of the same material with hexylamine yields hydrophobicity with a water contact angle around 138º as shown in Figure 3.7A, B. This chemically modulated non-adhesive and adhesive superhydrophobicity can be explained based on the Cassie–Baxter[39] and Cassie–Wenzel transition states[40] as depicted in Figure 3.8A-C. The availability of metastable trapped air in the hierarchical featured material controlled the heterogeneous wettability through modulating the fraction of contact area between beaded water droplets and solid interfaces, which was again optimized by post chemical modification with different small molecules

(having primary amine groups that mutually react with residual acrylate groups of the synthesized material). The fraction of contact area between beaded water droplets and hierarchically featured interfaces (modified with selected small molecules) was estimated using the following equation:

$$\cos \theta r = f_s \cos\theta - fa \qquad (1)$$

$$f_s + fa = 1 \qquad (2)$$

The fraction of contact area between the beaded aqueous phase and metastable trapped air in the hierarchical interfaces is denoted as *fa*, while *fs* depicts the fraction of contact area between the beaded aqueous phase and the chemically modified hierarchical interfaces. The fraction of contact area between the beaded liquid and metastable trapped air in the hierarchically featured polymeric materials that are prepared in the presence of different alkali metal salts and post modified with DA molecules is found to be above 0.85 as shown in Table 3.1. However, this fraction contact area of the liquid/air interface was reduced

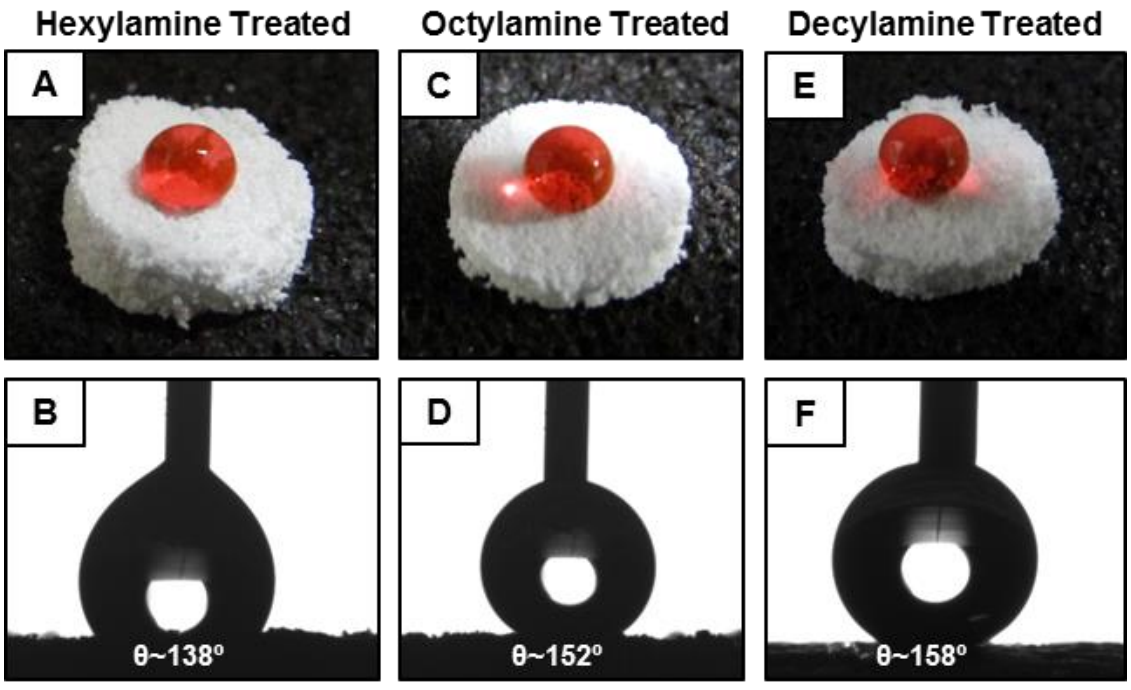

Figure 3.7. (A-F) Digital images (A, C, E) and contact angle images (B, D, F) of beaded water droplet on the polymeric material after post modification with hexylamine (A, B), octylamine (C, D) and decylamine (E, F) respectively.

after changing the post-chemical modification of polymeric monoliths from DA to octylamine (having a shorter alkyl chain) as shown in Table 3.1. On the other hand, the same polymeric materials that are post-chemically modified with even smaller hydrocarbon

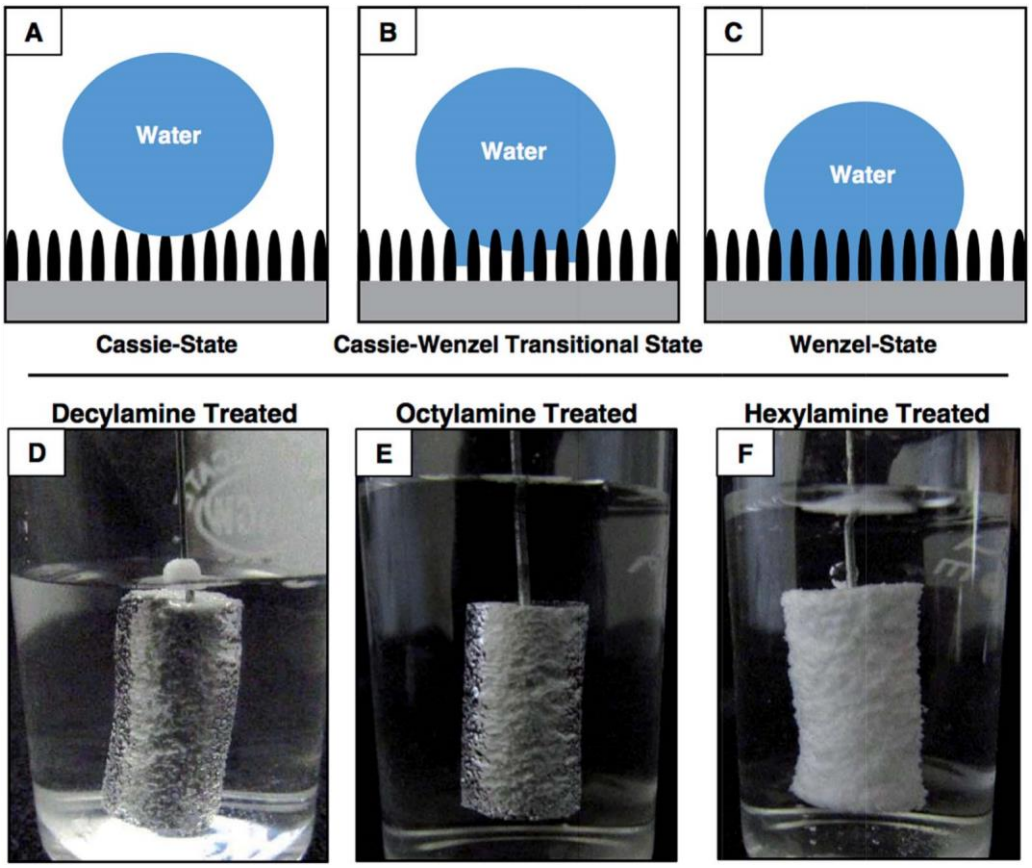

Figure 3.8 (A-C) Schematic Illustration of the heterogeneous (Cassie state (A) and Cassie–Wenzel transition state (B)) and homogeneous (Wenzel state; C) wettability of water droplets on the hierarchically featured interfaces. D-F) Digital images of the polymeric materials having the same hierarchical topography but with different chemical modification including decylamine (D), octylamine (E) and hexylamine (F) molecules, after submerging under water. The polymeric interfaces with decylamine and octylamine modifications appeared shiny due to the presence of meta-stable trapped air.

chain containing small molecules (i.e., hexylamine) were incapable of displaying adhesive/non-adhesive superhydrophobicity rather showed hydrophobicity (water contact angle 138º, Figure 3.7A,B) with homogeneous water wettability (Wenzel state, Figure 3.8C) as the hierarchical interfaces lacked metastable trapped air. Experiments were further designed for the direct and visual inspection of trapped metastable air in the chemically tailored hierarchical interfaces, where the same hierarchically featured (prepared in the

Alkali Metal Salts (10 mM)	Fraction Contact Area of Liquid/Air Interface (f_a)	
	Octylamine	Decylamine
Lithium Chloride	0.75	0.89
Sodium Chloride	0.77	0.91
Potassium Chloride	0.74	0.87
Rubidium Chloride	0.78	0.90
Cesium Chloride	0.77	0.91

Table 3.1. Illustrates the fraction contact area of liquid/air interface of the polymeric materials prepared in presence of various alkali metal salts after post modification with octylamine and decylamine.

presence of 10 mM LiCl) material that was post modified individually with decylamine, octylamine and hexylamine was submerged under water. The DA treated material appeared highly shiny under water, due to the presence of a large amount of metastable trapped air, whereas the same interface when treated with octylamine was found to be less shiny, and no shiny interface was noted for the same hierarchically featured interfaces that are treated with hexylamine as shown in Figure 3.8D-F. This simple demonstration unambiguously revealed the presence and absence of metastable trapped air in the same hierarchically featured interfaces depending on the selection of chemical functionalization of the same synthesized material. Thus, the current investigation clearly revealed that the biomimicked interfaces are more sensitive to the chemistry, in comparison to the hierarchical topography as a small variation in the hydrocarbon tail length can have a dramatic impact on the water wettability. The hierarchical topography is essential, but it does not demand very specific co-existence of micro/nanodomains in the hierarchically featured interfaces.

3.3.4. Physical/Chemical Durability of Biomimetic Wettability

The durability of nonadhesive superhydrophobicity in the synthesized material was examined in details. Here, I have selected a compressible material that was synthesized in the presence of LiCl (10 mM) and post modification with DA for various severe physical/chemical durability tests. Before subjecting the synthesized material to various

relevant durability tests, the water wettability in the interior of the material was also examined, wherein it was arbitrarily sliced into multiple pieces and interestingly, the freshly exposed interiors also displayed extreme water repellency (Figure 3.9A, B) with an advancing water contact angle above 150º and contact angle hysteresis below 10º. This simple demonstration unambiguously suggested the presence of three dimensional superhydrophobicity due to the presence of appropriate hierarchical features and the essential chemical functionalization throughout the material three dimensionally. A stream of water was exposed to the synthesized artificial lotus leaf-inspired interface, and the water stream readily bounced away from the interface (Figure 3.9C), which strongly revealed the existence of highly nonadhesive superhydrophobicity. Furthermore, the material was

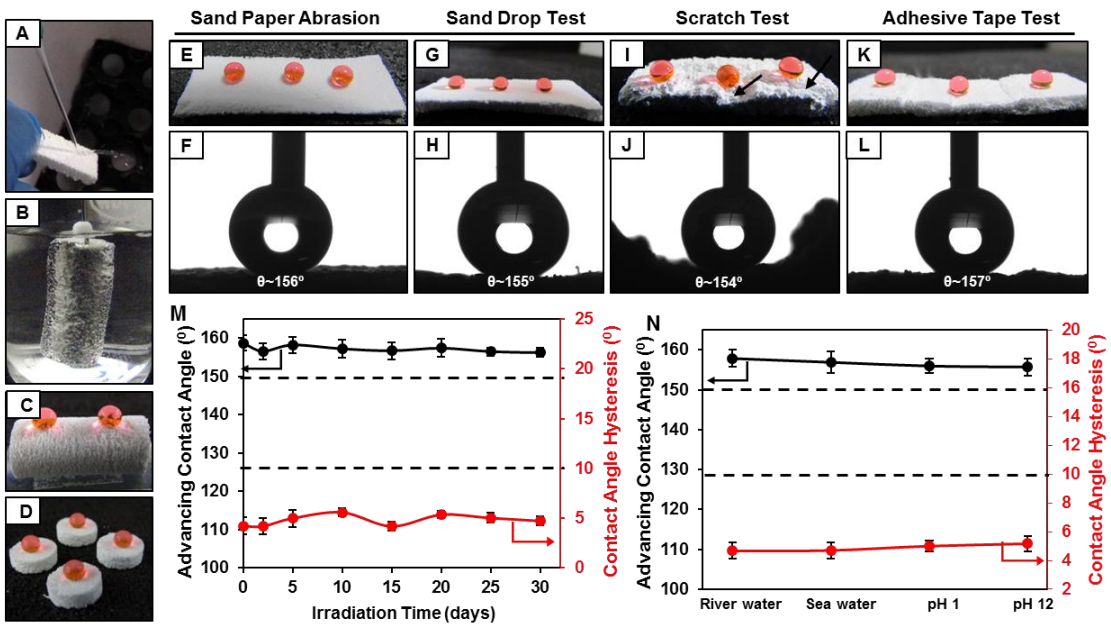

Figure 3.9. (A-B) Digital images of a beaded water droplet on the superhydrophobic polymeric material before (A) and after (B) slicing into multiple (four) pieces. C) Digital image displaying the bouncing of a water jet after hitting the superhydrophobic surface. D-K) Digital images (D, F, H, J) and water contact angle (E, G, I, K) of beaded water droplet on the synthesized polymeric material after sand paper abrasion (D, E), sand drop test (F, G), scratch test (H, I), and an adhesive tape test (J, K) respectively. L) Plot showing the change in the advancing contact angle (black) and contact angle hysteresis (red) of the polymeric material after exposing to UV radiation over 30 days. M) Plot showing the advancing contact angle (black) and contact angle hysteresis (red) of beaded water droplet on the superhydrophobic material after exposing to various chemically harsh aqueous phases including extremes of pH (1, 12), artificial sea water and river (Brahmaputra, Assam, India) water for 10 days.

subjected to a sand paper abrasion test where one part of the abrasive sand paper was attached to a microscopic glass slide and the abrasive side was exposed to the material and the material was moved back and forth multiple (five) times. During the abrasion procedure, the top portion of the material was sacrificed, however, the anti-wetting property remains intact as shown in Figure 3.9D, E. Moreover, 150 g of sand was poured on the superhydrophobic material from a height of 20 cm and the material remained non-adhesive superhydrophobic with an advancing water contact angle of 155º and contact angle hysteresis below 10º as shown in Figure 3.9F, G and no physical damage on the material was observed. Next, the superhydrophobic material was scratched deeply with a sharp edged needle over a large area and the material with physically damaged interfaces continued to repel beaded water droplets extremely with an advancing water contact angle of 154º (Figure 3.9H, I). Furthermore, adhesive tape test was performed where one side of the adhesive tape was immobilized on a glass slide and the other side was exposed to the synthesized polymeric material with an applied load of 200 g for facilitating a uniform contact between the adhesive tape and the polymeric material. Then, the adhesive tape was peeled off manually from the material and some top portion of the material was arbitrarily fractured and transferred onto the tape during this process, and eventually the interior of the polymeric material was exposed. However, the biomimicked wettability remained unperturbed even after incurring such severe physical damage as shown in Figure 3.9J, K. The as synthesized superhydrophobic material retained extremely durable water repellency with an advancing contact angle >150º and contact angle hysteresis <10º after incurring various kinds of severe physical abrasions because of the existence of three-dimensional biomimicked wettability in the material. Additionally, the superhydrophobic materials were exposed to UV radiation (λ_{max} = 265 nm and 385 nm) for 30 days. The anti-wetting properties of the materials were examined at regular time intervals and the material remained superhydrophobic with an advancing contact angle above 150º, and the contact angle hysteresis remained below 10º as shown in Figure 3.9L. Next, the same polymeric material was brought in contact with practically relevant and chemically challenging settings including extremes of pH (1 and 12), high ionic strength (artificial sea water) and river (Brahmaputra, Assam, India) water for the prolonged duration (10 days). However, the materials were found to have unaltered water repellency as shown in Figure 3.9M. This

impeccable chemical durability was attributed to the existence of robust and covalent bonding between the residual acrylate groups and primary amine groups of the selected small molecules through the 1, 4-conjugate addition reaction.

3.3.5. Selective Absorption and Filtration Based Separation of Contaminated Oils from Aqueous Phase in Severe Settings

Superhydrophobic interfaces have immense prospect in removing various forms of oil spillages through both selective absorption and gravity-driven filtration processes[42-51]. The polymeric materials that were synthesized in the presence of different alkali metal ions (10 mM) were initially screened for determining the oil absorption capacity. The polymeric

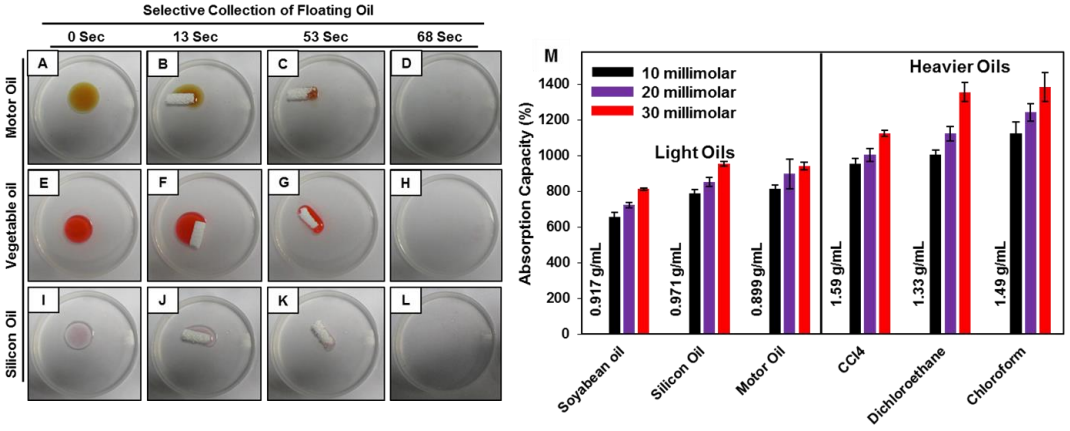

Figure 3.10. (A-L) Digital images showing the separation of a floating oil from the oil/water interface including motor oil (A-D), vegetable oil (E-H) and silicon oil (I-L) using the superhydrophobic polymeric material. M) Plot illustrating the oil (both light and heavy oils) absorption capacity of polymeric materials that are synthesized in the presence of different concentrations of LiCl including 10 mM (black), 20 mM (pink), and 30 mM (red) respectively.

material (that was synthesized in the presence of 10 mM LiCl), that shrunk the least (in comparison to other alkali metal doped material) after air drying, was the most efficient in the absorption of various oils. So, the same material was used in the rapid and selective separation of floating oils (vegetable oil, motor oil and silicone oil) as shown in Figure 3.10A-L. The selective oil-absorption (both heavy and light oils) capacity was estimated to be high by the polymeric materials that are synthesized in the presence of higher concentrations (20 mM and 30 mM) of LiCl as shown in Figure 3.10M. For instance, the motor oil (light oil) absorption increased from ~810 wt% to ~940 wt% on increasing the

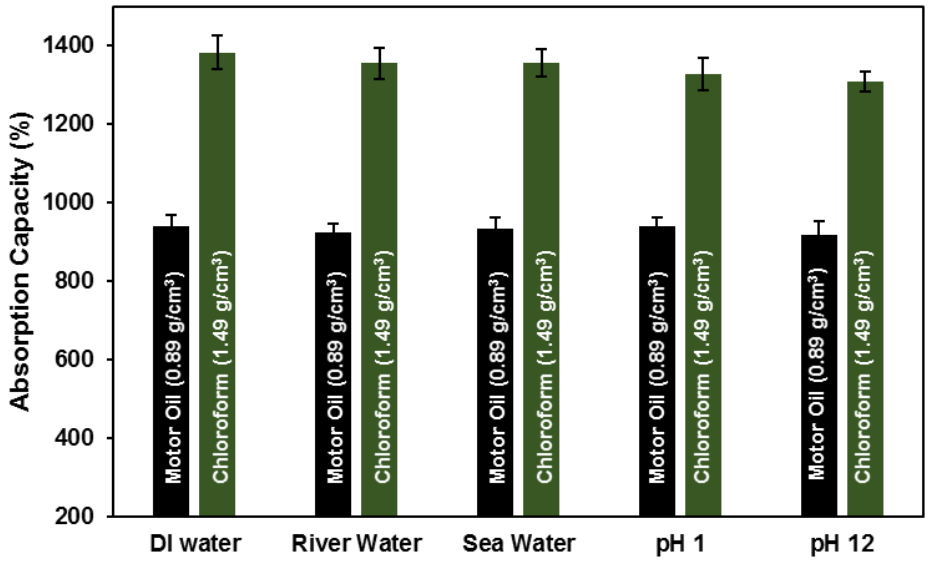

Figure 3.11. Plot accounting the selective oil absorption capacity of polymeric material that is prepared in the presence of LiCl (30 mM, post modified with decylamine) in various harsh aqueous chemical conditions including extremes of pH (pH 1 & 12), artificial sea water and river (Brahmaputra, Assam India) water for both lighter (Motor oil, black) and heavier (chloroform—model heavy oil; green) oils.

concentration of LiCl from 10 mM to 30 mM in the reaction mixture and the selective absorption of model heavy oil ($C_2H_4Cl_2$ denoted as DCE) also increased from ~1120 wt% (10 mM LiCl) to 1380 wt% (30 mM). This increasing trend of oil absorption by the polymeric materials that are synthesized in the presence of higher concentrations of LiCl is common irrespective of the density and viscosity of other selected oils in the oil/water mixture as shown in Figure 3.10M. The material that is synthesized in the presence of 30

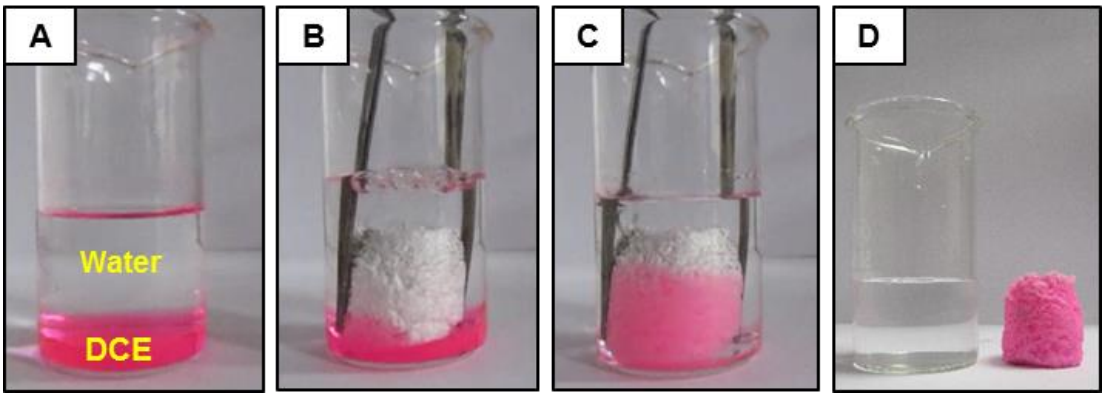

Figure 3.12. (A-D) Digital images showing the selective absorption of sediment oil (DCE; model oil) using the superhydrophobic polymeric material.

mM LiCl is most efficient in the selective absorption of both light and heavy oils. In addition to this, the oil absorption capacity of the polymeric material was also examined under practically relevant and severely challenging chemical settings including extremes of pH (1, 12), sea water and river (Brahmaputra, Assam, India) water (Figure 3.11). Thus, the synthesized material could be useful in the remediation of oil spills under diverse practical conditions. The same material was exploited further in the collection of sediment oil under water and the sediment oil (DCE as a model oil) under water was rapidly collected by the superhydrophobic material as shown in Figure 3.12A-D. However, collection of the absorbed oil from such material appeared to be difficult as the material is compressed to a certain extent. Application of high pressure damaged the integrity of the material.

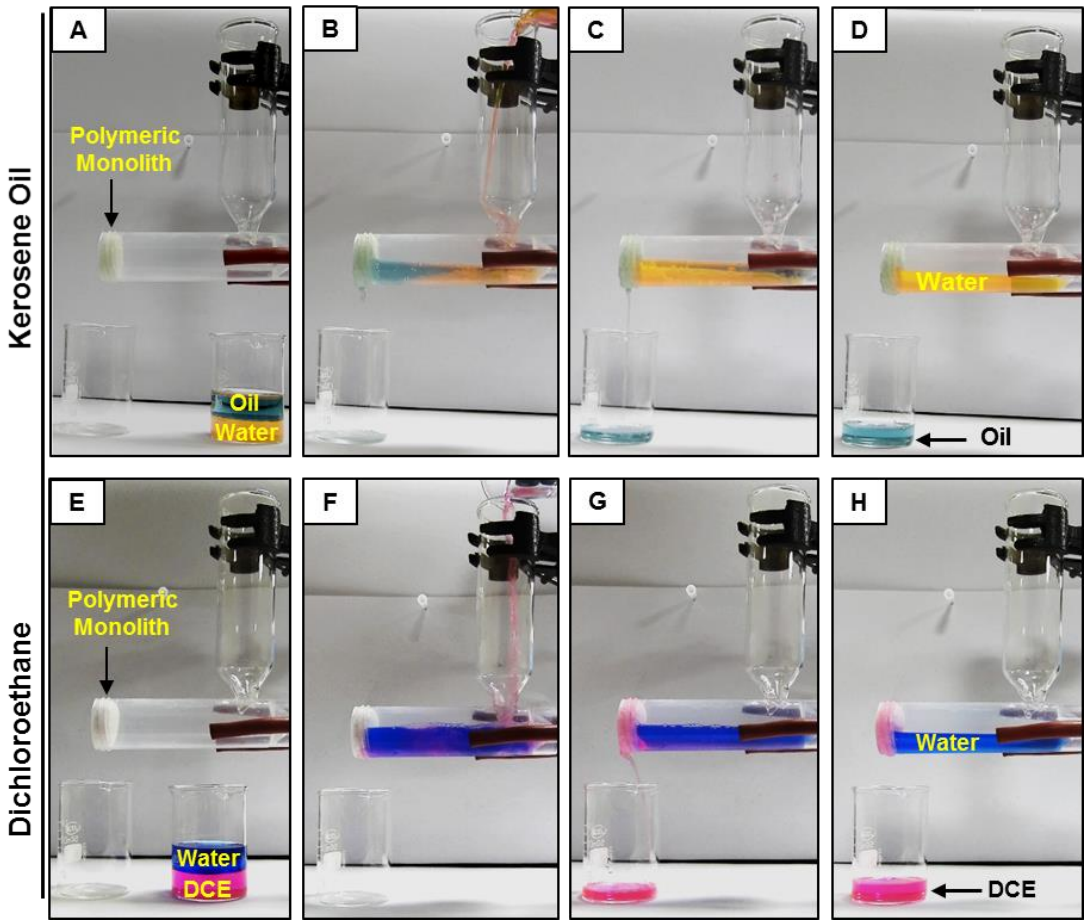

Figure 3.13. (A-H) Digital images showing the gravity driven separation of oil/water mixture (15 mL oil in 15 mL of water) using as synthesized polymeric material (prepared in presence of 30 mM of LiCl and post modified with decylamine), the lab-made prototype was capable of separating both light oil (kerosene; A-D) and heavy oil DCE (E-H).

Furthermore, this material was used in the demonstration of gravity driven oil/water separation, where both the light and heavy oils are separated from the oil/water mixture by the strategic use of the superhydrophobic monolith. The synthesized superhydrophobic material (diameter 2.7 cm and thickness 0.7 cm) was used as a filter where the oil phase was allowed to selectively pass through the material (the opening of the falcon tube was plugged with the compressible superhydrophobic material in the lab made prototype), but the water phase was extremely repelled irrespective of whether the oil or the water phase is first coming into contact with the superhydrophobic monolith (Figure 3.13A-H). The exposure of the aqueous phase to the superhydrophobic material does not block the passage of oil through the material. Furthermore, oil and aqueous phases were successfully separated from three phase oil/water mixtures that consisted of light oil, heavy oil and water. Thus, the current approach provided a single material for separating different forms of oil spills following both selective absorption and gravity driven filtration processes.

3.4. Conclusion

In this current chapter, a detailed study was performed to examine the impact of various alkali metal salts on the 1, 4-conjugate addition reaction mediated gelation of BPEI/5-Acl reaction mixture in ethanol. Alkali metal salt with smaller metal ion size are more efficient in facilitating gelation through the mutual reaction between acrylate and amine groups. These alkali metal salts accelerated both the growth of the polymeric nanocomplex, and the transformation of the reaction solution into a polymeric gel. This simple and single step process also allowed to tailor the hierarchical topography in the polymeric material just by changing the alkali metal salt in the reaction mixture. Furthermore, these alkali metal salts in the reaction mixture controlled the shrinkage and compressive modulus of the polymeric material. The synthesized material with tailored hierarchical topography was found to consist of residual acrylate functional groups, which makes it chemically reactive towards primary amines and eventually provided a simple basis to tailor the chemical functionality as well. This simple alkali metal salt assisted chemical approach having the ability to tailor topography and chemical functionality of the polymeric material allowed to examine the impact of these physical and chemical changes independently on the biomimicked water wettability. The synthesized material with lotus leaf-inspired durable interfaces was also explored for the separation and collection of various forms of oil spills following both

selective absorption and gravity driven filtration processes. This current chemical approach could be useful in several fundamental and applied studies including tissue engineering, catalysis etc.

References

(1) Wu, D.; Xu, F.; Sun, B.; Fu, R.; He, H.; Matyjaszewski, K. *Chem. Rev.* **2012**, *112*, 3959−4015.

(2) Jaggy, M.; Zhang, P.; Greiner, A. M.; Autenrieth, T. J.; Nedashkivska, V.; Efremov, A. N.; Blattner, C.; Bastmeyer, M.; Levkin, P. A. *Nano Lett*. **2015**, *15*, 7146−7154.

(3) Schwieger, W.; Machoke, A. G.; Weissenberger, T.; Inayat, A.; Selvam, T.; Klumpp, M.; Inayat, A. *Chem. Soc. Rev.* **2016**, *45*, 3353−3376.

(4) Das, S.; Heasman, P.; Ben, T.; Qiu, S. *Chem. Rev.* **2017**, *117*, 1515−1563.

(5) Hsu, C. H.; Huang, T. Y.; Chen, R. D.; Liu, Y. X.; Chin, T. Y.; Chen-Yang, Y. W.; Yeh, J. M. *ACS Biomater. Sci. Eng.* **2017**, *3*, 1527−1534.

(6) Li, X. M.; Reinhoudt, D.; Crego-Calama, M. *Chem. Soc. Rev.* **2007**, *36*, 1350−1368.

(7) Wen, L.; Tian, Y.; Jiang, L. *Angew. Chem. Int. Ed.* **2015**, *54*, 3387−3399.

(8) Feng, X.; Jiang, L. *Adv. Mater.* **2006**, *18*, 3063−3078.

(9) Yan, Y. Y.; Gao, N.; Barthlott, W. *Adv. Colloid Interface Sci*. **2011**, *169*, 80−105.

(10) Su, B.; Tian, Y.; Jiang, L. *J. Am. Chem. Soc*. **2016**, *138*, 1727−1748.

(11) Yao, X.; Song, Y.; Jiang, L. *Adv. Mater*. **2011**, *23*, 719−734.

(12) Yohe, S. T.; Colson, Y. L.; Grinstaff, M. W. *J. Am. Chem. Soc.* **2012**, *134*, 2016−2019.

(13) Ueda, E.; Levkin, P. A. *Adv. Mater*. **2013**, *25*, 1234−1247.

(14) Yu, C.; Cao, M.; Dong, Z.; Wang, J.; Li, K.; Jiang, L. *Adv. Funct. Mater.* **2016**, *26*, 3236−3243.

(15) Wen, G.; Guo, Z.; Liu, W. *Nanoscale* **2017**, *9*, 3338−3366.

(16) Li, S.; Huang, J.; Chen, Z.; Chena, G.; Lai, Y. *J. Mater. Chem. A* **2017**, *5*, 31−55.

(17) Yu, C.; Zhu, X.; Cao, M.; Yu, C.; Lic, K.; Jiang, L. *J. Mater.Chem. A* **2016**, *4*, 16865−16870.

(18) Zhang, X.; Zhi, D.; Sun, L.; Zhao, Y.; Tiwari, M. K.; Carmalt, C. J.; Parkin, I. P.; Lu, L. *J. Mater. Chem. A* **2018**, *6*, 357−362.

(19) Koch, K.; Bhushan, B.; Jung, Y. C.; Barthlott, W. *Soft Matter* **2009**, *5*, 1386−1393.

(20) Nishimura, R.; Hyodo, K.; Sawaguchi, H.; Yamamoto, Y.; Nonomura, Y.; Mayama, H.; Yokojima, S.; Nakamura, S.; Uchida, K. *J. Am. Chem. Soc.* **2016**, *138*, 10299−10303.

(21) Bird, J. C.; Dhiman, R.; Kwon, H. M.; Varanasi, K. K. *Nature* **2013**, *503*, 385−388.

(22) Feng, L.; Li, S.; Li, Y.; Li, H.; Zhang, L.; Zhai, J.; Song, Y.; Liu, B.; Jiang, L.; Zhu, D. *Adv. Mater*. **2002**, *14*, 1857−1860.

(23) Sun, T.; Feng, L.; Gao, X.; Jiang, L. *Acc. Chem. Res*. **2005**, *38*, 644−652.

(24) Rather, A. M.; Manna, U. *Chem. Mater*. **2016**, *28*, 8689−8699.

(25) Nelson, J. H.; Howells, P. N.; DeLullo, G. C.; Landen, G. L.; Henry, R. A. *J. Org. Chem.* **1980**, *45*, 1246−1249.

(26) Baik, T. G.; Luis, A. L.; Wang, L. C.; Krische, M. J. *J. Am. Chem. Soc.* **2001**, *123*, 5112−5113.

(27) Boiteau, J.; Imbos, R.; Minnaard, A. J.; Feringa, B. L. *Org. Lett.* **2003**, *5*, 681−684.

(28) Gini, F.; Hessen, B.; Minnaard, A. J. *Org. Lett.* **2005**, *7*, 5309−5312.

(29) Alexakis, A.; Backvall, J. E.; Krause, N.; P´amies, O.; Di´eguez, M. *Chem. Rev.* **2008**, *108*, 2796−2823.

(30) Hawner, C.; Alexakis, A. *Chem. Commun*. **2010**, *46*, 7295−7306.

(31) Schotes, C.; Mezzetti, A. *J. Org. Chem*. **2011**, *76*, 5862−5866.

(32) Simpson, A. J.; Lam, H. W. *Org. Lett*. **2013**, *15*, 2586−2589.

(33) Rather, A. M.; Mahato, S.; Maji, K.; Gogoi, N.; Manna, U. *Nanoscale* **2017**, *9*, 16154−16165.

(34) Parbat, D.; Manna, U. *Chem. Sci*. **2017**, *8*, 6092−6102.

(35) Rather, A. M.; Manna, U. *J. Mater. Chem. A* **2017**, *5*, 15208−15216.

(36) Das, A.; Deka, J.; Raidongia, K.; Manna, U. *Chem. Mater.* **2017**, *29*, 8720−8728.

(37) Deng, X.; Mammen, L.; Zhao, Y.; Lellig, P.; Mullen, K.; x Li, K.; Butt, H. J.; Vollmer, D. *Adv. Mater.* **2011**, *23*, 2962−2965.

(38) Uosaki, K.; Quayum, M. E.; Nihonyanagi, S.; Kondo, T. *Langmuir* **2004**, *20*, 1207−1212.

(39) Cassie, A. B. D.; Baxter, S. *Nature* **1945**, *155*, 21−22.

(40) Wang, S.; Jiang, L. *Adv. Mater.* **2007**, *19*, 3423−3424.

(41) Zhou, C.; Chen, Z.; Yang, H.; Hou, K.; Zeng, X.; Zheng, Y.; Cheng, J. *ACS Appl. Mater. Interfaces* **2017**, *9*, 9184−9194.

(42) Yuan, J. K.; Liu, X. G.; Akbulut, O.; Hu, J. Q.; Suib, S. L.; Kong, J.; Stelacci, F. *Nat. Nanotechnol*. **2008**, *3*, 332−336.

(43) Zhang, J.; Seeger, S. *Adv. Funct. Mater*. **2011**, *21*, 4699−4704.

(44) Hayase, G.; Kanamori, K.; Fukuchi, M.; Kaji, H.; Nakanishi, K. *Angew. Chem. Int. Ed* **2013**, *52*, 1986−1989.

(45) Jayaramulu, K.; Datta, K. K. R.; Rçsler, C.; Petr, M.; Otyepka, M.; Zboril, R.; Fischer, R. A. *Angew. Chem. Int. Ed.* **2016**, *55*, 1178−1182.

(46) Zhu, H.; Chen, D.; An, W.; Li, N.; Xu, Q.; Li, H.; He, J.; Lu, J. *Small* **2015**, *11*, 5222−5229.

(47) Feng, L.; Zhang, Z. Y.; Mai, Z. H.; Ma, Y. M.; Liu, B. Q.; Jiang, L.; Zhu, D. B. *Angew. Chem. Int. Ed*. **2004**, *43*, 2012−2014.

(48) Wang, B.; Guo, Z. G. *Chem. Commun.* **2013**, *49*, 9416−9418.

(49) Han, Z.; Li, B.; Mu, Z.; Niu, S.; Zhang, J.; Ren, L. *Small* **2017**, *13*, 1701121−32.

(50) Che, H.; Huo, M.; Peng, L.; Fang, T.; Liu, N.; Feng, L.; Wei, Y.; Yuan, J. *Angew. Chem. Int. Ed*. **2015**, *54*, 8934−8938.

(51) Wang, Z.; Wang, Y.; Liu, G. *Angew. Chem. Int. Ed*. **2016**, *55*, 1291−1294.

Chapter 4: Solvent-Controlled Michael Addition Reaction for Modulating Multiple Physical Properties in Polymeric Material*

The tailoring of different properties in polymeric material is challenging but useful for different fundamental and applied context. Here in this chapter, various physical properties of polymeric material (flexibility, shrinkage, porosity) were controlled with alteration in the reaction medium. Various alcoholic solvents (methanol to pentanol) used as a reaction medium for environment-friendly Michael addition reaction between amine and acrylate functionality are strategically exploited to control above mentioned physical properties in a polymeric material that is embedded with various bio-inspired water wettability. The appropriate selection of alcoholic solvent provided a highly flexible, durable and moldable superhydrophobic material, which can be even physically deformed with high compressive strain (75%) repetitively as well as can withstand various other physical manipulations without compromising the physical integrity and the embedded bio-inspired water wettability. Furthermore, the rose petal inspired adhesive superhydrophobic property was demonstrated for the controlled transfer of tiny water droplets and the lotus leaf mimicked nonadhesive superhydrophobic property was explored for selective absorption oil/water separation. The separated oil phase was selectively collected back by application of compressive force on the polymeric material.

*Rather, A. M.; Jana, N.; Begum, S.; Srivastava, H. K.; Manna, U. *Green Chem.* **2017**, *19*, 4527-4532.

Chapter 4

4.1. Introduction

Many relevant physical properties of a material are generally achieved through an appropriate optimization of both its topography and chemistry. In this context, bio-inspired artificial nonadhesive (roll-off angle <10°) superhydrophobicity (advancing contact angle >150°)[1] which provides a prospective avenue for various smart applications, including oil/water separation, open microfluidics, tissue engineering, and drug delivery[2-6] is developed through appropriate optimization of topography (hierarchical morphology) and chemistry (inert low surface energy coating) at the solid/air interface. Often, appropriate topography is tailored by adopting complex and tedious fabrication processes, while the essential chemical functionality is maintained through weak chemical interactions including ionic interactions, metal thiol interactions, silane interactions etc.[7,8] However, the materials with delicate chemical interfaces are highly labile and compromise their embedded anti-wetting property upon exposure to harsh physical/chemical manipulations (e.g. bending, scratching, squeezing, exposing to extreme pH or sea water, UV-exposure etc.), which are the prerequisites for practical applications.[9]

In the previous chapter, I have synthesized alkali metal salt assisted polymeric material for developing durable superhydrophobic material. However, such materials were found to be delicate under applied large (above 40%) compressive strain, bending, twisting etc, and the oil absorbed polymeric material breaks in pieces after manual squeezing of material during the recovery of absorbed oil. Here, I have prepared more durable and physical deformation tolerant material through a strategic use of reaction medium—that is alcoholic solvent. Adhesive superhydrophobicity on rose petal is an interesting class of naturally existing wettability.[10] The rose petal inspired adhesive superhydrophobic property was achieved through post modification with octylamine molecules which could be useful for prospective applications such as no loss transfer of tiny water droplets. The water droplets are beaded on such interfaces with high contact angle (above 150°) and high adhesive force (contact angle hysteresis above 10°) without spreading or spilling. Thus, the movement of the droplet is restricted even after the solid/air interface is titled above 10°. This principle has immense prospect in developing open microfluidic devices. [11-13] Such interfaces are mostly prepared by exploiting either the complex topography or the delicate chemistry of a material (i.e. metal–sulphur bond, metal–ion interactions) to attain the essential Cassie–

Wenzel transitional state.[14,15] However, the optimization of complex geometry is always challenging and the delicate chemistry is highly susceptible to damage in harsh practically relevant scenarios. In this chapter, the medium (i.e. alcoholic solvents, higher analogues of methanol) for the Michael addition reaction was strategically exploited for tailoring various relevant physical properties of the synthesized polymeric material including (1) the shrinkage (from ~63% to ~10%) after the removal of respective reaction medium, (2) the morphology, (3) the porosity and (4) the flexibility (e.g. compressive strain: from 0% to ~75%, bending, twisting etc.). Moreover, because the synthesized porous polymeric gel was chemically 'reactive' due to the presence of residual acrylate groups, the post-modification with appropriate primary amine containing small molecules again through the facile 1, 4-conjugate addition reaction is directed. The appropriate and facile physical/chemical optimizations eventually endowed the synthesized material with both adhesive and nonadhesive bulk bio-inspired superhydrophobicity. The embedded antifouling property is highly durable and capable of withstanding severe physical and chemical insults including the physical removal of the top surface of the material. Furthermore, the anti-wetting property remained intact during and even after successive (100 times) deformation (75%) of the synthesized material. The current synthetic approach is environmentally friendly as the fluorinated molecules, which are commonly used in the synthesis of conventional artificial bio-inspired interfaces[7,8] are associated with intractable diseases[17] were not integrated in the current design. Moreover, the superhydrophobic polymeric material was also exploited for selective absorption and collection of oil from oil/water interface. The synthesized material selectively absorbed only the oil phase from an oil/water mixture and the collected oil can be easily recovered in a separate container through manual squeezing of the porous polymeric material without damaging the integrity of the synthesized material.

4.2. Materials and Methods

4.2.1. Materials

Propanol, butanol, pentanol, hexanol were purchased from Thermo Fischer Scientific (Mumbai India). The details of all other materials and chemicals used in this chapter were previously mentioned in materials and method section of chapter 2.

4.2.2. General Considerations

The instruments used to characterize the synthesized polymeric material were same as discussed previously in the chapter 2.

4.2.3. Preparation of Polymeric Gels in Various Alcoholic Solvents

Before gelation of BPEI polymer in various alcoholic solvents, the BPEI and 5-Acl solutions were prepared in various alcoholic solvents—including methanol, ethanol, propanol, butanol, pentanol and hexanol separately by dissolving 0.5 g of BPEI and 1.325 g of 5-Acl in 10 mL of each alcoholic solvents. Afterwards solutions of BPEI and 5-Acl in same alcoholic solvent were mixed with appropriate composition (1 mL of 5-Acl and 0.3 mL of BPEI) and were kept for shaking. Over the time, the colorless mixtures of BPEI/5-Acl in alcoholic solvents were appeared as the turbid solution and eventually transformed into gel material except the mixture of BPEI/5-Acl in methanol. The gelation process was faster with increasing the hydrocarbon tail length in the alcoholic solvents and polymeric gel materials were appeared after 210 mins, 50 mins, and 20 mins of mixing BPEI/5-Acl in ethanol, propanol, and butanol. The same reaction mixture transformed into polymeric gel within 15 mins, when either pentanol or hexanol is used as reaction medium for 1, 4-conjugate addition reaction.

4.2.4. Physical and Chemical Stability Tests

Standard physical and chemical durability tests were applied on the polymeric materials (which were synthesized in pentanol solvent and post modified with ODA) to examine the robustness of the embedded antifouling property in the material were similar to the procedure that are discussed in the chapter 2.

4.2.5. Oil/Water Separation

The polymeric material prepared in pentanol solvent (post modified with ODA) was placed on the air/water interface where the oil droplet (motor oil, 1000 μL) was floating. The floated oil was soaked immediately and selectively by superhydrophobic material. Later the separated oil was collected in a discrete container by manually squeezing the oil soaked material.

4.2.5. Computational Methodology

The geometries of the reactants of primary amine, acrylate group and their corresponding transition states were fully optimized in the gas and also in different solvent mediums

(methanol, ethanol, propanol, butanol and pentanol) using quantum chemical methods of B3LYP/6-311++G(2d,2p). The effect of the solvent in the reaction process were considered using the polarizable continuum model (PCM) with the integral equation formalism variant (IEFPCM). Vibrational frequencies were performed at the same level of theory to characterize all the optimized structures as true minima or transition states on the potential energy surface. Intrinsic reaction coordinate (IRC)[19,20] analyses with mass weighted coordinates were performed at the same level of theory in gas phase and also in solvents to confirm the reactant structures. Gaussian 09 program package was used to perform all the calculations.[21] The topological properties of different transition states were analyzed in terms of electronic charge density at B3LYP/6-311++G(2d,2p) level using atoms in molecules (AIM) approach as implemented in AIMALL suite of program.[22] The input wave functions for AIM calculations were generated from Gaussian 09 program.

4.3. Results and Discussion

In this chapter, the branched polyethylenimine (BPEI) and small molecule dipentaerythritol penta-acrylate (5-Acl) were separately mixed (in appropriate composition) in different alcoholic solvents, having various hydrocarbon chain length from methanol to pentanol. These alcoholic solvents were used as the reaction medium for the mutual 1, 4-conjugate addition reaction between amine (from BPEI) and acrylate (from 5-Acl) groups. The gelation of BPEI polymer was observed in alcoholic solvents having longer alkyl chain. The colorless reaction mixture of BPEI/5-Acl (Figure 4.1A: the right most glass vial) in pentanol and hexanol transformed into an opaque gel material within 15 minutes through the formation of milky turbid solution, whereas, the mixture of BPEI/5-Acl in butanol appeared as a milky suspension (the second vial from the right, Figure 4.1B) due to the formation of polymeric nanocomplexes (NC) as confirmed by the DLS study. The gelation of the identical reaction mixtures of BPEI/5-Acl in butanol, propanol, and ethanol was sluggish as compared to that in pentanol and hexanol medium. The reaction solutions were transformed into gel materials after 20 mins, 50 mins (Figure 4.1C, D) and 210 mins in butanol, propanol and ethanol respectively. However, the same reaction mixture in methanol was incapable of forming gel material even after a couple of weeks and remained as a faint turbid solution. Furthermore, the DLS study (Figure. 4.1E) revealed that the growth of NC was delayed on decreasing the hydrocarbon chain length in the respective

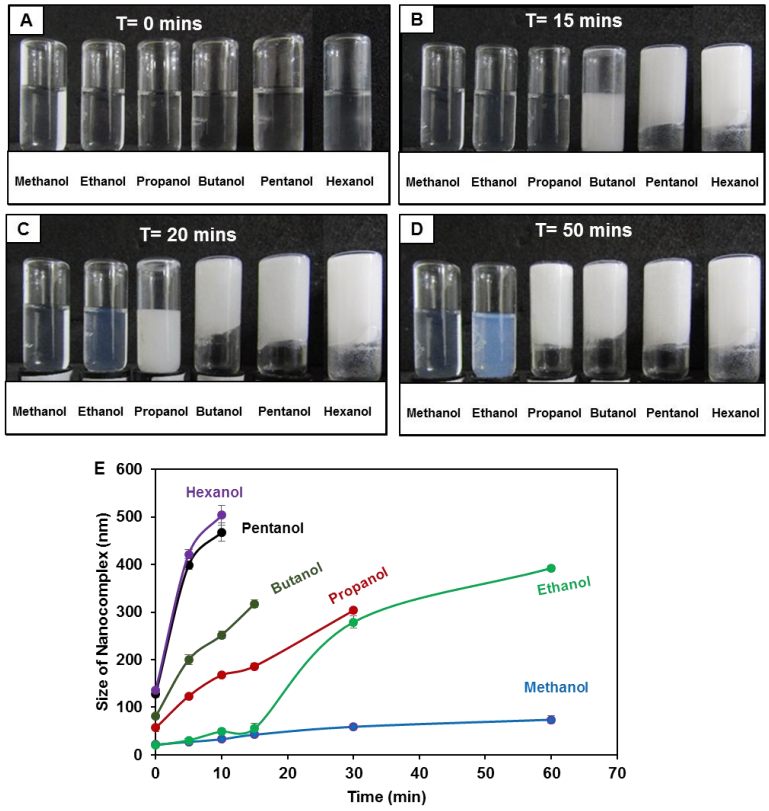

Figure 4.1. (A-D) Digital images of BPEI/5-Acl mixtures in methanol, ethanol, propanol, butanol, pentanol and hexanol at 0 min (A), after 15 mins (B), after 20 mins (C) and after 50 mins (D). E) DLS study on the mixture of 5-Acl/BPEI in hexanol, pentanol, butanol, propanol, ethanol and methanol solvent illustrating the progression in growth of the nano-complex in different alcoholic solvents.

alcoholic solvents. For instance, after 10 mins the size of nanocomplex in pentanol solvent is around 530 nm, whereas the growth of the nanocomplex is slow in methanol and the site of nanocomplex is estimated to be 20 nm as shown in Figure 4.1E. The reaction mixtures

Solvent Media	Vol used (mL)		Physical appearance
	5Acl	BPEI	
THF	1.0	0.30	Turns turbid in colour
Chloroform	1.0	0.30	No change in mixture
Acetone	1.0	0.30	No change in mixture
Ethyl acetate	NA	NA	BPEI not dissolved

Table 4.1. Accounts the effect of aprotic solvents in the reaction mixtures of BPEI and 5-Acl.

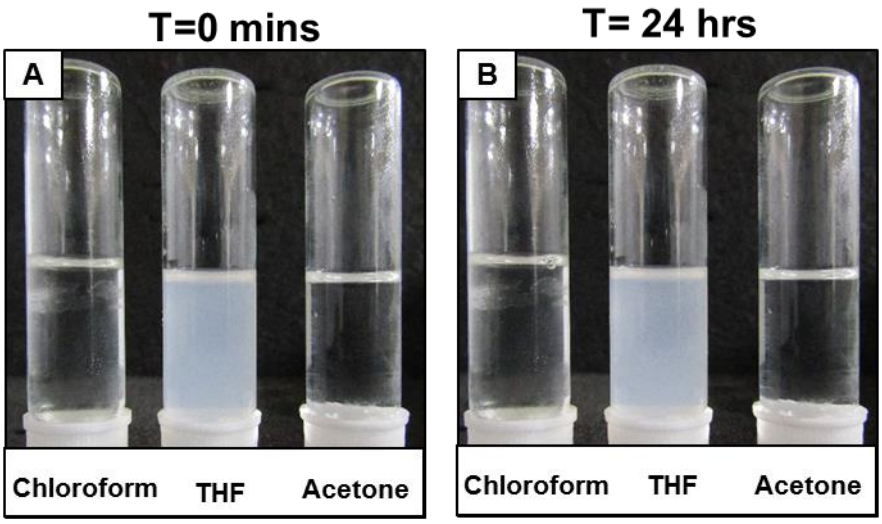

Figure 4.2. (A-B) Digital images displaying the reaction mixture of BPEI/5-Acl were incapable of forming gel in aprotic solvents (THF, chloroform and acetone) even after 24 h.

of BPEI and 5-Acl were noticed to be unable of forming a gel in aprotic solvents including THF, acetone and chloroform as is shown in Figure 4.2A-B. This simple study revealed the immense impact of alcoholic solvents on the gelation of BPEI polymer through 1, 4-

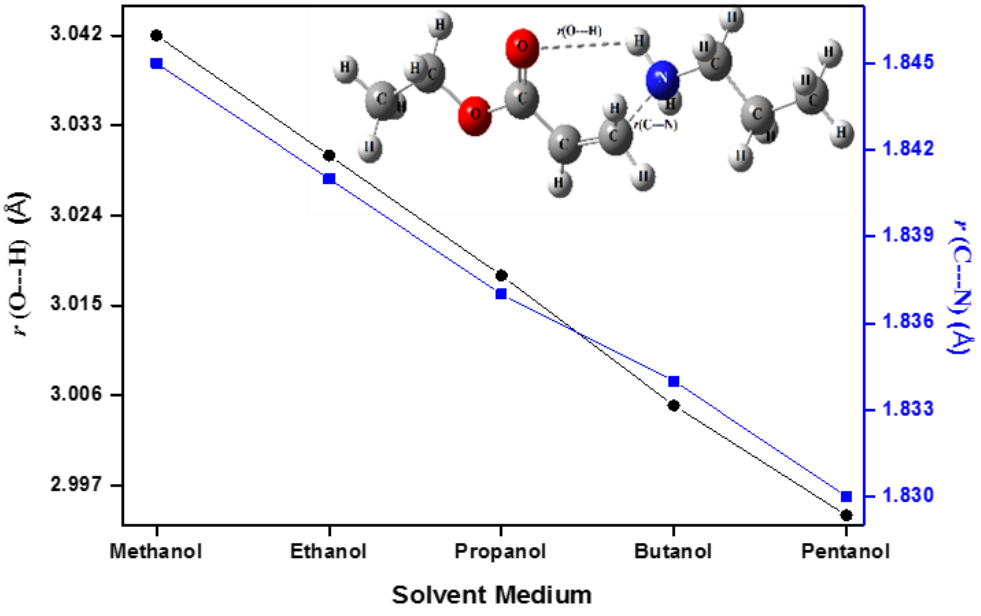

Figure 4.3. Plot displaying the Intermolecular bond distances r (O···H, black line) and r (C···N, blue line) in the transition states of the reaction between primary amine and acrylate group in different solvent mediums calculated at B3LYP/6-311++G(2d,2p) level of theory.

Solvent Medium	IE (kJ/mol)	SE (kJ/mol)	ρ (C···N)
Methanol	0.89	-21.06	0.018
Ethanol	0.99	-20.71	0.109
Propanol	1.09	-20.40	0.110
Butanol	1.18	-20.08	0.111
Pentanol	1.27	-19.78	0.112

Table 4.2. Interaction Energy (IE) and stabilization energy (SE) of the reactants in different solvent mediums along with electron density values (ρ) at bond critical points (BCP) for the intermolecular bond C---N in the transition states

conjugate addition reaction. I have notice that the gelation time for the reaction mixture of BPEI/5-Acl in hexanol solvent is also similar to pentanol, so I have decided to restrict my current study with alcoholic solvents from methanol to pentanol.

To understand the accelerated gelation of BPEI polymer in pentanol compared to that in methanol solvent, a preliminary computational study was performed on acrylate and amine moieties, which are mutually involved in the Michael addition reaction. The intermolecular bond distances r (O···H) and r (C···N) for transition states obtained for different solvents are shown in Figure 4.3. These intermolecular bond distances steadily decreased with the increase in the hydrocarbon chain length of alcoholic solvents. A shorter distance is likely to facilitate the reaction and can explain why gelation is fastest in pentanol and slowest in methanol. The topological parameter of electron density 'ρ' at bond critical points (BCP) for the new C···N bond formation in the transition states developed in various solvents is calculated. The ρ (C···N) value increases with the hydrocarbon chain length in the alcoholic solvents and follows the order methanol < ethanol < propanol < butanol < pentanol as is shown in Table 4.2. It reflects that the tendency to form the intermolecular C···N bond during the addition reaction between primary amine and acrylate group was highest in pentanol and least in methanol solvent. Furthermore, the interaction energy (IE) between primary amine and acrylate group was found to be maximum in pentanol and minimum in

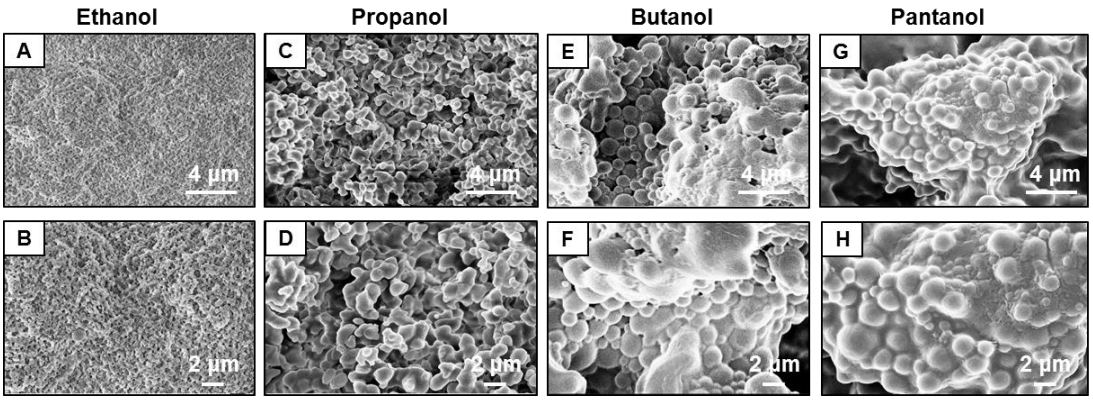

Figure 4.4. (A-H) FESEM images of the polymeric gel materials that were prepared in ethanol (A, B), propanol (C, D), butanol (E, F) and pentanol (G, H) respectively in low (A, C, E, G; scale bar: 4 µm) and high (B, D, F, H; scale bar: 2 µm) magnifications.

methanol. On the other hand, the reactants are stabilized in methanol and thus undergo the reaction slowly, which is opposite with the reaction in pentanol solvent. Thus, the DFT calculations clearly indicated that the bond distances and energy are most favorable for 1, 4-conjugate addition reaction in pentanol compared to other alcoholic solvents employed in this study.

Next, the topography of each polymeric material synthesized in various alcoholic solvents was characterized by FESEM study (Figure 4.4A-H). A significant change in the morphology was observed based on the variation of alcoholic solvent for mutual Michael

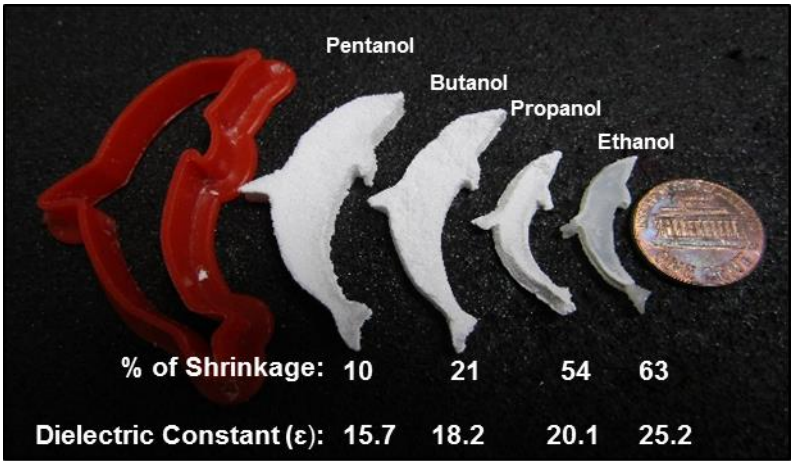

Figure 4.5. Digital image depicts the qualitative estimation of shrinkage of polymeric material prepared in pentanol, butanol, propanol, ethanol solvents after the removal of the respective solvents. Dolphin-shaped dough cutter (red) was used as a template for incurring the dolphin shape to each polymeric gel.

addition reaction between BPEI and 5-Acl. The polymeric materials that were prepared in pentanol and butanol were found with dominant micro domains, which comprised arbitrary association of granular submicron domains. A diffused and strongly interconnected

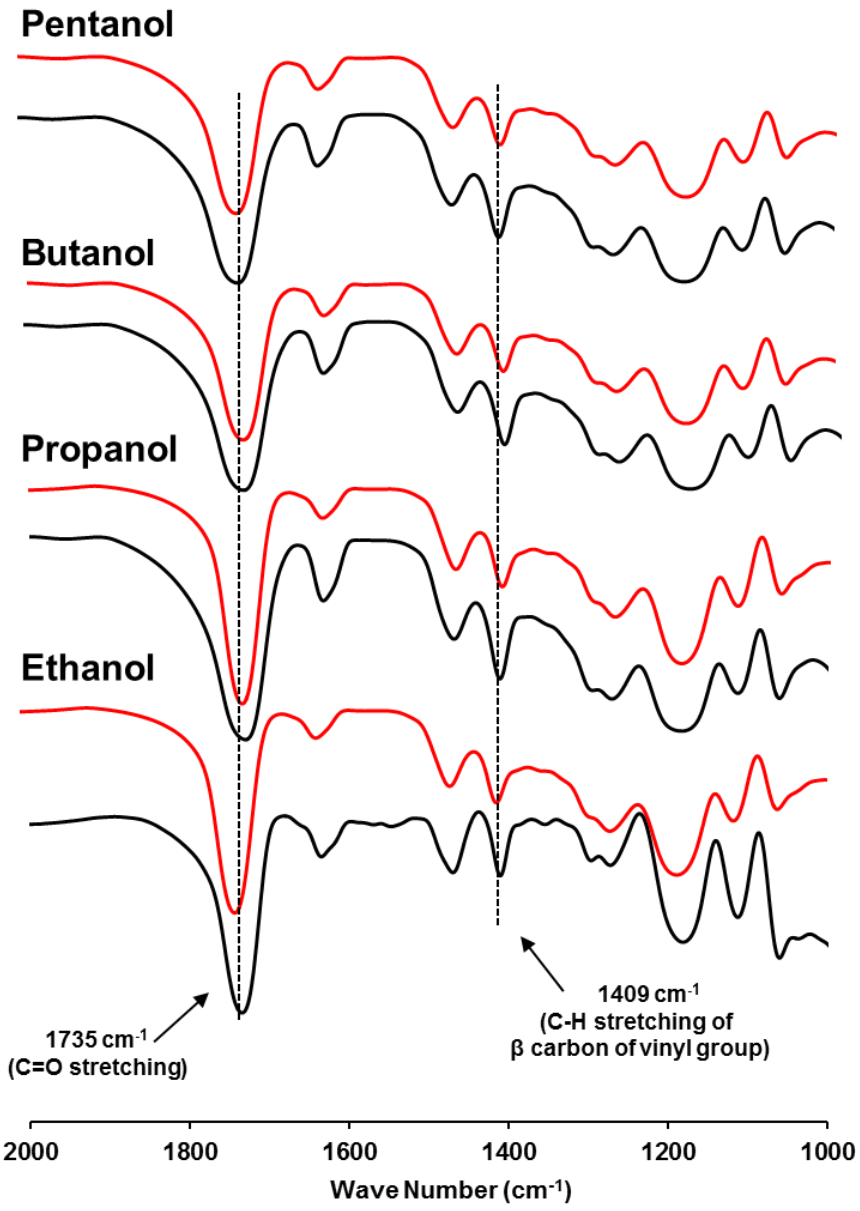

Figure 4.6. FTIR spectra of polymeric gel material that are synthesized in ethanol, propanol, butanol and pentanol solvent, before (black) and after (red) post chemical modification with octadecylamine. The peaks at 1735 cm^{-1} 1410 cm^{-1} corresponds to carbonyl streching and symmetric deformation of C-H bond for the β carbon of the vinyl group.

network of granular domains was found in the polymeric material, which was developed in pentanol solvent. This diffused interconnection of granular domains was likely to be instrumental in controlling the shrinkage of the polymeric material upon the complete removal of the alcoholic solvent. The use of pentanol with low dielectric constants (Ɛ= 15.68) leads to a nominal shrinkage of about 10% and the amount of shrinkage was found to be increased with decrease in the alkyl chain of alcoholic solvent media (Figure 4.5). The current approach provided a facile and scalable avenue to synthesize moldable polymeric material with different shapes. For proof of concept demonstration, a polymeric material with the shape of dolphin is developed as shown in Figure 4.5. The polymeric materials that are synthesized in alcoholic solvents having higher Ɛ values, are shrinked more in air drying, but the integrity and the shape of the molded material remained intact irrespective of the extent of shrinkages of the polymeric material. The material that is prepared using propanol (with Ɛ = 20.11) as external reaction solvent was significantly shrunk (~54%) after the removal of volatile solvents. In the extreme case, the shrinkage in the polymeric material that is prepared in ethanol (with Ɛ = 25.16), was noticed to be the maximum with ~63% and its morphology was completely different as shown in Figure 4.4A-B. The polymeric material, which was synthesized in propanol, lacked such diffused aggregation of sub-micro domains (Figure 4.4C, D). On the other hand, the polymeric material, which was synthesized in ethanol was found to be significantly less porous (0.023 cc g^{-1}) in comparison to that of the polymeric material that was synthesized in pentanol (0.041 cc g^{-1}) as confirmed from BET study. This increased porosity with diffused interconnected network in the material is likely to restrain its shrinkage after the removal of the respective alcoholic solvent. Moreover, the association of polymeric granular nano domains in ethanol is unable of providing appropriate micro/nano features (Figure 4.4A, B) that are essential to display extreme water repellency. The available chemical functionality in these polymeric materials developed in various alcoholic solvents, is examined with FTIR analysis. The appearance of IR peak at 1410 cm^{-1} (due to the symmetric deformation of the C–H bond for the β carbon of the vinyl group) (Black spectrum; Figure 4.6) unambiguously revealed the presence of residual acrylate groups in the polymeric material. The existence of residual acrylate groups in the polymeric material and the covalent post modification were investigated by FTIR study was primarily used as

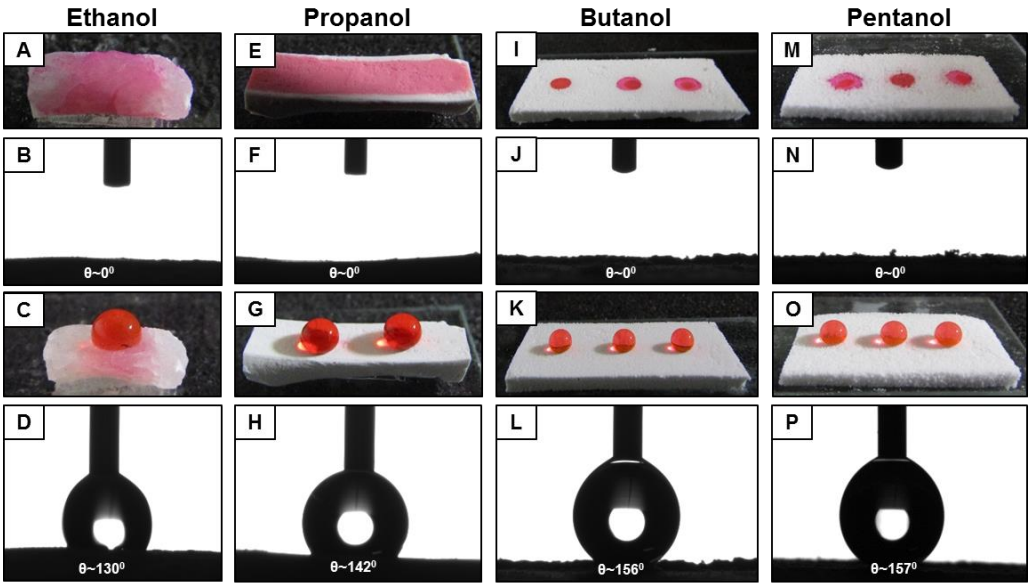

Figure 4.7 (A-P) Digital images (A, C, E, G, I, K, M, O) and water contact angle images (B, D, F, H, J, L N, P) of beaded water droplet on the polymeric material that are prepared using ethanol (A-D), propanol (E-H), butanol (I-L), pentanol (M-P) separately as reaction medium for 1, 4-conjugate addition reaction before (A-B, E-F, I-J, M-N) and after (C-D, G-H, K-L, O-P) post modification with octadecylamine.

the standard characterization tool in the past. Furthermore, the depletion of this peak after post treatment with primary amine containing small molecule (octadecylamine, ODA) indicated the post chemical modification of the material through 1, 4-conjugate addition reaction (Red spectrum; Figure 4.6). The existence of residual acrylate groups was also observed in the polymeric materials that were synthesized separately in ethanol, propanol, butanol and pentanol with FTIR spectral analysis (Figure 4.6). Similar to the material synthesized in ethanol the polymeric materials prepared in higher analogues of ethanol were found to be inherently hydrophilic and the beaded water droplets were completely soaked with contact angle of 0º as shown in Figure 4.7A-B, E-F, I-J, M-N. However, after post chemical modifications with ODA molecule, a significant change in the water wettability was observed and the materials that were prepared in propanol became hydrophobic with contact angle of above 140º (Figure 4.7G, H), whereas the butanol and pentanol mediated materials were able to exhibit bio-inspired artificial superhydrophobicity due to the appropriate coexistence of both chemistry and essential topography and the water droplet beaded on such interfaces with advancing water contact angle above 155º as shown Figure 4.7K-L, O-P.

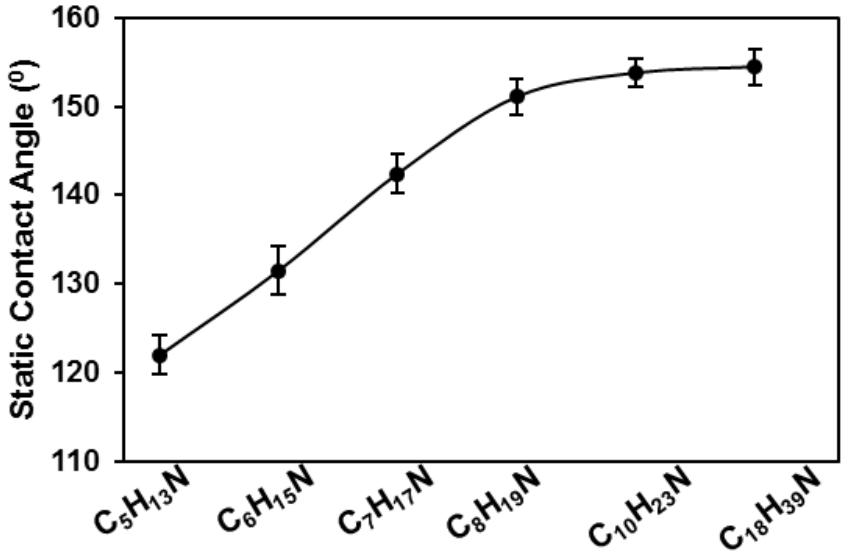

Figure 4.8. The plot accounts the static contact angles of water droplet on the polymeric gel material (that is prepared in pentanol solvent) after the post modification with pentylamine, hexylamine, heptylamine, octylamine, decylamine and octadecylamine, respectively.

The residual acrylate groups in the polymeric material that was synthesized in pentanol was further exploited for adopting various other types of water wettabilities including bio-inspired adhesive (θ_{Hys}>10°) superhydrophobicity (θ_{Adv}>150°) through a facile post chemical modification to the material with different amine containing small molecules (Figure 4.8). The amine 'reactive' polymeric material was post modified with primary amine containing small molecules and the hydrocarbon chain in the selected small molecules was gradually increasing from $–C_5H_{11}$ (pentylamine) to $–C_{10}H_{21}$ (decylamine). The incorporation of different amines in the material resulted in the progressive change in hydrophobicity with contact angle from 122° to 156°. Eventually, the polymeric materials were endowed with adhesive (roll off angle 18°) and nonadhesive (roll off angle 5.5°) superhydrophobicity after the post chemical modification with octylamine (Figure 4.9A-E) and decylamine molecules (Figure 4.9F-J), where the beaded (5 μL) water droplet rolled off on nonadhesive superhydrophobic interface on tilting the interface above 5.5° and the same water droplet remained immobilized until the adhesive superhydrophobic interface inclined ≥ 18°. Furthermore, the material displayed highly nonadhesive superhydrophobicity with a roll off angle below 2° after post chemical modification of the synthesized material (in pentanol) with ODA molecule as is shown in Figure 4.9K-O. The

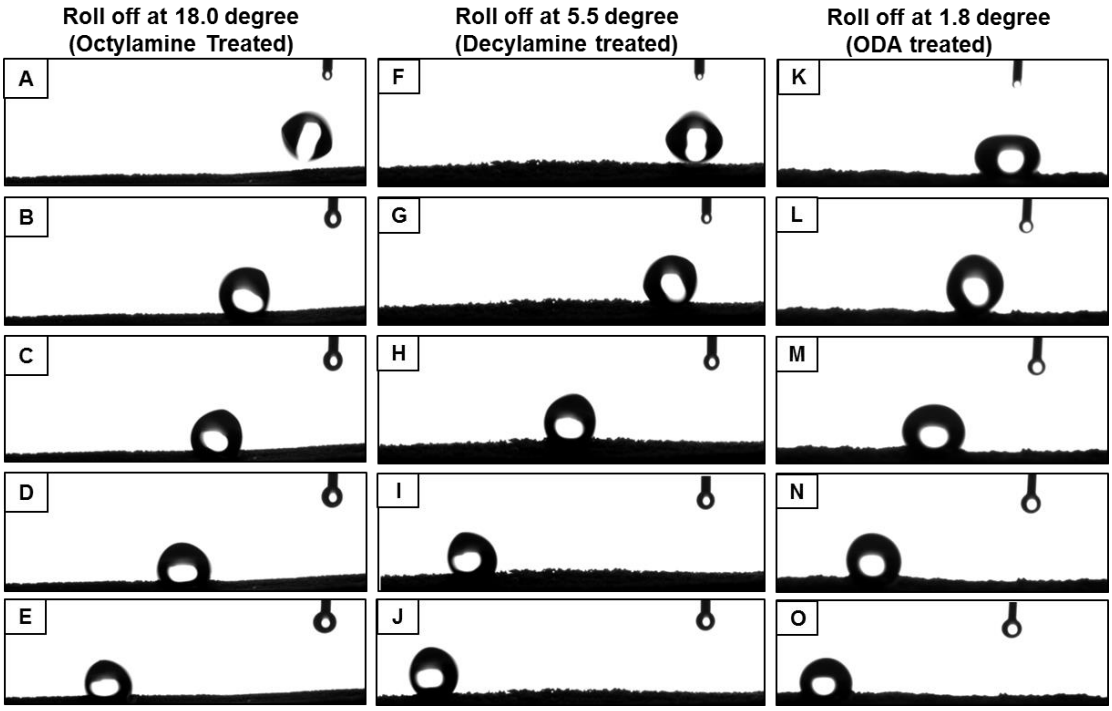

Figure 4.9. (A-O) Contact angle images showing the rolling of water droplet on the surface of polymeric material which was prepared in pentanol and post functionalization with octylamine (A-E, tilt angle: 18.0 degree), decylamine (F-J, tilt angle: 5.5 degree) and octadecylamine (K-O, tilt angle: 1.8 degree). The water droplet (4 μL) was dispensed from the 5 cm height on the surface of polymeric material.

bio-mimetic adhesive-superhydrophobicity was explored further to demonstrate the no-loss transfer of tiny water droplets by controlling the tilting angle of the interfaces as is shown in the Figure 4.10A-F. The water droplet remained immobile with a tilting angle of below

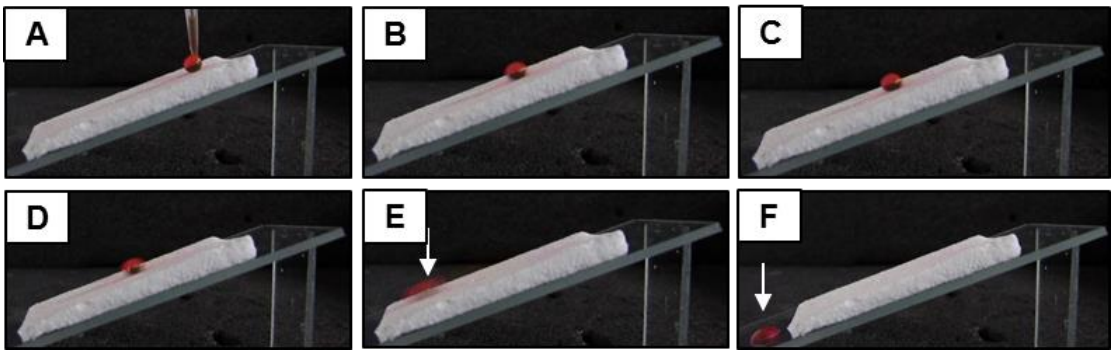

Figure 4.10. (A-F) Digital images depicting the pinning (A-C) and rolling (D-F) of beaded water droplet (red color aids visual inspection) on the surface of the polymeric material (which was prepared in pentanol and post functionalization with octylamine) after tilting the material at 15° (A-C) and 18° (D-F) respectively.

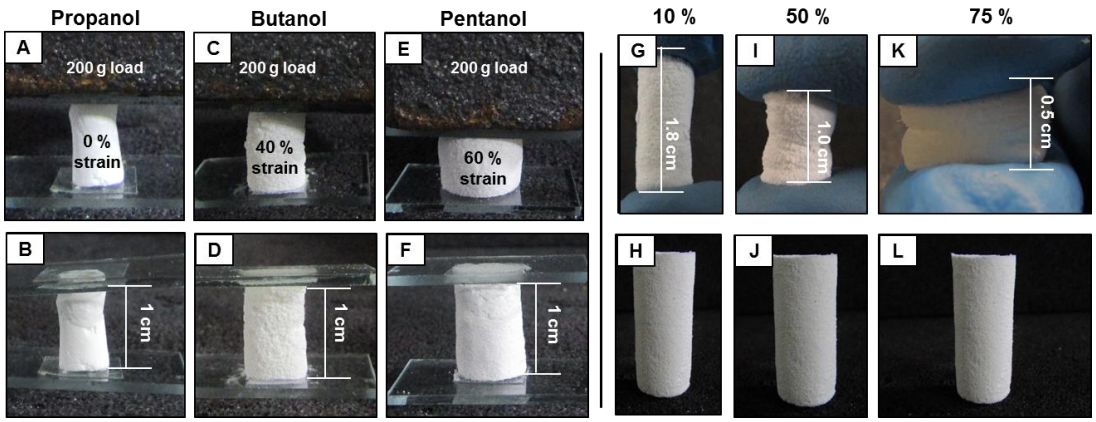

Figure 4.11 (A, C, E) Digital images depicting the percentage of compressive strain on the polymeric materials that were prepared in propanol, butanol, and pentanol, after the application of 200 g load. (B, D, F) Once the load was released, all polymeric materials were able to recover their original shapes and sizes; scale bar: 1 cm. G-L) Digital images of the polymeric material (prepared in pentanol solvent) after manual incurring of compressive strains with different extents including 10% (G), 50% (I) and 75% (K). H, J, L) The polymeric material recovered its native shapes after releasing the manual pressure.

18° (due to Cassie–Wenzel transition state) Figure 4.10A-C. However, the same water droplet rolled off when the substrate was titled ≥ 18° (Figure 4.10D-F). Hence, this property could be useful for smart open microfluidic applications where the controlled movement of the tiny water droplets could be achieved.

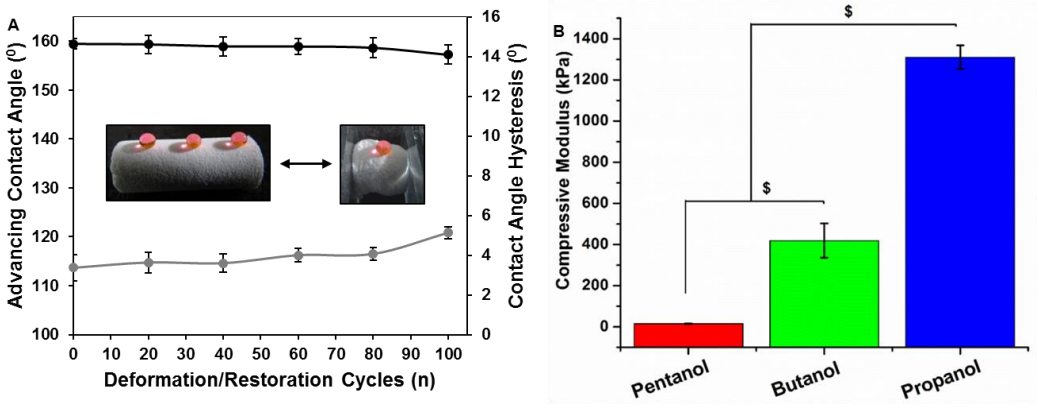

Figure 4.12. (A) Plot shows the advancing contact angle (black) and contact angle hysteresis (grey) of the beaded water droplet on the polymeric material (that was synthesized in pentanol and post-modified with octadecylamine) after incurring successive deformation (75%) and followed by relaxation after the applied pressure was released. The inset displays the water droplets on the material before and during incurring deformation. B) Plot depicting the compressive modulus of the polymeric materials prepared in propanol (blue), butanol (green) and pentanol (red) respectively.

Next, the synthesized materials prepared in different alcoholic solvents were first adhered and exposed to 200 g load (Figure 4.11A, C, E). No physical deformation was noticed for the polymeric material that was prepared in propanol solvent (Figure. 4.11A). However, the materials that were synthesized in butanol and pentanol were physically deformed. The compressive strains were measured to be 40% and 60%, respectively (Figure 4.11C, E) and their initial shape and size was recovered once the applied load was released (Figure. 4.11B, D, F). Moreover, the material synthesized in pentanol and post-modified with ODA molecules could be physically deformed with 75% strain (Figure 4.11G-L) without perturbing the physical integrity of the polymeric material. These physical deformation/recovery processes could be repeated for more than 100 times without compromising the extreme water repellency property (Figure 4.12A). Moreover, the compressive modulus was found to be higher for propanol compared to butanol and pentanol mediated materials as is shown in Figure 4.12B. Thus, the hardness and softness

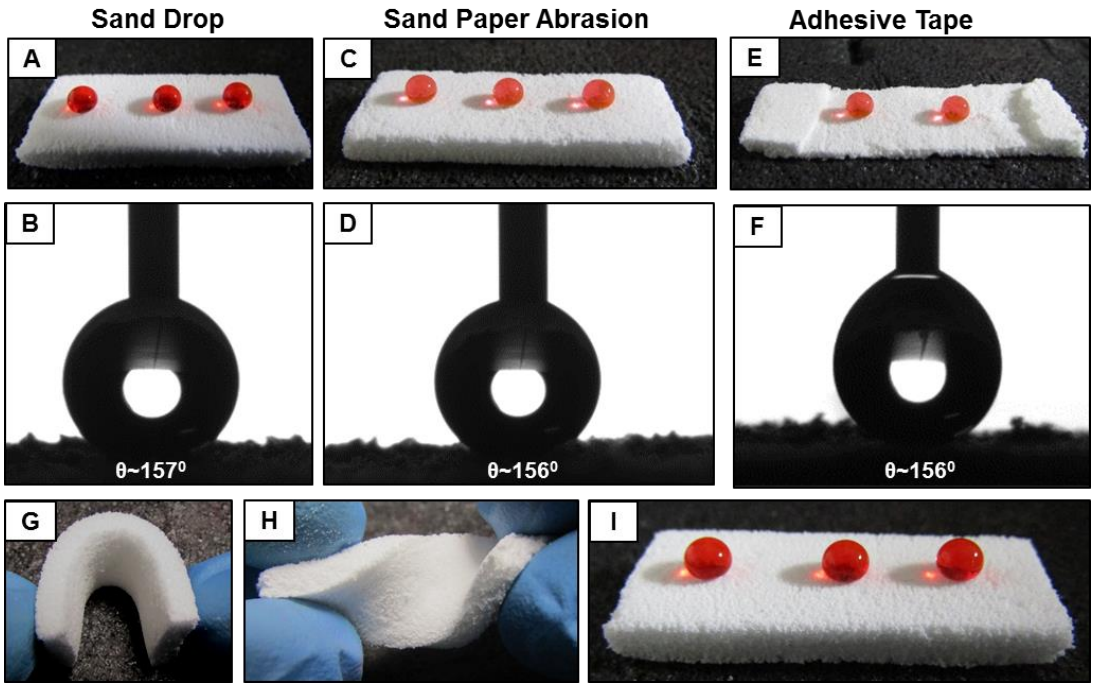

Figure 4.13. (A-F) Digital images (A, C, E) and contact angle images (B, D, F) of beaded water droplet on polymeric material prepared in pentanol solvent (post modified with ODA) after sand drop test (A, B), sand paper abrasion (C, D), adhesive tape test (E, F) respectively. G-I) Digital image of the same polymeric material during bending (G), twisting (H). I) Digital image of the beaded water droplets on the polymeric material after bending and twisting tests.

of the polymeric material can be further tailored depending on the selection of appropriate alcoholic solvent for the reaction mixture. Moreover, the same material was exposed to other physical deformations including sand drop test, sand paper abrasions and adhesive tape test, bending, twisting (Figure 4.13A-I). After incurring these physical deformations and severe abrasions, the antifouling property remained intact with $\theta_{Adv} > 150°$ and $\theta_{Hys} < 5°$ even after the removal of the top surface of the material particularly during the sand paper abrasion test and adhesive tape peeling test. The random fractures and arbitrary

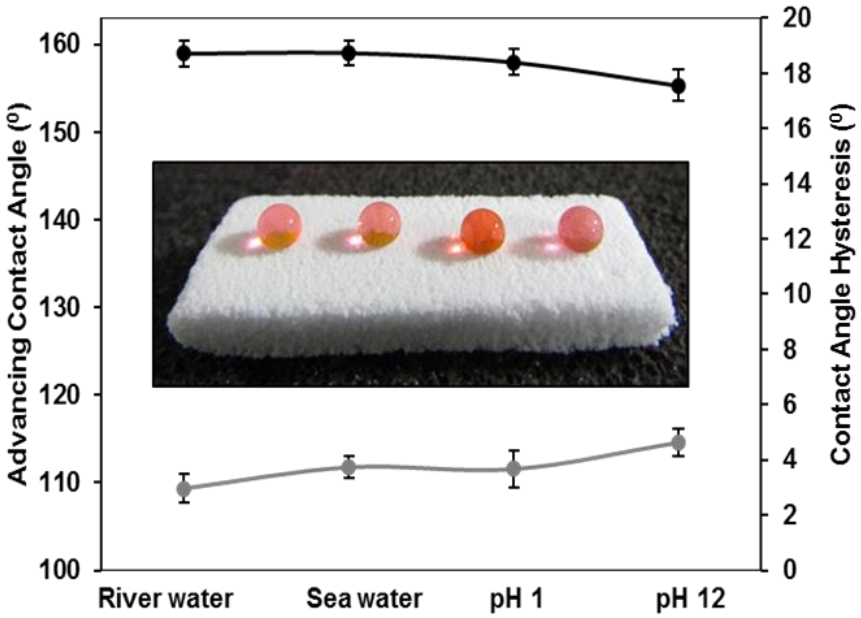

Figure 4.14. The plot showing the advancing contact angle (black) and contact angle hysterisis (grey) of the beaded water droplet on the polymeric material after exposure to various harsh chemically harsh environments and the digital image illustrating the ability of the material to repel chemically harsh aqueous droplets.

exposure of the interior of the material have no impact on the bio-inspired special wettability. In addition, the synthesized material also showed resistance to various harsh aqueous phases including extremes of pH (1 and 12), artificial sea water and river (Brahmaputra Assam, India) water as shown in Figure 4.14. Hence these results signify the existence of impeccable physical and chemical durability of the biomimicked wettability in synthesized polymeric material and this is likely due to the presence of covalent crosslinked network developed through the 1, 4-conjugate addition reaction. Subsequently, this durable and compressible superhydrophobic material was exploited in both

separation[18] and collection of floating oil (lighter than water) from air/water interfaces. The superhydrophobic material immediately and selectively soaked the floating oil on the aqueous phase (Figure 4.15A-D). The soaked oil can be collected in a separate container by squeezing the oil-laden polymeric material (Figure 4.15E, F) and the material regained its initial shape and size after releasing the applied pressure. This inherent ability of the material allowed to reuse this interface for repetitive oil/water separation. Moreover, the oil absorption capacity of polymeric materials prepared in butanol and pentanol that were displaying superhydrophobic property after ODA treatment was calculated for the range of oils and organic solvents and was found that the pentanol mediated polymeric material is showing high oil absorption capacity (Figure 4.15G) compared to butanol.

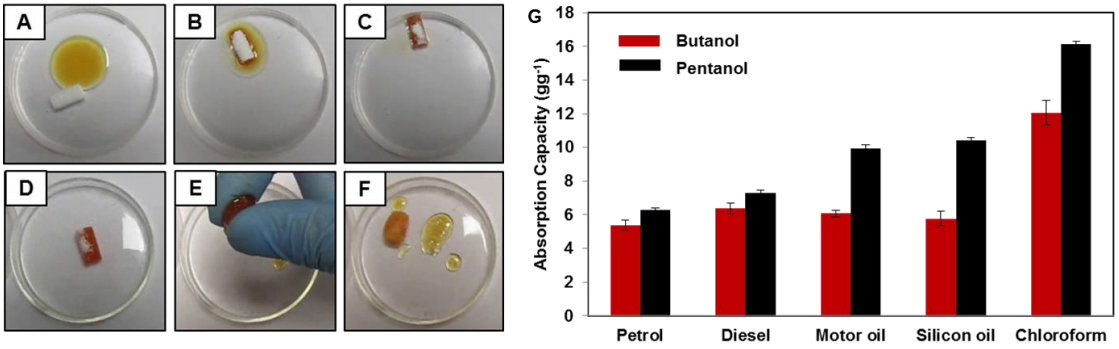

Figure 4.15. (A-F) Digital images showing the separation (A-D) of floating oil (motor oil) from air/water interface selectively using the polymeric material (post functionalized with ODA) and the oil was collected (E-F) from the material by manual compression. G) Plot illustrating the oil absorption capacity of polymeric materials prepared in presence of butanol (red) and pentanol (black) respectively.

4.4. Conclusion

In summary, a facile and scalable approach to synthesize polymeric material with tailored physical properties through the mutual Michael addition reaction between BPEI and 5-Acl with appropriate selection of alcoholic solvents is introduced. The appropriate selection of alcoholic solvents as reaction medium allowed to control various important physical (e.g. topography, flexibility, shrinkage etc.) properties. This approach was further extended to mimic the bio-inspired adhesive and nonadhesive wettability in the polymeric material with impeccable physical and chemical durability. The synthesized material withstands 75% compression multiple (100) times without compromising the physical integrity and the embedded anti-wetting property. Several significant features were added to the polymeric

material through the optimization of appropriate chemistry and topography. These special interfaces were also exploited in the no loss transfer of tiny water droplet and the selective collection and absorption of oil from oil/water interface. This simple and environment-friendly approach could be useful in developing various relevant functional materials for several other relevant and prospective applications of bio-inspired special water wettability in practical settings.

References

(1) Liu, K. S.; Yao, X.; Jiang, L. *Chem. Soc. Rev.* **2010**, *39*, 3240−3255.

(2) Li, X. M.; Reinhoudt, D.; Crego-Calama, M. *Chem. Soc. Rev.* **2007**, *36*, 1350−1368.

(3) Yao, X.; Song, Y.; Jiang, L. *Adv. Mater.* **2011**, *23*, 719−734.

(4) Ueda, E.; Levkin, P. A. *Adv. Mater.* **2013**, *25*, 1234−1247.

(5) Wen, L.; Tian, Y.; Jiang, L. *Angew. Chem., Int. Ed.* **2015**, *54*, 3387−3399.

(6) Gao, A.; Wu, Q.; Wang, D.; Ha, Y.; Chen, Z.; Yang, P. *Adv. Mater.* **2016**, *28*, 579−587.

(7) Yan, Y. Y.; Gao, N.; Barthlott, W. *Adv. Colloid Interface Sci.* **2011**, *169*, 80−105.

(8) Feng, X.; Jiang, L. *Adv. Mater.* **2006**, *18*, 3063−3078.

(9) Verho, T.; Bower, C.; Andrew, P.; Franssila, S.; Ikkala, O.; Ras, R. H. A. *Adv. Mater.* **2011**, *23*, 673−678.

(10) Jin, M. H.; Feng, X. L.; Feng, L.; Sun, T. L.; Zhai, J.; Li, T. J.; Jiang, L. *Adv. Mater.* **2005**, *17*, 1977−1981.

(11) Wang, Q.; Bai, J.; Dai, B.; Yang, Z.; Guo, S.; Yang, L.; He, Y.; Hana, J.; Zhu, J. *Chem. Commun.* **2017**, *53*, 2355−2358.

(12) Hong, X.; Gao, X.; Jiang, L. *J. Am. Chem. Soc.*, **2007**, *129*, 1478−1479.

(13) Zhu, H.; Guo, Z.; Liu, W. *Chem. Commun.* **2014**, *50*, 3900−3913.

(14) Tan, C.; Cai, P.; Xu, L.; Yang, N.; Xi, Z.; Li, Q. *Appl. Surf. Sci.*, **2015**, *349*, 516−523.

(15) Lai, Y.; Gao, X.; Zhuang, H.; Huang, J.; Lin, C.; Jiang, L. *Adv. Mater.* **2009**, *21*, 3799−3803.

(16) Danusso, F.; Ferruti, P. *Polymer* **1970**, *11*, 88−113.

(17) Hu, X. C.; Andrews, D. Q.; Lindstrom, A. B.; Bruton, T. A.; Schaider, L. A.; Grandjean, P.; Lohmann, R.; Carignan, C. C.; Blum, A.; Balan, S. A.; Higgins, C. P.; Sunderland, E. M. *Environ. Sci. Technol. Lett.* **2016**, 3, 344−350.

(18) Li, Y.; Zhang, Z.; Ge, B.; Men, X.; Xue, Q. *Green Chem.* **2016**, *18*, 5266−5272.

(19) Gonzalez, C.; Schlegel, H. B. *J. Chem. Phys.* **1989**, *90*, 2154−2161.

(20) Gonzalez, C.; Schlegel, H. B. *J. Phys. Chem.* **1990**, *94*, 5523−5527.

(21) Frisch, M. J.; Trucks, G. W.; Schlegel, H. B.; Scuseria, G. E.; Robb, M. A.; Cheeseman, J. R.; Scalmani, G.; Barone, V.; Mennucci, B.; Petersson, G. A.; Nakatsuji, H.; Caricato, M.; Li, X.; Hratchian, H. P.; Izmaylov, A. F.; Bloino, J.; Zheng, G.; Sonnenberg, J. L.; Hada, M.; Ehara, M. Toyota, K.; Fukuda, R.; Hasegawa, J.; Ishida, M.; Nakajima, T.;

Honda, Y.; Kitao, O.; Nakai, H.; Vreven, T.; Montgomery, J. A.; Peralta, J. E.; Ogliaro, F.; Bearpark, M.; Heyd, J. J.; Brothers, E.; Kudin, K. N.; Staroverov, V. N.; Kobayashi, R.; Normand, J.; Raghavachari, K.; Rendell, A.; Burant, J. C.; Iyengar, S. S.; Tomasi, J.; Cossi, M.; Rega, N.; Millam, J. M.; Klene, M.; Knox, J. E.; Cross, J. B.; Bakken, V.; Adamo, C.; Jaramillo, J.; Gomperts, R.; Stratmann, R. E.; Yazyev, O.; Austin, A. J.; Cammi, R.; Pomelli, C.; Ochterski, J. W.; Martin, R. L.; Morokuma, K.; Zakrzewski, V. G.; Voth, G. A.; Salvador, P.; Dannenberg, J. J.; Dapprich, S.; Daniels, A. D.; Farkas, Ö.; Foresman, J. B.; Ortiz, J. V.; Cioslowski, J. D.; Fox, J. *Gaussian 09* (Gaussian, Inc., Wallingford CT, **2009**).

(22) Keith, T. A.; AIMALL, version 13.11.04, TK Gristmill Software, Overland Park, KS, USA, **2013**, http://aim.tkgristmill.com.

Chapter 5: Rapid and Solvent Free Synthesis of Bulk Superhydrophobic Coating*

In this chapter, a single polymer is rapidly and covalently transformed into a chemically reactive and functional bulk polymeric coating through a catalyst-free mutual chemical reaction between acrylate and amine groups at ambient conditions in the absence of any external reaction solvent, which is unprecedented in the literature. This facile and external solvent free chemical approach provided a basis for developing biomimicked water wettability. The essential chemistry that conferred bio-inspired water wettability was optimized in the hierarchically featured polymeric material by post covalent functionalization of chemically reactive polymeric material with primary amine containing small molecules. The inherently sticky and "chemically reactive" polymeric gel having appropriate hierarchical topography is highly capable of providing substrate independent (irrespective of chemical compositions and mechanical strength of the substrates) stable coatings with robust bio-inspired extreme water repellency. The coating on different substrates doesn't demand any additional surface functionalities and the physical integrity as well as the anti-wetting property of the coatings remains intact under various physical and chemical insults.

*Rather, A. M.; Manna, U. *ACS Appl. Mater. Interfaces* **2018**, *10*, 23451−23457.

Chapter 5

5.1. Introduction

The "chemically reactive" interfaces that provided a facile and robust avenue for tailoring various relevant chemical functionalities[1–14] are fundamentally interesting and important for synthesizing smart and functional materials that have a wide range of potential applications including immobilization of desired bioactive molecules, synthesis of cell on a chip, controlled release of small molecules, multibiofunctionalization, smart sensing of various relevant chemical toxins and developing patterned interfaces etc.[1–17] Most often, such chemically reactive functional interfaces are ultrathin (in the scale of nanometers), featureless and were prepared commonly through multistep deposition processes such as layer by layer (LbL) deposition of reactive polymer and chemical vapor deposition (CVD) followed by an uncontrolled polymerization process.[1–7,9–11]

In the recent past, Lynn and co-workers[18,19] extended this concept of chemically reactive coating, and they strategically synthesized a hierarchically featured and chemically "reactive" interface for developing durable super-water-repellant coating for several prospective applications including open microfluidics, high-throughput screening of drug, controlled drug delivery, oil/water separation etc.[20–22] In general, the conventional and thin artificial superhydrophobic coatings are developed through appropriate co-optimization of (1) essential chemistry and (2) topography only over a few nanometers across the thickness of the artificial biomimicked interface.[23–26] Thus, a slight perturbation in either chemistry or controllable change in the topography in the conventional designing is expected to cause severe and permanent damage to the embedded special biomimicked wettability.[27–29] In comparison to the conventional approach, the hierarchically featured and chemically "reactive" thick coatings inherently yielded highly durable biomimicked interfaces. Such chemically reactive approaches are inherently capable of providing a facile basis for tailoring essential chemistry three dimensionally and allowed to trap metastable air across the thickness of the material and eventually provided bulk superhydrophobicity.[19] The synthesized bulk superhydrophobic materials are inherently capable of sustaining severe physical damages including physical erosion of the synthesized material. However, the examples of such chemically "reactive" and hierarchically featured coatings are very rare in the literature, and few functional polymers are mostly associated following tedious multistep/complex synthetic procedures in the reported approaches in the recent

literature.[18,19] Moreover, single polymer based rapid synthesis of chemically reactive and hierarchically featured interfaces without using any catalyst and external reaction solvent at ambient conditions is unprecedented in the literature. In this chapter, branched poly (ethylenimine) (BPEI, Figure 5.1A) is spontaneously converted into a "chemically reactive" and functional polymeric material through solvent-free and catalyst-free mutual addition reaction with other liquid reactants dipentaerythritol penta-acrylate (5-Acl, Figure 5.1A). On mixing the polymer (BPEI) and small molecule (5-Acl) in the absence of any external organic/aqueous solvents, a chemically reactive polymeric gel was spontaneously (within 30 seconds) formed through facile 1, 4-conjugate addition reaction (Figure 5.1B) between amine and acrylate groups at ambient conditions as shown in Figure 5.1C. This "reactive" and inherently sticky polymeric material was further exploited in developing substrate independent polymeric coatings that embedded with lotus leaf inspired artificial and durable bulk superhydrophobicity after covalent post chemical modification of the synthesized polymeric coating with octadecylamine (ODA) molecule (Figure 5.1D).

5.2. Materials and Methods

5.2.1. Materials

Plastic and card board were obtained from local shop in Guwahati city (Assam India). Whatman filter paper was purchased from GE Healthcare Services (Bangalore India). Aluminum foil was obtained from Parekh Aluminex Limited (PAL) Maharashtra India. Wood pieces were collected from a local construction site in IIT Guwahati campus and was rinsed thoroughly prior to use. The details of all other materials and chemicals used in this section are already discussed in the chapter 2.

5.2.2. General considerations

The instruments used in this section for characterization of synthesized materials were already discussed previously in the chapter 2.

5.2.3. Preparation of Solvent Free 'Reactive' Polymeric Gel and Post-Chemical Modifications

Branched poly (ethylenimine) (BPEI) and dipentaerythritol penta-acrylate (5-Acl) were mixed in a single container with appropriately selected molar ratios. The mixture instantly turns into semisolid gel within 30 seconds, then the gel material was taken out and was subsequently rinsed with THF for removing the unreacted reactants. Afterwards the

polymeric gel was transferred in the octadecylamine (ODA) solution (5 mg/mL of THF) for overnight. Other water wettabilities were obtained by post modifying the polymeric gel with different amine containing small molecules including propylamine (30 mg/mL), pentylamine (30 mg/mL), hexylamine (30 mg/mL), octylamine (30 mg/mL), decylamine (30 mg/mL) respectively. Next, the materials were rinsed with THF for one hour to remove the unreacted and loosely bound amine containing small molecules and were dried at ambient conditions. Afterwards the change in wettability was examined with digital images and contact angle measurements.

5.2.4. Coating on Various Substrates

The reactive polymeric composite films were fabricated by placing the highly sticky and chemically 'reactive' polymeric gel on the cleaned surface of various selected substrates including glass, wood, plastic, whatman filter paper, aluminum foil, card board. The polymeric gel was uniformly spread out using microscopic glass slide. Then the coated substrates were washed thoroughly for removing unreacted reactants. Thereafter, the substrates were post modified with ODA molecule for achieving the desired water wettability.

5.2.5. Physical and Chemical Abrasions

Various physical and chemical abrasions performed in this section were already discussed previously in the material and method section of the chapter 2.

5.3. Results and Discussion

Here, in this chapter, an unprecedented approach for rapid synthesis of covalently crosslinked, hierarchically featured and chemically reactive polymeric material was introduced without using any external reaction solvent and catalyst. The eco-friendly, solvent and catalyst-free synthesis approach provided a facile and rapid basis for adopting various important biomimicked interfaces that have enormous importance and prospective applications in practically relevant settings. In this current study (a) the strategic use of chemistry (b) the synthesis procedure and (c) the synthesized materials are completely different from previously discussed materials in the earlier chapters. Here in this current chapter, a series of controlled studies were performed, where the molar ratio ("mole to mole" ratio) of the liquid reactants (BPEI (the mole amount is calculated with respect to the repeating unit) and 5-Acl) was varied (from 1:3 to 1:5; BPEI:5-Acl) to achieve

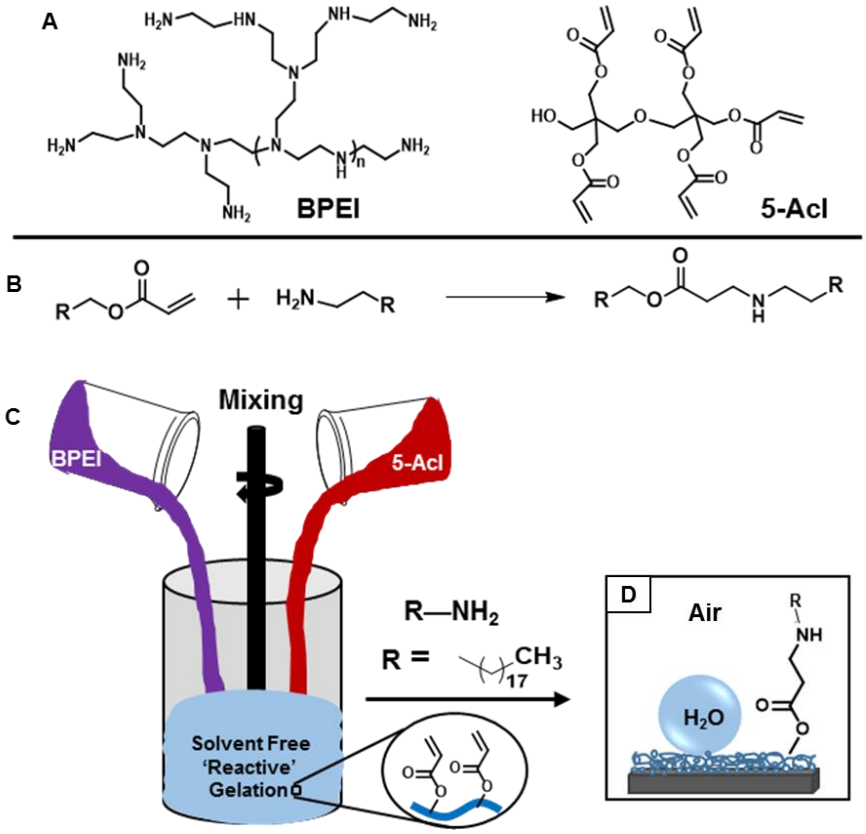

Figure 5.1. (A) Chemical structures of branched polyethylenimine (BPEI) and dipentaerythritol penta-acrylate (5-Acl). B) Schematic illustration of 1, 4-conjugate addition reaction between primary amine and acrylate moieties. C) Schematic illustrating the spontaneous synthesis of chemically "reactive" polymeric gel on continuous mixing of polymer (BPEI) and small molecules, without using any solvent and catalyst. D) Further, appropriate post chemical modifications with octadecylamine through 1, 4-conjugate addition reactions yielded superhydrophobicity.

biomimicked wettability through controlled optimization of (i) essential topography and (ii) appropriate chemistry. The colorless mixture (Figure 5.2A) with molar ratio 1 (BPEI):3 (5-Acl)) of liquid polymer (BPEI) and small molecules (5-Acl) was mixed rapidly to form an opaque gel (Figure 5.2E) within 30 seconds. The synthesized polymeric gel was inherently hydrophilic with water contact angle (WCA) of 73° and this WCA was increased from 73° to 85° after treatment with octadecylamine (ODA) molecules. This change in water wettability was further improved with varying the molar ratio of the selected reactants (BPEI and 5-Acl; 1:4) in the reaction mixture. On increasing the concentration of 5-Acl in the reaction mixture, the gel materials became more hydrophobic (with WCA of 120°) after ODA treatments (Figure 5.3A). The reaction mixture of BPEI/5-Acl with 1:5 molar ratio

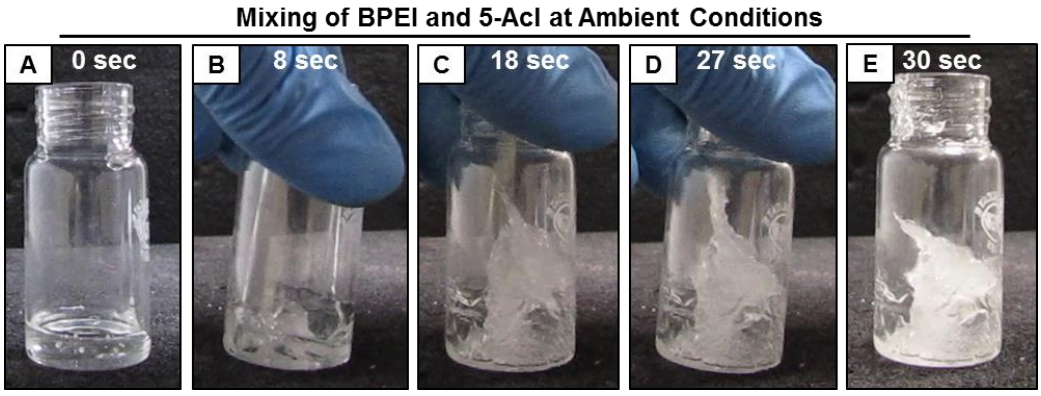

Figure 5.2 (A-D) Digital images illustrating the process of gelation on continuous mixing of BPEI and 5-Acl, where optically transparent mixture (A) of liquid reactants are transformed into opaque gel within 30 seconds (E).

yielded another hydrophilic material (Figure 5.3C, D); however, the synthesized chemically reactive material became superhydrophobic after ODA treatment, and the water droplet (red color aids visual inspection) beaded on the same gel material with an advancing water contact angle above 150° and contact angle hysteresis below 10° as shown in Figure 5.3E, F. This change in water wettability is mainly attributed to the inherent primary amine "reactivity" of the synthesized polymeric gel. The synthesized polymeric gel was loaded with residual acrylate groups as confirmed with standard FTIR spectral study. The IR peaks (Figure 5.3B, Black Spectrum) at 1735 cm^{-1} and 1410 cm^{-1} which correspond to the carbonyl stretching and symmetric deformation of the C−H bond for the β carbon of the vinyl groups unambiguously revealed the existence of acrylate groups in the synthesized polymeric gel. The depletion of the IR peak at 1410 cm^{-1} with respect to 1735 cm^{-1} (the internal standard, where carbonyl groups remained unperturbed in Michael addition reaction) after the postmodification with ODA molecules (Figure 5.3B, Red Spectrum) independently confirmed the presence of amine "reactive" functionality (i.e., residual acrylate groups) in the material and the covalent modification with desired chemistry in the material through robust 1, 4-conjugate addition reaction. The optimized chemistry in the polymeric gel conferred the biomimicked superhydrophobicity. Moreover, the microscopic morphology of the polymeric gel was investigated with FESEM study, where the top interface of the polymeric gel was noticed to have random porous structures as is shown in Figure 5.3G, H. This porosity appeared likely due to the removal of unreacted reactants

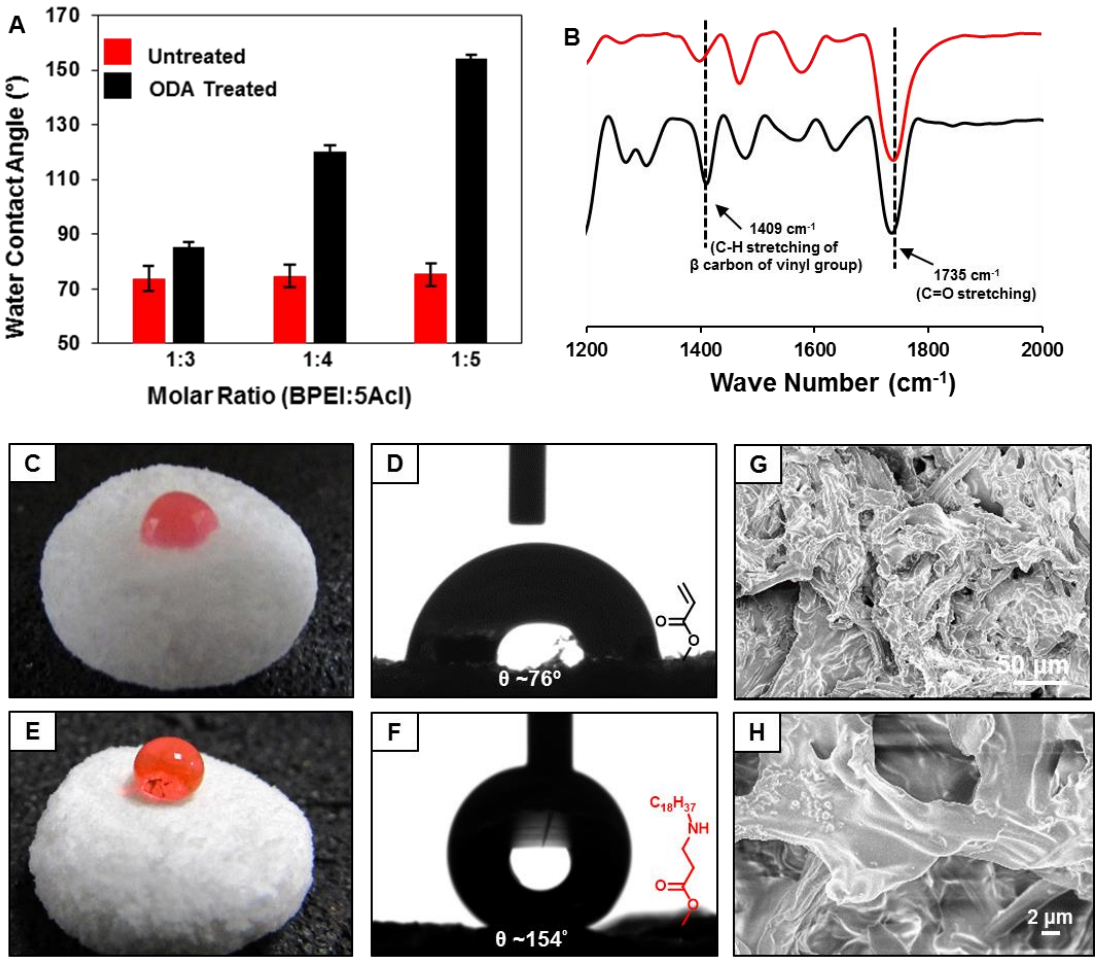

Figure 5.3. (A) The plot accounting for the change in contact angle of the chemically "reactive" polymeric gels that are prepared by mixing BPEI and 5-Acl with different molar ratio, before (red) and after (black) post treatment with ODA molecules. B) FTIR spectra of "reactive" polymeric gel before (black) and after (red) post functionalization with ODA molecules, where the IR peaks at 1735 cm^{-1} and 1410 cm^{-1} denoted the carbonyl stretching and symmetric deformation of the C−H bond for the β carbon of the vinyl group. C-F) Digital images (C, E) and contact angle images (D, F) of beaded water droplet on polymeric gel before (C, D) and after ODA treatment (E, F). G-H) FESEM images of solvent free polymeric gel with BPEI/5-Acl molar ratio of 1:5 in lower (G) and higher (H) magnifications.

during washing of the polymeric gel material. Thus, the "reactive" polymeric gel is embedded with appropriate hierarchical topography, which is an essential parameter for achieving anti-wetting property. Furthermore, this synthesized polymeric gel was capable of displaying inherently durable bulk superhydrophobicity, where the entire polymeric gel (molar ratio1:5 BPEI/5-Acl) that was post modified with ODA molecules was arbitrarily sliced into two parts to expose the interior of the material, and the interiors were observed

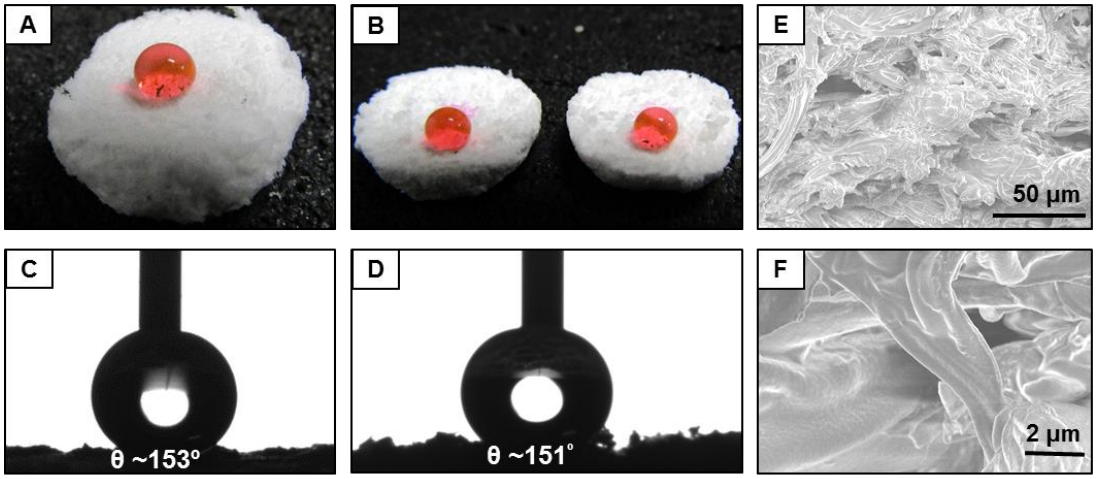

Figure 5.4. (A-D) Digital images (A, B) and water contact angle images (C, D) of beaded water droplet on solvent free polymeric gel (post modified with ODA) before (A, C) and after (B, D) slicing the material. E-F) FESEM images of the interior (bulk) of the polymeric material in lower (E) and higher (F) magnifications.

to be superhydrophobic as the freshly exposed interiors repelled the beaded water droplets with water contact angle above 150° as shown in Figure 5.4A-D. The topography of the material was also investigated in the bulk and was found the porous network similar to that of top surface (Figure 5.4E, F), which infers that the hierarchical topography and essential low surface energy coating is present all throughout the material. The compressive modulus of the gel materials prepared with different ratios of BPEI:5-Acl was calculated, and the gel materials that are prepared varying the molar ratio of BPEI:5-Acl are with similar compressive modulus as is shown in Figure 5.5. The facile chemical approach of synthesizing chemically "reactive" and porous polymeric gel allowed us to tailor various other wettabilities through appropriate post chemical modification in the polymeric gel material (molar composition of the BPEI and 5-Acl mixture was maintained to be 1:5). The post covalent modifications of the chemically reactive polymeric material with various small molecules (having primary amine groups and hydrophobic tails) were characterized with FTIR spectral studies, where the peak at 1410 cm^{-1} was significantly reduced after post chemical modification with selected small molecules, where all the IR peaks are normalized with respect to carbonyl streching (1735 cm^{-1}) as is shown in Figure 5.6. The chemically reactive (inherently hydrophilic) polymeric gel became moderately hydrophobic (WCA ~ 107°) and highly hydrophobic (120°) to superhydrophobic (θ>150°)

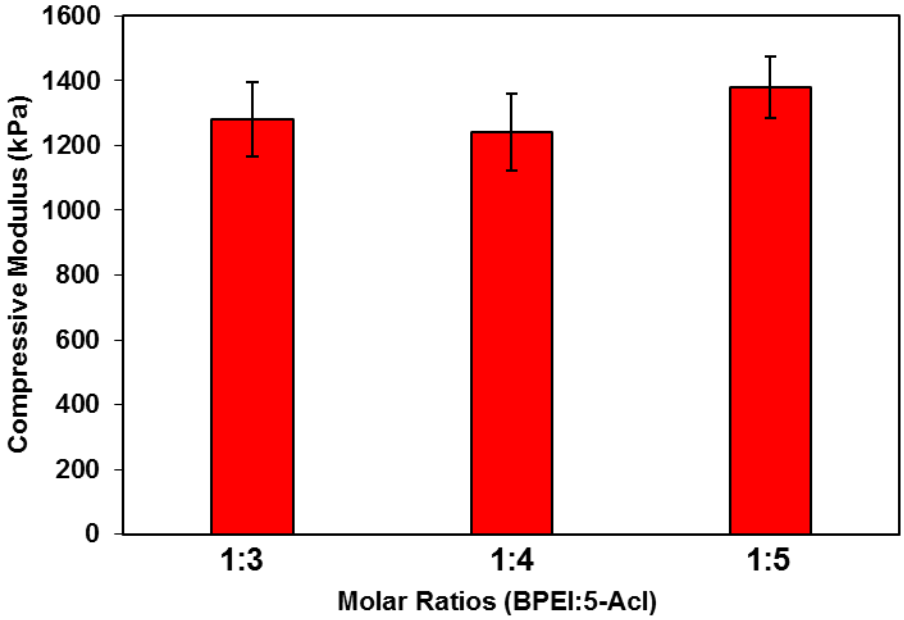

Figure 5.5. Plot accounting the compressive modulus of polymeric gels that are synthesized by changing composition (molar ratio) of the reactants (BPEI/5-Acl) including 1:3, 1:4, and 1:5, in absence of the external solvent.

on increasing the carbon number (from C5 to C18) in the primary amine containing small molecules, which were covalently attached on the polymeric gel through 1, 4-conjugate addition reaction as shown in Figure 5.7. Eventually, the same polymeric material is capable of displaying both homogeneous and heterogeneous wettability. This chemically "reactive" and inherently sticky gel was further coated on glass substrate and after post chemical modification with octadecylamine, the polymeric coating displayed superhydrophobicity with contact angle greater than 150º as is shown in Figure 5.8A, B. The stream of water was observed to readily bounce away after hitting the biomimicked interface (Figure 5.8C), and these simple studies supported the existence of nonadhesive durable superhydrophobicity. Moreover, the morphology of the coating was also found to be similar to the self-standing polymeric monolith as is shown in Figure 5.8D. The coating was further extended to other substrates irrespective of their chemical composition and wettability including glass, plastic film, aluminum foil, filter paper, and wood surface. An amount of 2.8 g of amine reactive gel, which was prepared just by mixing BPEI and 5-Acl (with 1:5 molar ratio), was placed on the surface of selected and cleaned substrates and spread out with one end of the microscopic glass slide uniformly over 21.6 cm^2 area. Then,

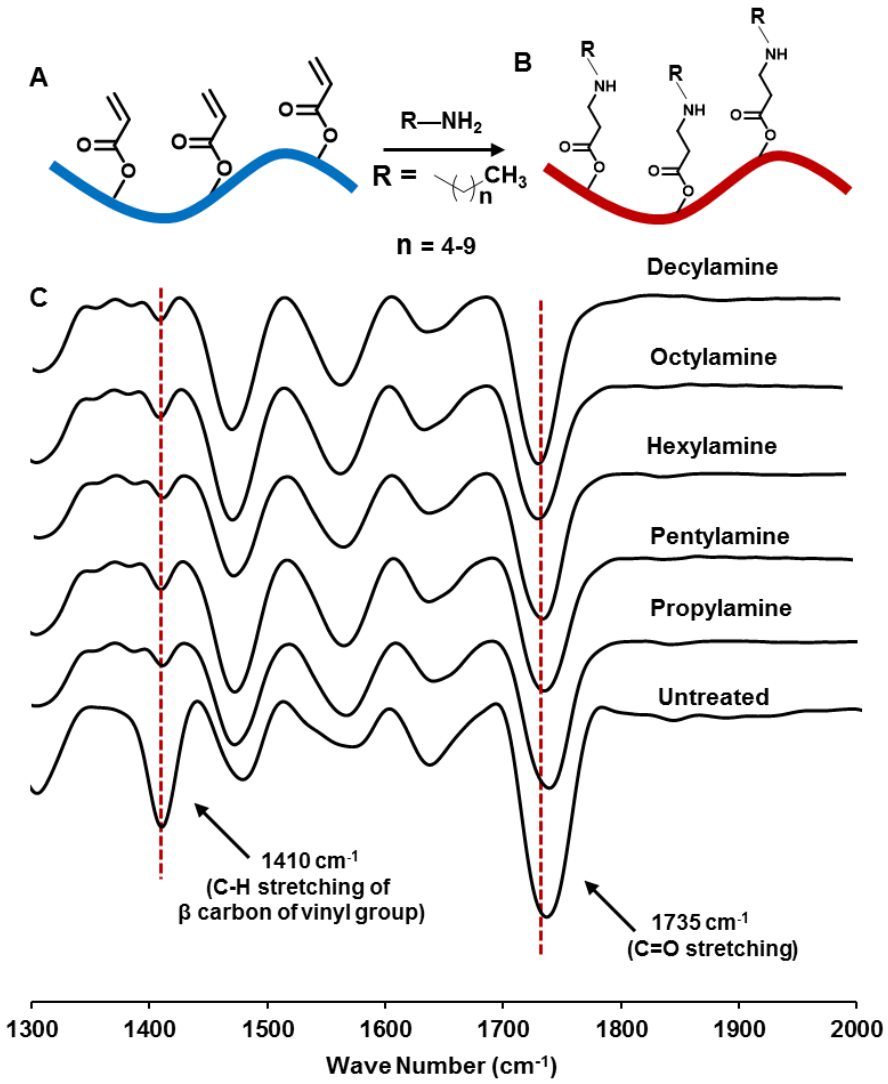

Figure 5.6. (A, B) Schematic illustration of polymeric gel having residual and reactive acrylate moieties and its post chemical modification with primary amine containing small molecules (having shorter or longer hydrocarbon tails (B). C) FTIR spectra of the solvent free and 'reactive' polymeric gel before and after post modification with various amine containing small molecules including propylamine, pentylamine, hexylamine, octylamine and decylamine respectively. The IR peaks at 1736 cm^{-1} and 1410 cm^{-1} denoted the carbonyl stretching and symmetric deformation of the C−H bond for the β carbon of the vinyl group respectively.

the extreme water wettability was adopted on covalently cross-linked "reactive" and polymeric coatings (555 μm ± 40 μm) through the appropriate post chemical modification with octadecylamine (Figure 5.8E-L). This simple approach provided a facile and substrate independent bulk superhydrophobic coating and the water droplets are beaded with high

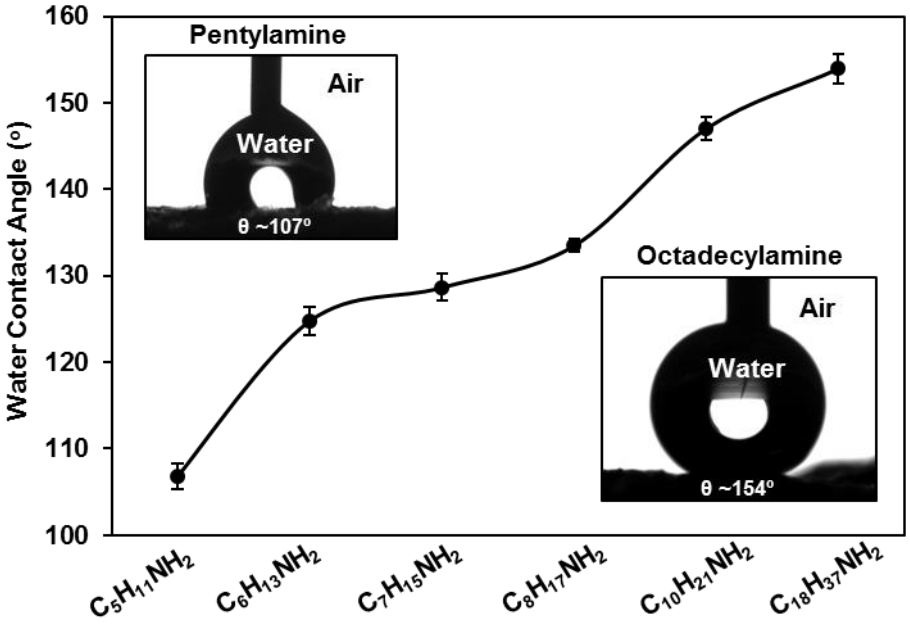

Figure 5.7. Plot showing the change in the water contact angle on the polymeric gel, after the post modification of the material with amine containing small molecules that have different hydrocarbon tail length; insets are the water contact angle (WCA) images of gel after post modification with pentylamine (WCA ~ 107°) and octadecylamine (WCA ~ 154°), respectively.

contact angles (above 150°) and low contact angle hysteresis (below 10°) as shown in Figure 5.8E-L. This current approach did not demand any additional surface modification on the selected substrates. Additionally, the durability of these coatings was examined in details where the polymeric coatings on Al foil, glass, and filter paper were strategically exposed to adhesive tape with 100 g of applied load, and during the peeling of the adhesive tape, some top portion of the film was transferred to the adhesive tape. However, the superhydrophobicity remained intact with the remaining portion of the coating on the selected substrates even after this severe physical damage as shown in Figure 5.9A-F. Hence, this simple study revealed the existence of strong interfacial interaction between the substrate and deposited film likely through nonspecific hydrogen bonding and electrostatic interaction, similar to that of nonspecific interactions in Mussel-inspired coatings.[30] Furthermore, the deposited polymeric coating is embedded with inherently durable bulk superhydrophobicity. The biomimicked coatings were then exposed to 100 g of sand from 15 cm distance, and the embedded special wettability was found to be unaffected (Figure

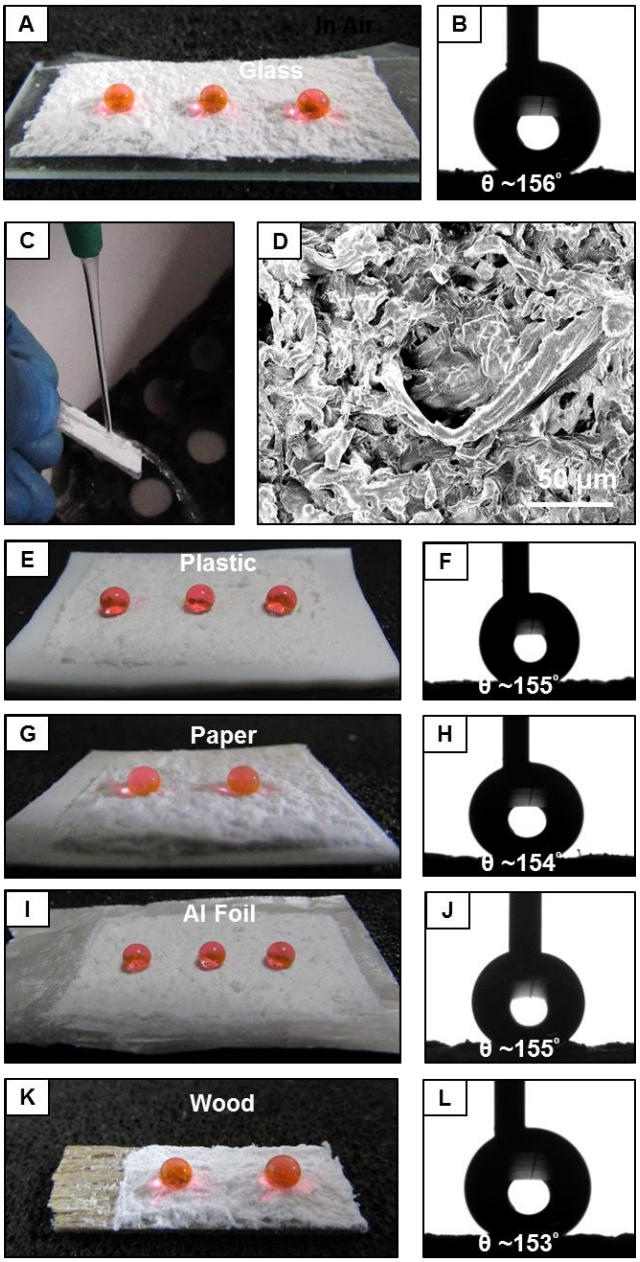

Figure 5.8. (A-B) Digital images (A) and contact angle images (B) of beaded water droplets on the polymeric coatings (post modified with ODA) on glass. C) Digital image showing the stream of water is bouncing away from superhydrophobic surface. D) FESEM image of solvent free polymeric gel coating on glass substrate with BPEI/5-Acl molar ratio of 1:5. E-L) Digital images (E, G, I, K,) and contact angle images (F, H, J, L) of beaded water droplets on the polymeric coatings on the various substrates including plastic (E, F), filter paper (G, H), aluminum foil (I, J), wood (K, L) respectively.

5.9G, H). Next, the superhydrophobic coating was exposed to UV irradiations (λ_{max}= 254 and 365 nm) for 5 days, and extreme water repellency was observed to be unaltered with

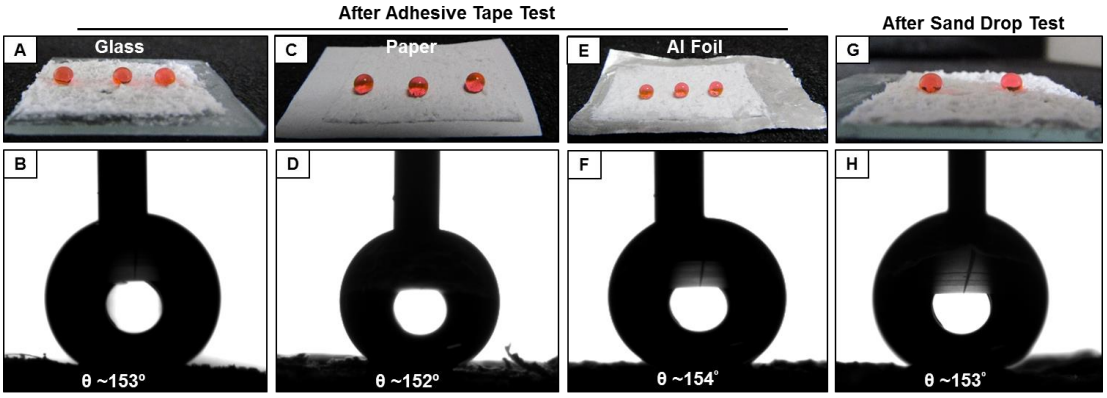

Figure 5.9. (A-F) Digital images (A, C, E) and water contact angle images (B, D, F) of polymeric coating on various substrates (post modified with ODA) after adhesive tape test including glass (A, B), filter paper (C, D), aluminum foil (E, F) after performing adhesive tape peeling test. G-H) Digital image (G) and contact angle image (H) of polymeric coating on glass substrate (post modified with ODA) after performing sand drop test.

advancing water contact angle above 150° after 5 days of exposure as is shown in Figure 5.10A-H. Further, these biomimicked interfaces were exposed to various complex aqueous phases including extremes of pH (1 and 12), artificial seawater and river (Brahmaputra River, Guwahati, India) water, however, the polymeric coating continued to repel these chemically complex phases with advancing contact angle above 150° and contact angle hysteresis below 10° (Figure 5.11). Thus, all these results signify the existence of both

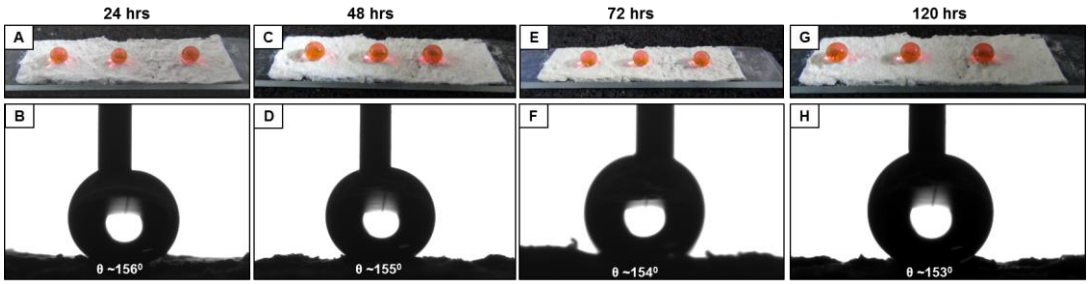

Figure 5.10. (A-H) Digital images (A, C, E, G) and contact angle images (B, D, F, H) of beaded water droplet on the polymeric coating (post modified with ODA) on glass substrate after continuous exposure to UV radiations at short (254 nm) and long (365 nm) wavelengths for 24 hours (A, B), 48 hours (C, D), 72 hours (E, F) and 120 hours (G, H) respectively.

physical and chemical durable superhydrophobicity in the as synthesized polymeric coatings. Hence, this current simple and rapid chemical approach provided a single avenue

for the synthesis of chemically reactive and covalently cross-linked polymeric coatings capable of displaying durable super-water repellency. This approach could be further

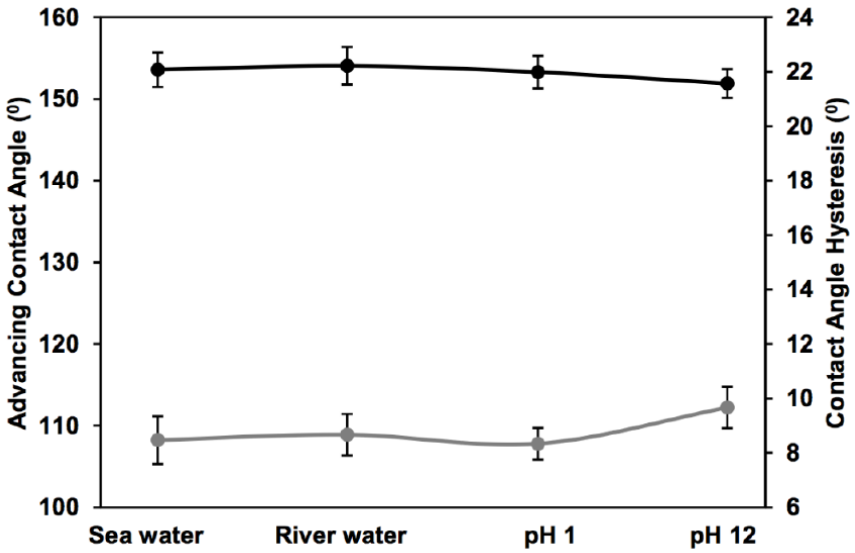

Figure 5.11. The plot accounting the advancing contact angle (black) and contact angle hysteresis (grey) of beaded harsh aqueous phases—including extremes of pH (1, 12), high ionic strength (artificial sea water) and river (Brahmaputra, Assam, India) on the polymeric coating after post modification with ODA.

exploited in developing other functional bio-interfaces and chemically patterned interfaces.[15–17] Thus, this material could be useful in synthesis of antibiofouling coating, drug delivery, anticorrosive coatings, tissue engineering, developing functional patterned interfaces, etc.[1–17,27–29,31]

5.4. Conclusion

In summary, a chemically "reactive" and covalently crosslinked functional polymeric interface is introduced through a solvent/catalyst-free facile and rapid 1, 4-conjugate addition reaction. Further, the presence of residual acrylate groups made this polymeric material inherently chemically reactive and were strategically used in covalent modification with primary amine containing hydrophobic small molecules for developing durable and bulk superhydrophobicity. Moreover, the inherently sticky and reactive gel was coated on various substrates irrespective of their nature and chemical composition. After the appropriate post chemical modification with essential low surface energy molecule, the polymeric coatings displayed superhydrophobicity with high physical and chemical durability. This simple and environmentally friendly single chemical approach could be

useful in synthesizing other functional interfaces (i.e., various chemically patterned interfaces, patterned wettability, etc.) for various smart and prospective applications in practically relevant diverse settings.

References

(1) Lahann, J.; Balcells, M.; Rodon, T.; Lee, J.; Choi, I. S.; Jensen, K. F.; Langer, R. *Langmuir* **2002**, *18*, 3632−3638.

(2) Lahann, J.; Balcells, M.; Lu, H.; Rodon, T.; Jensen, K. F.; Langer, R. *Anal. Chem.* **2003**, *75*, 2117−2122.

(3) Liang, Z.; Wang, Q. *Langmuir* **2004**, *20*, 9600−9606.

(4) Buck, M. E.; Zhang, J.; Lynn, D. M. *Adv. Mater.* **2007**, *19*, 3951−3955.

(5) Chen, H.; Lahann, J. *Langmuir* **2011**, *27*, 34−48.

(6) Deng, X.; Friedmann, C.; Lahann, J. *Angew. Chem.* **2011**, *123*, 6652−6656.

(7) Manova, R.; Van-Beek, T. A.; Zuilhof, H. *Angew. Chem., Int. Ed.* **2011**, *50*, 5428−5430.

(8) Spruell, J. M.; Wolffs, M.; Leibfarth, F. A.; Stahl, B. C.; Heo, J.; Connal, L. A.; Hu, J.; Hawker, C. J. *J. Am. Chem. Soc.* **2011**, *133*, 16698−16706.

(9) Broderick, A. H.; Azarin, S. M.; Buck, M. E.; Palecek, S. P.; Lynn, D. M. *Biomacromolecules* **2011**, *12*, 1998−2007.

(10) Bechler, S. L.; Lynn, D. M. *Biomacromolecules* **2012**, *13*, 1523−1532.

(11) Bally, F.; Cheng, K.; Nandivada, H.; Deng, X.; Ross, A. M.; Panades, A.; Lahann, J. *ACS Appl. Mater. Interfaces* **2013**, *5*, 9262−9268.

(12) Yoshii, T.; Onogi, S.; Shigemitsu, H.; Hamachi, I. *J. Am. Chem. Soc.* **2015**, *137*, 3360−3365.

(13) Carter, M. C. D.; Jennings, J.; Speetjens, F. W.; Lynn, D. M.; Mahanthappa, M. K. *Macromolecules* **2016**, *49*, 6268−6276.

(14) Liu, P.; Zhang, H.; He, W.; Li, H.; Jiang, J.; Liu, M.; Sun, H.; He, M.; Cui, J.; Jiang, L.; Yao, X. *ACS Nano* **2017**, *11*, 2248−2256.

(15) Bog, U.; Los, A. D.; Pereira, S.; Mueller, S. L.; Havenridge, S.; Parrillo, V.; Bruns, M.; Holmes, A. E.; Emmenegger, C. R.; Fuchs, H.; Hirtz, M. *ACS Appl. Mater. Interfaces* **2017**, *9*, 12109−12117.

(16) Chen, H. Y.; Hirtz, M.; Deng, X.; Laue, T.; Fuchs, H.; Lahann, J. *J. Am. Chem. Soc.* **2010**, *132*, 18023−18025.

(17) Li, J.; Li, L.; Du, X.; Feng, W.; Welle, A.; Trapp, O.; Grunze, M.; Hirtz, M.; Levkin, P. A. *Nano Lett.* **2015**, *15*, 675−681.

(18) Buck, M. E.; Schwartz, S. C.; Lynn, D. M. *Chem. Mater.* **2010**, *22*, 6319−6327.

(19) Manna, U.; Broderick, A. H.; Lynn, D. M. *Adv. Mater*. **2012**, *24*, 4291−4295.

(20) Yao, X.; Song, Y.; Jiang, L. *Adv. Mater.* **2011**, *23*, 719−734.

(21) Ueda, E.; Levkin, P. A. *Adv. Mater.* **2013**, *25*, 1234−1247.

(22) Wen, L.; Tian, Y.; Jiang, L. *Angew. Chem., Int. Ed.* **2015**, *54*, 3387−3399.

(23) Feng, L.; Li, S.; Li, Y.; Li, H.; Zhang, L.; Zhai, J.; Song, Y.; Liu, B.; Jiang, L.; Zhu, D. *Adv. Mater.* **2002**, *14*, 1857−1860.

(24) Li, X. M.; Reinhoudt, D.; Crego-Calama, M. *Chem. Soc. Rev*. **2007**, *36*, 1350−1368.

(25) Zhang, X.; Shi, F.; Niu, J.; Jiang, Y. G.; Wang, Z. Q. *J. Mater. Chem.* **2008**, *18*, 621−633.

(26) Yan, Y. Y.; Gao, N.; Barthlott, W. *Adv. Colloid Interface Sci.* **2011**, *169*, 80−105.

(27) Verho, T.; Bower, C.; Andrew, P.; Franssila, S.; Ikkala, O.; Ras, R. H. A. *Adv. Mater.* **2011**, *23*, 673−678.

(28) Feng, L.; Li, S.; Li, Y.; Li, H.; Zhang, L.; Zhai, J.; Song, Y.; Liu, B.; Jiang, L.; Zhu, D. *Adv. Mater.* **2002**, *14*, 1857−1860.

(29) Liu, M.; Wang, S.; Jiang, L. *Nat. Rev. Mater.* **2017**, *2*, 17036.

(30) Kang, S. M.; You, I.; Cho, W. K.; Shon, H. K.; Lee, T. G.; Choi, I. S.; Karp, J. M.; Lee, H. *Angew. Chem., Int. Ed.* **2010**, *49*, 9401−9404.

(31) Xu, Z.; Wang, L.; Yu, C.; Li, K.; Tian, Y.; Jiang, L. *Adv. Funct. Mater*. **2018**, *28*, 1703970−1703977.

Chapter 6: Synthesis of Stretchable Superhydrophobic Interface*

Stretchable and durable superhydrophobic materials are of potential interest for developing ultra-flexible electronics, flexible microfluidics, gas sensors, functional textiles, wearable devices etc. In general, the physical deformation of a material compromises the embedded antifouling property likely through perturbation in appropriate surface topography/chemistry, and appears as a potential 'Achilles' heel' of this prospective antifouling property in diverse practical settings. Here in this chapter, a highly stretchable and durable superhydrophobic membrane that strongly repels aqueous phase both in air and under oil is introduced by rationally exploiting a facile and robust 1, 4-conjugated addition reaction between amine and acrylate groups from branched poly (ethyleneimine) (BPEI) and dipentaerythritol penta-acrylate (5-Acl) respectively. An amine 'reactive' (due to the presence of residual acrylate groups) polymeric nanocomplexes which were formed on just mixing of BPEI and 5-Acl in ethanol, were directly immobilized on a BPEI modified polyurethane fibrous substrate to adopt appropriate hierarchical topography, and further post covalent modification of these immobilized 'reactive' nanocomplexes with strategically selected small molecules (i.e. octadecylamine) ensured the essential surface chemistry in the synthesized material. In the current design, scalable and facile dip coating (through covalent chemistry) followed by appropriate post chemical modifications yielded a highly durable superhydrophobicity, which is capable of enduring its anti-wetting property even at 150% tensile deformation of the material for 1000 times. Moreover, the synthesized material can survive exposure to various other physical and chemical insults, which are common in various severe practical settings. The synthesized material is further exploited in energy efficient and rapid separation of both heavy and light oils from complex (sea, river, extremes of pH etc.) aqueous phases with separation efficiency above 99% for multiple cycles.

* Rather, A. M.; Manna, U. *J. Mater. Chem. A* **2017**, *5*, 15208–15216

Chapter 6

6.1. Introduction

In the last couple of decades, several top-down and bottom-up approaches have been introduced to decorate planar or complex surfaces with appropriate hierarchical topography and essential low surface energy coating to achieve desired superhydrophobicity through stabilizing the metastable trapped air (Cassie–Baxter state).[1,2] However, the physical deformation of such materials due to stretching, is likely to damage the trapped metastable air pockets through perturbation of essential topography and chemistry at top of the material, and eventually compromise the embedded antifouling property.[3,4] While this phenomenon has been recently exploited in a specialized application (i.e. triggered release of small molecules),[5] it also appears as a potential 'Achilles' heel' of several prospective and relevant applications of extremely non-wetting interfaces at practical settings.[6–10]

Recently, stretchable superhydrophobic materials have emerged as a prospective avenue for developing ultra-flexible electronics, flexible microfluidics, gas sensors, functional textiles, wearable devices etc.[11–19] In the literature, few elegant approaches have been introduced to fabricate stretchable superhydrophobic materials adopting three-dimensional (3D) structures with appropriate hierarchy and chemistry by exploiting hierarchical wrinkles, polytetrafluoroethylene decorated polymeric nanostructures, polymeric hydrogels, crumpling of graphene, multilayers of polydopamine/Ag nanoparticles, blends of carbon nanofiber/paraffin etc.[3,11–15,20] However, in most of the cases, during the deformation process, the 3D topography in the synthesized materials is susceptible to change,[3,11–13] and their anti-wetting property gets compromised on large physical deformations even below 100% strain,[12,13] most likely due to perturbation in the essential topography and surface chemistry of the material, and that would be related to the presence of weak (and non-covalent) interfacial interaction between either the coating materials/the underlying substrate, or hierarchical topography /low surface energy coating. A few of the synthesized materials that are appropriate for sustaining high physical deformations without compromising their anti-wetting property[3,11,14,15,20] are susceptible to lose essential topography and chemistry during other physical manipulations (e.g. adhesive tape test, sand drop test, manual rubbing etc.) due to lack of strong interfacial interaction between the coating components and the substrates. For example, in a blend of carbon nanofiber/paraffin, the brittle carbon nanofibers are highly liable to erode away on exposure

to a regular physical abrasion process, due to lack of strong chemical interaction of carbon nanofiber with natural rubber.[3,14,20] Further, some of these synthesized materials are involved in essential low surface energy modification using fluorination chemistry[11,15] and the prolonged exposure to such materials is known to cause many intractable diseases.[21] Recently, Parkin and co-workers have developed a unique material that not only displays superhydrophobicity in air but also under oil; the material was synthesized by exploiting perfluorooctyltriethoxysilane-decorated dual-scale nanoparticles of titanium dioxide (TiO_2).[22] Inspired by this early demonstration, in the current chapter, a highly stretchable and durable superhydrophobic membrane was developed, that strongly repels aqueous phase both in air and under oil without applying any fluorination chemistry. Here in this chapter, a facile 1, 4-conjugate addition reaction[23–25] between amine and acrylate groups (Figure 6.1A, B) is (1) exploited for simple immobilization of 'reactive' nanocomplexes (RNC) on a selected fibrous substrates to achieve appropriate topography, and further (2) covalent modification of these immobilized 'reactive' nanocomplexes with primary amine-containing hydrophobic small molecule (i.e. octadecylamine) provided essential surface chemistry. Further, these stretchable and highly durable superhydrophobic membranes that displayed extreme water repellency both in air and under oil are explored in rapid separation/collection of both heavy and light oils from oil/water mixtures, where oil can be separated with a rate of ~115 mL min^{-1} with oil separation efficiency above 99% irrespective of the nature of contaminations (i.e. pH, salt etc.) in aqueous phases.

6.2. Materials and Methods

Dichloromethane (DCM) was purchased from Merck Life Science Pvt Ltd (Bangalore, India). Kerosene oil was obtained from a local shop in Guwahati city (Assam, India). Fibrous polyurethane (PU) fabric and cotton thread were purchased from a local shop in Guwahati city (Assam, India). The details of all other chemicals and materials used in this chapter, are already discussed in the chapter 2.

6.2.1. General Considerations

The instruments used to characterize the synthesized stretchable membrane were same as discussed previously in the chapter 2.

6.2.2. Coating of Fibrous Substrates with RNC and Post-Chemical Modifications

First, 1.325 g of 5-Acl and 0.5 g of BPEI was dissolved individually in 10 mL of ethanol. Mostly, three steps are involved to achieve the durable superhydrophobicity in fibrous substrates. (i) Selected fibrous substrates (PU fabric/cotton thread) were placed in a BPEI solution (10 mg BPEI per mL of ethanol) for three hours. After this BPEI treatment, PU fabric/cotton thread substrates were thoroughly rinsed with ethanol to remove loosely bound BPEI molecules and were dried at ambient conditions. (ii) The BPEI-treated fibrous substrates were transferred to a mixture of 5-Acl/BPEI (1 mL of 5-Acl and 0.3 mL of BPEI), and kept for 1 h, over this time, the reaction solution turned into a turbid liquid. Then the fibrous substrates were removed from the turbid mixture of BPEI/5-Acl and were thoroughly washed with THF for 1 h to remove the loosely bound nanocomplexes before (iii) transferring into octadecylamine (ODA) solution (5 mg mL^{-1} in THF) for overnight. After ODA treatment, fibrous substrates were further rinsed with THF for 1 h to remove the unreacted and loosely bound ODA molecules and were dried at ambient conditions, then the antiwetting property was analysed with visual inspection and water contact angle measurements. Other water wettability on the PU fabric were optimized by following similar post chemical modification of RNC-coated fibrous substrate with selected small molecules including propylamine (30 mg/mL), pentylamine (30 mg/mL) hexylamine (30 mg/mL), octylamine (30 mg/mL) and decylamine (30 mg/mL) in THF respectively. Afterwards, the fibrous substrates were further rinsed with THF for 1 h to remove unreacted and loosely bound corresponding small molecules from the material, and the post modified materials were allowed to air dry at ambient conditions. Later, the anti-wetting property was examined with digital images and contact angle measurements.

6.2.3. Physical and Chemical Durability Tests

Various complex and harsh physical/chemical durability tests were performed on the superhydrophobic PU fibrous substrate following the same protocol that are already discussed in the chapter 2.

6.2.3.1. Tensile Deformation Test

The superhydrophobic PU fibrous substrate was manually stretched with the different tensile strains. The streching percentage was calculated by measuring the change in length of material before and after incurring the tensile deformation using the following formula:

Percentage (%) of streching = [Final length – Initial length]/ [Initial length] x 100

6.2.3.2. Creasing and Bending Test

In this particular test, superhydrophobic PU fibrous substrate was manually creased with the index finger for 1-2 minutes, and at the end a clearly visible crease mark was noted on the substrate. Afterwards, the anti-wetting property on the creased interface was examined by visual inspection and contact angle measurement. The water droplets were beaded on the creased region with high contact angle (>150^{o}). Similarly the superhydrophobic PU fabric was manually twisted and bended several times and no change in the physical integrity as well as the anti-wetting property was observed. (See results and discussion section for more details).

6.2.4. Gravity Driven and Energy Efficient Oil/Water Separation

The superhydrophobic PU fibrous substrate was used as a membrane for gravity driven and selective filtration of oil/oily phase from oil/water mixture. As a proof of concept demonstration, an oil/water separation prototype was built in the lab using a centrifuge tube (50 mL, Falcon), and the stretchable membrane was wrapped on the opening of the tube, and a side hole was made at the other end of the tube for both pouring the oil/water mixture and collecting the separated water at the end—by rotating down the hole with appropriate inclination of the Falcon tube. This lab-made prototype was used in demonstration of oil/water separation, where aqueous phase is separately contaminated with heavier (DCM), lighter (kerosene) and highly viscous (silicone oil) oils. The oil/oily phase was selectively and readily passed through the superhydrphobic PU membrane and the filtration of aqueous phase was remained restricted. Control experiment was also performed with uncoated PU substrate in which both oil and water passes through the membrane.

6.3. Results and Discussion

6.3.1. 'Reactive' Coating on Fibrous Substrate and Characterization of Anti-Wetting Properties in Air and Under Oil

In chapter 2, I have shown that the reaction mixture of BPEI/5-Acl in ethanol was transformed into self standing polymeric gel via formation of turbid solution of polymeric nanocomplex. Here, in this chapter, this growing polymeric nanocomplexes is strategically used for decorating a BPEI treated fibrous substrate of polyurethane (PU) as shown in Figure 6.1. The synthesized nanocomplexes on mixing of BPEI/5-Acl in ethanol (Figure

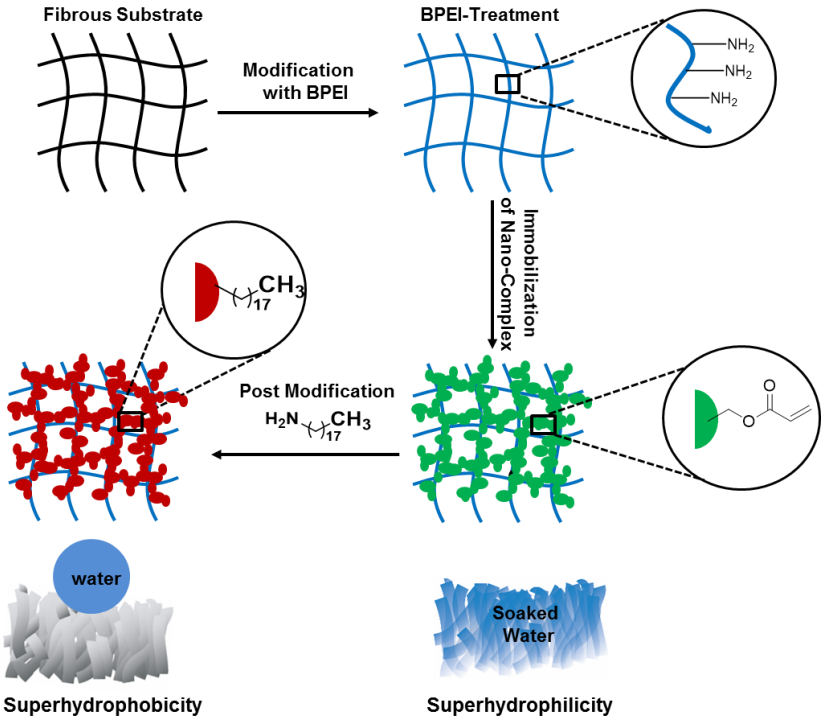

Figure 6.1. Schematic illustration of the synthesis of superhydrophobic PU fabric. In the first step, fibrous substrates are modified with BPEI polymer to install primary amine groups on the fibrous network. In the second step, the 'reactive' nanocomplexes are immobilized on the PU fabric, and in the third step, the PU fabric was chemically post-modified with ODA molecules to achieve nonadhesive superhydrophobicity.

6.2A-C) remained chemically reactive as shown in Figure 6.2D. FTIR peaks at 1410 cm^{-1} and 1739 cm^{-1} in the spectra are the characteristic peaks for the symmetric deformation of the C–H bond for the β carbon of the vinyl groups and the ester carbonyl stretching. Hence, the presence of these IR peaks revealed the presence of residual acrylate groups in the polymeric nanocomplexes (Figure 6.2D, black spectrum). The characteristic peak at 1410 cm^{-1} for residual acrylate groups was noticed to be depleted significantly after the post-chemical modification with amine containing small molecules (Figure 6.2D, red spectrum). The dynamic light scattering (DLS) study of the BPEI/5-Acl mixture in ethanol was performed in presence and absence of selected substrate (Figure 6.2E). The growth of the nanocomplexes was noticed to be faster in the presence of BPEI-treated PU fibrous substrate, and the nanocomplexes started to form immediately after mixing of BPEI and 5-Acl in ethanol at room temperature (20ºC). After 30 mins, the size of the nanocomplexes

in mixtures of BPEI/5-Acl in ethanol were observed to be 394 nm and 272 nm in the presence and absence of BPEI functionalized PU substrates respectively which revealed that the growth of the nanocomplexes is accelerated in the presence of BPEI-functionalized PU substrates solution as is shown in Figure 6.2E. This accelerated growth of nanocomplexes is due to the excess of amine functionalities in the BPEI treated fibrous substrate. The presence of BPEI functionalized PU substrate was kept in the BPEI/5-Acl mixture for 1 h, and during this period, the growing nanocomplexes are assumed to be deposited on the fibrous substrate through 1, 4-conjugate addition reaction, and the immobilization of these growing nanocomplexes would provide the appropriate topography to the material for achieving the desired anti-wetting property.

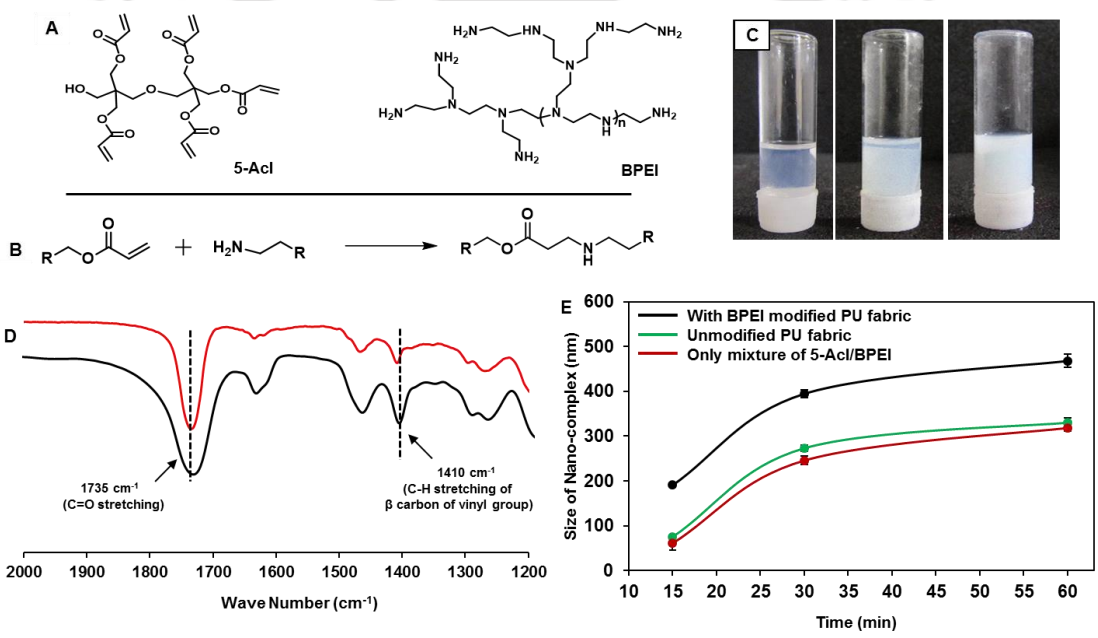

Figure 6.2. (A) The chemical structures of dipentaerythritol penta-acrylate (5-Acl) and branched poly (ethyleneimine) (BPEI). B) Schematic representation of 1, 4-conjugate addition reaction between illustrative primary amine and acrylate groups. C) Digital images showing appearance of turbidity in BPEI/5-Acl mixtures (after 1 h of mixing) in absence (left) and presence of unmodified (middle) and BPEI-modified (right) PU substrate. D) FTIR spectra of nano-complex before (black) and after (red) post-chemical treatment with octadecylamine molecules, the peaks at 1736 cm^{-1} and 1410 cm^{-1} denoted the carbonyl stretching and symmetric deformation of the C−H bond for the β carbon of the vinyl group respectively. E) The DLS study illustrating the growth of the reactive nanocomplex (RNC) in the mixture of 5-Acl/BPEI in ethanol in absence (red) and in presence of unmodified (green) and BPEI-modified (black) fibrous substrate with time.

The uncoated fibrous membrane was observed to be inherently superhydrophilic and it readily soaked up the beaded aqueous droplets (red color aids visual inspection) into the fibrous matrix with contact angle of 0º as shown in Figure 6.3A-B, and thus, the PU fibrous matrix remained superhydrophilic even after treatment with polymeric nanocomplex solution. However, this polymeric nanocomplex-coated fibrous PU matrix started to

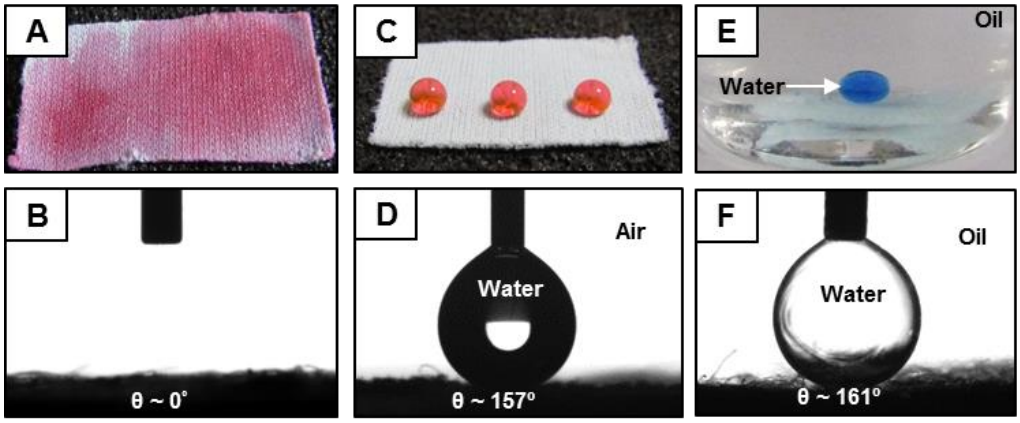

Figure 6.3. (A-F) Digital images (A, C, E) and water contact angle images (B, D, F) of water droplets (red and blue colour aids visual inspection) on uncoated (A, B) and nanocomplex-coated (C-F) PU substrate (nanocomplexes are functionalized with octadecylamine molecules) both in air (C, D) and under hexane (model oil) (E, F).

display extreme water repellency both in air and under oil after post chemical modification of the material with octadecylamine molecules, where the red and the blue colored water droplets were beaded on the material with advancing contact angle of 157º and 161º, and with contact angle hysteresis of 4º and 3º, respectively (Figure 6.3C-F). Next, the residual acrylate groups as confirmed with FTIR analysis in the nanocomplexes were rationally used in tailoring the water wettability in the nanocomplex-coated PU fibrous substrate through 1, 4-conjugate addition reaction with amine-containing small molecules, where the lengths of hydrocarbon chain of the amine-containing small molecules are strategically and gradually increased (from butylamine (C4) to octylamine (C8), for tailoring hydrophobicity in the synthesized material. It was eventually endowed with adhesive superhydrophobicity with advancing contact angle of ~152º and contact angle hysteresis of ~13º, after post-chemical modification of the nanocomplex coated PU membrane with octylamine (Figure 6.4E). Furthermore, the material displays the nonadhesive superhydrophobic property with

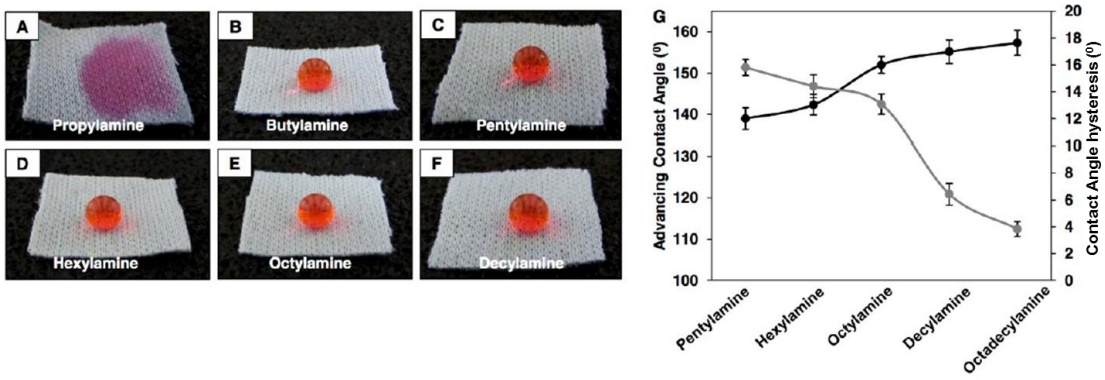

Figure 6.4. (A-F) Digital images depicting the wettability of liquid water (red color aids visual inspection) on the RNC coated PU substrate after post-chemical modification with various amine containing small molecules including propylamine (A), butylamine (B), pentylamine (C), hexylamine (D), octylamine (E) and decylamine (F). G) The plot accounting the advancing contact angle (black) and contact angle hysteresis (grey) of beaded water droplets on the RNC coated PU substrate after various post-chemical functionalizations.

advancing contact angle of 156º and contact angle hysteresis of 6º after post chemical modification with decylamine as is shown in Figure 6.4F, G. Hence, the wettability of the selected fibrous substrate can be tailored from hydrophilic to superhydrophobic (adhesive and nonadhesive) by tuning the hydrocarbon chain length of the amine containing small molecules. The topography of the PU fibers was examined with FESEM analysis, where smooth and featureless native PU fibers (Figure 6.5A) were found to be uniformly coated with random granular domains due to immobilization of growing nanocomplexes from BPEI/5-Acl mixture in ethanol as shown in Figure 6.5B, C. Thus, the developed topography of random granular domains uniformly deposited on every fiber of the PU fabric was found

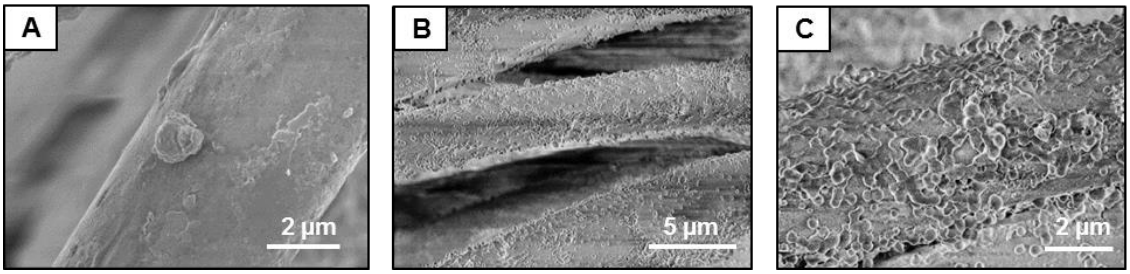

Figure 6.5 (A-C) FESEM images of the PU substrate before (A) and after immobilization of the RNC (B, C) at low (B) and higher magnifications (A, C).

to be appropriate to achieve desired superhydrophobicity that functions both in air and under oil.

6.3.2. Effect of Various Physical Deformations of the Membrane on its Antifouling Property

Elastomeric property of PU fibers has been strategically utilized in the past to develop various stretchable multifunctional materials. In this chapter, the same material (PU fabric) was further exploited in developing a stretchable and durable superhydrophobic material. The nanocomplex coated and chemically post-modified PU fibrous membrane was manually deformed with various extents of applied tensile strains, and the anti-wetting property of the material was noticed to remain unperturbed with advancing contact angle above 150º and contact angle hysteresis below 10º even after incurring 150% tensile deformation to the material Figure 6.6A-B. The reduction in advancing contact angle was measured to be only ~ 4º during the entire 150% tensile deformation of the material as is shown in Figure 6.6C. The water droplets beaded on the stretched (150% deformed) interface with advancing contact angle of ~154º (Figure 6.6B) and a stream of water was found to be readily bounced back from the stretched (150%) superhydrophobic PU membrane, which indicated the existence of robust and nonadhesive superhydrophobicity even for the physically deformed superhydrophobic interface. However, the material become adhesive superhydrophobic with advancing contact angle of ~153º and contact angle hysteresis of ~11º after 200% deformation of the interface (Figure 6.6C). The large deformation of the interface is likely to affect the topography or chemical functionality on the synthesized superhydrophobic interface. Next, the superhydrophobic PU fibrous membrane was exposed to physical deformation multiple times, where the material was stretched with 150% strain for 1000 times, and the anti-wetting property of the material remained intact with advancing water contact angle above 150º and contact angle hysteresis of below 10º during the entire process. After 1000 times of deformation with 150% strain, the advancing contact angle and contact angle hysteresis were measured to be ~153º and ~8º respectively. Therefore, the synthesized stretchable superhydrophobic PU membrane has highly durable anti-wetting property, which remained unaffected with large tensile deformation. Afterwards, the synthesized material was exposed to several other forms of physical manipulations that are commonly encountered in practical settings including

bending, creasing, twisting, rubbing etc., to examine the durability of the embedded anti-

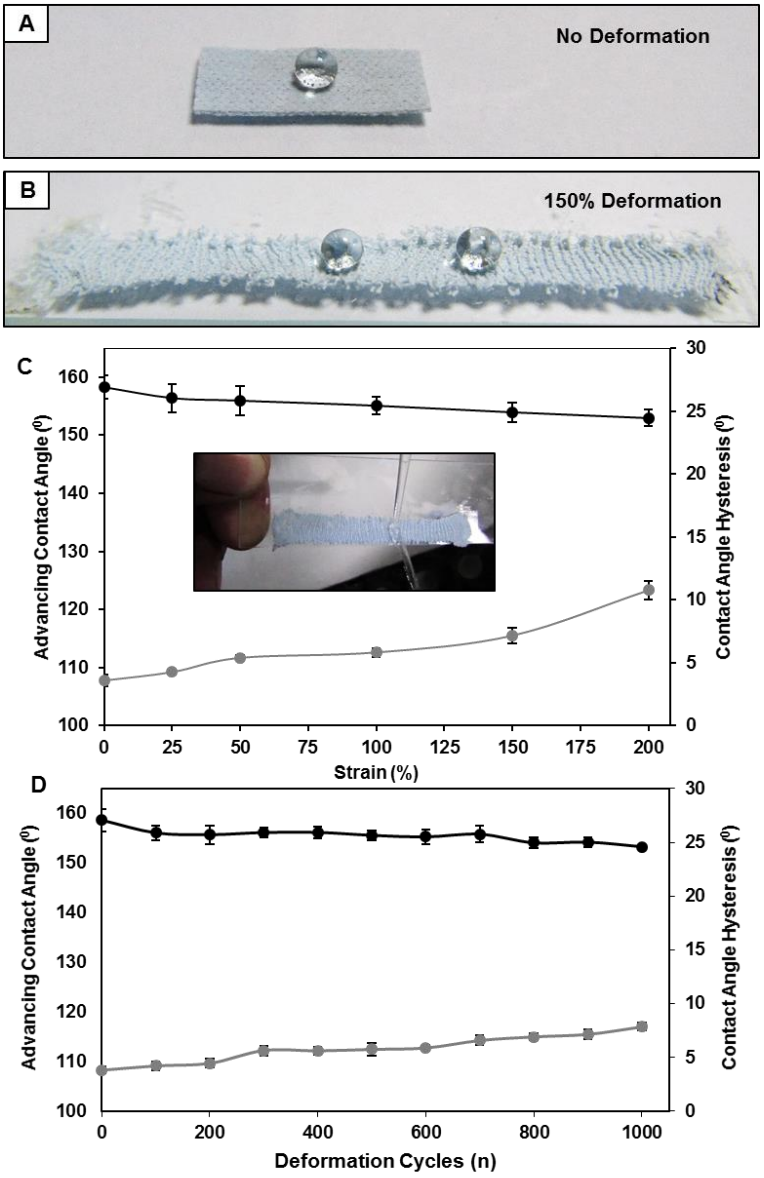

Figure 6.6. (A, B) Digital images of beaded water droplet on the superhydrophobic fibrous PU substrate before (A) and after incurring deformation with 150% strain (B). C) Plot accounting the advancing contact angle (black) and contact angle hysteresis (grey) of water droplet on the superhydrophobic PU substrate that was gradually deformed upto 200% strain and digital image (inset) depicting the bouncing of a jet of water on deformed (with 150% strain) superhydrophobic substrate. D) Plot illustrating the change in the advancing contact angle (black) and contact angle hysteresis (grey) of beaded water droplet on the superhydrophobic PU substrate after repetitive (100 times) deformation (with 150% strain) of synthesized interface.

wetting property. The synthesized superhydrophobic interface was capable of withstanding such challenging and complex scenarios (Figure 6.7A-D) with advancing contact angle

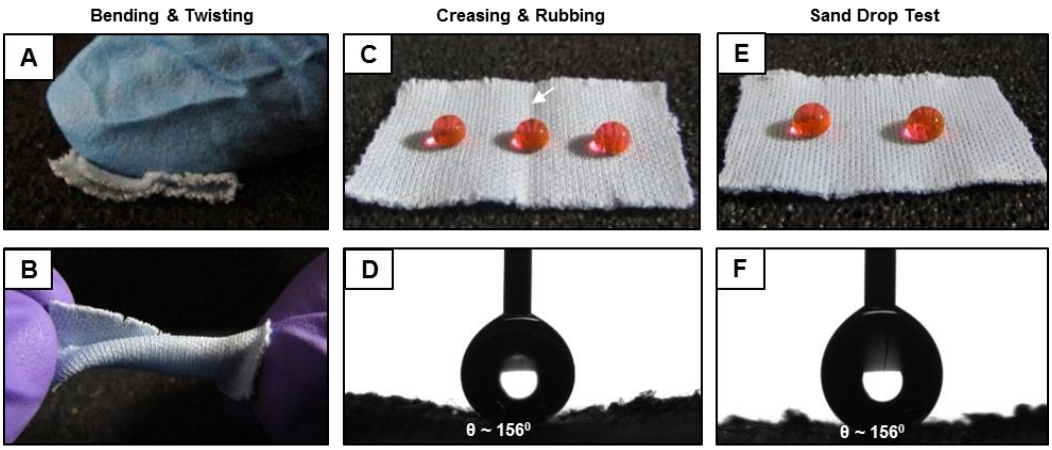

Figure 6.7. (A, B) Digital images of superhydrophobic PU substrate that is manually creased (A) and twisted (B). C-F) Digital images (C, E) and water contact angle images (D, F) of beaded water droplets on superhydrophobic PU substrate after manual rubbing and creasing (C, D); the water droplet was placed on the creased area as marked by white arrow of substrate and sand drop test (E, F).

above 150º and contact angle hysteresis of below 10º. The red colored (aiding visual inspection) water droplet beaded on the creased region of the material with advancing contact angle of ~156º as shown in Figure 6.7C, D. Moreover, 150 g of sand was constantly dropped on the same material from 20 cm height, and the material displayed extreme water

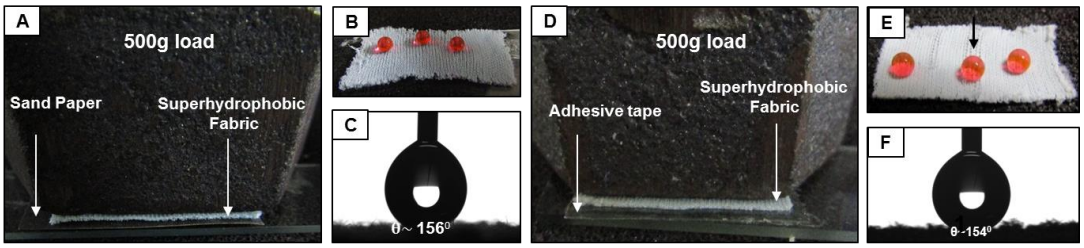

Figure 6.8. (A) Experimental setup for sand paper abrasion test, where superhydrophobic PU fabric was exposed to the sand paper with 500 g load. B-C) Digital image (B) and water contact angle image (C) of beaded water droplet on the superhydrophobic PU substrate after performing sand paper abrasion. D) Experimental setup for adhesive tape test, where superhydrophobic PU fabric was exposed to one of the surface of the double sided adhesive tape with 500 g load. E-F) Digital image (E) and contact angle images (F) of beaded water droplet on the superhydrophobic PU substrate after peeling off the adhesive tape.

repellency with advancing contact angle of ~156º, and no apparent change in physical appearance was noticed after the sand drop test (Figure 6.7E, F).

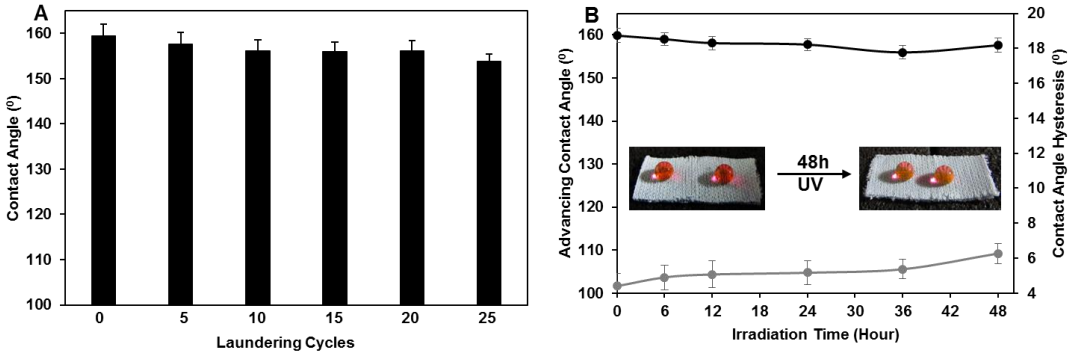

Figure 6.9. (A) The plot accounts the effect of successive (25 times) laundering tests on the water wettability. B) The plot illustrating the effect of prolonged (48 h) exposure of UV light on the wettability of the synthesized material.

Further, the stretchable superhydrophobic interface was rubbed with sandpaper under a load of 500 g across 5 cm distance back and forth for multiple times (5 times); although the minor deformation in the physical integrity of the membrane was noticed after sand paper abrasion, but the anti-wetting property remained intact with advancing contact angle of 156º as is evident in Figure 6.8A-C. Moreover, the material was exposed to adhesive tape with 500 g load to facilitate better contact between adhesive tape and superhydrophobic PU fabric. During the peeling of the adhesive tape, the physical integrity of the material was

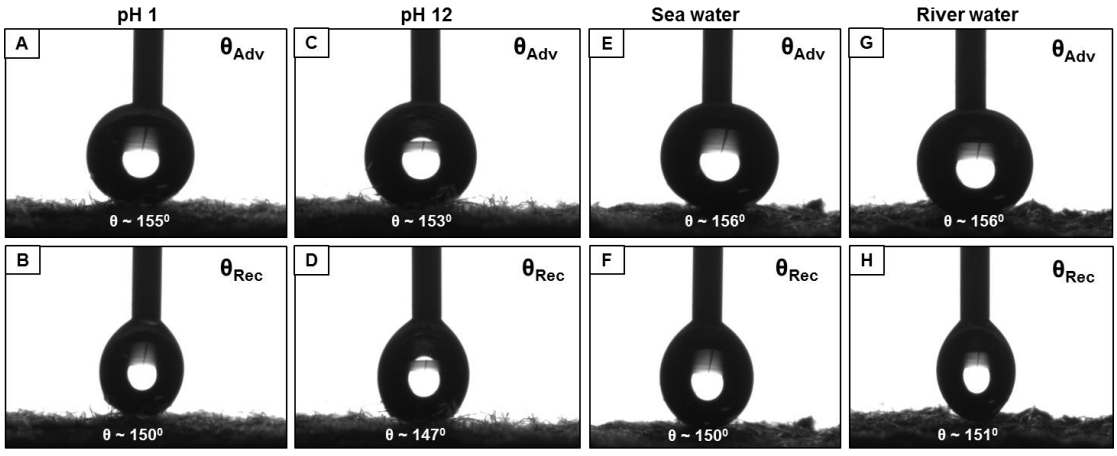

Figure 6.10. (A-H) Advancing (A, C, E, G) and receding (B, D, F, H) water contact angle images of the beaded water droplets on the superhydrophobic membrane after continuous exposure to complex aqueous phases including pH 1 (A, B), pH 12 (C, D), sea water (E, F), river (Brahmaputra, Assam India) water (G, H)) for 48 hours.

noticed to be affected in some regions as marked by the black arrow in Figure 6.8E; however, the superhydrophobicity of the material remained unperturbed with advancing contact angle of ~154º, including the area which is physically affected during this abrasion test (Figure 6.8E, F). Moreover, the superhydrophobic membrane was treated with a knife for multiple times, and the material continued to display extreme water repellency even after performing the test. In addition to these physical durability tests, a standard laundering test was performed on the superhydrophobic membrane following a reported protocol.[27] Briefly, the superhydrophobic membrane was washed in presence of 0.37 wt% of surfactant (SDS) for 30 mins and is considered as one cycle and the same was repeated for 25 cycles. However, the advancing water contact angle was measured to be above 153º even after performing the successive laundering test on the material for 25 cycles (Figure 6.9A). Moreover, the stretchable membrane was exposed to UV radiations at short (254 nm) and long (365 nm) wavelengths for 48 h and the extreme water repellant property of the stretchable membrane remained intact with advancing contact above 150º and contact angle hysteresis below 10º as is noted in Figure 6.9B. Moreover, the anti-wetting property in the material was observed to be unaffected with advancing water contact angle above 150º and contact angle hysteresis below 10º even after exposing the stretchable superhydrophobic

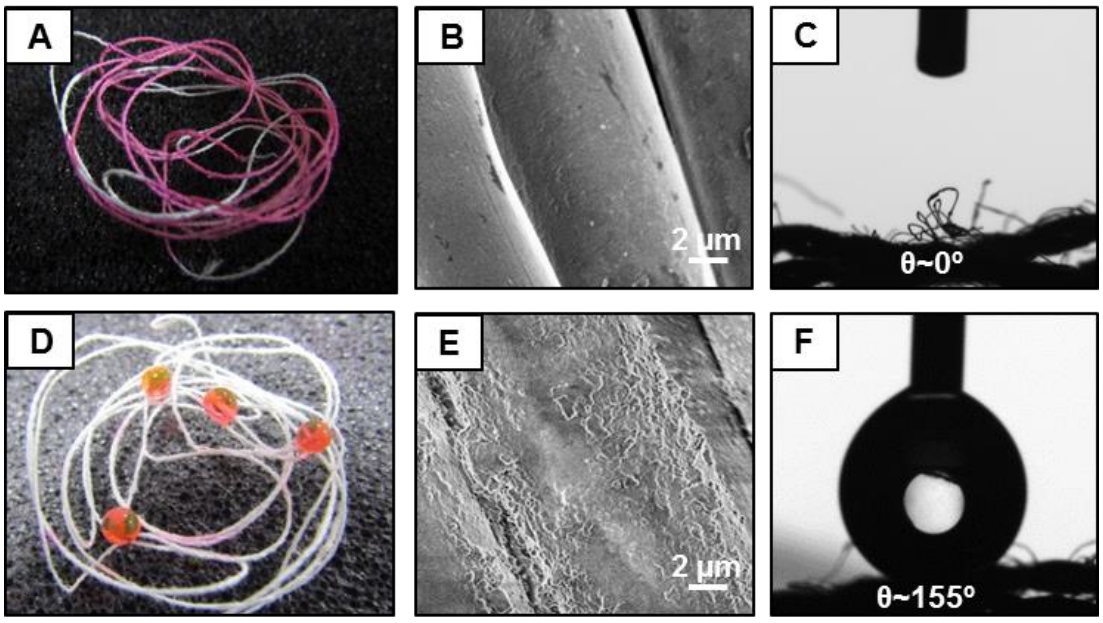

Figure 6.11. (A, C, D, F) Digital images (A, D) and contact angle images (C, F) of RNC coated cotton thread with beaded water droplets before (A, C) and after post modification with octadecylamine (D, F). B, E) FESEM images of uncoated cotton thread (B) and after immobilization (E) of RNC, respectively.

membrane to extremes of pH (1 and 12) and high ionic strength water (artificial sea water), river (Brahmaputra, Assam India) water for 48 h as shown in Figure 6.10A-H. This impeccable physical and chemical durability of the anti-wetting property of the stretchable superhydrophobicity is most likely due to i) existence of covalent cross-linkages in the immobilized nanocomplexes and (ii) the optimization of low surface energy in the material through the 1, 4-conjugate addition reaction between residual acrylate and primary amine groups. Furthermore, the approach was extended to coat other fibrous substrate (i.e. cotton thread, Figure 6.11A-B), and the successful immobilization of reactive nanocomplexes on the cotton thread was confirmed with FESEM analysis (Figure 6.11E). After appropriate post chemical modification with ODA molecule, the cotton thread displayed superhydrophobic property with advancing contact angle above 150^{o} as is shown in Figure 6.11F.

6.3.3. Gravity Driven Oil/Water Separation through Stretchable Superhydrophobic Membrane

In 2004, a seminal report by Jiang and co-workers exploited a porous metal mesh embedded with superhydrophobicity/superoleophilicity property for gravity driven and energy efficient oil/water separation, where the oil phase was passed selectively through the

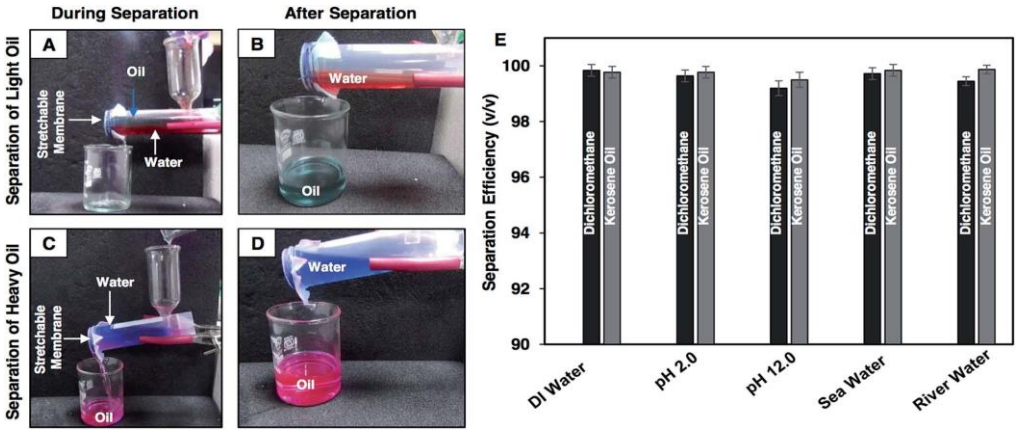

Figure 6.12. (A-D) Digital images illustrating the separation of both lighter oil (kerosene) (A, B) and model oil heavier (dichloromethane) (C, D) from corresponding oil/water mixtures using lab-made prototype, where the opening of a Falcon tube was covered with stretchable superhydrophobic PU membrane and another side hole was made at the other end of the tube to pour the oil/water mixture. E) Plot showing the collection efficiency for both the heavier and lighter oils from corresponding mixture of oil and complex aqueous (extremes of pH, sea water, river water) phases.

superhydrophobic porous mesh.[30] Since then, various other research groups have recapitulated this approach by exploiting various organic and inorganic superhydrophobic/superoleophilic coatings on non-stretchable porous substrates.[37,38] However, such coatings are highly susceptible to compromise their anti-wetting property on regular physical manipulations, and limiting the utility of the anti-wetting property at practical settings. Here, in this chapter, the stretchable PU membrane with durable superhydrophobicity, which is able to strongly repel aqueous phase both in air and under oil was explored in gravity driven separation and collection of oil from oil/water mixtures. As a proof of concept, an oil/water separation prototype was built in the lab using a Falcon

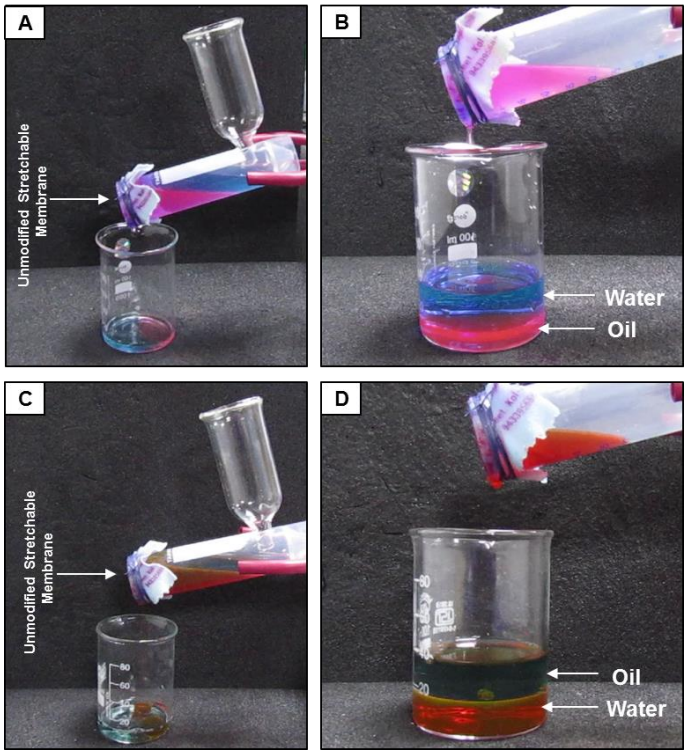

Figure 6.13. (A-D) Digital images illustrating the separation performance of both heavier, (DCM) (A, B) and lighter (kerosene) (C, D) oil/oily phase from corresponding oil/water mixtures using uncoated fibrous PU membrane, where both oil and water phases are passing through the fabric on pouring the oil /water mixture in the prototype.

tube, and the stretchable membrane was wrapped on the opening of the tube, and a side hole was made at the other end of the tube for both pouring the oil/water mixture and collecting the separated water at the end of the separation process. First, the oil/water

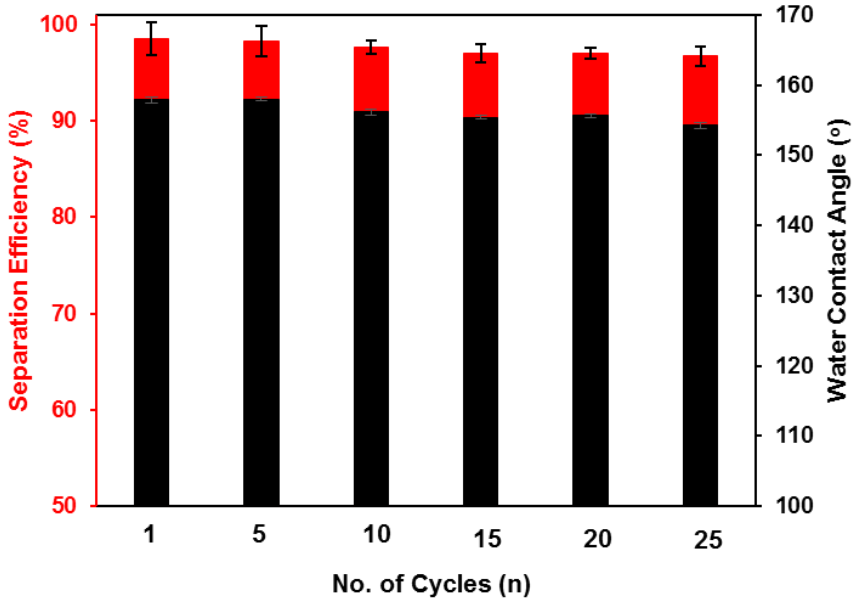

Figure 6.14. Plot showing the separation efficiency and water contact angle of superhydrophobic stretchable membrane for 25 cycles.

separation was demonstrated with kerosene oil—which is lighter (lower density) than water. A mixture of kerosene oil (30 mL) and water (30 mL) (colored red to aid visualization) was poured into the prototype, and the kerosene oil phase was selectively and readily passed through the stretchable PU membrane (Figure 6.12A, B) having durable superhydrophobicity, and was finally collected in a separate beaker with separation efficiency of 99.7%. A similar result was obtained with DCM (model oil) that is heavier than aqueous phase, where red-colored DCM was separated from the oil/water (blue color to aid visualization) mixture and was collected in a separate container (Figure 6.12C, D) with a flow rate of ~115 mL min^{-1} and separation efficiency of 99.8%. Moreover, the aqueous phases that are contaminated with either light fraction (kerosene) and/ or heavy fraction (DCM) oil/oily phases were separated under complex and harsh chemical compositions including extremes of pH (2 and 12), artificial sea water and river (Brahmaputra, Assam India) water, with separation efficiency above 99% as is noted in Figure 6.12E. The native PU membrane was explored for comparison study and was found that both the oil and water passed the uncoated (native) PU membrane on pouring the oil/water mixture of both heavy (DCM) oil and light (kerosene oil) oil separately as shown

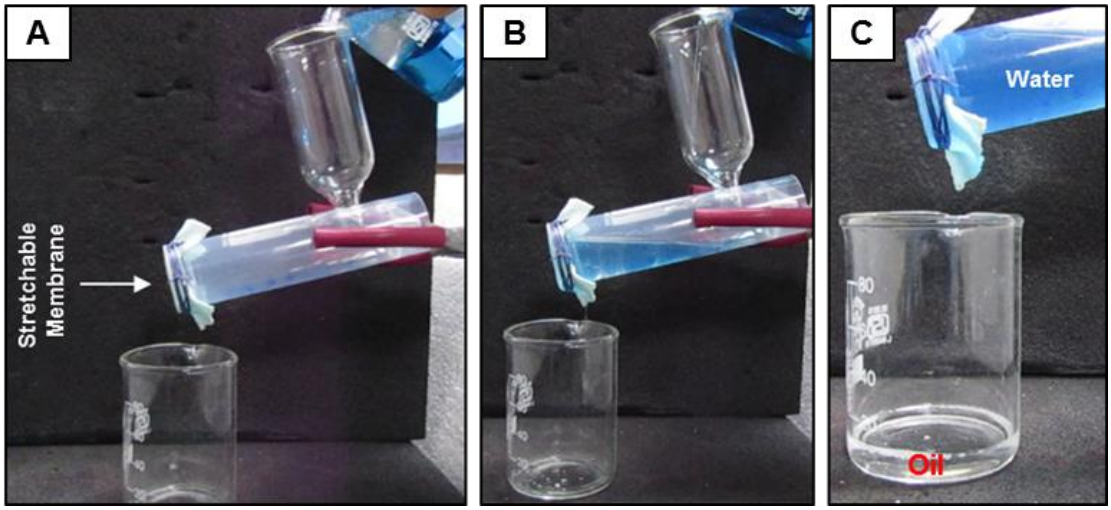

Figure 6.15. (A-C) Digital images depicting the separation of viscous oil (silicon oil) from oil/water mixture, blue color water (due to methylene blue dye) aids visual inspection.

in Figure 6.13A-D. Further, the superhydrophobic fibrous PU membrane can be repeatedly used in oil/water separation for more than 25 times without compromising the separation efficiency and the antiwetting property remained intact with advancing contact angle above 150º as shown in Figure 6.14. This superhydrophobic membrane is also capable of separating mixtures of highly viscous oil (Figure 6.15A-C). Silicone oil (20 mPa s), which is 22 times more viscous than water (0.89 mPa s), was selected here for the demonstration of oil/water separation and the oil was effectively separated with high separation efficiency. Next, the intrusion pressure (P) of the superhydrophobic membrane was experimentally estimated, which represents the maximum pressure generated by the water on the superhydrophobic membrane without any permeation of water. The intrusion pressure (P) was estimated from the following reported equation:[34]

$$P = \rho Hg$$

Where H is the maximum height of the liquid water that the superhydrophobic membrane can support, g stands for the gravitational acceleration and ρ is the density of the water. The average intrusion pressure for the water was estimated to be 4.89 kPa, and liquid water was unable to pass through this superhydrophobic membrane below the intrusion pressure.

6.4. Conclusion

In conclusion, here a highly stretchable membrane with durable superhydrophobic property which strongly repelled aqueous phase both in air and under oil is reported. The material was developed by simple and direct immobilization of growing nanocomplexes on a stretchable selected fibrous substrate, and the residual acrylate groups in the nanocomplexes were exploited in adopting the essential low surface energy of the material through 1, 4-conjugate addition reaction. This scalable and covalent dip coating approach provided a highly durable superhydrophobic property. The developed anti-wetting property remained intact even after 150% deformation of the material. Moreover, the synthesized material is capable of surviving under various harsh physical manipulations (including rubbing, twisting, adhesive tape peeling, sand drop test, knife test, exposure to UV light etc.) and chemically complex media (extremes of pH, sea water, river water etc.), without compromising the embedded superhydrophobic property. This stretchable superhydrophobic PU membrane is found to be appropriate for rapid separation of oils (both light and heavy) from complex aqueous phases with separation efficiency above 99%. This current approach might be useful in various other applications including gas sensing, wearable technology, biomedical applications, flexible microfluidics etc.

References

(1) Yan, Y. Y.; Gao, N.; Barthlott, W. *Adv. Colloid Interface Sci.* **2011**, *169*, 80–105.

(2) Feng, X.; Jiang, L. *Adv. Mater*. **2006**, *18*, 3063–3078.

(3) Wang, Y.; Shi, Y.; Pan, L.; Yang, M.; Peng, L.; Zong, S.; Shi, Y.; Yu, G. *Nano Lett.* **2014**, *14*, 4803–4809.

(4) Wu, D.; Wu, S.; Chen, Q.; Zhang, Y.; Yao, J.; Yao, X.; Niu, L.; Wang, J.; Jiang, L.; Sun, H. *Adv. Mater.* **2011**, *23*, 545–549.

(5) Wang, J.; Kaplan, J. A.; Colson, Y. L.; Grinstaff, M. W. *Angew. Chem., Int. Ed*. **2016**, *55*, 2796–2800.

(6) Schutzius, T. M.; Jung, S.; Maitra, T.; Graeber, G.; Ohme, M. K; Poulikakos, D. *Nature* **2015**, *82*, 527-535.

(7) Hou, Y.; Yu, M.; Chen, X.; Wang, Z.; Yao, S. *ACS Nano* **2015**, *9*, 71–81.

(8) Park, K. C.; Kim, P.; Grinthal, A.; He, N.; Fox, D.; Weaver, J. C.; Aizenberg, J. *Nature* **2016**, *531*, 78–82.

(9) Miljkovic, N.; Enright, R.; Nam, Y.; Lopez, K.; Dou, N.; Sac J.; Wang, E. N. *Nano Lett.* **2013**, *13*, 179–187.

(10) Verho, T.; Bower, C.; Andrew, P.; Franssila, S.; Ikkala, O.; Ras, R. H. *Adv. Mater.* **2011**, *23*, 673–678.

(11) Cho, S. J.; Nam, H.; Ryu, H.; Lim, G. *Adv. Funct. Mater.* **2013**, *23*, 5577–5584.

(12) Fatang, L.; Fenghe, S.; Qinmin, P. *J. Mater. Chem. A* **2014**, 2, 11365–11371.

(13) Jianfeng, Z.; Seunghwa, R.; Nicola, P.; Qiming, W.; Qing, T.; Markus, J. B.; Xuanhe, Z. *Nat. Mater*. **2013**, *12*, 321–325.

(14) Joseph, E.; Mates, W.; Bayer, S. I.; Palumbo, J. M.; Patrick, J.; Carroll, C.; Megaridis, M. *Nat. Commun.* **2015**, *6*, 8874–8882.

(15) Lee, W. K.; Jung, W. B.; Sidney, R.; Nagel, T.; Odom, W. *Nano Lett*. **2016**, *16*, 3774–3779.

(16) Uen, Y.; De, P. K.; Rosa, M. E. *Lab Chip* **2011**, *11*, 3249–3255.

(17) Yao, X.; Ju, J.; Yang, S.; Wang, J.; Jiang, L. *Adv. Mater*. **2014**, *26*, 1895–1900.

(18) Sun, J. Y.; Keplinger, C.; Whitesides, G. M; Suo, Z. *Adv. Mater.* **2014**, *26*, 7608–7614.

(19) Das, I.; De, G. *Sci. Rep.* **2015**, *5*, 18503–18510.

(20) Xin, H.; Tang, C.; He, Z.; Shao, H.; Xu, K.; Mei, J.; Lau, W. M. *Small* **2017**, *160*, 2353–2360.

(21) Hu, X. C.; Andrews, D. Q.; Lindstrom, A. B.; Bruton, T. A.; Schaider, L. A.; Grandjean, P.; Lohmann, R.; Carignan, C. C.; Blum, A.; Balan, S. A.; Higgins C. P.; Sunderland, E. M. *Environ. Sci. Technol. Lett.* **2016**, *3*, 344–350.

(22) Lu, Y.; Sathasivam, S.; Song, J.; Crick, C. R.; Carmalt, C. J.; Parkin, I. P. *Science* **2015**, *6*, 1132–1135.

(23) Ford, J.; Marder, S. R.; Yang, S. *Chem. Mater*. **2009**, *21*, 476–483.

(24) Wang, G.; Fang, Y.; Kim, P.; Hayek, A.; Weatherspoon, M. R.; Perry, J. W.; Sandhage, K. H.; Marder, S. R.; Jones, S. C. *Adv. Funct. Mater*. **2009**, *19*, 2768–2776.

(25) Parbat D.; Manna, U. *Chem. Sci*. **2017**, *8*, 6092–6102.

(26) Rather, A. M.; Manna, U. *Chem. Mater.* **2016**, *28*, 8689–8699.

(27) Xue, C.-H.; Li, Y.-R.; Zhang, P.; Ma, J.-Z.; Jia, S.-T.; *ACS Appl. Mater. Interfaces* **2014**, *6*, 10153–10161.

(28) Zhao, X.; Li, L.; Li, B.; Zhang, J.; Wang, A. *J. Mater. Chem. A* **2014**, *2*, 18281–18287.

(29) Li, B.; Zhang, J. *Carbon* **2015**, *93*, 648–658.

(30) Feng, L.; Zhang, Z. Y.; Mai, Z. H.; Ma, Y. M.; Liu, B. Q.; Jiang, L.; Zhu, D. B. *Angew. Chem., Int. Ed.* **2004**, *43*, 2012–2014.

(31) Ma, Q. L.; Cheng, H. F.; Fane, A. G.; Wang, R.; Zhang, H. *Small* **2016**, *12*, 2186–2202.

(32) Chu, Z. L.; Feng, Y. J.; Seeger, S. *Angew. Chem., Int. Ed.* **2015**, *54*, 2328–2338.

(33) Xue, Z.; Wang, S.; Lin, L.; Chen, L.; Liu, M.; Feng, L.; Jiang, L. *Adv. Mater.* **2011**, *23*, 4270–4273.

(34) Zhang, J.; Wu, L.; Zhang, Y.; Wang, A. *J. Mater. Chem. A* **2015**, *3*, 18475–18482.

Chapter 7: Compressible, Deformable and Durable Superhydrophobic Material for Absorption and Filtration Based Oil/Water Separation*

Oil contamination in aqueous phases by regular industrial discharges and accidental oil spillages during the production and transportation of oil is emerging as a global challenge due to its catastrophic effect on the aquatic ecosystem. Various materials—designed to remove the oil spillages are having the inherent limitations with respect to their durability, efficiency as well as their adverse impact on the environment. Here, a naturally abundant and environmental friendly fibrous substrate (i.e., a cotton ball) is strategically exploited in the energy-efficient and environmentally-friendly cleaning of different forms of oil-contamination, including floating light-oil, and sedimentary heavy-oil and emulsions, after the appropriate optimization of both the topography and the essential chemistry of the fibrous substrate through a catalyst-free, simple and scalable 1, 4-conjugate addition reaction between amine and acrylate groups under ambient conditions. The synthesized superhydrophobic cotton (SHC), that is capable of extreme repellency of water both in air and under oil, has provided a single avenue for both highly selective (1) absorption (with an efficiency above 2000 wt% for both heavy and light oils) and (2) gravity-driven active filtration of oil. The synthesized material is highly efficient in the separation of oil from aqueous phases that are chemically harsh, including extremes of pH (1 & 12), artificial seawater, river water etc. The embedded superhydrophobicity in the synthesized material remained unperturbed, even after prolonged (10 days) exposure to UV radiations (λ_{max} = 254 nm and 365 nm) and after incurring various and common physical manipulations. The synthesized material was repeatedly (100 times) used in removing oil contamination and the anti-wetting property remained intact with an advancing water contact angle of 157º and the oil/water separation efficiency remained around 95%. Further, the current approach provided a simple basis to separate oil from a complex three-phase oil/water mixture that was composed of a heavy-oil phase (the bottom layer), an aqueous phase (the middle layer), and a light-oil phase (the top layer), where the strategic application of SHC allowed the successful clean-up of oils through the complementary use of absorption and filtration processes.

***** Rather, A. M, Jana, N.; Hazarika. P.; U. Manna *J. Mater. Chem. A* **2017**, *5*, 23339-23348.

Chapter 7

7.1. Introduction

As I have discussed in the previous chapter, the growing water pollution because of regular oil-contamination from petro-chemical industrial discharge and frequent accidental oil spillages during oil production and transportation has a harsh and severe impact on the aqua-ecosystem around the globe.[1,2] There are some traditional oil/water separation processes, including chemical dispersants, burning of oil in situ, booms and skimmers etc.[2–5] However, most of them are either time or energy-consuming or lead to other secondary pollutions in the environment.[2–5] Furthermore, in practical settings, oil contamination is present in complex forms: (a) floating light oil, (b) sedimentary heavy oil and (c) emulsions in the aqueous phase. Thus, the synthesis of a material that has the potential to clean multiple forms of oil-contaminant following an eco-friendly and energy-efficient approach which would be useful in practically relevant diverse scenarios, including (i) preventing further oil contamination from industrial discharge and (ii) cleaning-up of oil spills that already exists in vast and open water reservoirs—is highly desirable to address this globally recognized challenge.[6,7]

In 2004, Jiang and co-workers introduced a formative demonstration of gravity-driven filtration-based oil/water separation by exploiting bio-inspired artificial superhydrophobicity. The oil phase was selectively allowed to pass through the superhydrophobic porous mesh.[8] Since then, several other research groups have extended this facile and energy-efficient approach for prospective oil/water separation using various two dimensional substrates (fabric, mesh etc.).[9–16] This approach is widely accepted and generally practiced for demonstrations of the facile separation of oil/water mixtures, and has an immense potential in preventing and controlling oil contamination in the aqueous phase in some practically relevant scenarios (e.g., the regular oil contamination from uncontrolled industrial waste water discharge in open water reservoirs), but at the same time this filtration process inherently demands appropriate precontainment and active filtration followed by the collection of two separated liquid phases at the end. This entire process may eventually appear to be highly expensive and impractical for removing oil contamination that is already present in open and vast water reservoirs.

As a complementary approach, a direct and selective absorption of oil from an oil/water mixture was demonstrated using again the basic principle of the superhydrophobic

property.[17–23] In general, two-dimensional objects are used in filtration-based oil/water separation. In the chapter 6, the synthesized stretchable and durable superhydrophobic membrane was explored for the filtration based oil/water separation of both heavy and light oils with high oil separation efficiency (99%) irrespective of the various chemical contaminations present in the aqueous phase. However, this two dimensional superhydrophobic material was inappropriate for absorption based oil/water separation. Here, in this chapter a completely different, highly compressible three-dimensional (3D) porous object (rather than using 2D substrates; mesh, fabric etc.) with a bioinspired anti-wetting property was successfully explored in the selective-absorption of oil from oil/water mixtures. This oil absorption process is a bulk phenomenon, as the oil phase is selectively absorbed three-dimensionally in such materials.[17–23] These absorption-based and filtration-based processes may be exploited together as complementary to each other for the comprehensive and facile clean-up of oil spills from an oil-contaminated aqueous phase in diverse and complex practically relevant scenarios. Generally, separate fabrication processes and geometrically different (2D substrates for filtration and 3D substrates for selective absorption) substrates are associated in the fabrication of appropriate individual materials for absorption-based and filtration-based oil/water separation. Furthermore, often the artificial bio-inspired special wettability gets compromised during common physical manipulations (bending, twisting, shrinking etc.) and deformations, likely due to perturbation in the appropriate co-existence of topography and chemistry in the reported materials.[24–29] On the other hand, in most proof of concept demonstrations of artificial superhydrophobicity, weak or delicate chemistries are associated for adopting essential low surface energy coatings, which are mostly achieved through functionalization with various analogues of silane[9,11,14,18,19,30–32] or metal–thiol bonds[10,33–35] and metal–ion interactions.[15,36,37] However, the silane-based chemistry is well known to be labile upon prolonged UV exposure,[38–40] the metal–thiol bonds and metal–ion interactions are generally susceptible to damage in severe aqueous phases (e.g., extremes of pH, sea water, etc.). These severe physical and chemical durability aspects are highly relevant for outdoor applications of artificial superhydrophobicity.[41] Thus, even after several proof-of-concept demonstrations of lotus-leaf-inspired interfaces, the further design of a (i) scalable, (ii) highly durable and (iii) single superhydrophobic material through (iv) a simple fabrication

process, which would be capable of both filtration-based and absorption-based oil/water separation, is essential for comprehensive and environmental-friendly oil/water separation in diverse and practically relevant circumstances, and would be of potential interest for addressing this globally recognized oil contamination challenges.

Here, in this chapter, a compressible, deformable and durable single superhydrophobic material is introduced for both absorption-based and filtration-based separation of oil and water from diverse types (floating oil, sedimentary oil, emulsion droplets) of oil/water mixtures. In this current design, a naturally abundant and environmentally friendly fibrous cotton was selected as a general substrate which was capable of displaying extreme water repellency both in air and under oil, after the adaptation of the appropriate topography and chemistry in the material through a facile and scalable 1, 4-conjugate addition reaction between amine and acrylate groups at ambient conditions, without use of any catalyst. In the literature, the fibers of cotton fabrics are mostly modified to achieve superhydrophobicity, which is generally used in filtration-based oil/water separation. The integrity and alignment of the fibers in the cotton fabric and in a naturally abundant cotton ball are entirely different, and the shape of a fibrous cotton ball is easily deformed during regular physical manipulations. Reports on physically and chemically durable superhydrophobic coatings on naturally abundant cotton balls are rare in the literature. The current chemical approach provided a highly durable anti-wetting property, which remained unperturbed after incurring successive (1000 times) manual compression and other physical manipulations, and even after exposure to UV radiations and harsh aqueous chemical environments. The synthesized spongy and fibrous superhydrophobic material was highly efficient in selectively absorbing (above 2000 wt%) as well as filtering the oil phase even after repeated (100 times) uses, without compromising the embedded anti-wetting property. Along with separation of floating oil, sedimentary oil and emulsion droplets, this superhydrophobic material was also capable of separating a three-phase oil/water mixture composed of both heavy and light oils along with an aqueous phase. Thus, this current approach provided a general avenue that could be useful in comprehensive, energy-efficient and environmentally-friendly clean-up of oil-spills from diverse scenarios at practically relevant settings.

7.2. Materials and Methods

7.2.1. Materials

Motor oil was purchased from Castrol India Limited. Dichloromethane (DCM) and chloroform was purchased from Merck Life Science Pvt Ltd (Bangalore, India). Kerosene oil and vegetable oils were obtained from a local shop in Guwahati city (Assam, India). Cotton was procured from a local medical shop in Guwahati city (Assam, India). Hexane and ethyl acetate was obtained from RANKEM (Maharashtra, India). The details of all other materials and chemicals used in this chapter are already mentioned previously in the chapter 2.

7.2.2. General Considerations

The instruments used to characterize the synthesized superhydrophobic cotton were same as already discussed in the chapter 2.

7.2.3. Fabrication of Superhydrophobic/Superoleophilic cotton

The naturally abundant cotton having both superhydrophilic and superoleophilic property in air was transformed into superhydrophobic cotton by adopting the previously described method for the fabrication of stretchable superhydrophobic membrane as mentioned in the chapter 6.

7.2.4. Physical and Chemical Stability Tests

7.2.4.1. Adhesive Tape Test

The adhesive tape test was performed on the superhydrophobic cotton substrate following the same protocol that is already discussed in the chapter 2.

7.2.4.2. Compressive Strain Test

In this particular test, first, the superhydrophobic cotton was manually compressed to various extents of compressive strain from 10% to 80%. However, after releasing the applied pressure, the material returned to its original shape and the water contact angle was measured before, during application of load and after releasing the applied load. Furthermore, the same material was deformed with compressive strain of 80% for 1000 times using 500 g load, and the anti-wetting property was examined at regular intervals by measuring the water contact angle. The same material was manually bended, twisted and even arbitrarily fragmented in multiple parts, and the contact angle of the beaded liquid water droplet was measured after incurring each physical manipulation test.

7.2.5. Absorption Based Separation of Oil from Oil/Water Mixture

Various light oils (vegetable oil, motor oil, silicon oil etc) were removed using superhydrophobic cotton from the oil/water mixture. 1 mL of oil (red dyed, for visual inspection) was placed on the air/water interface before bringing the superhydrophobic cotton (SHC) in contact with the floating oil. The SHC remained floating on the air/water interface, was capable of collecting the floating oil within 30 seconds. Further, the same experiment was repeated for uncoated cotton, however, the uncoated cotton was appeared to be inappropriate in removing oil under same conditions. Next, the SHC was explored in collection of the bulk oil phase from the oil/water mixtures, irrespective of the location of oils (light and heavy) in the respective oil/water mixture. For the proof of concept demonstration, single pieces of SHC was exposed to oil/water mixture that was composed of 5 mL of motor oil and 30 mL of water. The oil phase was instantly soaked by the SHC and the separated oil was collected by squeezing the material manually. On the other hand, a piece of SHC was brought in contact with the sediment model (DCM) oil under water, and a similar demonstration was further performed with uncoated cotton.

7.2.6. Filtration of Oil Under Water Against Gravity

To demonstrate active and selective filtration of oil under water using SHC, a lab-made set-up was developed using a glass dropper, where the wide opening of a glass dropper was plugged with SHC. Then, the blocked end of the dropper was brought in contact with the sediment model oil (5 mL of chloroform that was dyed with nile-red for facile visual inspection) under water. Immediately, the oil phase was selectively penetrated through the SHC—which was plugged at wide end of the glass dropper, and the oil phase was accumulated within the glass dropper. Then, other end opening of the dropper was closed with index finger and finally the dropper was taken out from aqueous phase, and the separated oil was collected in a separate glass vial by lifting the finger from the end opening. In this way, all the oil phase from the oil/water mixture, was collected with high separation efficiency. Moreover, the same experiment was extended to separate oil/water mixture, where aqueous phase is contaminated with various harsh chemical conditions (acidic pH 1, alkaline pH 12), artificial sea water and river (Brahmaputra, Assam India) water.

7.2.7. Gravity-Driven Oil/Water Separation

Another prototype was developed in the lab using a centrifuge tube (50 mL, falcon tube) and glass funnel, where the small opening of glass funnel was plugged with SHC prior to integrate with the tube, Then respective oil/water mixtures that were consisted with two phases (DCM or Kerosene oil/Water) or three phases (DCM/Water/Kerosene oil) were poured on the prototype through glass funnel. Oil phase was selectively passed through the SHC cotton irrespective of the density and nature of the used oils. The water in oil emulsion was also separated successfully using the same set-up. Further, the similar set-up was also developed with uncoated cotton to examine the oil/water separation performance for comparative analysis.

7.3. Results and Discussion

7.3.1. Synthesis of Fibrous Material with Selective Super-Liquid Wettability

The 1, 4-conjugate addition reaction between acrylate and amine groups was successfully exploited for the synthesis of various functional polymeric material coatings at ambient conditions.[42–48] The strategic use of this facile and robust chemical approach allowed the regulation of both the topography and the chemical functionality throughout the coatings, and eventually yielded materials with the desired liquid wettability.[46–50] Here, in this chapter, a durable and compressible three dimensional (3D) superhydrophobic material is developed using cotton fibers. The same synthetic procedure that is mentioned in chapter 6 was adopted for coating cotton balls with chemically reactive nanocomplex, and further appropriate post chemical modification with hydrophobic small molecule, provided desired durable superhydrophobicity. The synthesized material was capable of displaying extreme and opposite (superhydrophobicity and superoleophilicity) wettability for water and oil. Further the material was exploited in environmentally-friendly and comprehensive cleaning of oil/oily contaminants by adopting facile and energy-efficient absorption and filtration principles. The naturally abundant fibrous cotton is inherently hydrophilic (Figure 7.1A-D) and capable of soaking up the aqueous phase (red and blue colors aid visual inspection) immediately after beading the droplets on the uncoated cotton both in air (Figure. 7.1A, B) and under oil (Figure 7.1C, D). The successful surface modification is generally achieved through grafting polymers;[51] here, in this chapter, the hydrophilic fibrous cotton was first functionalized with BPEI polymer prior to immobilizing ‘amine-

reactive' nanocomplexes following the similar procedure as briefly described in chapter 6. The fibrous cotton has hydroxyl groups, which are likely to interact with BPEI polymer through electrostatic interaction and hydrogen bonding.[52] This BPEI modification is important for achieving the durable and stable coating of NC on the fibrous substrate. After the post-chemical modification of the NC coated fibrous substrate with octadecylamine

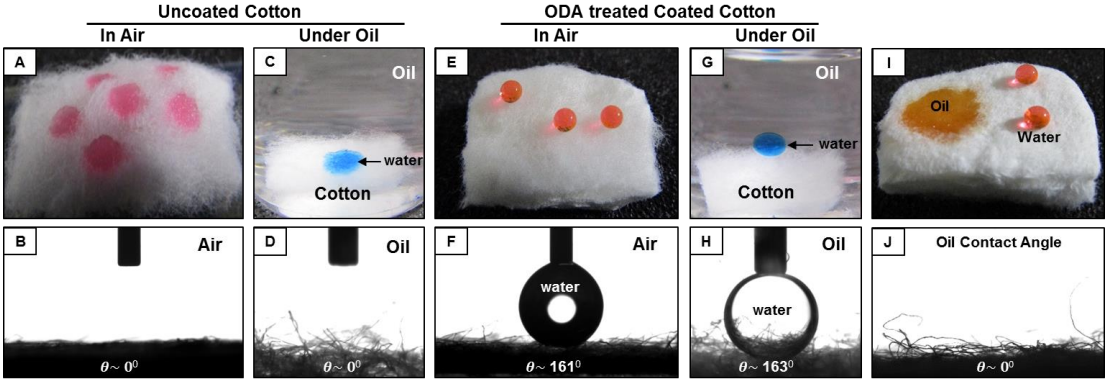

Figure 7.1. (A-H) Digital images (A, C, E, G) and water contact angle images (B, D, F, H) of beaded water droplets on both uncoated cotton (A-D) and nanocomplex-coated cotton (post modified with ODA) (E-H) in air (A, B, E, F) and under oil (C, D, G, H). I, J) Digital image (I) and oil contact angle (J) of the beaded water and oil droplets on SHC in air.

(ODA) molecule through a 1, 4-conjugate addition reaction, the material was able to display extreme water repellency both in air (Figure 7.1E) and under oil (Figure 7.1G), with advancing contact angles of 161º and 163º, respectively, as shown in Figure 7.1F, H. While this SHC has extreme repellence of the aqueous phase, it was noticed that the oil phase readily soaked in the same material, with a contact angle of 0º, as shown in Figure 7.1I, J. This selective and contrasting wettability of oil and water on the SHC provided a simple basis to separate oil through both selective filtration and absorption based processes.

The reactivity of the hierarchical domains of the coated fibrous cotton was confirmed with standard FTIR analysis, which was widely used in characterizing the 1, 4-conjugate addition reaction in the past.[43–50] The appearance of IR peaks at 1410 cm^{-1} and 1739 cm^{-1} that are characteristic peaks for the symmetric deformation of the C–H bond for the β carbon of the vinyl group and the ester carbonyl stretching denotes the presence of residual acrylate groups in the polymeric nanocomplex coated cotton, as shown in Figure 7.2A (black spectrum). Further, the depletion of the IR peak intensity at 1410 cm^{-1} with respect to the normalized carbonyl stretching at 1739 cm^{-1} (Figure 7.2A, red spectrum) after the

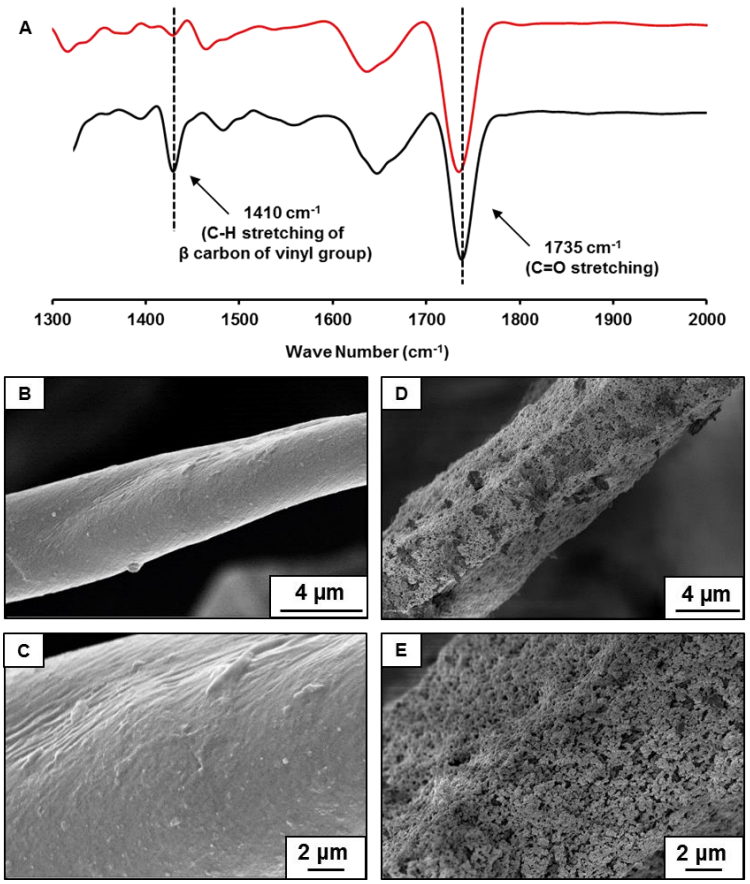

Figure 7.2. (A) FTIR spectra of nanocomplex-coated cotton before (black) and after (red) treatment with octadecylamine. The peaks at 1736 cm^{-1} and 1410 cm^{-1} correspond to the carbonyl stretching and symmetric deformation of the C–H bond for the β carbon of the vinyl group, respectively. B-E) FESEM images of fibrous cotton before (B, C) and after (D, E) immobilization of the nanocomplex at low (B, D) and high (C, E) magnifications.

post modification of the NC coated cotton with ODA molecule revealed the successful post-chemical modification, through 1, 4-conjugate addition reaction. Moreover, the successful and uniform coating of the polymeric nanocomplex on the fibrous substrate was investigated with FESEM study. The featureless and smooth uncoated fibrous cotton (Figure 7.2B, C) was observed to be coated uniformly with a porous polymeric topography on each fiber of the selected substrate that consists of randomly arranged granular hierarchical domains, as shown in Figure 7.2D, E. The existing topography in the material was found to be appropriate to display the desired anti-wetting property, after post covalent-

modification of the 'amine-reactive' polymeric coating with ODA molecule through a 1, 4-conjugate addition reaction.

7.3.2. Durability of Three Dimensional (3D) Superhydrophobicity

The opposite and extremes of oil (superoleophilicity) and water (superhydrophobicity) wettability, which were recognized at the surface of the superhydrophobic material was found to be present three-dimensionally in the modified fibrous cotton. The NC coated fibrous cotton post-modified with ODA molecule was arbitrarily sliced into four parts, and the freshly exposed interiors of the fibrous substrate were exposed to both oil and water in air. All the exposed solid/air interfaces were capable of displaying superoleophilicity (with an oil contact angle of 0º) and superhydrophobicity with an advancing water contact angle above 155º in air, as shown in Figure 7.3. Hence, the hierarchical topography developed by covalent immobilization of reactive polymeric nanocomplexes and the essential low surface energy coating is appropriately optimized all throughout the fibrous cotton substrate. Next, various standard physical durability tests including bending, twisting, and

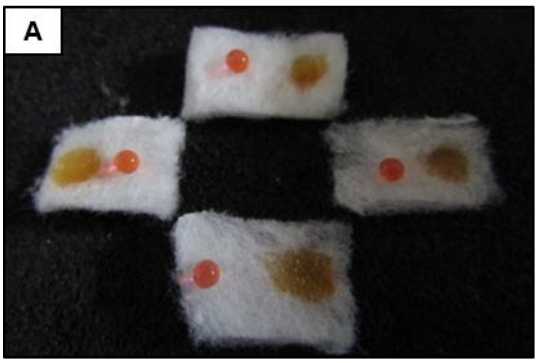

Table 7.1. Detailed oil and water wettability on these four pieces of SHC

No. of pieces	θ_{Adv} (º)		θ_{Hys} (º)	
	Water	Oil	Water	Oil
1	156.2	0	8.1	NA
2	155.4	0	7.7	NA
3	155.7	0	7.9	NA
4	156.3	0	8.4	NA

Figure 7.3. (A) Digital image of SHC that were manually sliced in four pieces with random preference and both oil and water droplets were beaded on all four pieces of SHC. **Table 7.1** displays the detailed oil and water wettability on these four pieces of SHC.

creasing were performed on this superhydrophobic cotton (SHC) which are expected to be executed at the practical settings. Primarily, the SHC was compressed manually with 500 g load, after releasing the load, the material regained its original position (Figure 7.4A, B). The anti-wetting property remains intact with advancing contact angle of above 150º after 1000 times of manual compression as shown in Figure 7.4C, D. Furthermore, the SHC was deformed with various extents of applied compressive strain from 20% to 80% and the

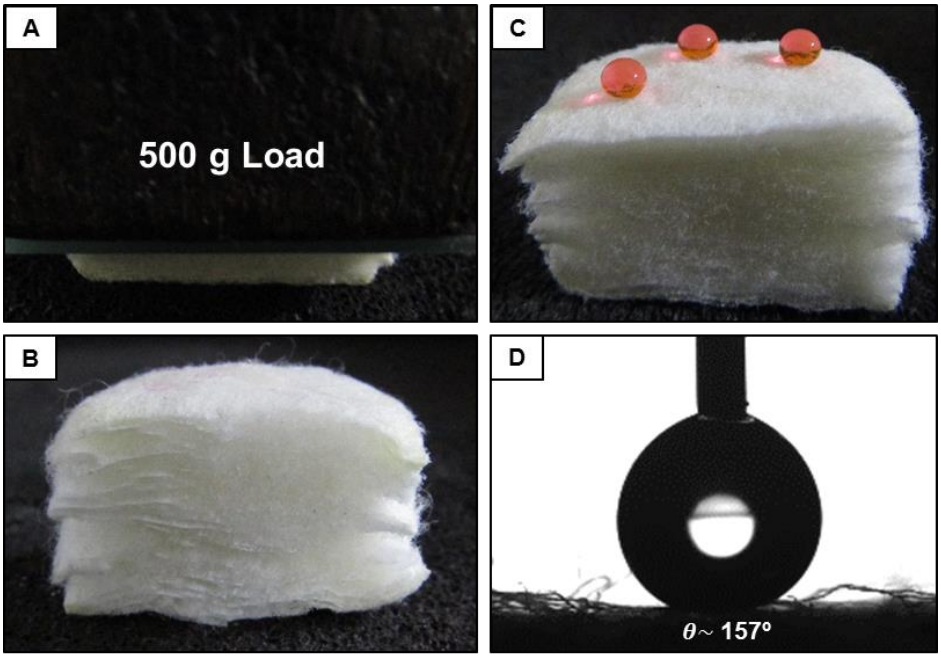

Figure 7.4. (A) Digital image of compressed SHC after application of 500 g load. After releasing the load, the SHC was capable of recovering its native dimension (B). C, D) Digital image (C) and water contact angle (D) of beaded water droplet on SHC, after performing the compression/recovery tests (with 500 g load) for 1000 times.

embedded superhydrophobicity in the SHC remained intact with an advancing water contact angle above 155º and contact angle hysteresis below 10º as shown in Figure 7.5A-J. The same material was repetitively compressed with 80% compressive strain for 1000

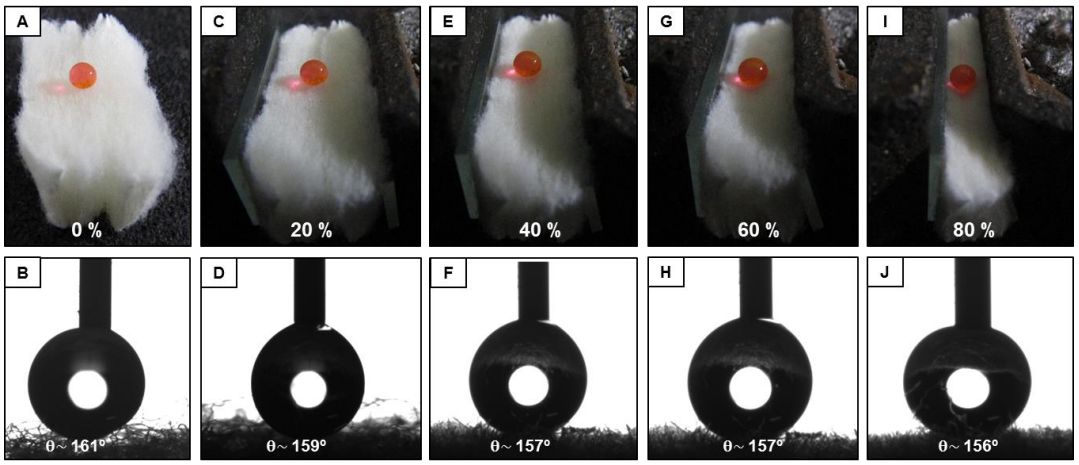

Figure 7.5. (A-J) Digital images (A, C, E, G, I) and water contact angle (B, D, F, H, J) of beaded water droplet on SHC that are deformed with compressive strain of 0% (A-B), 20% (C, D), 40% (E, F), 60% (G, H) and 80% (I, J) respectively.

cycles. However, the material remained capable of displaying extreme water repellency with an advancing water contact angle above 155º and with contact angle hysteresis below 10º respectively throughout the 100 times deformation process (Figure 7.6A). In the recent

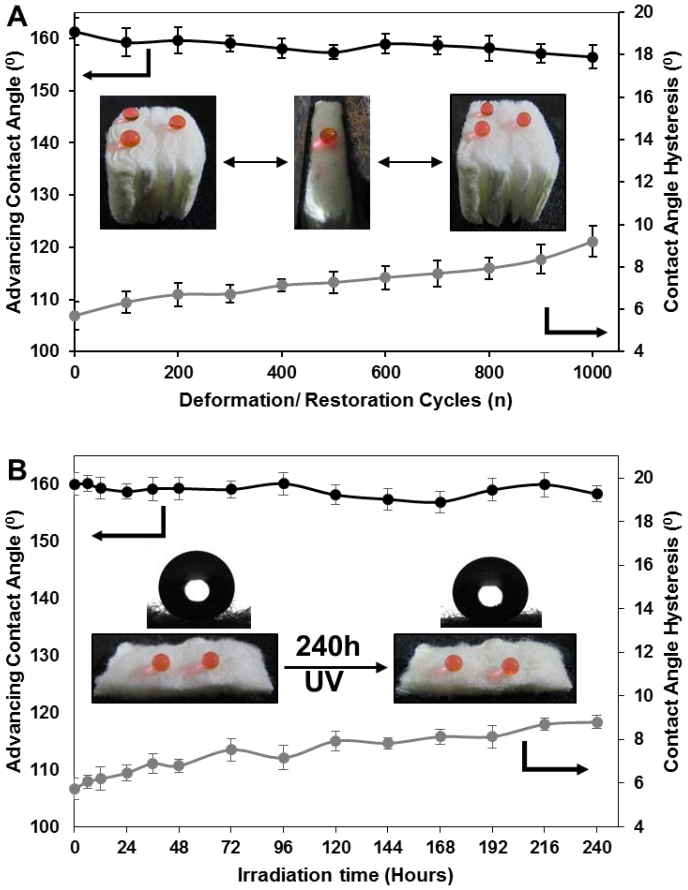

Figure 7.6. (A) Plot illustrating the change in the advancing contact angle (black) and contact angle hysteresis (grey) of beaded water droplet on SHC with incurring the successive deformation with 80% compressive strain for 1000 cycles. The inset digital images of beaded aqueous (red aids visual inspection) droplets before (left image), during (middle image) compression and after (right-most image) releasing the applied pressure. B) Plot displaying the change in advancing contact angle (black) and hysteresis (grey) of contact angle of beaded water droplets on SHC after irradiating the material under UV light; the inset is the contact angle images of beaded water droplets on SHC before and after exposure to UV radiation for 240 hours (10 days).

past, covalent bonding and other relatively strong interactions were adopted in superhydrophobic materials to provide improved interfacial interaction between the surface of the hydrophilic hierarchical topography and the top inert coatings. However, most of these interactions would be labile to the exposure of UV radiations or chemically harsh

aqueous phases, which are highly relevant circumstances for the outdoor applications of the bio-inspired property. Next, the synthesized superhydrophobic cotton was exposed to ultraviolet (UV) radiations at both the shorter (254 nm) and longer (365 nm) wavelengths for prolonged duration. Even after continuous exposure for 10 days to UV radiations, the SHC showed extreme repellency to the aqueous phase with an advancing water contact angle of above 150º and contact angle hysteresis below 10º, as shown in Figure 7.6B. The durability of the anti-wetting property was further demonstrated by arbitrarily rapturing the SHC using adhesive tape, and the exposed fibers of the fibrous substrate were displaying superhydrophobic property as is noted in Figure 7.7A, B. Next, this superhydrophobic

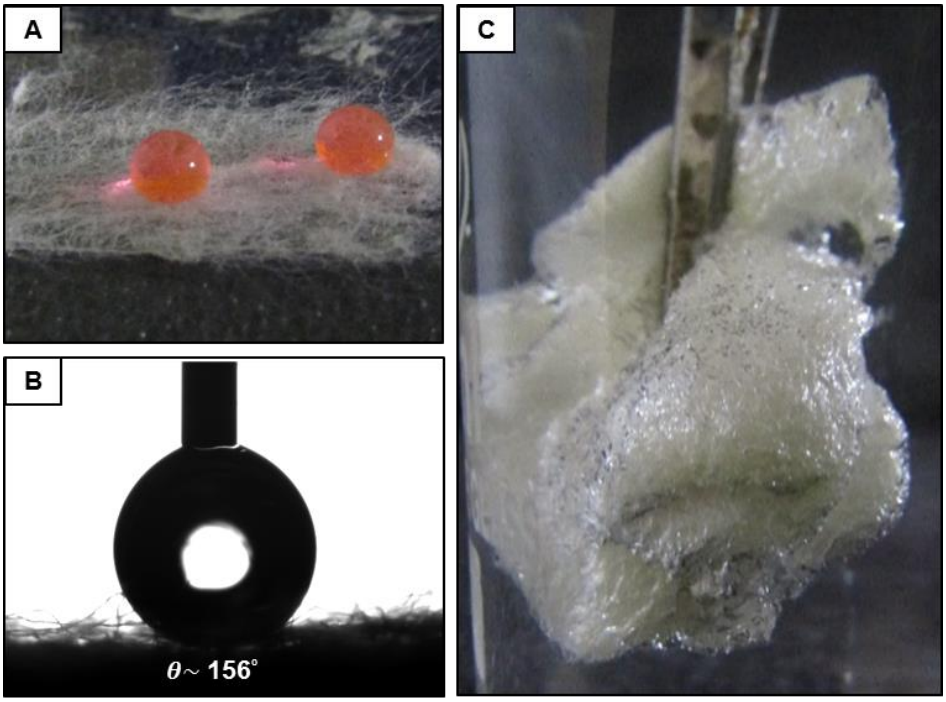

Figure 7.7. (A, B) Digital image (A) and contact angle image (B) of beaded water droplet on SHC after arbitrarily tearing the material using adhesive tape peeling test. C) Digital image of superhydrophobic cotton (SHC) which was submerged under water.

cotton was submerged under water, the solid/water interface appeared as shiny (Figure 7.7C), which is attributed to the presence of trapped air that confers the extreme heterogeneous wettability, and this simple study eventually revalidated the existence of a stable Cassie–Baxter state.[53] Hence, these all studies infers that the synthesized superhydrophobic fibrous cotton has durable anti-wetting property present three

dimensionally in the cotton ball. Next, the SHC was exposed to diverse and severe chemical conditions, including highly acidic (pH 1), alkaline (pH 12), artificial sea water and river (Brahmaputra Assam India) water for 96 hours. However, the anti-wetting property of the SHC remained intact with an advancing contact angle above 155° and contact angle hysteresis below 10°, as shown in Figure 7.8A-H. This impeccable physical and chemical

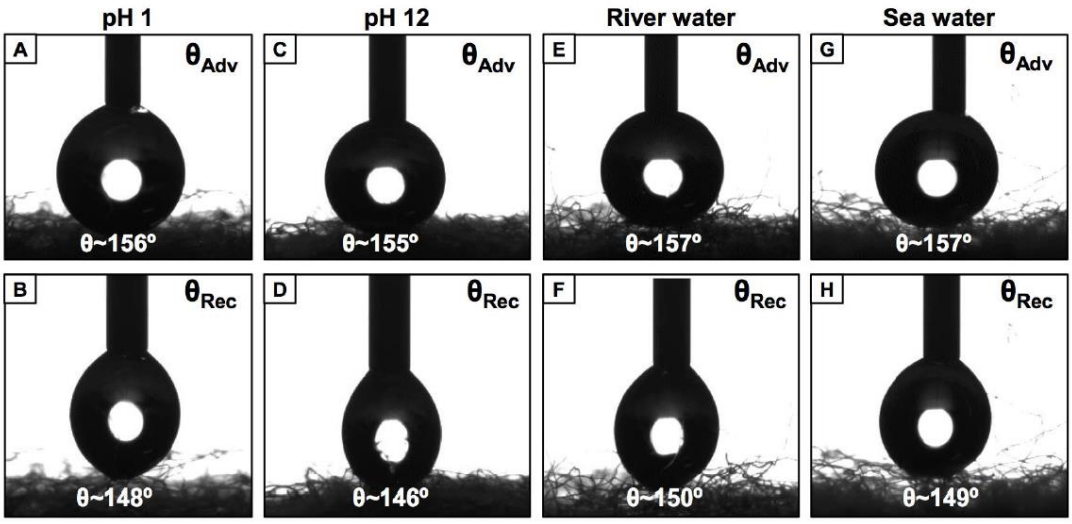

Figure 7.8. (A-H) The advancing (A, C, E, G) and receding (B, D, F, H) water contact angle images of beaded water droplet on SHC after exposing the material in various complex aqueous mediums including highly acidic medium of pH 1 (A-B), highly alkaline medium of pH 12 (C-D), river (Brahmaputra Assam India) water (E-F) and artificial sea water (G-H) respectively, for 96 hours.

durability of the superhydrophobic cotton is likely due to the presence of covalent crosslinking of reactive nanocomplexes on the selected fibrous substrate and the covalent optimization of essential low surface energy coating on the immobilized polymeric nanocomplexes.

7.3.3 Selective Absorption-Based Oil/Water Separation

Next, the three-dimensional superhydrophobic fibrous substrate with impeccable physical and chemical durability was strategically exploited in energy-efficient and environmentally-friendly oil/water separation from diverse and practically relevant scenarios. First, various light oils (e.g., vegetable oil, silicon oil and motor oil) with a density lower than water, which were floating on the air/water interface, were removed through the spontaneous and selective absorption of the oil phases by the SHC, as shown in Figure 7.9A-L. The SHC can float and move easily on the air/water interface due to its

inherent light weight and the presence of its extreme water repellency property, which eventually provided a facile basis for the complete removal of floating multiple oil droplets from the air/water interface, as depicted in Figure 7.9M-P. The absorbed oil was collected in a separate container by manual squeezing of the material. In contrast, the uncoated cotton was unable to collect any traces of the floating oil droplets. The uncoated cotton instantly soaked up the aqueous phase, and the water soaked cotton was absolutely inappropriate to absorb any traces of oil; rather, the floating oil phase on the air/water interface was repelled by the uncoated cotton, as shown in Figure 7.10A-H. Furthermore, this absorption-based

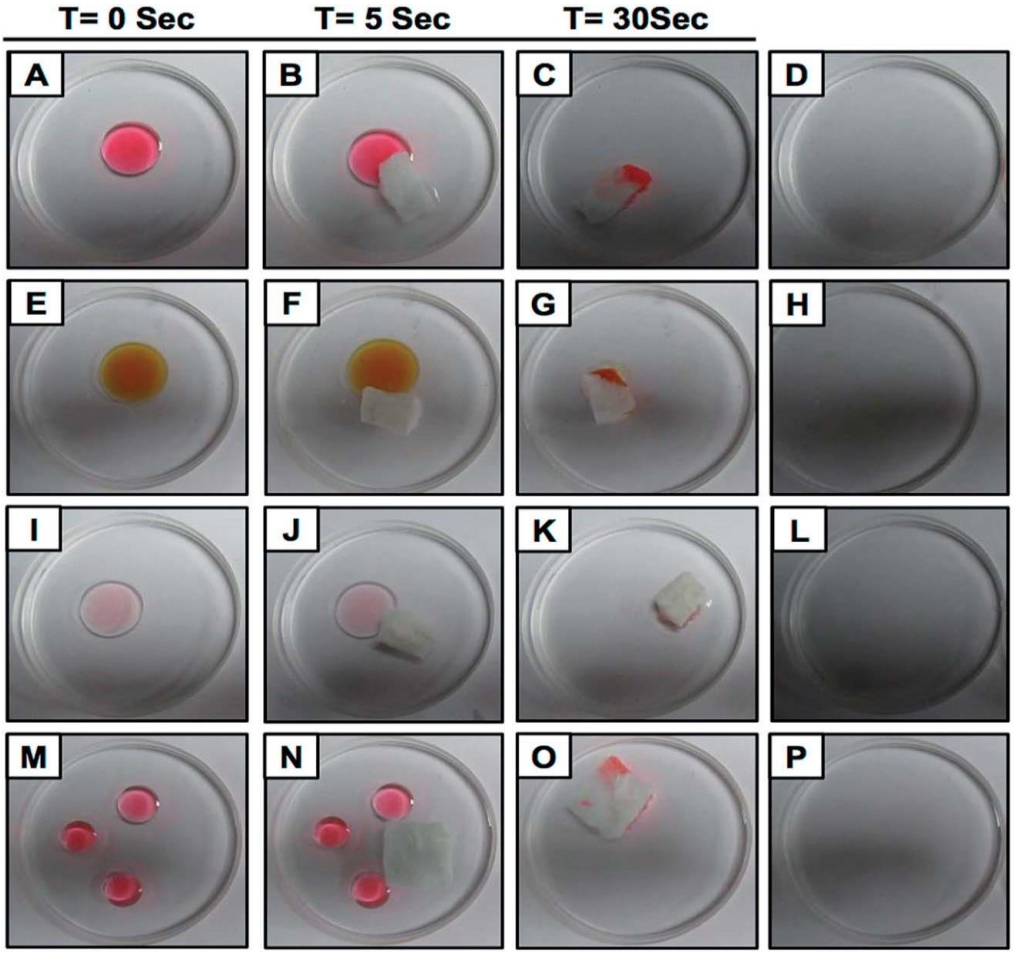

Figure 7.9. (A-L) Digital images illustrating the separation of floating droplets of various oils, including vegetable oil (A-D), motor oil (E-H), silicone oil (I-L), using SHC. 1 mL of oil was placed on the air/water interface in a Petri dish, then the superhydrophobic (SHP) cotton was placed on the water surface and the SHP cotton selectively absorbed the oil from the oil/water interface within 30 seconds. (M-P) Demonstrating the collection of multiple (three) droplets of vegetable oil from the air/water interface using superhydrophobic cotton.

selective oil collection by the SHC was extended to separate bulk oil/water mixtures irrespective of the density of the oils and their locations (both above and under the aqueous phase), which resembles practically relevant circumstances, where the oil contaminants (light or heavy) are either floating on the air/water interface or are sedimented on the bottom of open water reservoirs (river, lake, sea etc.). As a proof-of-concept demonstration, a piece

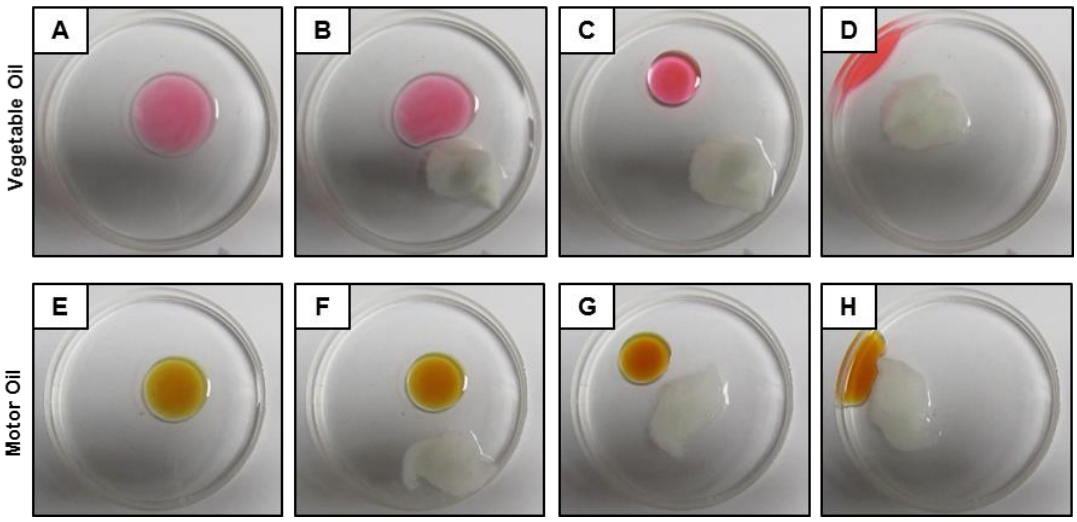

Figure 7.10. (A-H) Digital images showing the interaction between uncoated cotton and different types of oils including vegetable oil (A-D) and motor oil (E-H) respectively. Oils are repelled by the native cotton.

of SHC was brought in contact with a bulk oil/water mixture consisting of 5 mL of motor oil (light oil) and 30 mL of water (Figure 7.11A). The motor oil was selectively and rapidly soaked into the material (Figure 7.11B, C), and the oil-soaked SHC remained floating on the top of the aqueous phase due to its extreme water repelling property even after contamination with oil as shown in Figure 7.11C. The oil-soaked superhydrophobic cotton was removed from the water without any traces of water as characterized by visual inspection and the absorbed oil was squeezed manually to recover the oil. Next, the same absorption principle was exploited further to remove sedimentary heavy model-oil (DCM, red color aids visual inspection, present at the bottom of water) from the oil/water mixture (10 mL of DCM and 20 mL of water). The sedimentary oil (red color aids visual inspection) was instantly and selectively absorbed by the SHC under water (Figure 7.11E, F), and no trace of water (blue color aids visual inspection) was noticed in the SHC after exposing the material to the oil phase under water, which is again due to its extreme water repellency

property. In contrast, the uncoated cotton was completely wetted by water (blue color) prior to bringing it into contact with the sedimentary oil under water (Figure 7.11G, H) and thus, the uncoated cotton became absolutely ineffective for removing the sedimentary oil under water. The synthesized SHC is capable of absorbing a large volume (with respect to the mass of SHC) of both heavy and light oils (e.g., chloroform, dichloromethane (DCM),

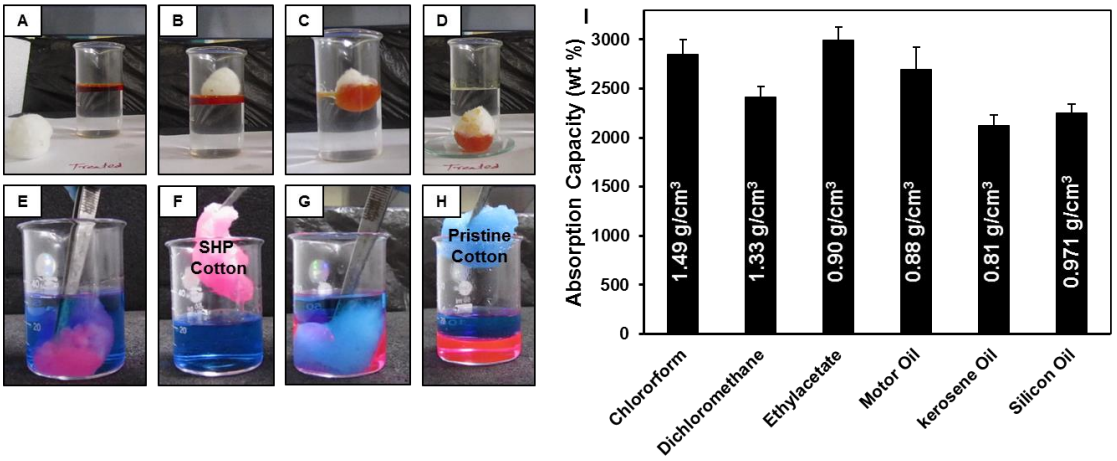

Figure 7.11. (A-D) Digital images depicting the selective absorption of layered oil that is floating on the aqueous phase, using SHC. E-F) Digital images illustrating the successful collection/separation of heavy model-oil (DCM) under water (blue color aids visual inspection) using superhydrophobic cotton; however the native cotton (G-H) was inappropriate for collecting oil under water, and rather collected the aqueous phase (blue color) selectively. I) Plot illustrating the maximum absorption capacity of SHC for absorbing various oils irrespective of chemical compositions, densities and viscosities of the oils.

silicone oil, ethyl-acetate, motor oil, kerosene oil), due to its highly porous and fibrous three dimensional network, and the absorption capacity was calculated to be well above 2000 wt%, irrespective of the density and viscosity of the oils (Figure 7.11I). Further, the SHC was found to be highly capable of separating oil and water with a separation efficiency above 97%, irrespective of the chemical composition and density of the used oils, as shown in Figure 7.12A. This oil/water separation process was further repeated with oil/water mixture having complex aqueous phases, including extremes of pH (1 and 12), artificial sea water and river (Brahmaputra, Assam India) water. However, the SHC was found to be highly efficient with separation efficiency above 95% in the selective removal of oil from an oil/water mixture, irrespective of the presence of complex chemical composition in the aqueous phases, as shown in Figure 7.12B. Hence, these studies implied that the

synthesized superhydrophobic cotton has immense potential in removing oil/oily phases from respective oil/water mixtures irrespective of their locations and the densities of the used oil/oily phases, with a high absorption capacity and separation efficiency. Further, the absorbed oil was recovered from the SHC by a simple and rapid manual squeezing process, unlike the refluxing approach,[54] which is inherently time and energy consuming processes.

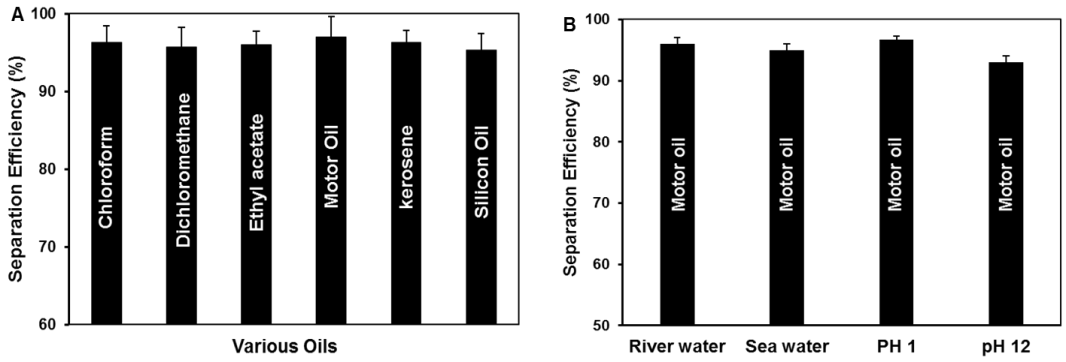

Figure 7.12. (A) Plot showing the efficiency for separating various oils and organic solvents from oil /water mixtures. B) Plot showing the ability of SHC for separating motor oil in different harsh chemical environments, including highly acidic (pH 1), highly alkaline (pH 12), artificial sea water and river (Brahmaputra Assam, India) water.

7.3.4. Selective Filtration of Oil through Superhydrophobic Cotton

The potential of the SHC in absorption based separation of oil and water under diverse conditions, including an air/water interface and under water was demonstrated in the previous section. Further, this material was explored in another energy-efficient and environmental-friendly oil/water separation process that is selective filtration of oil and oily contaminants from oil/water mixtures. This active filtration would be useful in preventing regular oil contamination during industrial waste water discharge. As a proof-of-concept demonstration, a lab-based prototype was developed using a glass tube, where wide opening of a glass tube was plugged with SHC for the removal of sedimentary oil and was followed by collection of the separated oil from the SHC, without refluxing and physically deforming the material. The ingress of sedimentary oil was rapid and selective through the plugged SHC under water, and the oil phase was further filtered through the SHC and was accumulated within the glass tube against the gravity, unlike a conventional gravity driven filtration process,[8] as shown in Figure 7.13A-C. Then, the other end of the prototype was manually capped with an index finger and the whole prototype was taken out of the

oil/water mixture. The separated oil in the prototype was collected in a separate container by uncapping the top end of the prototype. This process was successfully repeated for multiple times to remove and collect the sedimentary oil under water, as shown in Figure 7.13D. However, a similar prototype—that was prepared with uncoated cotton—was completely unable to extract any sedimentary oil under water due to the its pre-wetting with aqueous phase and hence, remains inept to collect any traces of oil, as shown in Figure

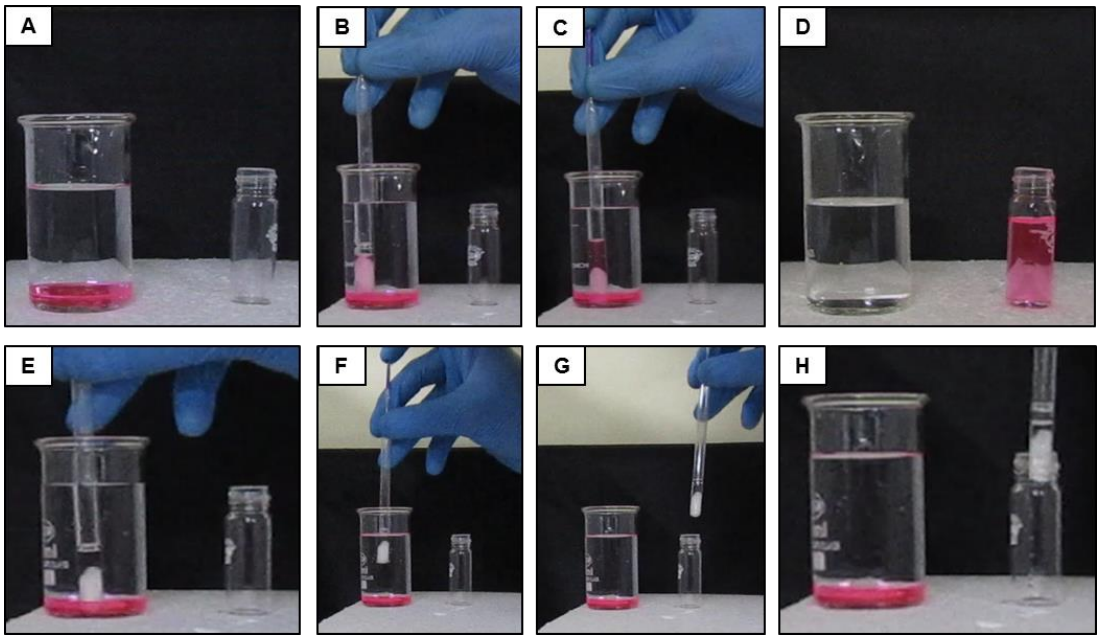

Figure 7.13. (A-D) Digital images illustrating the selective filtration of oil (model oil, chloroform, red dyed for easy visualization) under water against gravity using a lab-based prototype where the wider opening of the glass dropper was plugged with SHC. E-H) Digital images illustrating the inability of native cotton in collecting the sediment oil under water.

7.13E-H. Moreover, this prototype was also explored to separate oil from various complex and practically relevant conditions, including highly acidic (pH 1), alkaline (pH 12), artificial sea water and river (Brahmaputra, Assam, India) water (Figure 7.14A-H). The as prepared prototype was found to be highly efficient in separation of oil in presence of these complex aqueous mediums. Another prototype was developed in the lab using falcon tube and a glass funnel, where the SHC was fixed on the small opening of the glass funnel placed above the falcon tube for conventional and gravity-driven filtration of an oil/water mixture that consisted of 20 mL of water and 20 mL of DCM (model oil, red color aids visual inspection). The oil/water mixture was separated spontaneously as the oil phase was

selectively filtered through the SHC, while the aqueous phase (blue color aids visual inspection) remained accumulated above the SHC due to presence of superhydrophobic

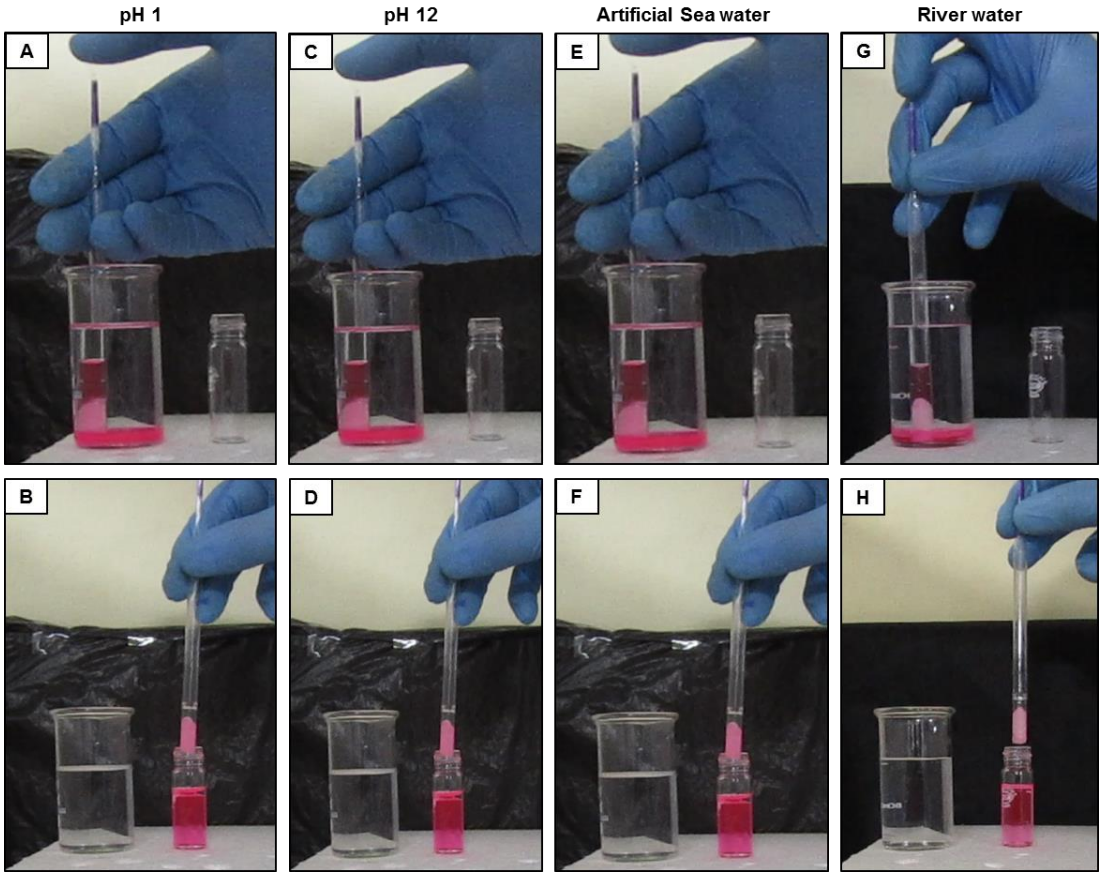

Figure 7.14. (A-H) Digital images illustrating the collection of sediment oil under water by filtration through SHC—but against the gravity in various complex aqueous phases including highly acidic medium of pH 1 (A, B), highly alkaline medium of pH 12 (C, D), artificial sea water (E, F) and river (Brahmaputra Assam India) water (G, H).

and superoleophilic property as is shown in Figure 7.15A, B. In comparison, the untreated cotton allowed filtration of both oil and water phases and eventually both the oil and water phases are collected in separate container (Figure 7.15C, D). Moreover, the same piece of SHC was repeatedly used for separating an oil/water mixture following the gravity-driven filtration principle, and around 95% of the oil was collected from the oil/water mixture even after successive use of the SHC for 100 times, as shown in Figure 7.16A. Moreover, the anti-wetting property of this SHC cotton was examined regularly after the repeated use in an oil/water separation process, and the material was displaying extreme water repellency

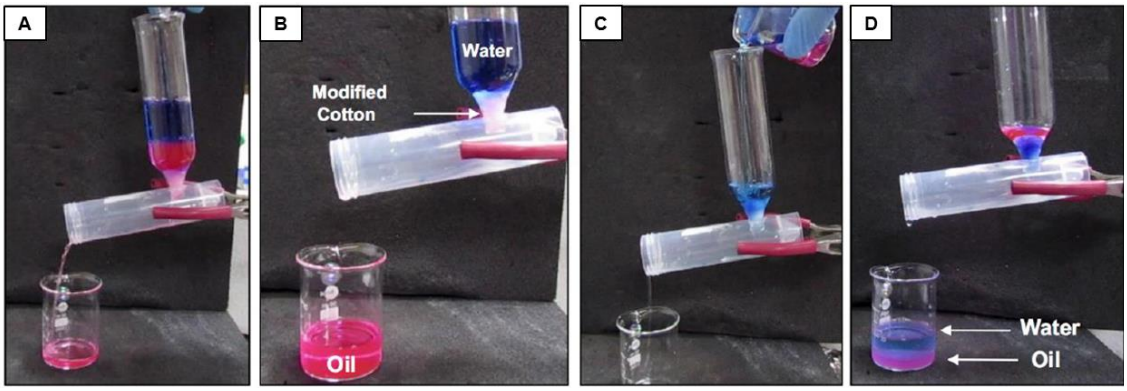

Figure 7.15. (A-D) Digital images illustrating the ability of both SHC (A-B) and the native cotton (C-D) in the gravity driven separation of oil/water mixture (20 mL DCM and 20 mL of water).

towards the beaded water droplets with an advancing water contact angle of above 157º and with contact angle hysteresis of below 10º, even after 100 times of successive use of the same material in oil/water separation as shown in Figure 7.16B.

This lab made prototype was further explored in gravity-driven selective filtration of oils from a complex oil/water mixture (Figure 7.17A-D) where the blue colored (aids visual inspection) aqueous phase was sandwiched between heavy (bottom layer, bright pink colored DCM) and light (top layer, green colored kerosene oil) oils. When the three phase oil/water mixture was poured into the prototype, both the heavy and light oils were actively

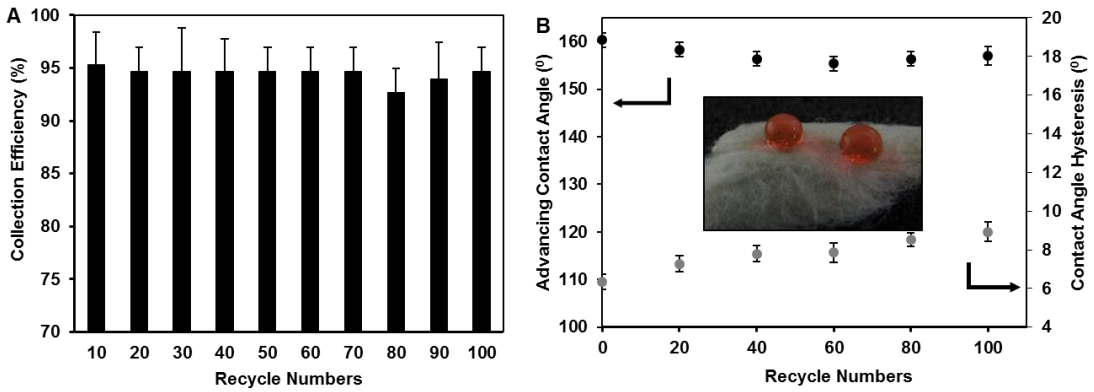

Figure 7.16. (A) Plot showing the ability of SHC for repetitive use in gravity-driven filtration of an oil/water mixture for 100 times. B) Plot illustrating the variation in the advancing contact angle (black) and contact angle hysteresis (grey) of superhydrophobic cotton after successive use in oil/water separation (inset is the digital image of superhydrophobic cotton after 100 times of oil/water separation).

filtered through SHC and were collected in a separate container that was placed under the prototype, as shown in Figure 7.17B-D, whereas the blue-colored aqueous phase remained accumulated above the SHC due to restricted ingression of the water phase, as shown in Figure 7.17E. At the end, it was noticed that a small fraction of oil remained above the accumulated aqueous phase, which had not passed through the SHC. Then, another complementary approach—that is selective absorption of oil by the SHC was strategically

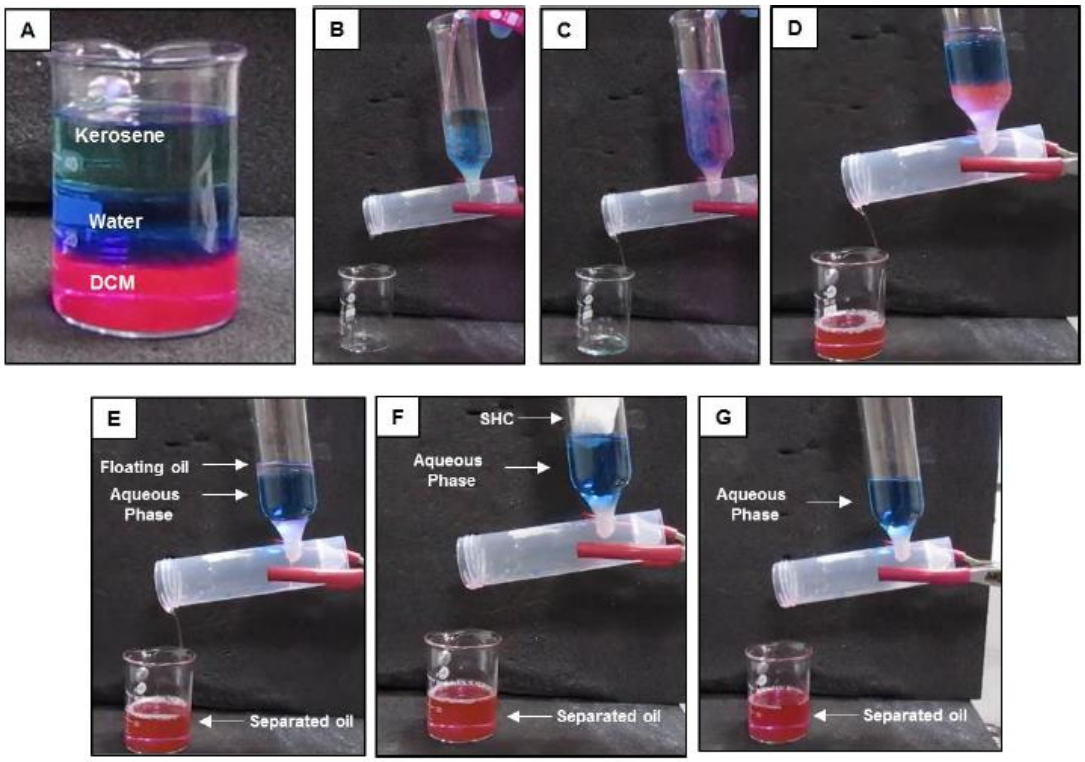

Figure 7.17. (A) Digital image of three phases oil/water mixture that consisted of kerosene (at top), aqueous phase (at middle) and DCM (model heavy oil, at bottom). B-E) Digital images illustrating the oil/water separation by the gravity driven filtration process, and small fraction of floating oil was finally removed through absorption process (F). Pieces of SHC were strategically exploited during complimentary use of both the filtration and absorption processes.

applied to remove this floating oil above the aqueous (blue aids visual inspection) phase, as shown in Figure 7.17F-G. Thus, this simple study unambiguously revealed the potential of the complementary use of selective filtration and absorption principles in the comprehensive cleaning of oil spills in practically relevant complex circumstances, and in this context, the performance of the synthesized SHC cotton was found to be exceptional (Figure 7.17G).

Moreover, this approach was further extended to separate even water-in-oil emulsion (Figure7.18A). The model oil phase (DCM) was labelled with fluorescent dye (Nile red) for better visual inspection of the separation process. The pink and turbid emulsion was poured into the prototype that was plugged with SHC, and the oil phase was instantly separated from the aqueous phase by selective filtration through the SHC, and was eventually collected in a separate container that was placed under the lab-made oil/water separating system, as shown in Figure 7.18D. The successful separation of water droplets from the oil phase was further verified by optical microscope imaging (Figure 7.18E-F). Even though this material is capable of separating diverse forms of oil spills, it remained inherently incapable of separating oil-in-water emulsions due to the presence of excess amount of water in such emulsions limits the SHC to be exposed to the oil phase and hence remained unable to separate the oil-in-water emulsion.

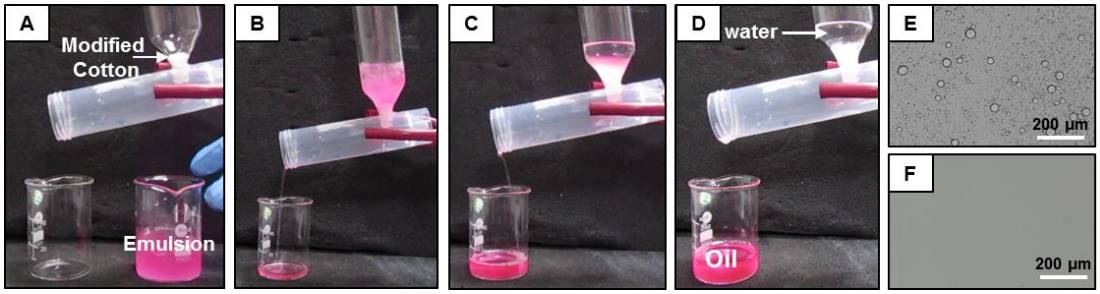

Figure 7.18. (A-D) Digital images revealing the ability of SHC in gravity driven filtration based emulsion (5 mL of water in 20 mL of DCM) separation. E-F) Microscopic images of water in oil emulsion before (E) and after separation (F) respectively.

7.4. Conclusion

In conclusion, here, a naturally abundant and three-dimensional-fibrous substrate was exploited in the eco-friendly separation of oil and water, irrespective of the density and viscosity of the oils, after appropriate optimization of topography/chemistry through a facile and catalyst-free 1, 4-conjugate addition reaction. The synthesized material was capable of displaying extreme water repellency both in air and under oil, and this anti-wetting property remained intact even after incurring various common physical manipulations (e.g., bending, twisting and compressing) that are highly relevant at practical settings. The adapted chemistry in this design provided a highly stable material that can survive after prolonged (10 days) exposure to UV radiations and complex aqueous phases

(such as extremes of pH, sea water, river water etc.). The fibrous superhydrophobic/superoleophilic material with exemplary durability was highly efficient (with a separation efficiency ~ 99%) for separating different forms of oils (including floating light oil, sedimentary heavy oil, and emulsion) from aqueous media, through selective absorption process. The same material was also repetitively used in filtration based oil/water separation for 100 times with a high separation efficiency (above 95%) and without compromising its anti-wetting property. Hence, this material has a potential for both (i) preventing oil contamination by adopting an active-filtration process and (ii) cleaning up accidental oil-spills from vast and open water resources (seas, rivers, lakes etc.) through the selective absorption process, both in air and under water.

References

(1) Peterson, C. H.; Rice, S. D.; Short, J. W.; Esler, D.; Bodkin, J. L.; Ballachey, B. E.; Irons, D. B. *Science* **2003**, *302*, 2082–2086.

(2) Brussaard, C. P. D.; Peperzak, L.; Beggah, S.; Wick, L. Y.; Wuerz, B.; Weber, J.; Arey, J. S.; Burg, B.; Jonas, A.; Huisman, J.; Meer, J. R. *Nat. Commun.* **2016**, *7*, 11206–11217.

(3) Nordvik, A. B.; Simmons, J. L.; Bitting, K. R.; Lewis, A.; Stromkristiansen, T. *Spill Sci. Technol. Bull.* **1996**, *3*, 107–122.

(4) Al-Majed, A. A.; Adebayo, A. R.; Hossain, M. E. *J. Environ. Manage*. **2012**, *113*, 213–227.

(5) Nyankson, E.; Decuir, M. J.; Gupta, R. B. *ACS Sustainable Chem. Eng.* **2015**, *3*, 920–931.

(6) Chu, Z. L.; Feng, Y. J.; Seeger, S. *Angew. Chem. Int. Ed.* **2015**, *54*, 2328–2338.

(7) Ma, Q. L.; Cheng, H. F.; Fane, A. G.; Wang, R.; Zhang, H. *Small* **2016**, *12*, 2186–2202.

(8) Feng, L.; Zhang, Z. Y.; Mai, Z. H.; Ma, Y. M.; Liu, B. Q.; Jiang, L.; Zhu, D. B. *Angew. Chem. Int. Ed*. **2004**, *43*, 2012–2014.

(9) Crick, C. R.; Gibbons, J. A.; Parkin, I. P. *J. Mater. Chem. A* **2013**, *1*, 5943–5948.

(10) Wang, B.; Guo, Z. G. *Chem. Commun.* **2013**, *49*, 9416–9418.

(11) Zhou, X. Y.; Zhang, Z. Z.; Xu, X. H.; Guo, F.; Zhu, X. T.; Men, X. H.; Ge, B. *ACS Appl. Mater. Interfaces* **2013**, *5*, 7208–7214.

(12) Xue, Z. X.; Cao, Y. Z.; Liu, N.; Feng, L.; Jiang, L. *J. Mater. Chem. A* **2014**, *2*, 2445–2460.

(13) Che, H.; Huo, M.; Peng, L.; Fang, T.; Liu, N.; Feng, L.; Wei, Y.; Yuan, J. *Angew. Chem. Int. Ed*. **2015**, *54*, 8934–8938.

(14) Wang, Z.; Wang, Y.; Liu, G. *Angew. Chem. Int. Ed*. **2016**, *55*, 1291–1294.

(15) Han, Z.; Li, B.; Mu, Z.; Niu, S.; Zhang, J.; Ren, L. *Small* **2017**, *13*, 1701121–1701132.

(16) Rather, A. M.; Manna, U. *J. Mater. Chem. A* **2017**, *5*, 15208–15216.

(17) Yuan, J. K.; Liu, X. G.; Akbulut, O.; Hu, J. Q.; Suib, S. L.; Kong, J.; Stelacci, F. *Nat. Nanotechnol.* **2008**, *3*, 332–336.

(18) Zhang, J.; Seeger, S. *Adv. Funct. Mater*. **2011**, *21*, 4699–4704.

(19) Nguyen, D. D.; Tai, N. H.; Lee, S. B.; Kuo, W. S. *Energy Environ. Sci*., **2012**, *5*, 7908–7912.

(20) Calcagnile, P.; Fragouli, D.; Bayer, I. S.; Anyfantis, G. C.; Martiradonna, L.; Cozzoli, P. D.; Cingolani, R.; Athanassiou, A. *ACS Nano*, **2012**, *6*, 5413–5419.

(21) Zhu, Q.; Chu, Y.; Wang, Z. K.; Chen, N.; Lin, L.; Liua, F. T.; Pan, Q. M.; *J. Mater. Chem. A* **2013**, *1*, 5386–5393.

(22) Zhu, H.; Chen, D.; An, W.; Li, N.; Xu, Q.; Li, H.; He, J.; Lu, J. *Small* **2015**, *11*, 5222–5229.

(23) Ge, J.; Zhao, H. Y.; Zhu, H. W.; Huang, J.; Shi, L. A.; Yu, S. H. *Adv. Mater.* **2016**, *28*, 10459–10490.

(24) Jianfeng, Z.; Seunghwa, R.; Nicola, P.; Qiming, W.; Qing, T.; Markus, J. B.; Xuanhe, Z. *Nat. Mater.* **2013**, *12*, 321–325.

(25) Cho, S. J.; Nam, H.; Ryu, H.; Lim, G. *Adv. Funct. Mater.* **2013**, *23*, 5577–5584.

(26) Fatang, L.; Fenghe, S.; Qinmin, P. *J. Mater. Chem. A* 2014, *2*, 11365–11371.

(27) Callies, M.; Quere, D. *Soft Matter* **2005**, *1*, 55–61.

(28) Verho, T.; Bower, C.; Andrew, P.; Franssila, S.; Ikkala, O.; Ras, R. H. A. *Adv. Mater.* **2011**, *23*, 673–678.

(29) Xue, C. H.; Ma, J. Z. *J. Mater. Chem. A* **2013**, *1*, 4146–4161.

(30) Li, X. M.; Reinhoudt, D.; Crego-Calama, M. *Chem. Soc. Rev.* **2007**, *36*, 1350–1368.

(31) Yan, Y. Y.; Gao, N.; Barthlott, W. *Adv. Colloid Interface Sci.* **2011**, *169*, 80–105.

(32) Gao, X.; Zhou, J.; Du, R.; Xie, Z.; Deng, S.; Liu, R.; Liu, Z.; Zhang, J. *Adv. Mater.* **2016**, *28*, 168–173.

(33) Toma, M.; Loget, G.; Corn, R. M. *ACS Appl. Mater. Interfaces* **2014**, *6*, 11110–11117.

(34) Mo, X.; Wu, Y.; Zhang, J.; Hang, T.; Li, M. *Langmuir* **2015**, *31*, 10850–10858.

(35) Osicka, J.; Il˘cikov´a, M.; Popelka, A.; Filip, J.; Bertok, T.; Tkac, J.; Kasak, P. *Langmuir* **2016**, *32*, 5491–5499.

(36) Tan, C.; Cai, P.; Xu, L.; Yang, N.; Xi, Z.; Li, Q. *Appl. Surf. Sci.* **2015**, *349*, 516–523.

(37) Zhou, C.; Chen, Z.; Yang, H.; Hou, K.; Zeng, X.; Zheng, Y.; Cheng, J. *ACS Appl. Mater. Interfaces* **2017**, *9*, 9184–9194.

(38) Sugimura, H.; Ushiyama, K.; Hozumi, A.; Takai, O. *Langmuir* **2000**, *16*, 885–888.

(39) Uosaki, K.; Quayum, M. E.; Nihonyanagi, S.; Kondo, T. *Langmuir* **2004**, *20*, 1207–121.

(40) Kwak, G.; Lee, M.; Yong, K. *Langmuir* **2010**, *26*, 9964–9967.

(41) Tian, X.; Verho, T.; Ras, R. H. A. *Science* **2016**, *352*, 142–143.

(42) Lynn, D. M.; Langer, R. *J. Am. Chem. Soc.* **2000**, *122*, 1076–1078.

(43) Farrer, R. A.; LaFratta, C. N.; Li, L.; Praino, J.; Naughton, M. J.; Saleh, B. E. A.; Teich, M. C.; Fourkas, J. T. *J. Am. Chem. Soc.* **2006**, *128*, 1796–1797.

(44) Weatherspoon, M. R.; Dickerson, M. B.; Wang, G.; Cai, Y.; Shian, S.; Jones, S. C.; Marder, S. R.; Sandhage, K. H. *Angew. Chem. Int. Ed.* **2007**, *46*, 5724–5727.

(45) Ford, J.; Marder, S. R.; Yang, S. *Chem. Mater.* **2009**, *21*, 476–483.

(46) Bechler, S. L.; Lynn, D. M. *Biomacromolecules* **2012**, *13*, 1523–1532.

(47) Rather, A. M.; Manna, U. *Chem. Mater*. **2016**, *28*, 8689–8699.

(48) Parbat, D.; Manna, U. *Chem. Sci*. **2017**, *8*, 6092–6102.

(49) Parbat, D.; Gaffar, S.; Rather, A. M.; Gupta, A.; Manna, U. *Chem. Sci.* **2017**, *8*, 6542–6554.

(50) Rather, A. M.; Mahato, S.; Maji, K.; Gogoi, N.; Manna, U. *Nanoscale* **2017**, *9*, 16154–16165.

(51) Chen, Y.; Gan, T.; Ma, C.; Wang, L.; Zhang, G. *J. Phys. Chem. B* **2016**, *120*, 4715–4722.

(52) Wu, M.; Ma, B.; Pan, T.; Chen, S.; Sun, J. *Adv. Funct. Mater.* **2016**, *26*, 569–576.

(53) Cassie, A. B. D.; Baxter, S. *Nature* **1945**, *155*, 21–22.

(54) Vibhute, A. M.; Muvvala, V.; Sureshan, K. M. *Angew. Chem. Int. Ed.* **2016**, *55*, 7782–7785.

Chapter 8. Conclusion and Future Directions

This chapter presents a general summary of the work described in the current thesis and the possible future directions of the research associated to this work is also provided. In the current thesis, a facile and rapid chemical reaction at ambient conditions was adopted to develop various functional polymeric materials where initially doping of NaCl accelerated the gelation of synthetic branched polymer through strategic use of facile Michael addition reaction between amine and acrylate functionalities in ethanol. The synthesized material was embedded with durable and bulk superhydrophobicity after appropriate post chemical modification with amine containing small molecule (decylamine) through 1, 4-conjugate addition reaction. This facile synthesis enables to fabricate the polymeric materials with different shapes and sizes. The impact of various alkali metal salts including LiCl, NaCl, KCl, RbCl and CsCl on the gelation of branched polymer was studied in details, where various alkali metal ions has different impact on the gelation of BPEI polymer. The rate of gelation was faster with decrease in the size of alkali metal ion. Moreover, the presence of various alkali metal salts in the reaction mixture provided polymeric materials with different topographies without affecting the existence of residual reactive acrylate functionalities in the synthesized material. The polymeric materials with different topographies are highly efficient in displaying nonadhesive superhydrophobicity after post chemical modification with decylamine. However, a slight change in the post chemical optimization by varying the hydrocarbon tail length—caused significant change in water wettability. Hence this study allowed to evaluate the dependence of physical/chemical parameters towards superhydrophobicity. Next, various physical properties (shrinkage, porosity, mechanical strength) and the anti-wetting property of the polymeric material was further tailored with change in the alcoholic solvent of the reaction medium, where composition of reactants remained unaltered. The gelation rate was noted to be faster with increase in the alkyl chain of the alcoholic solvent from methanol to pentanol/hexanol. A preliminary computational study on the acrylate and amine functionalities in various alcoholic solvents revealed that the intermolecular bond distances steadily decreased with increase in the hydrocarbon chain length of the alcoholic solvents and this improved interaction is likely to facilitate the 1, 4-conjugate addition reaction and resulted in faster gelation in higher analogues of methanol. The instant and rapid gelation of BPEI polymer

without using any solvent and catalyst provided a stable and bulk superhydrophobic coatings on various substrates irrespective of their nature and chemical compositions. The developed coatings were highly durable against various physical and chemical insults including adhesive tape test, sand drop test, exposure to various pH (1, 12), artificial sea water, river water as well as under UV exposure. Synthesized superhydrophobic materials were demonstrated for self-cleaning of the deposited dust, controlled transfer of tiny water droplets etc. This facile and scalable 1, 4-conjugate addition reaction between amine and acrylate functionalities of BPEI and 5-Acl provided reactive polymeric nanocomplexes which were further strategically used for developing stretchable and durable superhydrophobic membrane. The anti-wetting property of the membrane remained intact after incurring various physical abrasions (i, e., bending, twisting, winding) and even after inducing 150% tensile strain repetitively for 1000 cycles. This highly durable and stretchable superhydrophobic membrane was further explored for gravity-driven and energy-efficient oil/water separation with high separation efficiency (above 99%) for lighter and heavier oils irrespective of the contamination of the aqueous phase. Moreover, a highly compressible, deformable and durable superhydrophobic material was developed using a naturally abundant and inherently hydrophilic fibrous substrate (cotton ball). The superhydrophobic/superoleophilic property in the fibrous substrate was developed through covalent immobilization of the reactive polymeric nanocomplexes followed by appropriate post chemical modification with octadecylamine. The bio-inspired anti-wetting property remained intact after various physical and chemical abrasions and even after 80% of compressive strain for 1000 cycles. The three dimensional porous and fibrous substrate with durable and bulk superhydrophobic property was further explored for both the absorption and filtration based oil/water separation of lighter and heavier oils with high absorption capacity (above 2000 wt%) and separation efficiency (above 99%), irrespective of the density of the used oils. Furthermore, the same superhydrophobic fibrous and porous material was repetitively used for oil/water separation for 100 consecutive cycles.

Considering the research work in this thesis, a number of research projects could be taken up in the future with respect to the prospective and relevant applications. Some prospective future research directions are briefly mentioned in the following section.

(i) Recently, superhydrophobic patterned interfaces are emerged as potential avenue for various applications—including water harvesting as similar to that of desert beetle back, open channel microfluidic systems, dynamic solution transfer, biospecific cell adhesive surfaces etc., where the hydrophilic domains present on the superhydrophobic interfaces in order to confine, collect or transport small volumes of aqueous solution. My current design of chemically reactive polymeric material developed through the gelation of BPEI polymer that consists of residual and reactive acrylate moieties, would allowed to selectively functionalize with hydrophobic and hydrophilic amine containing small molecules to develop durable chemically patterned interfaces for the above mentioned applications with improved performance in practically relevant settings.

(ii) The stretchable superhydrophobic interfaces have recently received an enormous attention due to its inherent ability for various potential applications at practical context include wearable devices, gas sensors, flexible electronics etc. However, the synthesis of durable and stretchable superhydrophobic interfaces is challenging. I have introduced a facile avenue to develop such interfaces. Now, such design can be further extended for developing various functional materials for practically relevant above mentioned applications.

(iii) Water pollution caused due to frequent oil spill accidents and continuous discharge of oil contaminated wastewater from oil-refinery plants impose a severe challenges worldwide. In the current thesis, the highly compressible, deformable and tolerant superhydrophobic cotton was fabricated and subsequently demonstrated for the oil/water separation of various types of oils irrespective of their density and locations. This approach can be further extended to other porous substrates for improving the oil absorption capacity.

(iv) In the recent past, the bulk superhydrophobic materials have been explored for the controlled and sustained release of embedded drug like small molecules. The presence of metastable trapped air layer (presence of Cassie-Baxter state) at the surface and in the interior of bulk superhydrophobic materials provides the means for the slow infiltration of water and there by promotes the slow and controlled release of embedded drug like small molecules. Hence, the synthesized polymeric material with controlled water wettability in the current thesis has an immense prospective for the controlled and sustained release of

post loaded drug molecules for future endeavors. Such principle is highly relevant for various biomedical applications.

List of Publication Based on Research Work

(A) Papers Published in Peer-Reviewed Journals (Part of Thesis)

1. **A. M. Rather**, U. Manna. Facile Synthesis of Tunable and Durable Bulk Superhydrophobic Material from Amine "Reactive" Polymeric Gel. *Chem. Mater*. **2016**, *28*, 8689–8699.
2. **A. M. Rather**, A. Shome, S. Kumar, B. K. Bhunia, B. B. Mandal, H. K. Srivastava, U. Manna. Alkali Metal-ion Assisted Michael Addition Reaction in Controlled Tailoring of Topography in a Superhydrophobic Polymeric Monolith. *J. Mater. Chem. A* **2018**, *6*, 17019–17031.
3. **A. M. Rather**, N. Jana, S. Begum, H. K. Srivastava, U. Manna. Exceptional Control on Physical Properties of a Polymeric Material through Alcoholic Solvent Mediated Environment-Friendly Michael Addition Reaction**.** *Green Chem*. **2017**, *19*, 4527–4532.
4. **A. M. Rather**, U. Manna. Green and Rapid Synthesis of Durable and Super-Oil (under Water) and Water (in Air) Repellent Interfaces. *ACS, Appl. Mater. Interface* **2018,** *10***,** 23451–23457.
5. **A. M. Rather**, U. Manna. Stretchable and Durable Superhydrophobicity that Acts both in Air and Under Oil. *J. Mater. Chem. A* **2017,** *5*, 15208–15216.
6. **A. M. Rather**, N. Jana, P. Hazarika, U. Manna. Sustainable Polymeric Material for the Facile and Repetitive Removal of Oil-Spills through the Complementary use of Both Selective-Absorption and Active-Filtration Processes. *J. Mater. Chem. A* **2017**, *5*, 23339–23348.

(B) Other Publications

1. **A. M. Rather**, S. Mahato, K. Maji, Gogoi, N. Gogoi, U. Manna. 'Reactive' Nano-Complex Coated Medical Cotton: A Facile Avenue for Tailored Release of Small Molecules. *Nanoscale* **2017**, *9*, 16154–16165.
2. **A. M. Rather**, A. Shome, B. K. Bhunia, B. B. Mandal, U. Manna, Simultaneous and Controlled Release of Two Different Bioactive Small Molecules from Nature Inspired Single Material. *J. Mater. Chem. B* **2018**, *6*, 7692–7702.
3. A. Das, J. Deka, **A. M. Rather**, B. K. Bhunia, P. P. Saikia, B. B. Mandal, K. Raidongia, U. Manna**.** Strategic Formulation of Graphene Oxide Sheets for Flexible Monoliths and Robust Polymeric Coatings Embedded with Durable Bioinspired Wettability. *ACS Appl. Mater. Interface* **2017**, *9*, 42354−42365.

4. D. Parbat, S. Gaffar, **A. M. Rather**, A. Gupta, U. Manna. A General and Facile Chemical Avenue for the Controlled and Extreme Regulation of Water Wettability in Air and Oil Wettability under Water. *Chem. Sci*. **2017**, *8*, 6542–6554.
5. A. Das, S. Sengupta, J. Deka, **A. M. Rather**, K. Raidongia, U. Manna. Synthesis of Fish Scale and Lotus Leaf Mimicking, Stretchable and Durable Multilayers. *J. Mater. Chem. A* **2018,** *6*, 15993–16002.
6. A. Shome, **A. M. Rather**, U. Manna, Aloe Vera Mucilage Derived Highly Tolerant Underwater Superoleophobic Coating. *J. Mater. Chem. A* **2018**, *6*, 22465–22471.

Conferences/Seminars Attended

- Presented poster entitled "Facile Fabrication of Durable Bulk Superhydrophobic Material from Amine Reactive Formable Gel" in ***Chemical Research Society of India (CRSI-2016)*** at Guwahati University Assam, India.
- Presented poster entitled "Facile Fabrication of Durable Bulk Superhydrophobic Material from Amine Reactive Polymeric Gel" in ***'Research Conclave '17*** organized by Students' Academic Board (SAB), IIT Guwahati.
- Presented poster entitled "Synthesis of Stretchable and Durable Superhydrophobic Surface" in ***'Chemconvene 2017'*** organized by Department of Chemistry, IIT Guwahati.
- Presented poster entitled "Synthesis of Durable Amine Reactive Polymeric Material" ***International Conference on Sophisticated Instruments in Modern Research, 2017*** *(ICSIMR-2017),* organized by 'CIF IIT Guwahati'.
- Presented poster entitled "Fabrication of Durable Bulk Superhydrophobic Material from Amine Reactive Polymeric Gel" ***Advances in Polymer Science & Technology, 2017*** at Radisson Blu Hotel 'New Delhi' organized by 'Asian Polymeric Association and IIT Delhi'.
- Delivered an oral talk entitled "Facile Fabrication of Bulk Superhydrophobic Material from Amine Reactive Polymeric Gel" ***Advances in Polymer Science & Technology, 2017*** at Radisson Blu Hotel 'New Delhi' organized by 'Asian Polymeric Association and IIT Delhi'.
- Presented poster entitled "Stretchable and Durable Superhydrophobicity That Acts both in Air and Under Oil" in ***International Conference on Advanced Nanomaterials and***

Nanotechnology (ICANN-2017) conducted by Centre for Nanotechnology, Indian Institute of Technology Guwahati in 2017.

- Delivered an oral talk entitled "Highly Elastic and Robust Water Repellent Property that Performs both in Air as well as after Oil Contamination" at Annual Chemical Engineering Festival ***Reflux 2018*** organized by Department of Chemical Engineering, IIT Guwahati, India.
- Presented poster entitled "Smart Polymeric Material for Inclusive Oil/Water Separation through Complementary Use of Selective-Absorption and Gravity Driven-Filtration Process" in ***'Research Conclave'*** (2018) organized by Students' Academic Board (SAB), IIT Guwahati.
- Presented Model based on "Stretchable and Porous Superhydrophobic Fibrous Substrate for Oil Spill Cleanup" in ***'Research Conclave'*** (2018) organized by Students' Academic Board (SAB), IIT Guwahati.
- Delivered an oral talk entitled "Smart Polymeric Material for Oil/Water Separation through Selective Absorption and Gravity Driven-Filtration Process" at ***two days workshop on Nanoscience-opportunities and challenges*** (2018) organized by department of chemistry and physics of IUST Kashmir.

Awards and Achievements

- Received *Departmental Best Poster Award* in **'Research Conclave '2017** organized by Students' Academic Board (SAB), IIT Guwahati.
- Received *Institute Best Poster Award* in **Research Conclave '2017** organized by Students' Academic Board (SAB), IIT Guwahati.
- Received *Best Poster Award* in **'Chemconvene 2017'** organized by Department of Chemistry, IIT Guwahati.
- Received *Best poster Award* in **International Conference on Sophisticated Instruments in Modern Research, 2017 (ICSIMR-2017***),* organized by 'CIF IIT Guwahati'.
- Received *Best poster Award* in **International Conference on Advanced Nanomaterials and Nanotechnology (ICANN-2017)** conducted by Centre for Nanotechnology, IIT Guwahati.

- Received *Best Oral Presentation Award* in International Conference on **Advances in Polymer Science & Technology, 2017** at Radisson Blu Hotel 'New Delhi' organized by 'Asian Polymeric Association and IIT Delhi'.
- Received *Tertiary Prize Award* in ISBE 2017, Bionic Innovation Competition organized by **'Journal of Bionic Engineering & National-Local Joint Engineering Laboratory of Bionic Engineering**, Jilin University' China.